552951

Analysis Report for the CRA-2009 PABC Culebra Flow and Transport Calculations

AP-144

Task Number: 1.2.5

Report Date: 2/3/2010

Author: Kristopher L. Kuhlman, 6712, Repository Performance Department — 2/3/10 Date

Technical Review: Ahmed E. Ismail, 6711, Performance Assessment Department — 2/3/2010 Date

QA Review: Mario J. Chavez, 6710, Carlsbad Programs Group — 2/3/2010 Date

Management Review: Christi Leigh, 6712, Manager, Repository Performance Department — 2/3/2010 Date

WIPP:1.2.5:PA:QA-L:549013

Contents

List of Figures

List of Tables

1 Introduction

The Waste Isolation Pilot Plant (WIPP), located in southeastern New Mexico, has been developed by the U.S. Department of Energy (DOE) for the geologic (deep underground) disposal of transuranic (TRU) waste. Containment of TRU waste at the WIPP is regulated by the U.S. Environmental Protection Agency (EPA) according to the regulations set forth in Title 40 of the Code of Federal Regulations (CFR), Part 191 (U.S. EPA, 1993). The DOE demonstrates compliance with the containment requirements according to the Certification Criteria in Title 40 CFR Part 194 (U.S. EPA, 1996) by means of performance assessment (PA) calculations performed by Sandia National Laboratories (SNL). WIPP PA calculations estimate the probability and consequence of potential radionuclide releases from the repository to the accessible environment for a regulatory period of 10,000 years after facility closure. The models are maintained and updated with new information as part of a recertification process that occurs at five-year intervals after the first waste is received at the site.

PA calculations were included in the 1996 Compliance Certification Application (CCA) (U.S. DOE, 1996), and in a subsequent Performance Assessment Verification Test (PAVT) (MacKinnon and Freeze, 1997a; 1997b; 1997c). Based in part on the CCA and PAVT PA calculations, the EPA certified that the WIPP met the containment criteria in the regulations and was approved for disposal of transuranic waste in May 1998 (U.S. EPA, 1998). PA calculations were also an integral part of the 2004 Compliance Recertification Application (CRA-2004). During their review of the CRA-2004, the EPA requested an additional PA calculation, referred to as the CRA-2004 Performance Assessment Baseline Calculation (PABC) (Leigh et al., 2004), be conducted with modified assumptions and parameter values (Cotsworth, 2005).

Since the CRA-2004 PABC (PABC-2004), additional PA calculations were completed for and documented in the 2009 Compliance Recertification Application (CRA-2009). The CRA-2009 PA resulted from continued review of the PABC-2004, including a number of technical changes and corrections, as well as updates to parameters and improvements to the PA computer codes (Clayton et al., 2008). The EPA has requested that additional information, which was received between the commencement of the CRA-2009 PA (December 2007) and the submittal of the CRA-2009 (March 2009), be included in an additional PA calculation (Cotsworth, 2009), referred to as the CRA-2009 Performance Assessment Baseline Calculation (PABC-2009). The PABC-2009 analysis is guided by analysis plan AP-145 (Clayton, 2009a). This report documents the Culebra flow and radionuclide transport analysis for the PABC-2009 and is compared with the results from the PABC-2004 PA. The EPA requested (Cotsworth, 2009) the PABC-2009 transport calculations utilize the newly conceptualized hydrologic model from AP-114 Task 5 (Hart et al., 2008) and the newly calibrated transmissivity fields from AP-114 Task 7 (Hart et al., 2009). The EPA also requested (Kelly, 2009) the PABC-2009 use revised K_d ranges in the Culebra radionuclide transport calculations.

This analysis report documents the efforts to evaluate the effects of potential future potash mining on the flow and transport in the Culebra Member of the Rustler Formation, in the vicinity of the Waste Isolation Pilot Plant (WIPP), approximately 26 miles southeast of Carlsbad, New Mexico. It is an update of analyses done for the PABC-2004 (Lowry and Kanney, 2005), which updates CCA analyses (Ramsey and Wallace, 1996).

Radionuclide movement through the Culebra is a function of the groundwater flow-field and the transport properties of the radionuclide species being considered. Groundwater flow velocity and direction are highly dependent upon the magnitude and the spatial variability of hydraulic transmissivity (the T-field). WIPP PA considers the potential that future potash mining in the McNutt potash zone of the Salado Formation underlying the Rustler Formation will cause subsidence in the Culebra and hence increase Culebra transmissivity.

The Culebra flow and transport analysis in this report begins with results from Latin Hypercube Sampling (LHS) (Kirchner, 2010) and the calibrated Culebra T-fields (Hart et al., 2009). Cumulative releases of radionuclides through the Culebra to the accessible environment (the Culebra outside the WIPP land withdrawal boundary (LWB)) are inputs to CCDFGF (Camphouse, 2010). Discussion of the data flow between the different elements of PA can be found in the PABC-2009 summary report (Clayton et al., 2010).

The work reported herein was conducted under the analysis plan for the Calculation of Culebra Flow and Transport PABC-2009 (AP-144), (Kuhlman, 2009), which is a subset of the work broadly described by AP-145, the analysis plan for the CRA-2009 Performance Assessment Baseline Calculation(Clayton, 2009a)

This report documents the analysis performed regarding the release mechanism related to groundwater flow and transport through the Culebra. The analysis report associated with AP-114 Task 5 (Hart et al., 2008) documents the development of the 1000 base T-fields (before calibration) for the Culebra and the analysis report associated with AP-114 Task 7 (Hart et al., 2009) documents the subsequent calibration and selection of 100 calibrated realizations from the base T-fields for use in the PA analysis outlined here. Background information on groundwater flow and solute transport within the Culebra is presented in Section 2. The effects of potash mining on the flow-field (Section 3 and Appendix 1) and the transport of radionuclides through these flow-fields (Section 4 and Appendix 2) are both covered in this report. Results of the flow and transport calculations are summarized and conclusions are drawn in Section 5.

2 Background

The WIPP repository is located approximately 26 miles (42 kilometers) southeast of Carlsbad, New Mexico. The disposal horizon of the WIPP is approximately 2,150 feet (655 meters) below the ground surface in the Salado Formation of the Delaware Basin. The Salado is regionally extensive, consisting predominantly of halite, a low permeability evaporite (Powers et al., 1978).

The Rustler Formation is located stratigraphically above the Salado Formation and is of particular importance in estimating the potential for radionuclide releases from the WIPP because it contains the most hydraulically transmissive units above the repository. In the vicinity of the WIPP, the Rustler consists of evaporite units interbedded with carbonates and siliciclastic units (Vine, 1963; Holt and Powers, 1988). The Culebra Dolomite Member has been identified as the most transmissive unit in the Rustler Formation and consequently it is the most likely pathway for subsurface transport of radionuclides from the WIPP panels to the accessible environment outside the LWB.

The Culebra is an approximately 7.75 meter thick fractured dolomite with nonuniform properties in both the horizontal and vertical directions (Holt, 1997). There are multiple scales of porosity and permeability within the Culebra ranging from microfractures to potentially large vuggy zones. Flow occurs through fractures, vugs and, to some extent, through intergranular pores. The large permeability contrast between the different scales of interconnected porosity suggests a dual porosity conceptualization consisting of advective porosity (i.e., fracture porosity) and diffusive porosity (i.e., matrix porosity). The advective porosity is the void space comprised of the highly transmissive portions of the rock such as large open fractures and/or interconnected vugs. The diffusional porosity represents the intragranular porosity potentially including microfractures or vugs. Tracer tests conducted in the Culebra at the WIPP site have shown characteristics of both advective transport and matrix diffusion(Meigs et al., 2000).

Although the Culebra properties vary in the vertical direction, the error introduced by modeling the Culebra in two rather than three dimensions has been determined to be negligible for the objective of groundwater flow and radionuclide transport calculations(Corbet, 1995).

Potash mining in the WIPP area involves resource extraction below the Culebra dolomite in the McNutt Potash zone, a subsection of the larger Salado Formation that underlies the Rustler Formation. It is hypothesized that subsidence of the Culebra due to potash mining leads to fracturing and unconsolidation, resulting in higher Culebra transmissivities. This increase in transmissivity may significantly change the regional groundwater flow pattern in the Culebra and additionally the transport of any nuclides entering the aquifer from the underlying repository. WIPP PA includes mining scenario calculations to estimate the impact potash mining may have on groundwater flow and radionuclide transport.

The key steps in estimating radionuclide transport through the Culebra include:

1. Construction of base geostatistical realizations of Culebra hydraulic transmissivity (T), anisotropy, storativity, and recharge fields (collectively referred to as "T-fields");
2. Calibration of the T-fields to observed heads;
3. Modifying the T-fields to account for potential subsidence due to potash mining beneath the Culebra;
4. Calculating steady-state groundwater flow-fields for each mining-modified T-field; and
5. Calculating radionuclide transport through the Culebra for each flow-field. Culebra transport simulations calculate the cumulative discharge at the WIPP LWB over the 10,000-year regulatory period due to a source located at the center of the waste panel area. The source releases 1 kg for each of several radionuclides over the first 50 years of the simulation.

The work reported herein includes steps 3-5. The construction of base geostatistical realizations of Culebra T-fields (step 1) was covered in AP-114 Task 5 (Hart et al., 2008), and the calibration of these T-fields (step 2) was covered in AP-114 Task 7(Hart et al., 2009).

3 Culebra T-Field Mining Modifications and Flow-field Calculations

3.1 Overview

The PABC-2009 Culebra T-field mining modifications and flow-field calculations largely follow the procedure used in the PABC-2004 (Lowry and Kanney, 2005), with two exceptions: 1) a new definition of the region containing minable potash is used, and 2) the new T-fields developed and calibrated as part of AP-114 Tasks 5 and 7 are used as inputs. The procedure for this analysis is summarized below:

1. Obtain the sampled values for the random mining modification factor (100 vectors x 3 replicates);
2. Map potential areas of future potash mining onto the groundwater modeling domain for both full- and partial-mining scenarios;
3. Apply the mining modification factor to the 100 stochastically calibrated T-fields from AP-114 Task 7 (Hart et al., 2009), producing 600 mining-modified T-fields (100 vectors × 2 mining scenarios × 3 replicates);
4. Perform steady-state flow simulations for each of the 600 mining-modified T-fields using MODFLOW-2000 (also known as MODFLOW or MF2K);
5. Perform particle tracking using the new mining-affected flow-fields to determine advective travel times to the LWB; and
6. Refine the flow-field to a finer grid size and re-execute MODFLOW to create flow-fields as input for the Culebra radionuclide transport calculations.

This analysis report represents the latest effort in characterizing mining effects in the Culebra and highlights the differences and additions relative to past calculations (Ramsey and Wallace, 1996; Lowry, 2003a; 2003b; Lowry, 2004). The reader is encouraged to review the past documents for further background information.

The PABC-2009 models two categories of mining-impacted transmissivity fields: partial mining with only mining outside the LWB and full mining with regions both inside and outside the LWB mined.

Starting with the 100 stochastically calibrated T-fields from Hart et al., (2009), T-fields are modified to reflect the effects of mining by multiplying the transmissivity value in cells that lie within designated mining zones by a random factor uniformly sampled between 1 and 1000. The range of this factor is set by the EPA in regulation 40 CFR 194.32(b) (U.S. EPA, 1996). The scaling factor for each T-field is provided from Latin Hypercube Sampling (LHS), (Kirchner, 2010).

A forward steady-state flow simulation is run for each new T-field under each mining scenario (full and partial) across three replicates of mining factors, resulting in 600 simulations. Particle tracking is performed on both the 100 original and 600 modified flow-fields to compare the flow path and groundwater travel time from a point above the center of the WIPP disposal panels to the LWB. CDFs are produced for each mining scenario and compared to the undisturbed scenario. The CDFs describe the probability of a conservative tracer (i.e., a "marked" water particle) reaching the LWB at a given

time. In addition to comparing travel times, particle-tracking directions are also examined to determine the effect on the regional flow direction in the WIPP area due to mining.

The parameter fields for the mining scenarios are then copied to a finer grid and the resulting flow-fields are passed to the transport analysis, which performs radionuclide transport modeling in the Culebra.

3.2 Approach

3.2.1 Modeling Assumptions

Besides assumptions inherent in all modeling exercises (e.g., physical processes can be adequately parameterized and estimated on a numerical grid), there are several assumptions that are specific and important to the PABC-2009 analysis. Those assumptions are as follows:

1. It is assumed that the boundary conditions along the model domain edges are known and are not dependent on mining (internal fixed-head cells are modified). The reasoning for this assumption is described in Section 3.3.1.
2. It is assumed that the flow field, over the duration of the particle tracking and transport times, can be represented by steady-state conditions. This is related to the first assumption; the boundary conditions are also assumed to remain constant over time. This assumption is necessary since data do not exist that can predict the transient conditions in the Culebra at the site over the time frames involved (>10,000 years).
3. It is assumed that the mining effects can be adequately represented with a single mining factor that increases the transmissivity uniformly across the potential mining zones within the Culebra. This is directed by EPA regulation 40 CFR 194.32(b) (U.S. EPA, 1996).

Further assumptions related to the flow modeling and calibration of the T-fields can be found in AP-114 Task 5 (Hart et al., 2008) and Task 7 (Hart et al., 2009).

3.2.2 Potash Mining Parameter Modifications

Potash mining in the region surrounding WIPP involves underground excavation in the McNutt Potash zone of the upper Salado Formation, which is located stratigraphically above the WIPP repository horizon, but below the Culebra Member of the Rustler Formation (see Figure 3-1). It is hypothesized that subsidence due to collapse of the underground voids created in the McNutt potash zone during mining will lead to increased permeability in the Rustler Formation, due to increased fracturing. The purpose of the mining scenario calculations is to determine the impact of potash mining on groundwater flow directions and transport velocities in the Culebra. This analysis largely represents a re-application of the methods used in PABC-2004 (Lowry and Kanney, 2005), with a few minor exceptions:

1. The definition of the regions where minable potash is believed to exist, obtained from the Bureau of Land Management (BLM) (Cranston, 2009), has been updated.
2. The configuration of the MODFLOW model that mining modifications are being applied to has changed (see Figure 3-2):
    a. The eastern limit of the model domain has moved 6 km east.

b. The no-flow boundary condition present along the western edge of the PABC-2004 model has been eliminated in the southern half of the model domain.
c. The "halite-sandwiched" region of the Culebra (east of either the M2/H2 or M3/H3 Rustler halite margins) is now constant head.

3. The way the mining-modified areas interact with internal boundary conditions of the flow model has changed, due to the change in the boundary conditions (there were no internal boundary conditions in the PABC-2004 MODFLOW model).

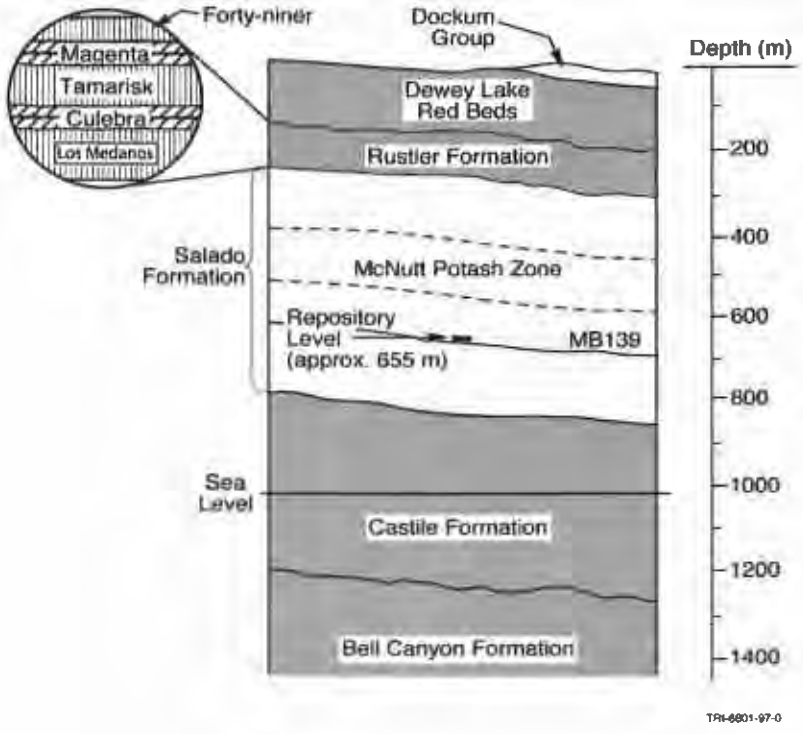

Figure 3-1. Generalized stratigraphy near WIPP

3.2.3 Software and Run Control

The mining-modified Culebra flow-fields and particle tracks were produced on the WIPP PA Pentium 4 Cluster using MODFLOW(Harbaugh et al., 2000), DTRKMF (Rudeen, 2003), and several utility codes (see Appendix 4 for code listings).

With the exception of the conversion of the potash definition shapefile to ASCII, the calculations were performed under formal run control(Long, 2010). The run control scripts extracted executables and input files from access-controlled repositories, performed the calculations in access-controlled directories, and stored the output files in access-controlled repositories. The Run Control Coordinator performed the calculations using a reserved account (`run_mast`) on the cluster. Input and output files were archived using the CVS version control system.

The mining modification simulations were run using an input file (`mining_mods.inp`) that drives the run control Python program ReadScript.py (Kirchner, 2008). The run control program creates the required directory structure, checks out the required input files, executes the main Bash shell script

(`run_mining_mods.sh`), and checks the results back into CVS. This driving Bash shell script performs five major functions (see Appendix 1 for a detailed narrative of the process):

1. Convert potash definition shapefile to ASCII files indicating mining-affected MODFOW model cells;
2. Modify MODFLOW model properties in response to mining;
3. Run MODFLOW and DTRKMF for each of 700 scenarios (600 mined + 100 original) using original 100 m grid;
4. Convert MODFLOW input data to 50 m transport grid; and
5. Run MODFLOW for each of 600 mined scenarios using 50 m transport grid, converting output to format required for VTRAN2.

3.2.4 Radionuclide Transport Calculations

The steady-state flow-fields are computed using MODFLOW after adjustments to account for potential effects of potash mining. These flow results are used as inputs to the SECOTP2D solute transport model, which predicts the fate of radionuclides released from a point located directly over the center of the waste disposal panels. This portion of the analysis is largely unmodified from the analysis done for PABC-2004 (Lowry and Kanney, 2005), aside from the changes in K_d ranges and the MODFLOW velocity fields used as inputs.

3.3 Model Domain and Discretization

The eastern limit of the MODFLOW model domain used in the PABC-2009 analysis (Hart et al., 2008) is extended eastward, compared to the MODFLOW domain used in the PABC-2004 analysis (see both boundaries in Figure 3-2). This change was made in order to locate the boundary in an area where halite is present in all of the non-dolomite members of the Rustler Formation, simplifying the specification of the eastern model boundary condition. The new extent of the model domain is 601700 m to 630000 m *x* and 3566500 m to 3597100 m *y* (see Table 3-1 for these and other relevant UTM NAD27 Zone 13 coordinates). The MODFLOW flow model domain is aligned with the primary compass directions and is aerially discretized into 100 m square cells, yielding a model that is 284 cells or 28.4 km wide (east-west) by 307 cells or 30.7 km tall (north-south). The Culebra is modeled as a single horizontal layer of uniform 7.75 m vertical thickness.

Table 3-1. UTM NAD27 Zone 13 coordinates defining extents of model domains

Domain Corner	UTM NAD27 X [m]	UTM NAD27 Y [m]
MODFLOW Flow Model Domain		
Northeast	630,000	3,597,200
Northwest	601,700	3,597,200
Southwest	601,700	3,566,500
Southeast	630,000	3,566,500
WIPP Land Withdrawal Boundary		
Northeast	616,941	3,585,109
Northwest	610,495	3,585,068
Southwest	610,567	3,578,623
Southeast	617,015	3,578,681
SECOTP2D Transport Model Domain		
Northeast	617,750	3,583,000
Northwest	610,250	3,583,000
Southwest	610,250	3,577,600
Southeast	617,750	3,577,600

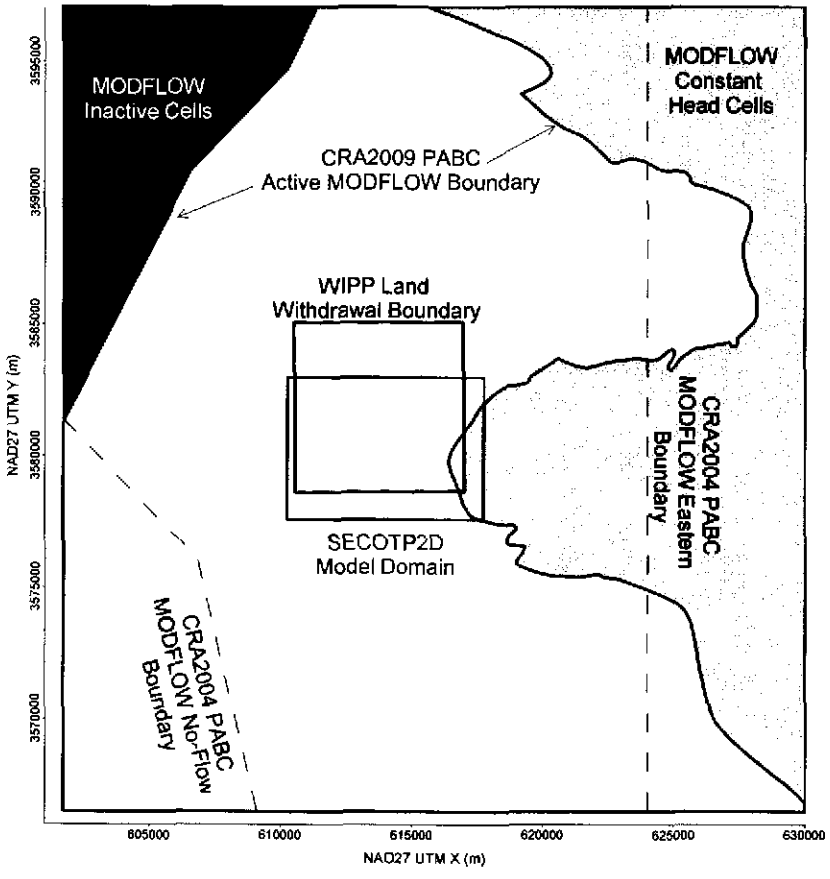

Figure 3-2. PABC-2004 (black dashed line) and PABC-2009 (solid blue line) MODFLOW domains, SECOTP2D transport domain (red), and WIPP LWB shown for comparison.

3.3.1 Boundary and Initial Conditions

Like the model domain and discretization, the boundary and initial conditions used in the PABC-2009 are described fully in AP-114 Task 7 (Hart et al., 2009). Freshwater head data were used from May 2007, consisting of 44 head measurements across the modeling domain; see AP-114 Task 6 (Johnson, 2009) for details regarding the calculation of freshwater head values. A multi-parameter parametric surface is used to fill initial head values everywhere except in the constant-head zone east of the halite margin (Hart et al., 2009).

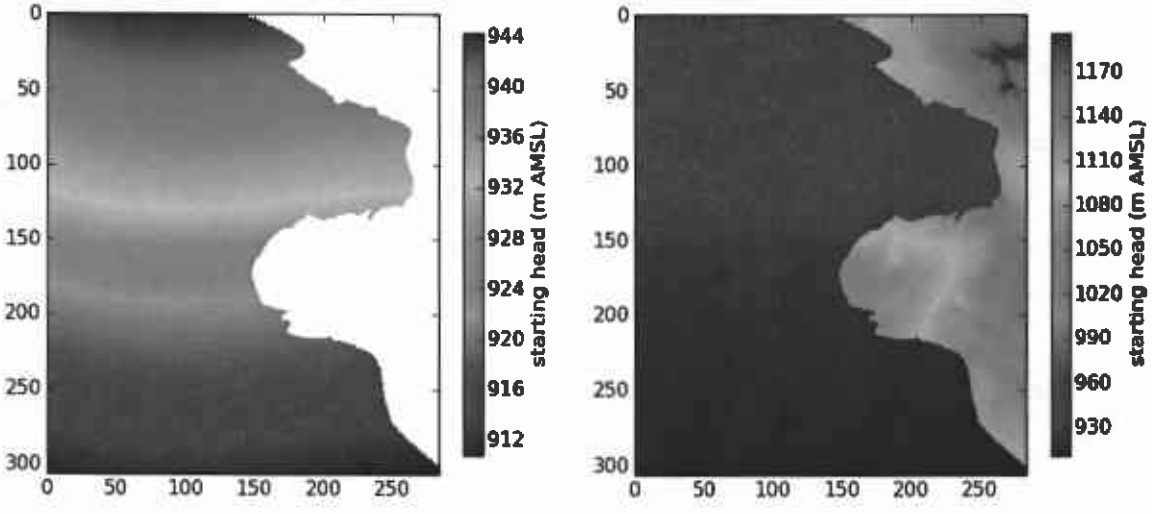

Figure 3-3. Initial and boundary heads for non-constant-head portion of domain (left) and entire domain (right) (Hart et al., 2009). Coordinates are cell-based.

The model boundary conditions along straight-line portions of the north, west, and south edges of the domain are specified head. The parametric function values determining the initial heads are assigned to constant-head cells and kept fixed throughout the simulation. Since simulations are steady state, determination of the initial heads is important only in relation to setting the fixed boundary conditions. The constant-head region associated with the halite-sandwiched portion of the Culebra (light gray region in Figure 3-2) is specified head, set to the land surface elevation (see right plot in Figure 3-3). The piecewise-linear boundary in the northwest corner is a no-flow boundary and is parallel to the Nash Draw groundwater divide (implemented using no-flow cells indicated with dark gray in Figure 3-2). The axis of Nash Draw is interpreted as a regional groundwater divide, draining the Rustler units to the east (and also by symmetry to the west). The initial head contours across the non-constant-head portion of the modeling domain are shown in more detail (only the values specified by the parametric equation) in the left plot of Figure 3-3. The effects of potential potash mining on the boundary conditions must be considered because the extent of minable potash ore extends beyond the modeling domain (see Figure 3-4). Regional flow rates within the flow model are controlled by the boundary conditions and the hydraulic conductivity distribution. The regional gradient across the domain is approximately

$$(943.9\ \text{m} - 911.6\ \text{m})/30.7\ \text{km} = 0.00105 \quad (1)$$

For the current grid, we average the constant heads along the non-halite-sandwiched portion of the northern boundary (columns 1-140, 943.9 m), subtract the average heads along the entire southern boundary (911.6 m), and then divide by the north-south model domain distance (30.7 km). It is assumed that mining impacts would not significantly change this regional gradient and thus the specified initial conditions for the mining scenarios are identical to those in AP-114 Task 7 (Hart et al., 2009). In addition, the CCA, CRA-2004, and PABC-2004 all used this same conceptualization (keeping the outer boundary conditions fixed between the mining and non-mining scenarios); the same conceptualization is maintained to allow for comparisons between the different models.

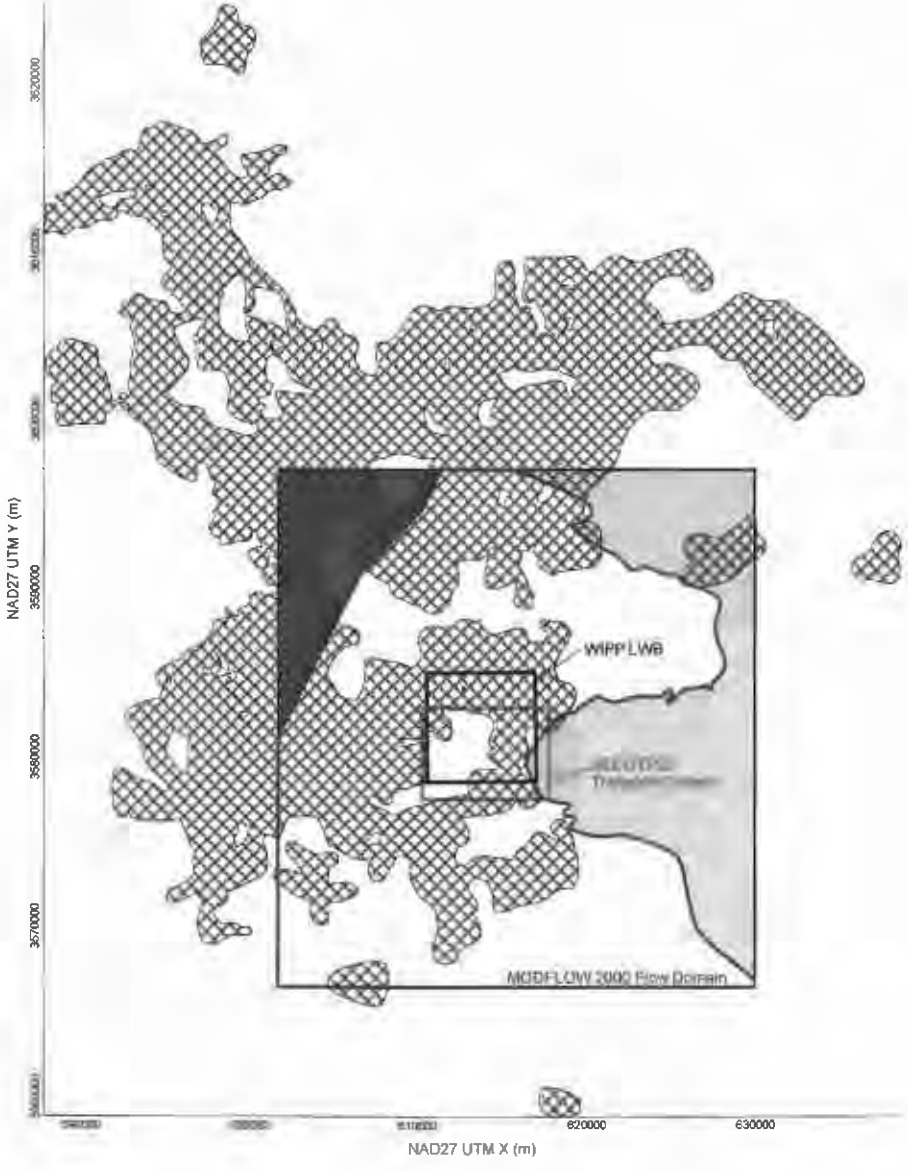

Figure 3-4. Comparison of minable potash to the flow and transport modeling domains; green hatched area from BLM shapefile (Cranston, 2009)

3.3.2 Determination of Potential Mining Areas

The 2009 version of the Bureau of Land Management (BLM) map indicating the distribution of minable potash ore was obtained from BLM as an ESRI shapefile (Cranston, 2009). The conversion of this shapefile to an integer matrix corresponding to Culebra MODFLOW model cells (indicating whether a model cell was affected by mining or not) is explained in Section A1.1.

Since the potash-mining horizon is located in the Salado Formation, below the Culebra, the areas disturbed by mining activities in the Culebra are larger than mined areas in the Salado due to angle-of-draw effects; the subsidence effects do not propagate up vertically, but instead they propagate up and out at 45° angles between horizontal and vertical. The final conclusion is that a 253-m-wide collar was to be added to the mining-impacted areas (Ramsey and Wallace, 1996; Bertram, 1995). This is considered a conservative estimate of the angle-of-draw effects. To accommodate the angle of draw, the mining zone boundaries, as overlaid on the current model grid, were extended outward three cells (300 m) in the x- and y-directions, and two cells (283 m) in the diagonal directions (see Figure 3-5 for an illustration of the mining-expansion stencil). The PABC-2009 modeling domain and mining zones for the full-mining case are shown in comparison to the 1996 CCA and the CRA-2004 delineations in Figure 3-6. The comparison of the current and previous partial-mining cases is shown in Figure 3-7. A close-up of the WIPP site and the distribution of minable potash is shown in Figure 3-8; it illustrates how the definition inside the WIPP LWB has changed significantly since PABC-2004. For the PABC-2004, the closest minable potash was approximately 1,230 m from the center of the WIPP panels in the southeast direction; for PABC-2009, this distance has reduced to approximately 670 m (in a more easterly direction).

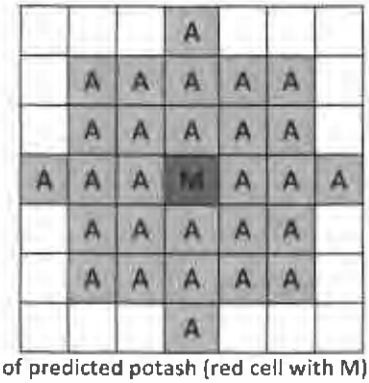

Figure 3-5. Stencil used to expand areas of predicted potash (red cell with M) to model cells affected by mining-related subsidence from 45° angle of draw (blue cells with A)

The output of this mining-area delineation is a file that contains one value for each cell in the grid. A value of 1 means the cell lies within a potential mining-affected zone, and a value of 0 means that it is outside a potential mining-affected zone. See section A1.3 for a detailed narrative description of the calculation of the mining-modified areas.

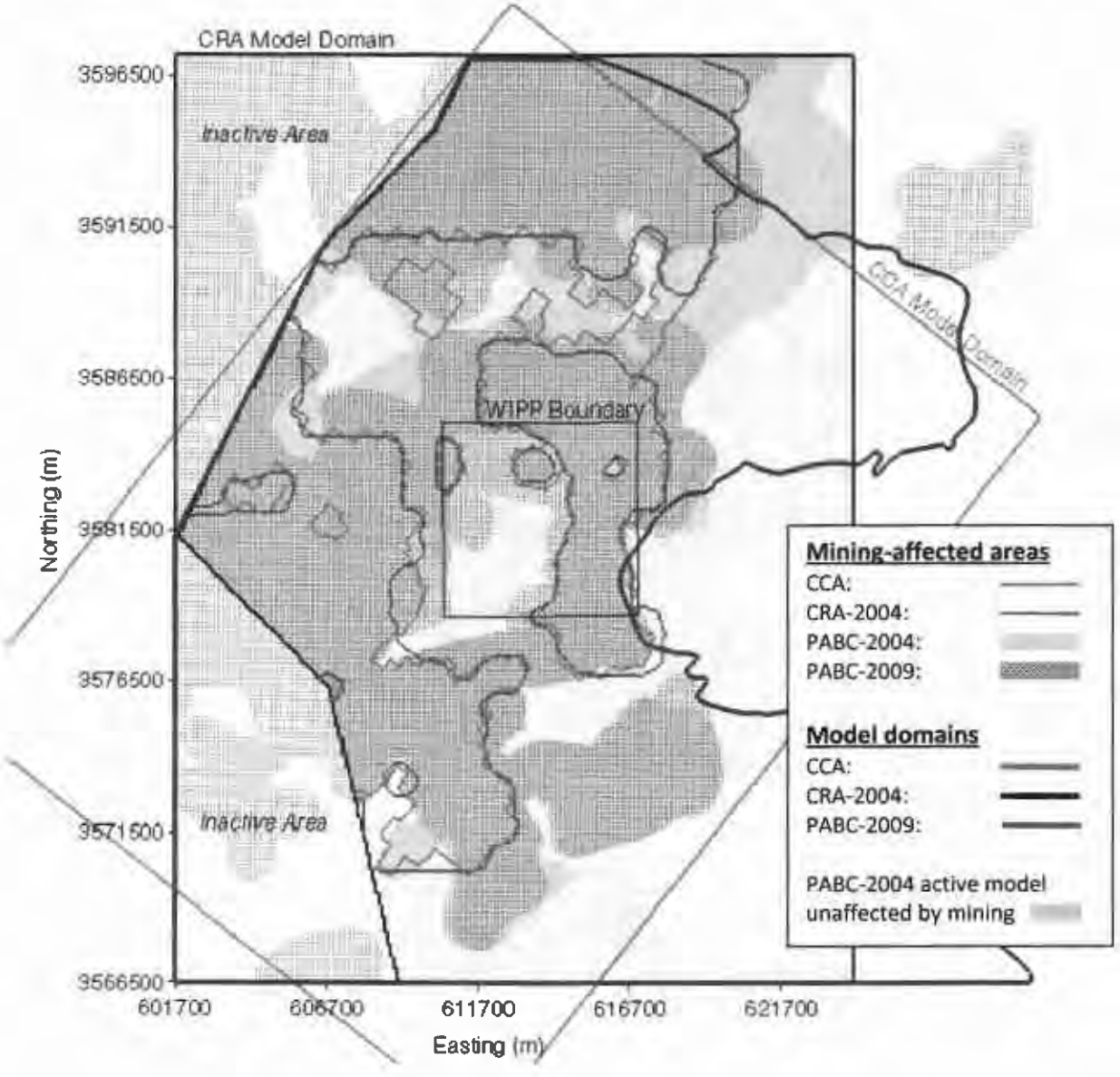

Figure 3-6. Definitions of mining-affected areas in full-mining scenario between current and previous models. Base image is Figure 3.2 from Lowry and Kanney (2005).

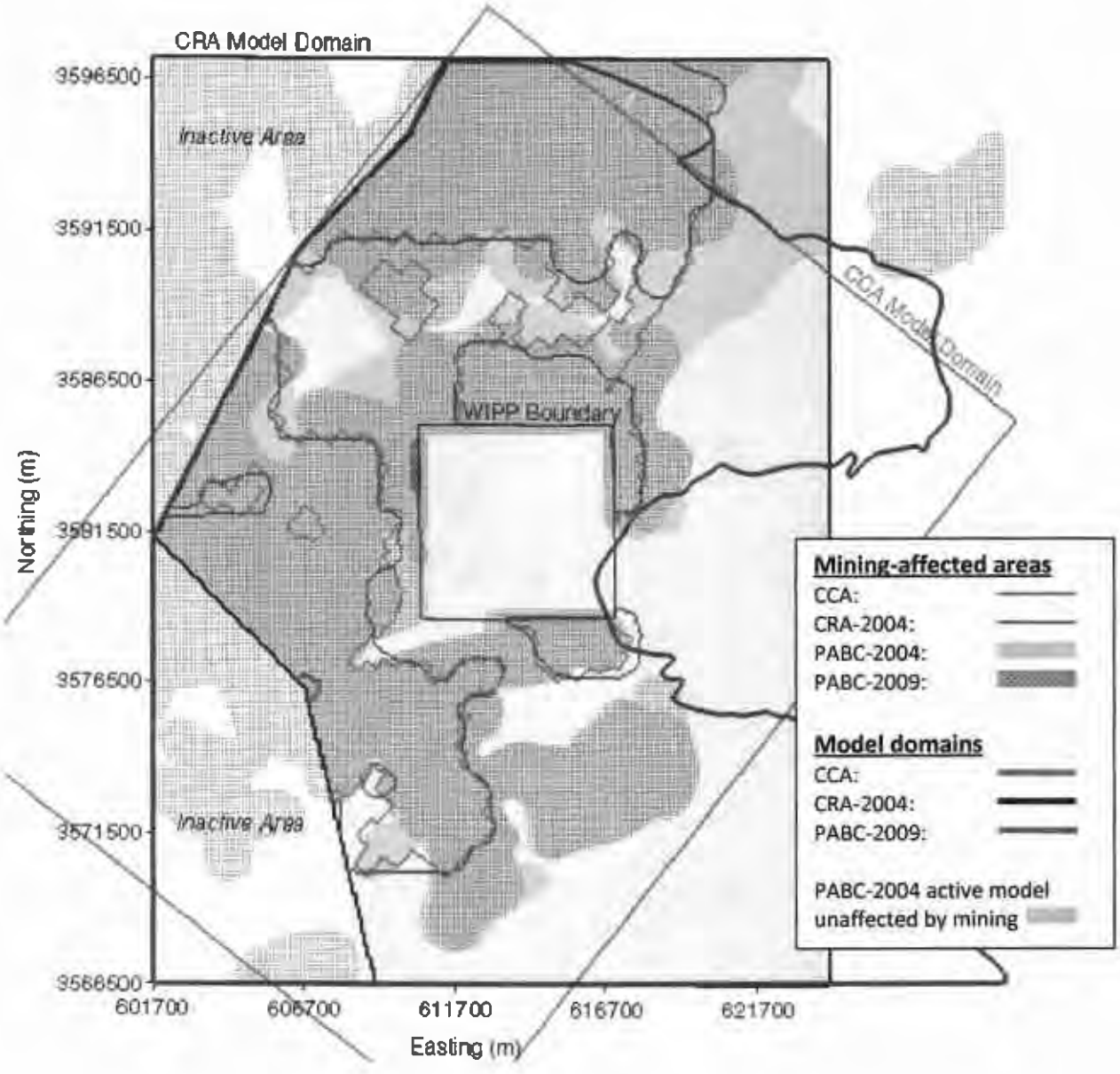

Figure 3-7. Definitions of partial-mining-affected areas between current and previous applications; base image is Figure 3.3 from Lowry and Kanney (2005).

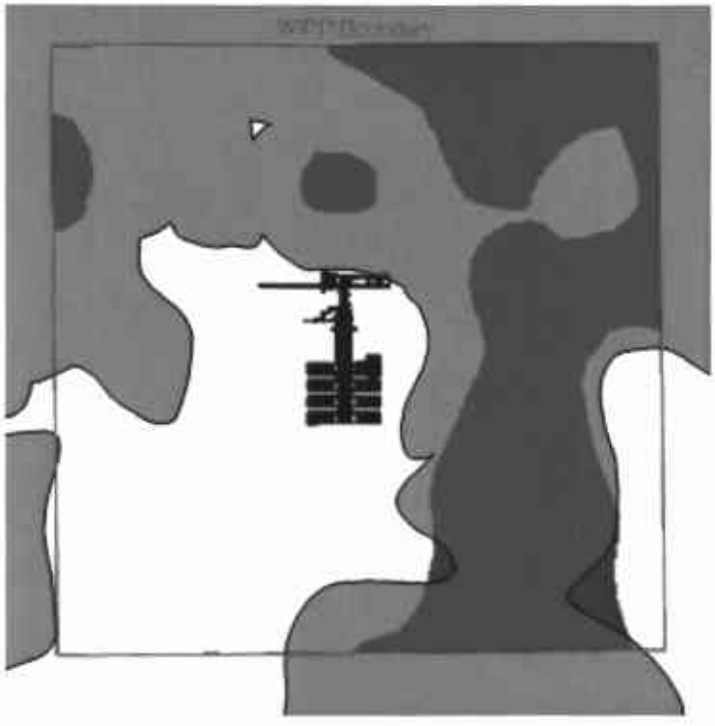

Figure 3-8. Comparison of minable potash distribution inside WIPP LWB for PABC-2004 (dark gray) and PABC-2009 (transluscent green). The WIPP repository plan is shown for comparison, from Figure 3.6 of Lowry and Kanney (2005)

3.3.3 Use of Mining Zones in Forward Simulations

The calibration process in Hart et al., (2009) produces 100 sets of transmissivity, horizontal anisotropy, storativity, and areal recharge fields (often referred to simply as "the T-fields" because in previous versions only transmissivity was calibrated) that each minimize the error between observed and model-calculated head distributions. The hydrologic conceptual model produces an ensemble of 1000 uncalibrated parameter fields (Hart et al., 2008). Two hundred of these were randomly sampled from the ensemble and calibrated; the best 100 were selected as the final calibrated set based on their ability to recreate observed head data (Hart et al., 2009). To simulate the effects of mining, each selected T-field is multiplied by its own unique mining scaling factor in areas of potential mining, and MODFLOW is run with these mining-modified T-fields to produce the mining-affected head and flow distributions. The cell-by-cell flow budget files are used in particle tracking and radionuclide transport calculations. To demonstrate stability in mean results, three different sets of mining factors are used, each set forming a replicate (given here as R1, R2, and R3). Thus, for each mining scenario (full and partial), three sets of 100 mining-altered T-fields and related cell-by-cell flow budgets are produced.

3.3.4 Particle Tracking Simulations

In each realization, a single conservative particle is tracked from the UTM NAD27 coordinate $x = 6135975$ m, $y = 35813852$ m (i.e., the location of monitoring well C-2737, directly above the center of the WIPP waste panels) to the LWB (Table 3-1) for each combination of T-field, replicate, and mining scenario using the DTRKMF code. Two main outputs are generated from the suite of particle tracks. First, plots are constructed showing the individual tracks for all 100 T-fields in each scenario for each

replicate (six plots total). This allows visual comparison of the prevailing flow directions for the full- and partial-mining scenarios and the qualitative comparison of the variability of the tracking direction. Secondly, CDFs are constructed for each replicate and scenario, which describe the probability that a water particle will cross the LWB in a given amount of time. The six plots and the CDFs are presented in Section 3.4.

3.4 Particle Tracking Results

Particle tracks were computed using DTRKMF (Rudeen, 2003), which uses the binary cell-by-cell flow budget files produced by MODFLOW-2000. In flow calculations, the full 7.75 m thickness of the Culebra is used, while for transport and particle tracking purposes the thickness is reduced to 4.0 m to focus all flow through the lower, more permeable portion of the Culebra (Holt, 1997). An average value of 16% porosity is used for the particle tracking calculations, as was used in AP-114 Task 7 (Hart et al., 2009). Porosity directly affects transport, but is not needed for the calibration of the flow model.

Particle tracking is performed to allow comparison between the two mining scenarios and the non-mining scenario, which was not used in the SECOTP2D radionuclide transport calculations. The particle tracking results illustrate the advective pathway taken by a marked water particle and do not take into consideration retardation, dispersion, or molecular diffusion. The particle tracks also allow easier comparison of the 600 results (each a 1D trace) in a single plot, in contrast showing 600 sets of concentrations (each a 2D field) produced from SECOTP2D.

3.4.1 Particle Travel Times

Compared to the non-mining scenario (results already given in AP-114 Task 7 (Hart et al., 2009)), the travel times for the partial-mining scenarios are longer, while travel times for the full-mining scenarios are shorter. The median travel time across all three replicates for the full-mining scenario is approximately 0.689 times the median travel time of the non-mined scenario (see Table 3-2, Figure 3-9 and Figure 3-10 for summary statistics and comparison to PABC-2004 results). All advective particle travel times are plotted, but it should be noted that the regulatory limit for radionuclide transport modeling is 10,000 years, taking into consideration retardation, diffusion, and dispersion (which don't apply to particle track modeling). The median travel time across all three replicates for the partial-mining scenario is 3.034 times greater than for the non-mining scenario. For PABC-2004, travel times in both the full- and partial-mining scenarios were slower (longer) than for the non-mining scenario. The CDFs for the full-, partial-, and non-mining scenarios are shown in Figure 3-9.

Table 3-2. Particle tracking travel time statistics (years); PABC-2004 statistics from Table 3.22 of Lowry and Kanney (2005)

		PABC-2009			PABC-2004		
Replicate	Statistic	Full	Partial	No Mining	Full	Partial	No Mining
R1	Median	5,138	22,581	N/A	64,026	117,815	N/A
	Max	200,260	91,119		2,175,165	2,727,191	
	Min	1,591	5,042		2,130	5,185	
R2	Median	4,956	21,999		80,801	148,489	
	Max	94,852	84,929		2,059,263	1,667,084	
	Min	1,421	5,037		2,463	4,855	
R3	Median	5,560	22,537		74,315	118,919	
	Max	93,172	86,758		1,779,512	3,128,693	
	Min	1,421	4,505		2,507	3,314	
Global	Median	5,084	22,376	7,374	70,170	131,705	18,289
	Max	200,260	91,119	73,912	2,175,165	3,128,693	101,205
	Min	1,421	4,505	2,618	2,130	3,314	3,111

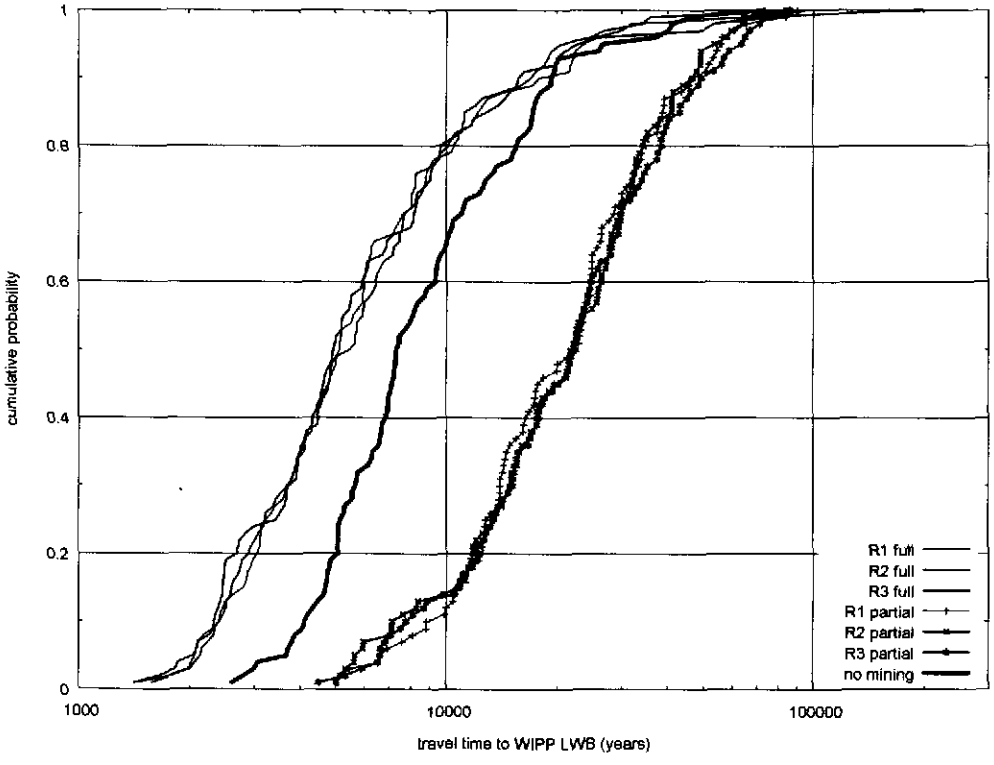

Figure 3-9. CDF of advective particle travel times from the center of the WIPP waste panels to the WIPP LWB for full, partial, and non-mining scenarios

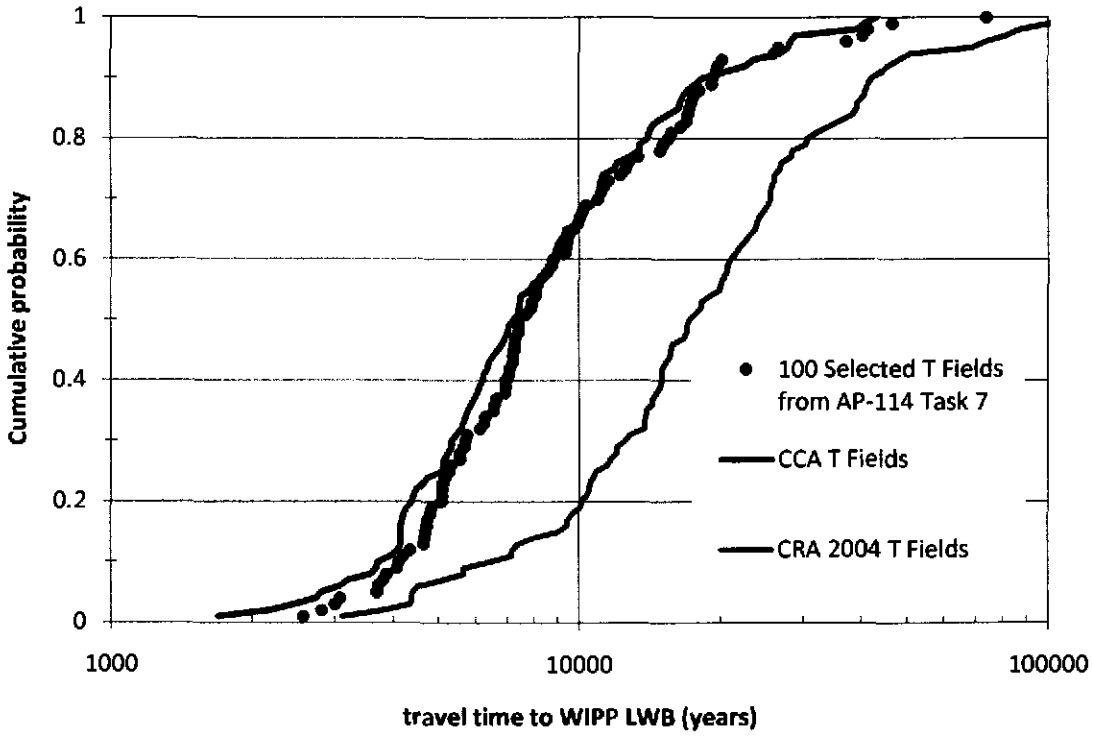

Figure 3-10. Comparison of advective particle travel time CDFs for PABC-2009, PABC-2004, and CCA.

3.4.2 Flow Directions

The particle track directions for the non-, full-, and partial-mining scenarios for the PABC-2009 are illustrated in Figure 3-11 to Figure 3-14. Like past mining scenario calculations (i.e., PABC-2004), there is a strong similarity between the three replicates (R1, R2, and R3) for each scenario (full or partial mining), although the travel directions for the PABC-2009 are different than for the PABC-2004 (Lowry and Kanney, 2005). A larger amount of minable ore inside the WIPP LWB, especially the ore immediately to the east of the particle release point, leads to different effects of full mining on travel times, compared to PABC-2004. Nearly all particles immediately go east to this boundary and then move south along it towards to the edge of the LWB at approximately $x = 612.75$ km (see Figure 3-12 and Figure 3-15). This is in contrast to the partial-mining scenario where the tracking directions are more similar to the non-mining scenario, but more evenly distributed spatially along the southern boundary. In the non-mining scenario, most of the particles exit near the high-transmissivity zone at approximately $x = 615$ km.

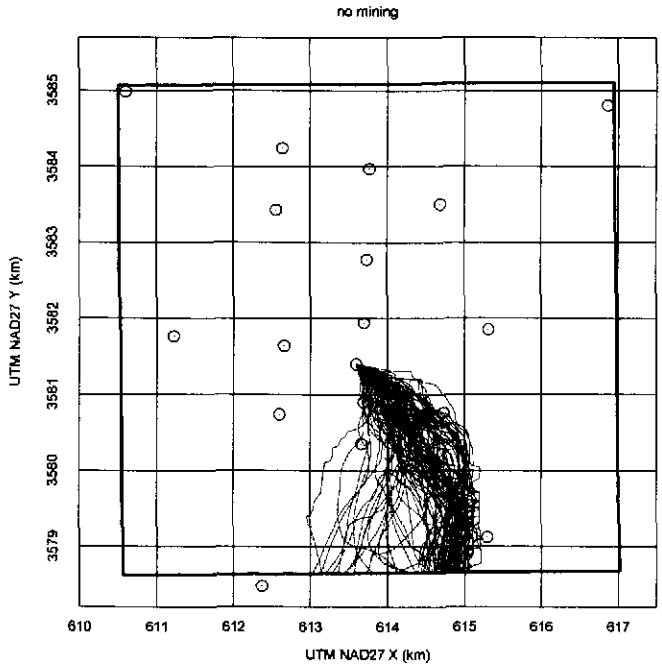

Figure 3-11. Particle tracks for non-mining scenario; black box is WIPP LWB, green circles are Culebra monitoring well locations.

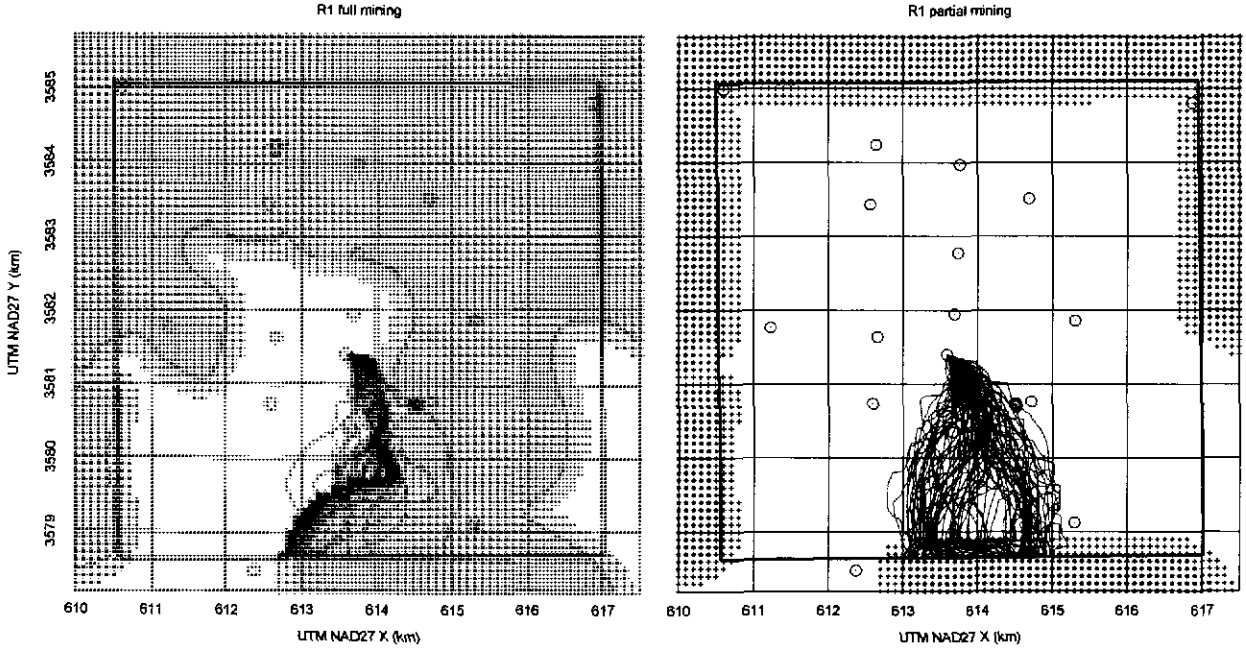

Figure 3-12. Particle tracks for R1. Small magenta squares and black crosses indicate centers of MODFLOW cells located within potash and mining-affected areas, respectively; thin black line is minable potash definition.

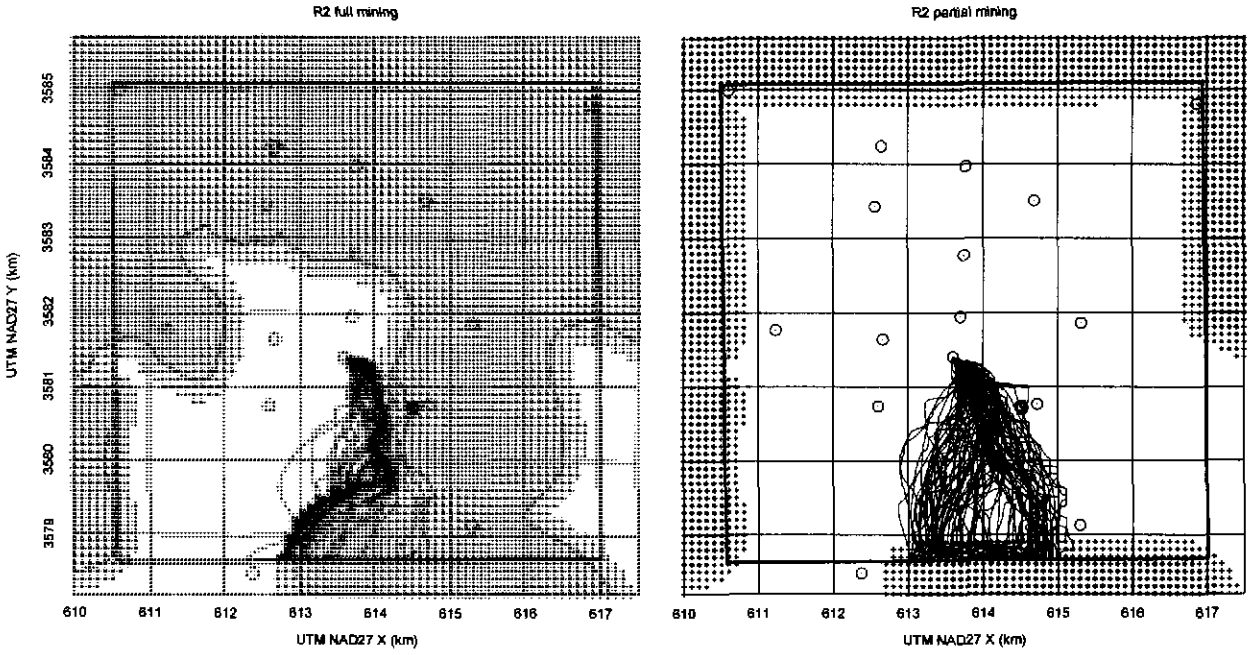

Figure 3-13. Particle tracks for R2. Small magenta squares and black crosses indicate centers of MODFLOW cells located within potash and mining-affected areas, respectively; thin black line is minable potash definition.

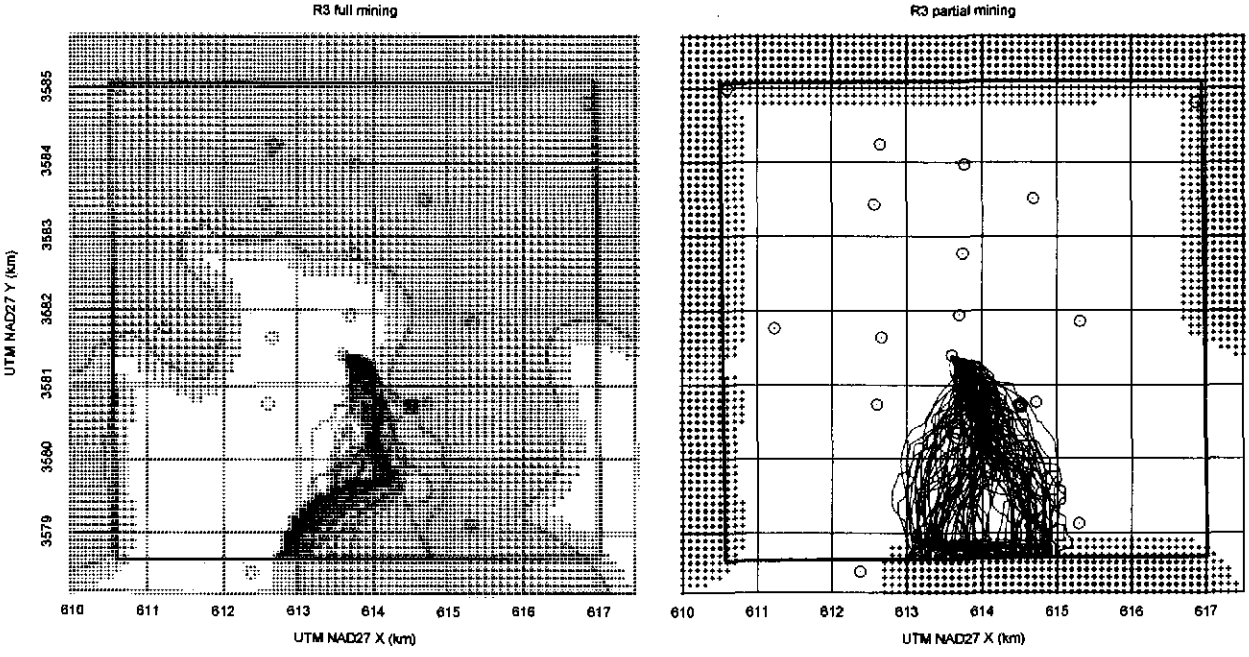

Figure 3-14. Particle tracks for R3. Small magenta squares and black crosses indicate centers of MODFLOW cells located within potash and mining-affected areas, respectively; thin black line is minable potash definition.

High-transmissivity areas corresponding to the mining-affected zones create preferential pathways through the system (see oranges and yellows in Figure 3-16). These preferential pathways result in higher velocities and flow rates through the mining zone and therefore relatively slower velocities in the non-mined areas. In the partial-mining scenario, where there is no mining inside the WIPP LWB, the preferential pathway goes "around" the LWB, rather than through it (similar to behavior seen in both

mining scenarios for PABC-2004). In the full-mining scenario, the mined regions are closer to the release point than in PABC-2004 (see Figure 3-8 for comparison), giving the particles a high-transmissivity pathway from the release point to the LWB, resulting in shorter travel times than the non-mined scenario (this behavior is different from that predicted using the PABC-2004 model). A comparison of the median, maximum, and minimum travel times for each scenario is presented in Table 3-2.

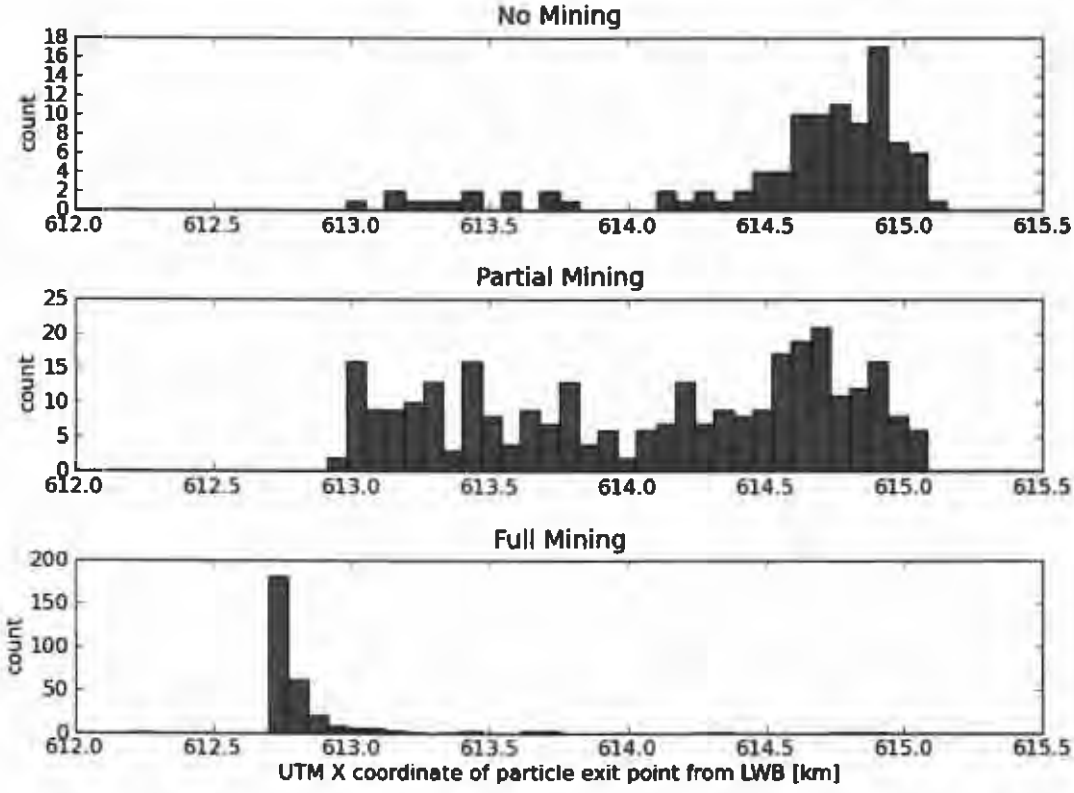

Figure 3-15. Histograms of particle *x*-coordinates at exit point from LWB; full and partial-mining include all three replicates (note different vertical scales between plots; no mining contains 100 particles while mining scenarios include 300 particles)

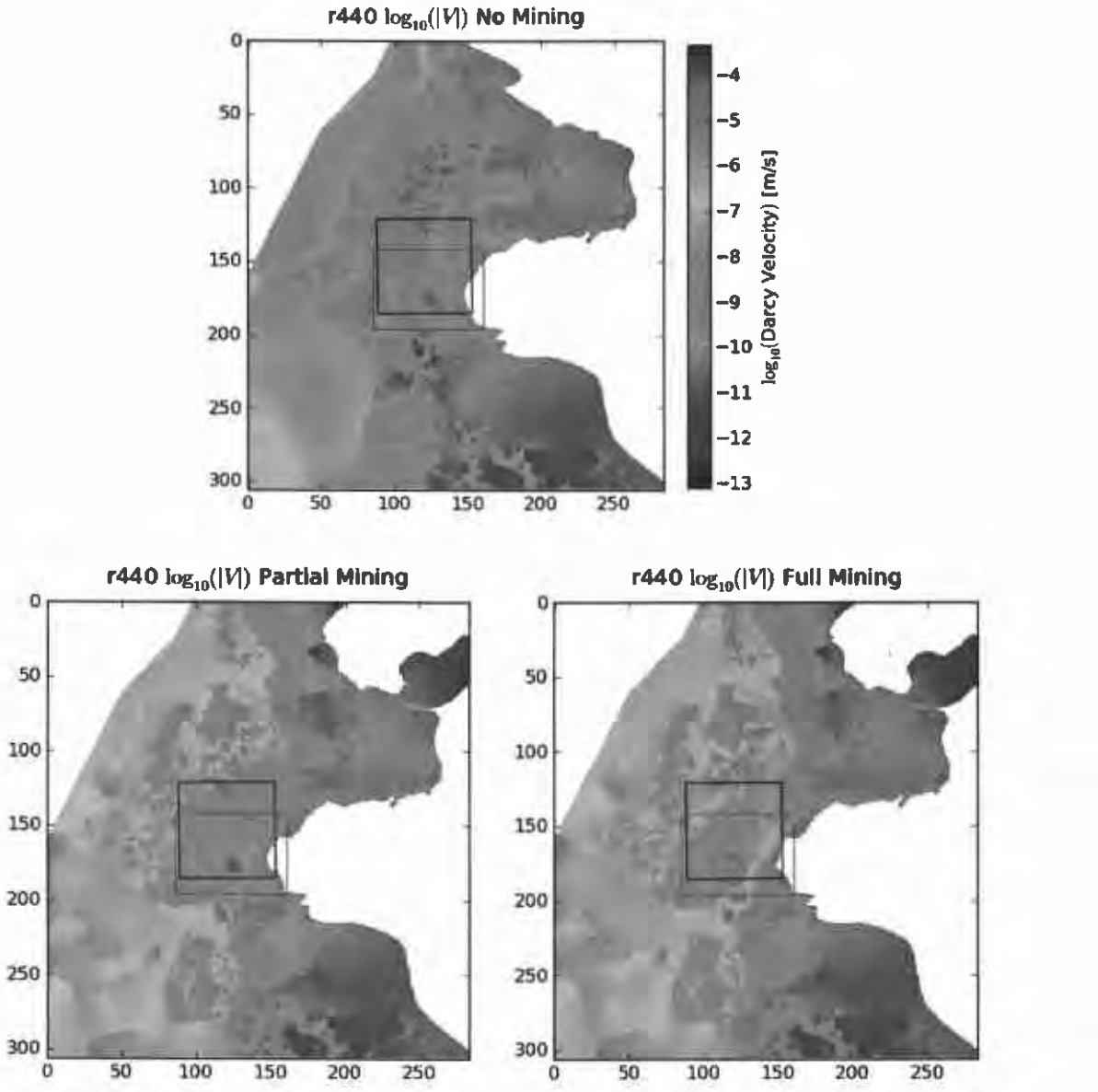

Figure 3-16. Magnitude of Darcy flux for r440 R2 for no, partial, and full-mining scenarios using cell-based coordinates; LWB (black) and SECOTP model domain (red) shown for reference.

3.4.3 Particle Speeds

Instantaneous speeds (the magnitude of particle velocities) were calculated from the DTRKMF particle locations and times using backwards finite differences,

$$v(t_{i+1}) = \frac{\sqrt{[x(t_i) - x(t_{i+1})]^2 + [y(t_i) - y(t_{i+1})]^2}}{t_{i+1} - t_i} \quad (2)$$

where a subscript *i* indicates the previous time step (a record or line in the DTRKMF output file) and a subscript *i*+1 is the current time step. This approach assumes a straight line connects the locations at the beginning and ends of the step, so it is potentially underestimating speeds, but step sizes are small

and error should be minimal; these values should be used for qualitative comparisons between realizations and scenarios, rather than quantitative estimates of true particle velocities.

In Figure 3-17 through Figure 3-20, the color of the diamond indicates the particle velocity; the dots are located at the midpoint of the step, e.g., $x_{\text{midpt}} = \frac{1}{2}[x(t_i) + x(t_{i+1})]$, $y_{\text{midpt}} = \frac{1}{2}[y(t_i) + y(t_{i+1})]$. In the no-mining case (Figure 3-17), the highest particle velocities are in the southeastern portion of the particle swarm, corresponding to the high-transmissivity pathway (Hart et al., 2009) exiting the LWB at approximately X=614,750 m (Figure 3-15). The effects of the full-mining scenario are clearly evident in the left portions of Figure 3-18 through Figure 3-20; high particle velocities (yellows and oranges) are found along the margin of the mining-affected areas, where particles enter the increased-transmissivity region. For comparison, in the partial-mining scenario the particles are relatively slowed down and more evenly distributed in the region between the release point and the southern WIPP LWB.

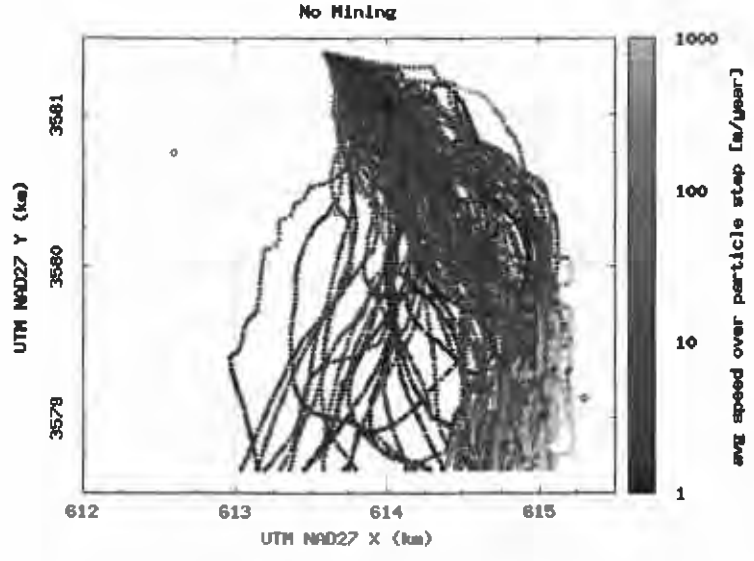

Figure 3-17.Particle speeds for non-mining scenario computed from DTRKMF results

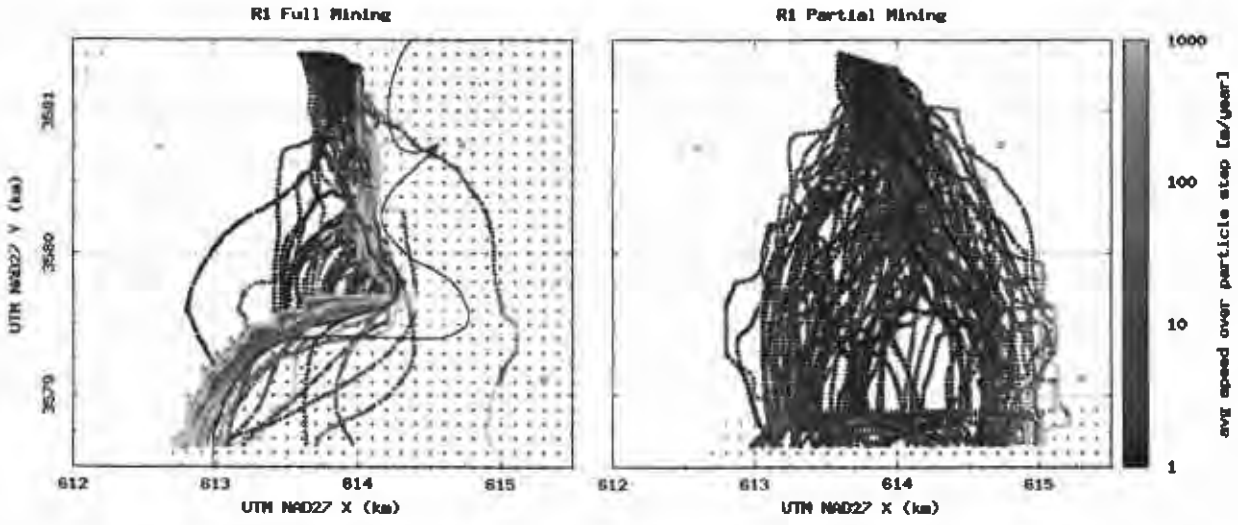

Figure 3-18. Particle speeds for R1, computed from DTRKMF results

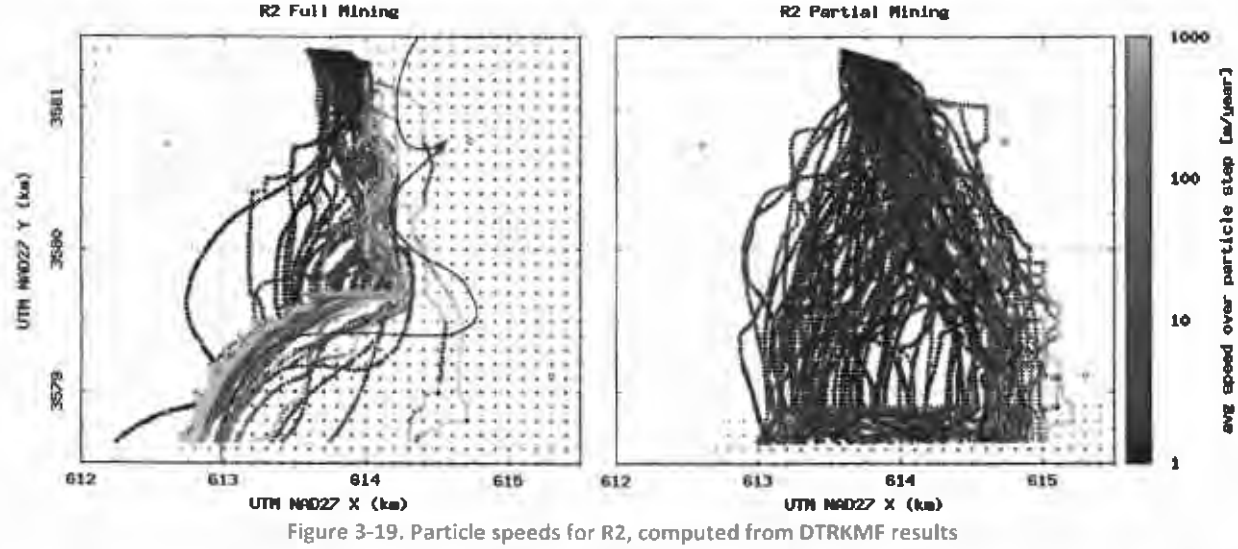

Figure 3-19. Particle speeds for R2, computed from DTRKMF results

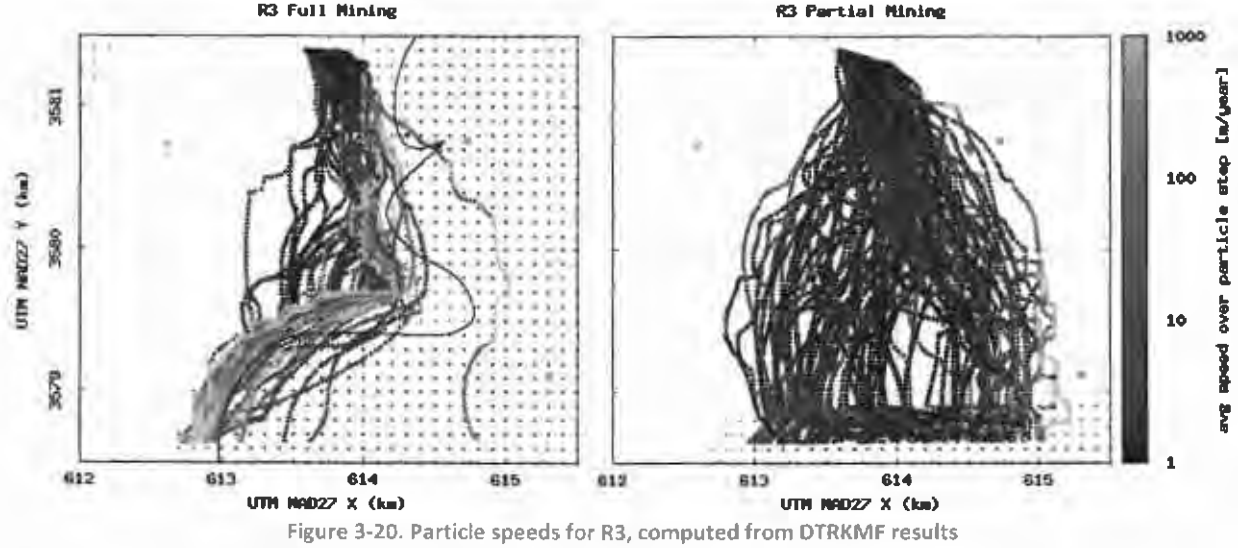

Figure 3-20. Particle speeds for R3, computed from DTRKMF results

3.5 Particle Tracking Discussion

Correlation analysis for the PABC-2009 particle tracking calculations shows that travel time and the random mining factor are weakly correlated for the partial- (Figure 3-21) or full-mining (Figure 3-22) scenarios. This is similar to what was observed for the PABC-2004 (Lowry and Kanney, 2005). The high scatter in Figure 3-21 and Figure 3-22 indicates that the transmissivity spatial distribution plays the more significant role in determining the travel time than the mining factor does. See Appendix 1 (Figure A1-9) for a cross-sectional comparison of transmissivity for each mining type, showing that the variability in the transmissivity due to calibration is on the same order as that due to mining for a single realization. The mining factor plays a weak but slightly larger role in explaining the observed variance for the partial-mining realizations (Figure 3-22) than the full-mining realizations (Figure 3-21), based on the larger (but still very small) R^2 value for the straight-line fit of $\log_{10}$ travel times to mining factors.

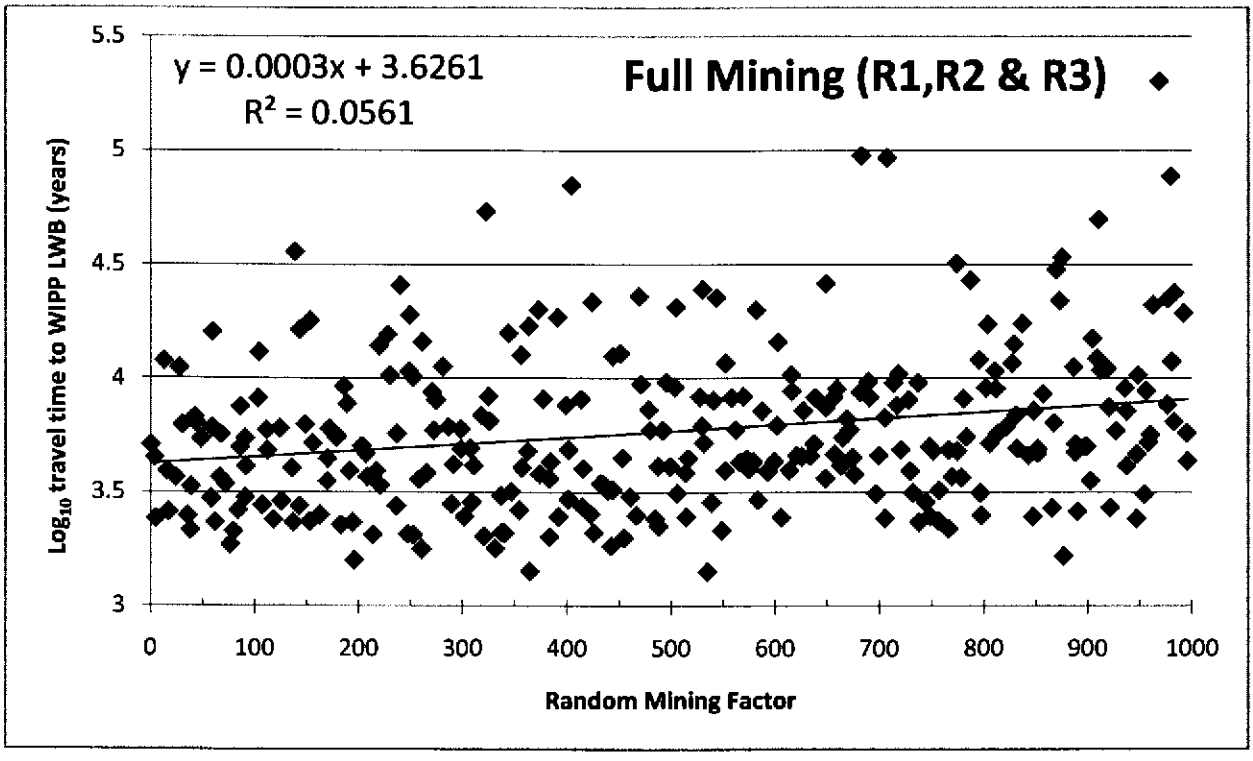

Figure 3-21. Mining factor and travel time to WIPP LWB for full-mining scenario (all replicates)

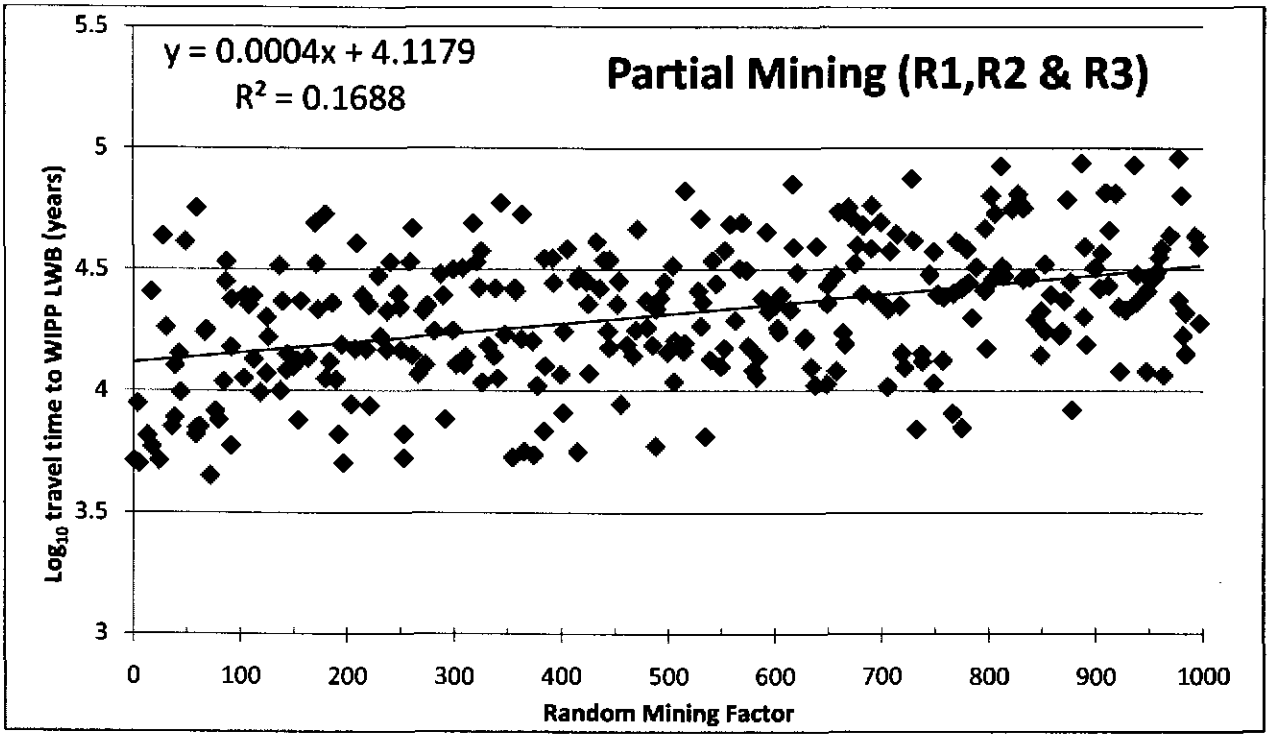

Figure 3-22. Mining factor and travel time to WIPP LWB for partial-mining scenario (all replicates)

4 Radionuclide Transport Calculations

4.1 Background and Theoretical Overview

The Culebra radionuclide transport calculations are performed using SECOTP2D, a two-dimensional, dual-porosity solute transport code developed to simulate radionuclide transport through fractured porous media (Salari and Blaine, 1996; Ramsey, 1997). This section describes the process for incorporating the MODFLOW flow-fields into the Culebra transport model, an overview of the theory underlying the SECOTP2D code, and a description of the parameters used in the Culebra transport calculations.

4.1.1 Relationship Between Flow and Transport Modeling Domains

The spatial domain used for the transport calculations, in relation to the groundwater modeling domain and the LWB, is shown in Figure 3-2. The UTM coordinates of the extent of the transport domain are given in Table 3-1.

The domain used in the transport calculations is a subregion of that used for the groundwater flow calculations. This subregion is approximately 7.5 km by 5.4 km, aligned with the principal compass directions and the principal directions of the groundwater flow domain. The transport domain extends beyond the boundaries of the WIPP LWB in the east-west direction (approximately 250 m to the west and approximately 750 m to the east). Since the undisturbed groundwater flow direction is generally north to south, the transport domain is shifted so that it extends from a point midway between the center of the waste panels and the northern LWB to approximately 1 km beyond the southern edge of the LWB. The transport calculations use a uniform computational grid composed of square 50 m cells, created by subdividing MODFLOW flow model cells into four equal-sized cells.

4.1.2 Flow-Field Extraction

Several issues need to be addressed when using the results of the MODFLOW groundwater flow calculations as input to the SECOTP2D Culebra transport calculations:

1. The MODFLOW code outputs the volumetric flux [m^3/s] across the face of each cell in the computational mesh, while the SECOTP2D code suite expects the flow-field in terms of the Darcy or specific discharge [m/s] at cell faces.
2. The computational domain used in the transport calculations is a sub-region of that used in the groundwater flow calculations.
3. The origin of the two-dimensional MODFLOW computational mesh is the northwest corner of the groundwater flow modeling domain (i.e., spreadsheet convention), while the origin of the SECOTP2D computational mesh is the southwest corner of the transport model domain (i.e., Cartesian coordinate convention).
4. The sense of coordinate system used by MODFLOW also differs from that used by SECOTP2D; the positive y-direction in MODFLOW is opposite (increasing to the south) that of SECOTP2D (increasing to the north) and thus the flux in the y-direction has different sense in the two systems.

5. MODFLOW defines the x-direction flux for a given cell index as the flux through that cell's right face while SECOTP2D defines it as the flux through the neighboring cell's left face.

The specific discharge or Darcy velocity [m/s] across the cell face is computed by dividing the volumetric flux across the cell face by its area (see Figure 4-1);

$$u = \frac{Q_x}{A_x} = \frac{Q_x}{\Delta y \cdot \Delta z} \tag{3}$$

$$v = \frac{Q_y}{A_y} = \frac{Q_y}{\Delta x \cdot \Delta z} \tag{4}$$

where u, v are the specific discharge values (Darcy velocity) across the cell face in the x- and y-directions, Q_x, Q_y are the volumetric fluxes [m^3/s] across the cell faces, and A_x, A_y are areas of the cell faces perpendicular to the x- and y-directions [m^2], respectively.

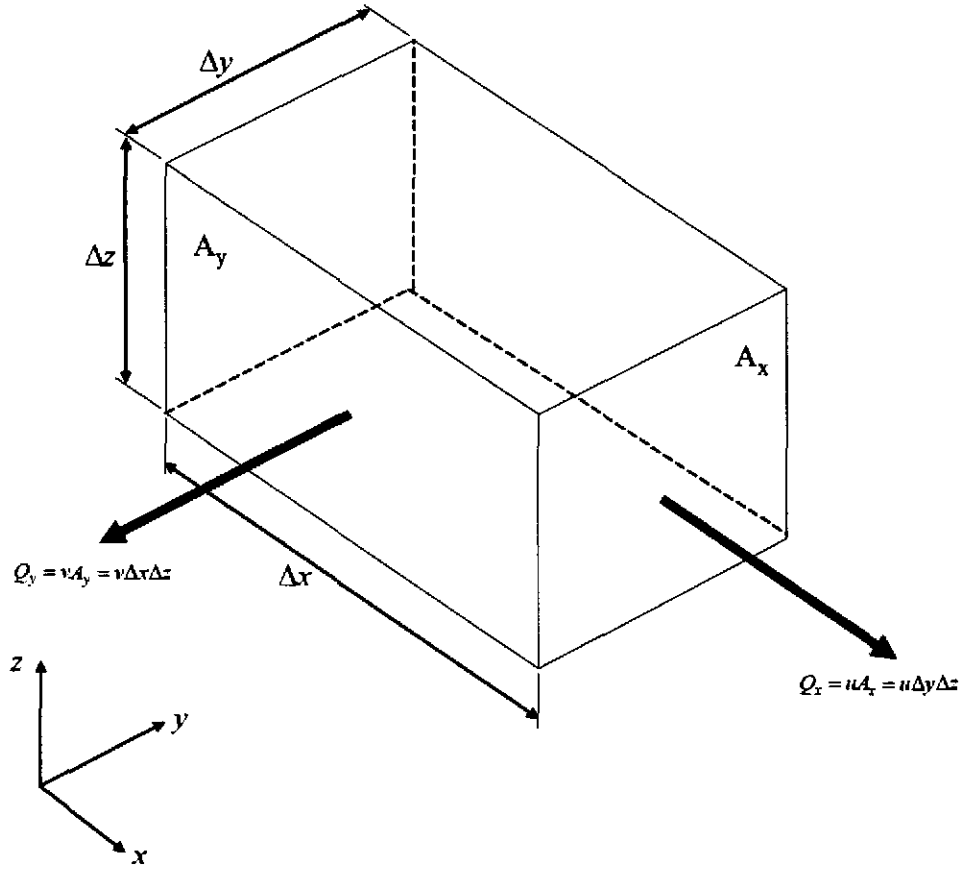

Figure 4-1. MODFLOW volumetric flux and Darcy velocity; A_y is perpendicular to the arrow pointing left; A_x is perpendicular to the arrow pointing right

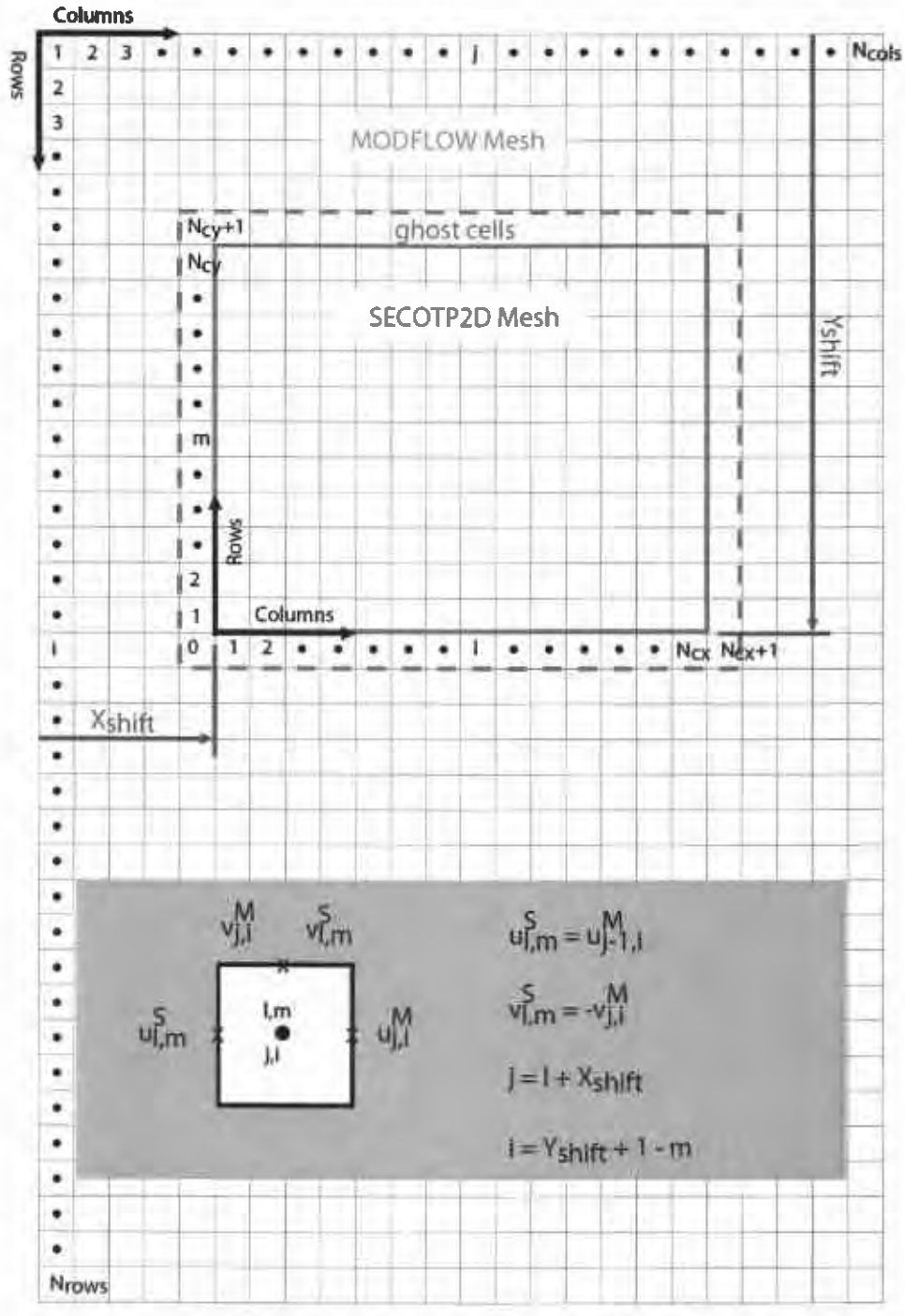

Figure 4-2. Velocity transfer between MODFLOW and SECOTP2D meshes

The remaining issues can be dealt with as outlined below and illustrated in Figure 4-2. Let (j, i) be the x-direction and y-direction indices of a cell in the MODFLOW mesh with $j = 1, \ldots, N_{\text{cols}}$ and $i = 1, \ldots, N_{\text{rows}}$. Let (l, m) be the indices of the same cell referenced to the SECOTP2D mesh with $l = 0, \ldots, N_{cx} + 1$ and $m = 0, \ldots, N_{cy} + 1$. Note that the SECOTP2D mesh uses a border of ghost cells

that extend one cell beyond the boundaries of the transport domain in order to implement boundary conditions.

Since the positive *y*-direction of the two meshes are opposite in sense, we must have

$$v^S_{l,m} = -v^M_{i,j} \tag{5}$$

where the superscript S denotes the SECOTP2D velocity and M denotes the MODFLOW velocity. The difference in conventions regarding which face to associate with a given cell can be written as

$$u^S_{l,m} = u^M_{j-1,i} \tag{6}$$

Let X_{shift} be the x-direction distance (in number of cells) between the origin of the MODFLOW mesh and the SECOTP2D. Let Y_{shift} represent the corresponding distance in the y-direction. The MODFLOW cell indices corresponding to the cell (l, m) in the SECOTP2D mesh are then given by

$$j = l + X_{\text{shift}} \tag{7}$$

$$i = Y_{\text{shift}} + 1 - m \tag{8}$$

The rules specified by equations 5 and 8 may be summarized by the following pseudo-code algorithm:

for $l = 1$ to N_{cx} do
  for $m = 1$ to N_{cy} do
    $j \leftarrow l + X_{\text{shift}}$
    $i \leftarrow Y_{\text{shift}} + 1 - m$
    $u^S_{l,m} \leftarrow u^M_{j-1,i}$
    $v^S_{l,m} \leftarrow -v^M_{i,j}$
  end for
end for

4.1.3 VTRAN2 Output Summary

Figure 4-3 shows ensemble average and standard deviation distributions for Darcy velocity (from VTRAN output). Each figure is either an average or standard deviation across 300 realizations (3 replicates × 100 realizations). The WIPP LWB, panel outline, and release locations are indicated on each of the six plots.

The top two plots in Figure 4-3 show the average magnitude of $\log_{10}$ Darcy velocity (color plot) and scaled vectors (only one of every five is plotted for clarity) indicating direction. Although color scales are consistent in each row, arrow sizes are not. The high-transmissivity pathway observed during the SNL-14 pumping test (the north-south feature located in southern half of the domain approximately following column 95) is also apparent in both the full- and partial-mining scenarios, as it was in the unmined MODFLOW scenarios (Hart et al., 2009). The edges of the areas affected by potash mining can be seen in the color plots. In the full-mining case this appears as the blue irregular shape occupying the west half of the transport model domain and in the partial-mining case the the edge of the affects of

mining can be seen just inside the WIPP LWB (see Section 3.3.2 for discussion and illustration of mining-affected areas).

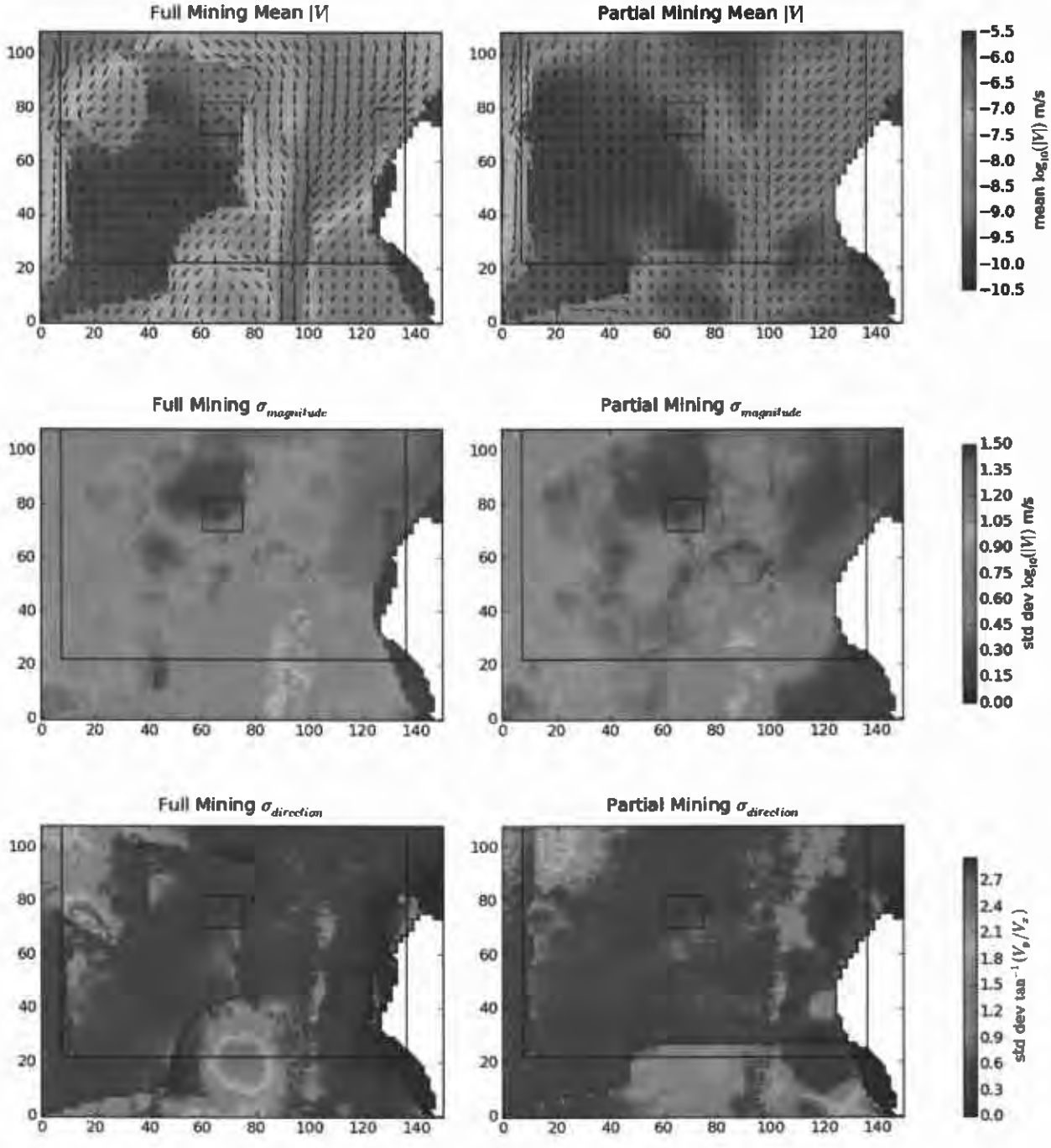

Figure 4-3. Ensemble average and standard deviation of Darcy flow velocity magnitude $|V|$ and direction V_{dir} from VTRAN2 (each figure is constructed from 300 realizations); SECOTP2D cell-based coordinates. Outer black line is the LWB, small black box outlines the WIPP panels, with the yellow star at the release point (C-2737).

The middle two plots in Figure 4-3 show the variability in the magnitude of the $\log_{10}$ Darcy velocity. The highest variability (red to yellow) is associated with the southern part of the high-T pathway, at or south

of where the pathway crosses the WIPP LWB. The high-T pathway is the estimated distribution of T associated with the response observed due to pumping SNL-14 (Hart et al., 2009). The bottom two plots show variability in the direction of the Darcy velocity. In the full-mining case, there is high variability (red) in the direction at the WIPP LWB west of the high-T pathway and along the northwest boundary of the non-mining area (west and north of the release point). Both of these regions of high direction variance are in areas that are affected by potash mining located immediately next to non-mining areas. Low variability (blues) in both the magnitude and direction of the Darcy velocity across all the realizations is found inside the non-mining areas.

Example VTRAN2 output for a single MODFLOW realization (r440) is shown in the six plots in Appendix 1 (Figure A1-11). R1 and R3 have relatively high mining factors (663.4 and 902.6, respectively), while R2 has a moderate mining factor (77.07).

4.1.4 Solute Transport Modeling

The SECOTP2D code assumes parallel-plate fracturing where fluid flow is restricted to the advective continuum (fractures) and mass is transferred between the advective and diffusive (matrix) continua via molecular diffusion. The dual-porosity conceptualization is illustrated in Figure 4-4. Retardation is permitted in both the advective and diffusive domains assuming linear equilibrium isotherms. Radioactive decay is accounted for through the use of multiple straight decay chains.

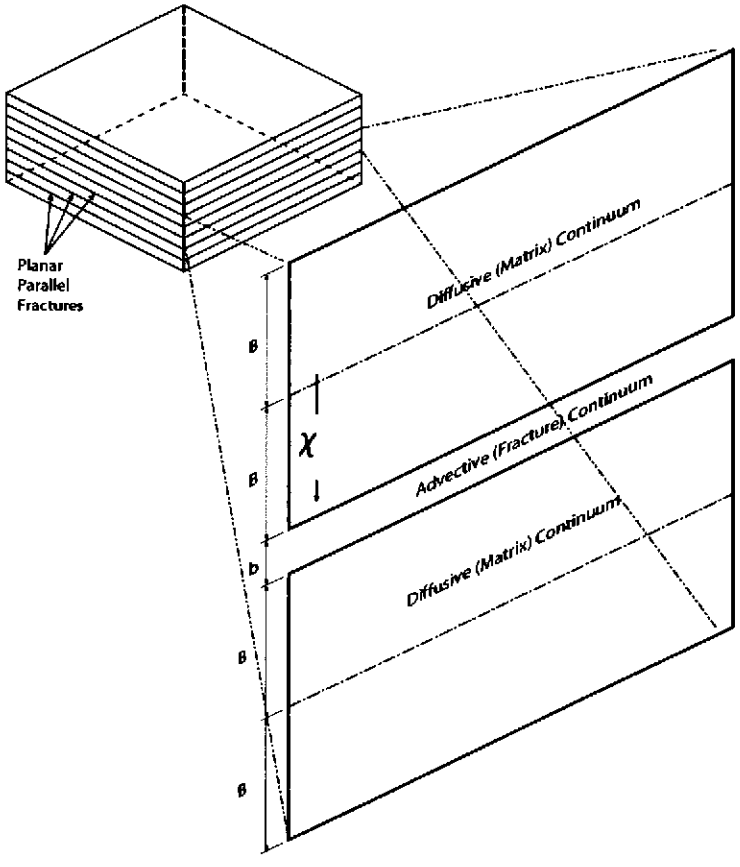

Figure 4-4. Dual-Porosity Conceptual Model

SECOTP2D solves the following partial differential equation (PDE) for radionuclide transport in the advective (i.e., fracture) continuum:

$$\phi R_\ell \frac{\partial C_\ell}{\partial t} = \nabla \cdot (\phi \boldsymbol{D}_\ell \nabla C_\ell - \boldsymbol{V} C_\ell) - \phi R_\ell \lambda_\ell C_\ell + \phi R_{\ell-1} \lambda_{\ell-1} C_{\ell-1} + Q_\ell + \Gamma_\ell \quad (9)$$

where $\ell = 1, \cdots, N_s$ is a species index (N_s is the number of species), C_ℓ is the unknown concentration of the ℓ^{th} radionuclide in the advective continuum [kg/m^3], $\boldsymbol{V}$ is the specific discharge vector [m/s], $\boldsymbol{D}_\ell$ is the second-rank hydrodynamic dispersion tensor [m^2/s], ϕ is the dimensionless advective porosity, R_ℓ is the dimensionless retardation coefficient, λ_ℓ is the radioactive species decay constant [1/s], Q_ℓ is the specific injection rate [kg/(m^3·s)], and Γ_ℓ is the mass transfer coefficient between the advective and diffusive continua per unit volume [kg/(m^3·s)]. Only the dependent concentration variables (C_ℓ) and the mass transfer coefficient (Γ_ℓ) are both spatially and temporally variable. Flow velocities (the vector $\boldsymbol{V}$ and its components u and v) are spatially variable, but steady state. All other parameters in the equations are constant in space and time for each realization.

The concentration C_ℓ is defined as the mass of the ℓ^{th} radionuclide per unit volume of pore fluid. The advective porosity ϕ is defined as the ratio of the advective pore volume to the total volume. Similarly, the specific injection rate Q_ℓ is defined as the rate of mass injected per unit bulk volume per time. Terms in equation 9 involving $\ell - 1$ are omitted for species that are parents of their respective decay chains ($\ell = 1$). The advective transport equation is linear in C_ℓ and is solved simultaneously for all N_s species in a given decay chain.

The vector flow-field $\boldsymbol{V}$ is assumed to be independent of the solute concentration. The flow-field is obtained from MODFLOW and is scaled by a random factor between 1 and 2.25 to account for the potential impact of climate change (Corbet and Swift, 1996).

The product $\phi \boldsymbol{D}_\ell$ is defined as

$$\phi \boldsymbol{D}_\ell = \frac{1}{|\boldsymbol{V}|} \begin{bmatrix} u & -v \\ v & u \end{bmatrix} \begin{bmatrix} \alpha_L & 0 \\ 0 & \alpha_T \end{bmatrix} \begin{bmatrix} u & v \\ v & u \end{bmatrix} + \phi \tau D_\ell^* \quad (10)$$

where α_L and α_T are the longitudinal and transverse dispersivities of the advective continuum [m], u and v are the scalar x- and y-components of the specific discharge vector [m/s], D_ℓ^* is the free water molecular diffusion coefficient [m^2/s], and τ is the dimensionless advective tortuosity defined as the ratio of the fluid particle flow path length to the length of the porous medium. Note that WIPP PA takes no direct credit for hydrodynamic dispersion in Culebra transport calculations; only mixing due to molecular diffusion is allowed (i.e., $\alpha_L = \alpha_T = 0$ in equation 10 and therefore $\phi \boldsymbol{D}_\ell = \phi \tau D_\ell^*$). WIPP PA treats the free liquid molecular diffusion coefficient as a function of both radionuclide species and oxidation state.

The retardation coefficient R_ℓ is defined by:

$$R_\ell = 1 + \rho_s K_d^\ell \frac{1 - \phi}{\phi} \quad (11)$$

where ρ_s is the Culebra dolomite grain density [kg/m^3] and K_d^ℓ is the distribution coefficient of the ℓ^{th} radionuclide [m^3/kg], equation 11 completely describes the linear isotherm for radionuclide sorption to the Culebra.

SECOTP2D solves the following one-dimensional PDE for diffusional radionuclide transport in the matrix continuum:

$$\phi' R'_\ell \frac{\partial C'_\ell}{\partial t} - \frac{\partial}{\partial \chi}\left(\phi' D'_\ell \frac{\partial C'_\ell}{\partial \chi}\right) = -\phi' R'_\ell \lambda_\ell C'_\ell + \phi' R'_{\ell-1} \lambda_{\ell-1} C'_{\ell-1} \tag{12}$$

where C'_ℓ is the unknown concentration of the ℓ^{th} radionuclide in the diffusive continuum [kg/m^3], χ is the spatial coordinate originating from the symmetry line of a matrix block (as shown in Figure 4-4), and D'_ℓ is the matrix diffusion coefficient. The matrix diffusion coefficient is defined as:

$$D'_\ell = \tau' D^*_\ell \tag{13}$$

where τ' is the matrix tortuosity. All other symbols in equation 12 for diffusive transport have analogous meaning as those in equation 9 for advective transport except that the prime denotes diffusive-continuum properties.

The governing equations for the advective (9) and diffusive (12) continua are coupled through the mass transfer term, Γ_ℓ. Applying Fick's law at the interface between the two continua results in the mass-transfer equation:

$$\Gamma_\ell = -\frac{2\phi}{b}\left(\phi' D'_\ell \frac{\partial C'_\ell}{\partial \chi}\bigg|_{\chi=B}\right) \tag{14}$$

where B is the matrix half-block length [m], b is the fracture aperture [m] (see Figure 4-4), the term in parentheses represents the mass flux per unit area of contact between the advective and diffusive continua. The term $2\phi/b$ represents the specific surface area (ratio of surface area to bulk volume) of the coupled system. In the parallel-plate formulation used in SECOTP2D, the fracture aperture is defined in terms of advective porosity and matrix half-block length by:

$$b = \frac{\phi B}{1-\phi} \tag{15}$$

4.1.5 Model Parameters

The transport equations for the advective and diffusive continua described in Section 4.1.4 contain many parameters, which must be obtained from measurements, theoretical considerations, or expert judgment. In general, WIPP PA treats some process model parameters as deterministic and others as uncertain. Uncertain parameters are represented by probability distributions, and sampled values of uncertain parameters are used in a probabilistic (Monte Carlo) modeling approach to predict repository performance.

The parameters can be divided into physical parameters and chemical parameters. The physical parameters are generally properties of the porous Culebra material. The chemical parameters are

generally properties of the radionuclide species transported. Some chemical parameters are functions of the oxidation state as well as species.

WIPP PA treats the following Culebra physical transport parameters as deterministic:

1. advective continuum longitudinal and transverse dispersivity (α_L, α_T);
2. fracture tortuosity (τ);
3. matrix tortuosity (τ');
4. skin resistance factor; and
5. Culebra material grain density (ρ_s).

The WIPP PA Parameter Database (PAPDB) designations for these parameters, along with the values used in this analysis, are shown in Table 4-1; these parameter values have not changed since the CCA. Table 4-1 shows that no credit is taken for dispersion in the transport of radionuclides in the Culebra ($\alpha_L = \alpha_T = 0$).

Table 4-1. Deterministic physical transport parameters

Model Parameter	MATERIAL:PROPERTY	Value	Units
Longitudinal dispersivity	CULEBRA:DISP_L	0	m
Transverse dispersivity	CULEBRA:DISPT_L	0	m
Fracture tortuosity	CULEBRA:FTORT	1.0	-
Matrix tortuosity	CULEBRA:DTORT	0.11	-
Skin resistance	CULEBRA:SKIN_RES	0	-
Material grain density	CULEBRA:DNSGRAIN	2820	kg/m^3

WIPP PA treats the following Culebra physical transport parameters as subjectively uncertain:

1. advective (fracture) porosity (ϕ);
2. diffusive (matrix) porosity (ϕ');
3. matrix half-block length (B);
4. climate index;
5. flow-field index; and
6. mining factor.

The PAPDB designations for these parameters, along with the probability distributions used in this analysis are shown in Table 4-2. Note that these parameter distributions have not changed since the CCA. The sampled values for any given analysis will depend upon the random seed used in the sampling algorithm.

Potential climatic changes are simulated as leading to an increase in hydraulic gradients in the Culebra. This is implemented as a uniform increase in the steady-state velocity fields by the multiplier CLIMTIDX at the beginning of the simulation (Corbet and Swift, 1996). Calibrated MODFLOW realizations and mining factors are mapped from one to the other (a different mapping for each replicate) using the integer index TRANS_IDX.

See Appendix 2 (Table A2-3) for sampled values of APOROS, DPOROS, HMBLKLT, and CLIMTIDX used in analysis, and see Appendix 1 (Table A1-12) for values of MINP_FAC and TRANS_IDX used in the analysis.

Table 4-2. Uncertain physical parameters

Model Parameter	MATERIAL:PROPERTY	Units	Distribution	Range	Median
Advective porosity	CULEBRA:APOROS	-	log-uniform	[1.00E-4,1.00E-2]	1.000E-3
Diffusive porosity	CULEBRA:DPOROS	-	cumulative	[1.00E-1,2.50E-1]	1.600E-1
Matrix half-block length	CULEBRA:HMBLKLT	m	uniform	[5.00E-2,5.00E-1]	2.750E-1
Climate index	GLOBAL:CLIMTIDX	-	cumulative	[1.00E+0,2.25E+0]	1.170E+0
Flow-field index	GLOBAL:TRANSIDX	-	uniform	[0.00E+0,1.00E+0]	5.000E-1
Mining factor	CULEBRA:MINP_FAC	-	uniform	[1.00E+0,1.00E+3]	5.005E+2

WIPP PA treats the following radionuclide chemical parameters as deterministic:

1. radionuclide atomic weight;
2. radionuclide half-life; and
3. radionuclide free liquid molecular diffusion coefficient (D_ℓ^*).

The PAPDB designations for these parameters, along with the values used in this analysis, are shown in Table 4-3. Note that these parameter values have not changed since the CCA.

Table 4-3. Deterministic chemical parameters

Model Parameter	MATERIAL:PROPERTY	Value	Units
Atomic Weight[1]			
^{241}Am	AM241:ATWEIGHT	2.41057E-01	kg/mole
^{239}Pu	PU239:ATWEIGHT	2.39052E-01	kg/mole
^{230}Th	TH230:ATWEIGHT	2.30033E-01	kg/mole
^{234}U	U234:ATWEIGHT	2.34041E-01	kg/mole
Half-life ($t_{1/2}$)[1,2]			
^{241}Am	AM241:HALFLIFE	1.36400E+10	s
^{239}Pu	PU239:HALFLIFE	7.59400E+11	s
^{230}Th	TH230:HALFLIFE	2.43000E+12	s
^{234}U	U234:HALFLIFE	7.71600E+12	s
Molecular diffusion coefficient[3]			
Am(III)	AM+3:MD0	3.00000E-10	m^2/s
Pu(III)	PU+3:MD0	3.00000E-10	m^2/s
Pu(IV)	PU+4:MD0	1.53000E-10	m^2/s
Th(IV)	TH+4:MD0	1.53000E-10	m^2/s
U(IV)	U+4:MD0	1.53000E-10	m^2/s
U(VI)	U+6:MD0	4.26000E-10	m^2/s

1. Atomic weight and half-life used to calculate specific activity
2. $\lambda_\ell = (\ln 2)/t_{1/2}$
3. Free-liquid diffusion coefficient is a function of species and oxidation state

WIPP PA treats the following radionuclide chemical parameters as subjectively uncertain:

1. oxidation state; and
2. matrix distribution coefficient (K_d^ℓ).

The PAPDB designations for these parameters, along with the probability distributions used in this analysis, are shown in Table 4-4. Note that the lower bounds of the K_d ranges for constituents modeled (except U(VI)) were lowered (Clayton, 2009b), as requested by the EPA in the third 2009 completeness letter (Kelly, 2009). The oxidation states and upper limits on the K_d parameter distributions have not changed since the CCA. The sampled values for any given analysis will depend upon the random seed used in the sampling algorithm.

Table 4-4. Uncertain chemical parameters

Model Parameter	MATERIAL:PROPERTY	Units	Distribution	Range	Median
Oxidation state index	GLOBAL:OXSTAT	-	uniform	[0.00E+0, 1.00E+0]	5.00E-1
Matrix distribution coefficient					
Am(III)	AM+3:MKD_AM	m^3/kg	log-uniform	[5.00E-3, 4.00E-1]	4.50E-2
Pu(III)	PU+3:MKD_PU	m^3/kg	log-uniform	[5.00E-3, 4.00E-1]	4.50E-2
Pu(IV)	PU+4:MKD_PU	m^3/kg	log-uniform	[5.00E-4, 1.00E+1]	7.10E-2
Th(IV)	TH+4:MKD_TH	m^3/kg	log-uniform	[5.00E-4, 1.00E+1]	7.10E-2
U(IV)	U+4:MKD_U	m^3/kg	log-uniform	[5.00E-4, 1.00E+1]	7.10E-2
U(VI)	U+6:MKD_U	m^3/kg	log-uniform	[3.00E-5, 2.00E-2]	7.70E-4

4.2 Transport Results

Radionuclide transport calculations for the Culebra were performed with the SECOTP2D code suite as described in Section 4.1. All calculations were performed on the WIPP Alpha Cluster under formal run control procedures (Long, 2010).

The prediction of interest in the Culebra transport calculations is the cumulative release of radionuclides at the LWB during the 10,000-year regulatory period. In each transport simulation, 1 kg of each of four radionuclides is released at the center of the waste panel area during the first 50 years after repository closure. This unit mass release at the initial simulation time is subsequently scaled and time shifted in the CCDFGF analysis (Camphouse, 2010). The radionuclides transported in the Culebra are ^{241}Am, ^{234}U, ^{230}Th and ^{239}Pu. Pu may be present in either the Pu(III) or Pu(IV) oxidation state; U may be present as U(IV) or U(VI), depending on the values of OXSTAT; mixed high- and low-oxidation states do not occur.

Transport calculations were performed for both full-mining and partial-mining scenarios. The partial-mining scenario assumes potash is only mined outside the LWB, while full mining assumes that all reserves are exploited both inside and outside the LWB. The effect of mining enters the transport calculations through the Culebra flow-field computed using MODFLOW (see Section 3).

A total of 300 realizations (three replicates of 100 vectors each) were required for both full- and partial-mining conditions; 600 Culebra transport simulations were performed. Along with the input files referenced above, the output (CAMDAT database) files from these simulations are stored in CMS library LIBPABC09_ST2D, class PABC09-0 on the WIPP PA Alpha Cluster. The naming convention for the CAMDAT database files is: ST2D3_PABC09_R*r*_M*m*_V*vvv*.CDB, where $r \in \{1,2,3\}$, $m \in \{F,P\}$, and $vvv \in \{001,002,\ldots,100\}$. See (Long, 2010) for a complete description of the run control procedures used to perform the Culebra transport calculations. In each transport simulation, 1 kg of each of four radionuclides (^{241}Am, ^{234}U, ^{230}Th, and ^{239}Pu) is released in the Culebra at the location of observation well C-2737 (the center of the WIPP waste panels). Transport of the ^{230}Th daughter product of ^{234}U decay is calculated and tracked as a separate species. In the following discussion, ^{230}Th will refer to the ^{234}U daughter product and ^{230}ThA will refer to that released at the center of the waste panel area.

4.2.1 Radionuclide Transport Under Partial-Mining Conditions

Under partial-mining conditions, only ^{234}U and its daughter product ^{230}Th had a significant number of vectors (37 and 21, respectively) where radionuclides were transported to the LWB during the course of the 10,000-year simulation. Only five vectors of ^{239}Pu and ^{230}ThA reached a 10^{-9} kg cumulative release threshold (Table 4-5), and ^{241}Am had no vectors surpassing a 10^{-9} kg criterion. The 10^{-9} kg cumulative release reporting or significance threshold is somewhat arbitrary, but is chosen to compare to results reported previously in PABC-2004 (Lowry and Kanney, 2005).

Table 4-5. Number of vectors exceeding the 10^{-9} kg cumulative release threshold during the 10,000 year simulation

	partial			full		
	R1	**R2**	**R3**	**R1**	**R2**	**R3**
^{241}Am	0	0	0	8	10	3
^{239}Pu	3	1	1	20	27	22
^{234}U	11	14	12	48	50	47
^{230}Th	5	10	6	36	38	42
^{230}ThA	2	3	0	21	31	29

The total numbers of vectors with releases greater than the 10^{-9} kg criterion, tabulated in Table 4-5, are shown in Figure 4-5 as histograms of log cumulative releases. The individual histograms in Figure 4-5 are arranged similar to the rows and columns in Table 4-5 through Table 4-8. The histograms give more information about the distribution of vectors with cumulative releases greater than the 10^{-9} kg criterion, rather than just the total number of them.

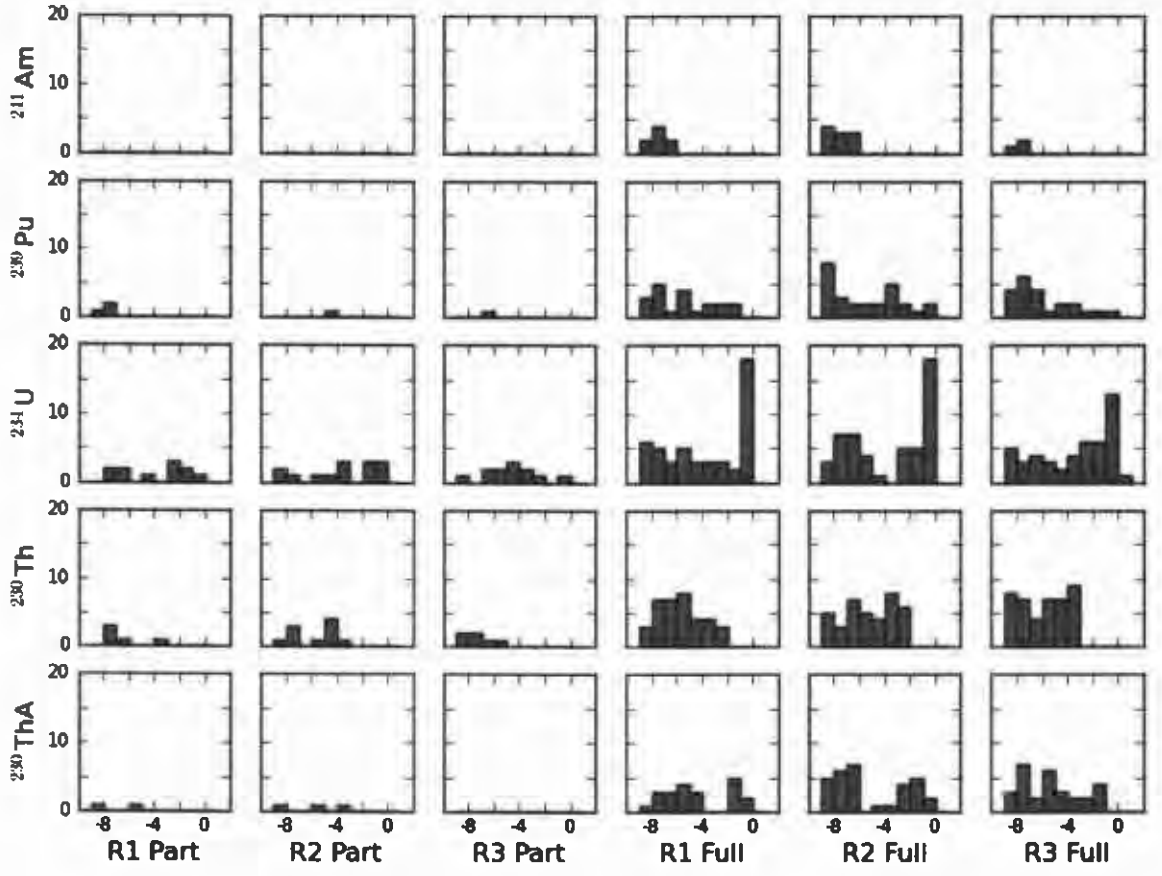

Figure 4-5. Histograms showing distribution of cumulative releases greater than 10^{-9} kg, each *x*-axis is $\log_{10}$ cumulative release (kg), each *y*-axis is number of vectors per bin (bins are one log cycle wide).

Table 4-6 shows the maximum cumulative release predicted for each group of 100 vectors, including all vectors (not just those greater than the 10^{-9} kg criterion). These values correspond to the rightmost bar in the histograms shown in Figure 4-5. The results for ^{241}Am are very low and are likely caused by numerical dispersion, as the concentrations reported are so low as to be physically unrealistic. The maximum masses reported reaching the WIPP LWB are smaller than can validly be simulated using SECOTP2D and can therefore be considered to be effectively zero.

Table 4-6. Maximum cumulative release (kg) within each group of 100 vectors at 10,000 years

	partial			full		
	R1	R2	R3	R1	R2	R3
^{241}Am	4.6e-27	7.4e-20	4.3e-23	1.1e-07	7.5e-07#	8.6e-08
^{239}Pu	3.9e-08	3.3e-05	5.7e-07	3.3e-02	2.5e-01#	1.1e-01
^{234}U	7.1e-01	7.5e-01	2.5e-01	9.9e-01	9.9e-01	1.0e+00#
^{230}Th	9.9e-04	1.0e-04	1.9e-06	4.2e-03#	2.6e-03	9.2e-04
^{230}ThA	8.5e-06	9.5e-04	2.6e-12	2.1e-01#	1.8e-01	6.6e-02

# Indicates the largest maximum release for each radionuclide

The identities of the vectors that produced the largest cumulative releases in Table 4-6 are listed in Table 4-7. In R1, the highest releases of ^{234}U and both ^{230}Th are from V098. Similarly, in R2 and R3, the same vector that had the highest release of ^{234}U also had the highest release of ^{230}Th.

Table 4-7. Vector number corresponding to maximum cumulative release to WIPP LWB over 10,000 years (see Table 4-6)

	partial			full		
	R1	**R2**	**R3**	**R1**	**R2**	**R3**
^{241}Am	V018	V099	V053	V033	V099#	V057
^{239}Pu	V071	V050	V040	V100	V050#	V004
^{234}U	V098	V033	V036	V098	V088	V036#
^{230}Th	V098	V033	V036	V057#	V012	V084
^{230}ThA	V098	V045	V097	V098#	V045	V097

# Indicates the largest maximum release for each radionuclide

Table 4-8 shows the median cumulative releases for each set of 100 vectors (including those less than the 10^{-9} kg threshold, which were left out of Table 4-5 and Figure 4-5). The median concentrations for all radionuclides in Table 4-8 are so low as to be physically unrealistic (not just ^{241}Am), and are essentially zero. These near-zero median concentrations indicate that under partial-mining conditions at least half of the vectors have essentially no simulated transport to the LWB.

Table 4-8. Median concentration at 10,000 years across all 100 vectors for each species and mining scenario

	partial			full		
	R1	**R2**	**R3**	**R1**	**R2**	**R3**
^{241}Am	0.0e+00	0.0e+00	0.0e+00	1.3e-17	3.7e-17	3.6e-17
^{239}Pu	0.0e+00	0.0e+00	0.0e+00	3.5e-14	3.2e-15	3.4e-14
^{234}U	4.0e-39	0.0e+00	0.0e+00	3.2e-10	1.1e-09	2.0e-10
^{230}Th	2.7e-38	0.0e+00	1.9e-39	2.1e-11	4.5e-12	8.6e-13
^{230}ThA	0.0e+00	0.0e+00	0.0e+00	1.4e-13	1.2e-15	1.7e-14

4.2.2 Radionuclide Transport Under Full-Mining Conditions

Under full-mining conditions, all five simulated species had significant numbers of vectors transporting cumulative releases greater than the 10^{-9} kg threshold to the LWB during the course of the 10,000-year simulation (see the right half of Table 4-5). Releases greater than 10^{-9} kg were calculated for all simulated radionuclides for all three replicates.

The simulated constituents sorted by the numbers of vectors exceeding the 10^{-9} kg cumulative release threshold were ^{234}U, ^{230}Th, ^{230}ThA, ^{239}Pu, and ^{241}Am, in descending order. Nearly half of the ^{234}U vectors surpassed the 10^{-9} kg cumulative release threshold.

Figure 4-5 shows the distribution of these vectors with cumulative releases greater than the 10^{-9} kg threshold; there are more vectors plotted than in the partial-mining case, and they are on average at higher concentrations. Figure 4-5 shows that approximately 15 vectors from each full-mining replicate

transported at least 10% of the ^{234}U mass injected to the LWB in 10,000 years (tall bars in the ^{234}U row between 10^{-1} and 10^{0}).

Table 4-6 shows that the maximum full-mining ^{234}U releases (all three replicates) essentially transported the entire 1 kg of injected mass beyond the WIPP LWB. The identities of the vectors that produced the largest cumulative releases are listed in Table 4-7.

The five vectors with the largest cumulative releases to the LWB (all from the full-mining scenario) have their radionuclide distributions plotted at 10,000 years in Figure 4-6 through Figure 4-10, which all share the same $\log_{10}$ concentration color scale.

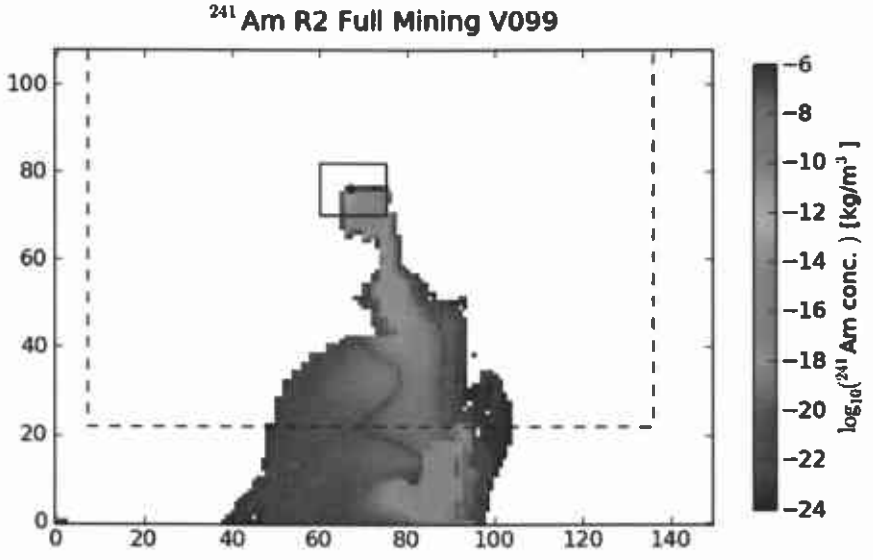

Figure 4-6. Log_{10}-distribution of ^{241}Am at 10,000 years for the vector with the largest cumulative release of ^{241}Am to the LWB (dashed line); SECOTP2D cell-based coordinates

Concentrations of ^{241}Am are relatively low compared to the other radionuclides, even for the vector with the largest cumulative release (see blues and greens in Figure 4-6). ^{234}U concentrations are shown to be highest south of the LWB (see darkest reds in Figure 4-8), consistent with the statement that nearly all the mass had been transported that far already.

The two ^{230}Th distributions are slightly different (they also correspond to different vectors and flow-fields). ^{230}ThA has higher concentrations near the release point (see Figure 4-10), while ^{230}Th is more evenly distributed because it is a decay product of ^{234}U (see Figure 4-9).

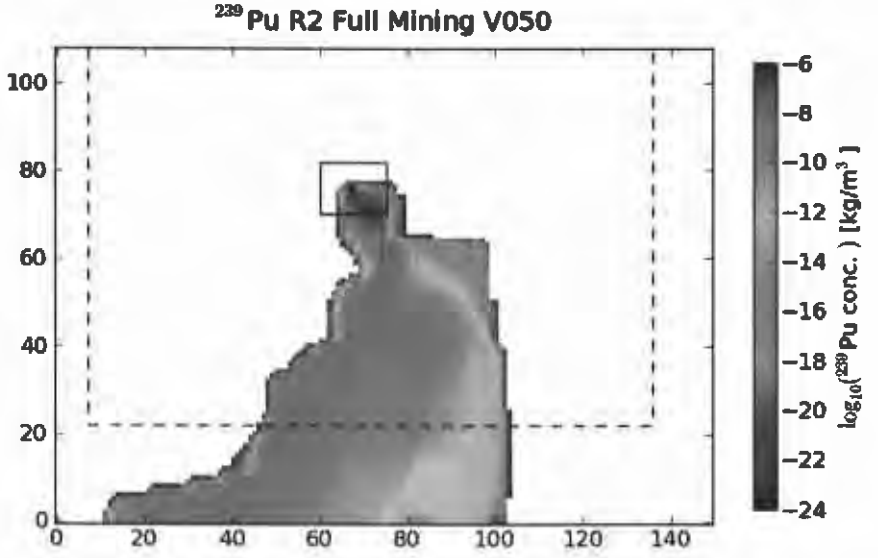

Figure 4-7. Log_{10}-distribution of ^{239}Pu at 10,000 years for the vector with the largest cumulative release of ^{239}Pu to the LWB (dashed line); SECOTP2D cell-based coordinates

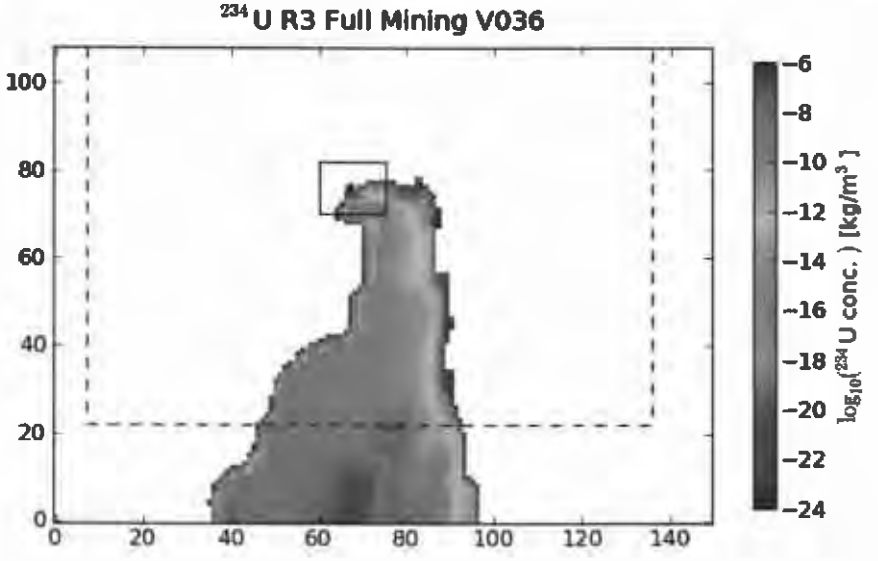

Figure 4-8. Log_{10}-distribution of ^{234}U at 10,000 years for the vector with the largest cumulative release of ^{234}U to the LWB (dashed line); SECOTP2D cell-based coordinates

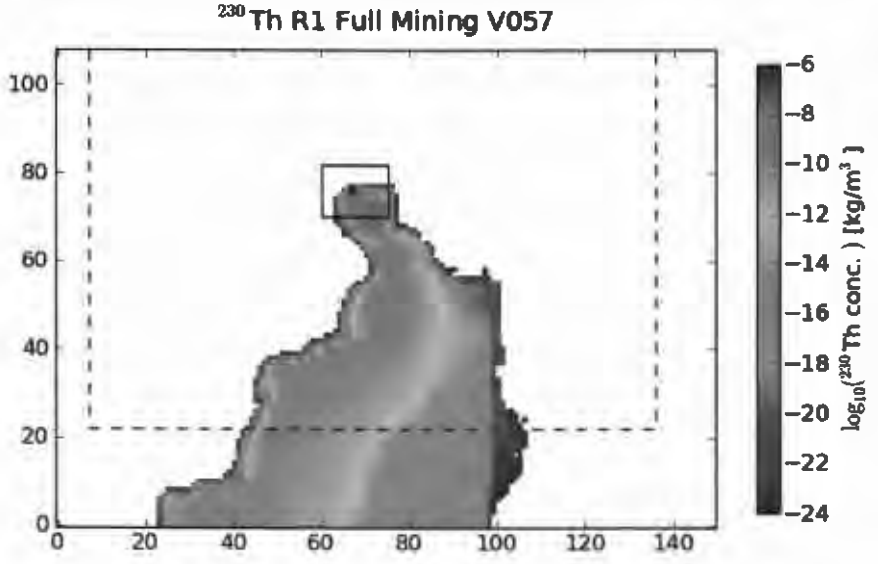

Figure 4-9. Log_{10}-distribution of ^{230}Th (daughter product) at 10,000 years for the vector with the largest cumulative release of ^{230}Th to the LWB (dashed line); SECOTP2D cell-based coordinates

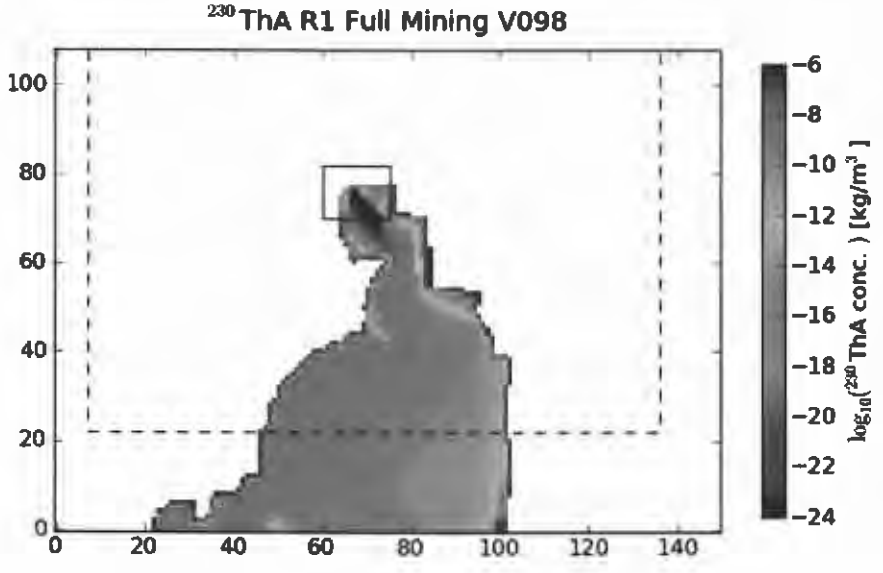

Figure 4-10. Log_{10}-distribution of ^{230}ThA (released ^{230}Th) at 10,000 years for the vector with the largest cumulative release of ^{230}ThA to the LWB (dashed line); SECOTP2D cell-based coordinates

4.3 Transport Summary

In summary, under partial-mining conditions, few vectors showed significant transport of radionuclides to the LWB during the 10,000-year simulation, while under full-mining conditions, a large portion of the vectors showed mass transport to the LWB. ^{234}U and its ^{230}Th daughter product had the largest cumulative masses transported to the WIPP LWB. Comparing these results to those for the PABC-2004, there is much more transport of radionuclides through the Culebra to the LWB. Similar to the PABC-

2004, ^{234}U and ^{230}Th have the largest number of vectors with significant releases to the WIPP LWB during the 10,000-year simulation.

These significant increases in radionuclide transport to the LWB can be attributed to three main changes since the PABC-2004:

1. **Speedup due to mining:** The definition of minable potash, obtained from the BLM (Cranston, 2009), has changed significantly, especially inside the LWB (see Figure 3-8). Minable potash ore is now located in close proximity (approximately 670 m) to the center of the WIPP disposal panels.
2. **Speedup due to decrease in radionuclide retardation:** The lower limits of the matrix distribution coefficient (K_d) distributions were decreased several orders of magnitude, as requested by EPA (Kelly, 2009). Lower limits of the K_d ranges for Am(III) and Pu(III) were reduced from 2.0E-2 to 5.0E-3 m^3/kg; lower limits for Pu(IV), Th(IV), and U(IV) were reduced from 7.0E-1 to 5.0E-4 m^3/kg; the lower limit for U(VI) was not changed. Lower K_d values result in smaller retardation coefficients (see equation 11 in Section 4.1.4), and were requested to reflect the increase in organic ligand content in the WIPP inventory.
3. **Speedup due to MODFLOW calibration:** The consistent presence of a high-transmissivity zone in the southeastern portion of the WIPP site in all the calibrated realizations of the MODFLOW model(Hart et al., 2009) creates a pathway for radionuclides to leave the LWB (see Figure 4-3). This feature was confirmed through the interpretation of pumping tests at SNL-14, and the data from this test were included as calibration targets (Hart et al., 2009). The presence of this pathway leads to predictions of advective particle travel times to the LWB more consistent with CCA model predictions than PABC-2004 (see Figure 3-10).

5 Summary and Conclusions

The 100 transmissivity fields resulting from calibration to both steady-state and transient observed freshwater heads in the Culebra (Hart et al., 2009) were modified to account for potential effects due to mining potash from the Salado Formation above the repository. A definition of the areal extent of minable potash was obtained from the Bureau of Land Management (Cranston, 2009) and used to define areas where Culebra transmissivity was increased by a randomly sampled mining factor ($1 \leq \texttt{MINP\_FACT} \leq 1000$). Two mining scenarios were developed: a full-mining scenario with all minable potash removed and a partial-mining scenario with only potash outside the WIPP LWB removed.

The mining-modified transmissvities were inputs to a MODFLOW flow model, which was used by DTRKMF to compute advective particle tracks from a release point at the center of the WIPP waste panels to the edge of the WIPP LWB. Results show that for the partial-mining scenario, the median particle travel time of 22,376 years is 3.03 times greater than for the non-mining scenario (7,374 years); the median particle travel time for the partial-mining scenario in PABC-2004 was 7.06 times greater than for the non-mining scenario. In contrast to the PABC-2004, the full-mining scenario decreased median travel time to 5,084 years, a factor of 1.45 *faster* than for the non-mining scenario; the median particle

travel time for the full-mining scenario in PABC-2004 was 3.84 times slower than for the non-mining scenario. For the partial-mining scenario, the increase in transmissivity due to mining increases the relative flow rate through the mining zones, with a corresponding decrease in flow through the non-mining zones. This decrease in flow through the non-mining zones produces longer travel times for the partial-mining scenario. For the full-mining scenario, the potash definition from BLM (Cranston, 2009) locates minable potash ore half the distance from the C-2737 release point than in PABC-2004 (see Figure 3-8). This new shortened distance from the release point to minable potash (in the full-mining scenario) reverses the slowing-down trend observed in the PABC-2004 analysis.

Like the PABC-2004 calculations, a very weak positive correlation was found between the travel times and the random mining factor (the higher the random mining factor, the longer the particle travel time – see Figure 3-21 and Figure 3-22). As the mining factor is increased, the flow through the non-mining areas is decreased, producing longer travel times and the positive correlation. Most of the advective particle travel time variability is due to differences in the base T-fields and not the random mining factor.

Culebra radionuclide transport calculations used the same MODFLOW flow-fields as DTRKMF, but refined the solution mesh to focus on a smaller subset of the domain focused on the WIPP LWB. The flow-fields computed using this smaller refined grid were additionally multiplied by a randomly sampled multiplier ($1 \leq$ CLIMTIDX ≤ 2.25) to account for potential increases in hydraulic gradients due to climate change (Corbet and Swift, 1996).

Many more Culebra radionuclide transport vectors showed significant movement of radionuclides to the LWB during the 10,000-year transport simulations under full-mining conditions, compared to PABC-2004. The mass of ^{234}U and its ^{230}Th daughter product transported to the WIPP LWB during the 10,000 year regulatory period were the largest of the five simulated radionuclides, with a few vectors essentially transporting the entire injected mass of ^{234}U to the LWB. The large increase in radionuclide transport can be attributed to three factors:

1. changes in the definition of minable potash,
2. changes in the lower limit of the K_d ranges, and
3. presence of a high-transmissivity pathway out of the southeast portion of the LWB, supported by the SNL-14 pumping test.

The cumulative mass of each radionuclide transported to the WIPP LWB, reported every 50 years, is the prediction used from this analysis in the subsequent CCDFGF analysis (Camphouse, 2010). The source term introduced in the Culebra in this modeling exercise is a unit mass at the beginning of the 10,000 year regulatory period, which is scaled and time-shifted based on other sampled parameters to produce predicted release to the accessible environment (the subsurface outside the WIPP LWB).

6 Bibliography

Bertram, S.G., 1995. *Record of FEP Screening Work, FEP ID#NS-11: Subsidence Associated with Mining Inside or Outside the Controlled Area*. Carlsbad, NM: Sandia National Laboratories. ERMS 230761.

Camphouse, R.C., 2010. *Analysis Package for CCDFGF: CRA-2009 Performance Assessment Baseline Calculation*. Carlsbad, NM: Sandia National Laboratories. In Progress.

Chavez, M., 2006. *NP 19-1 Software Requirements, Revision 12*. Carlsbad, NM: Sandia National Laboratories.

Chavez, M., 2008. *NP 9-1 Analyses, Revision 7*. Carlsbad, NM: Sandia National Laboratories.

Clayton, D.J., 2009a. *Analysis Plan for the CRA-2009 Performance Assessment Baseline Calculation, AP-145 Revision 0*. Carlsbad, NM: Sandia National Laboratories. ERMS 551603.

Clayton, D.J., 2009b. *Update to the K_d values for the PABC-2009*. Carlsbad, NM: Sandia National Laboratories. ERMS 552395.

Clayton, D.J., Camphouse, R.C., Garner, J.W., Ismail, A.E., Kirchner, T.B., Kuhlman, K.L. and Nemer, M.B., 2010. *Summary Report of the CRA-2009 Performance Assessment Baseline Calculation*. Carlsbad, NM: Sandia National Laboratories. In progress.

Clayton, D.J., Dunagan, S., Garner, J.W., Ismail, A.E., Kirchner, T.B., Kirkes, G.R. and Nemer, M.B., 2008. *Summary Report of the 2009 Compliance Recertification Application Performance Assessment*. Carlsbad, NM: Sandia National Laboratories. ERMS 548862.

Corbet, T., 1995. *Record of FEP Screening Work FEP ID# NS-9 Justification of SECO2D Approximation for PA Transport Calculotion*. Carlsbad, NM: Sandia National Laboratories. ERMS 230802.

Corbet, T. and Swift, P., 1996. *Parameters required for SECOFL2D: Climate Index*. Carlsbad, NM: Sandia National Laboratories. ERMS 237465.

Cotsworth, E., 2005. *EPA Letter on Conducting the Performance Assessment Baseline Change (PABC) Verification Test*. Washington, D.C.: U.S. Environmental Protection Agency, Office of Radiation and Indoor Air. ERMS 538858.

Cotsworth, E., 2009. *EPA CRA-2009 First Set of Completeness Comments*. Washington, D.C.: U.S. Environmental Protection Agency, Office of Radiation and Indoor Air. ERMS 551444.

Cranston, C.C., 2009. *Minable Potash Ore*. Carlsbad, NM: Bureau of Land Management. ERMS 551120.

ESRI, 1998. *ESRI Shapefile Technical Description - An ESRI White Paper*. Redlands, CA: Environmental Systems Research Institute, Inc.

Harbaugh, A.W., Banta, E.R., Hill, M.C. and McDonald, M.G., 2000. *MODFLOW 2000: The U.S. Geological Survey Modular Ground-Water Model User Guide*. Reston, VA: U.S. Geological Survey. OFR 00-92.

Hart, D.B., 2010. *WIPP PA Validation Document for MODFLOW-2000 Version 1.6: addenda for direct solver*. Carlsbad, NM: Sandia National Laboratories. ERMS 552422.

Hart, D.B., Beauheim, R.L. and McKenna, S.A., 2009. *Analysis Report for Task 7 of AP-114: Calibration of Culebra Transmissivity Fields*. Carlsbad, NM: Sandia National Laboratories. ERMS 552391.

Hart, D.B., Holt, R.M. and McKenna, S.A., 2008. *Analysis Report for Task 5 of AP-114: Generation of Revised Base Transmissivity Fields*. Carlsbad, NM: Sandia National Laboratories. ERMS 549597.

Holt, R.M., 1997. *Conceptual Model for Transport Processes in the Culebra Dolomite Member of the Rustler Formotion*. Carlsbad, NM: Sandia National Laboratories. SAND97-0194.

Holt, R.M. and Powers, D.W., 1988. *Facies Voriability ond Post-Depositionol Alteration Within the Rustler Formation in the Vicinity of the Waste Isolotion Pilot Plant, Southeastern New Mexico*. Carlsbad, NM: WIPP Project Office. ERMS 242145.

Johnson, P.B., 2009. *Routine Colculations Report In Support of Task 6 of AP-114: Potentiometric Surfoce, Adjusted to Equivalent Freshwater Heads, of the Culebra Dolomite member of the Rustler Formation neor the WIPP Site, Revision 2*. Carlsbad, NM: Sandia National Laboratories. ERMS 551116.

Kelly, T.E., 2009. *EPA Third Letter Requesting Additional Information on the CRA-2009*. Washington, D.C.: U.S. EPA Office of Radiation and Indoor Air. ERMS 552374.

Kirchner, T., 2008. *User's Guide to CVS, ReadScript.py, ond Related Utilities, Version 1.00*. Carlsbad, NM: Sandia National Laboratories. ERMS 550579.

Kirchner, T.B., 2010. *Generation of the LHS Samples for the AP-145 (PABC09) PA calculations*. Carlsbad, NM: Sandia National Laboratories. In Progress.

Kuhlman, K.L., 2009. *AP-144 Analysis Plan for the Calculation of Culebra Flow and Transport for CRA2009PABC*. Sandia National Laboratories. ERMS 551676.

Leigh, C.D., Kanney, J.F., Brush, L.H., Garner, J.W., Kirkes, G.R., Lowry, T., Nemer, M.B., Stein, J.S., Vugrin, E.D., Wagner, S. and Kirchner, T.B., 2004. *2004 Compliance Recertification Application Performance Assessment Baseline Calculation, Revision 0*. Carlsbad, NM: Sandia National Laboratories. ERMS 541521.

Long, J.J., 2010. *Execution of Performonce Assessment Codes for the CRA-2009 Performance Assessment Baseline Calculation*. Carlsbad, NM: Sandia National Laboratories. In Progress.

Lowry, T.L., 2003a. *Analysis Report, Task 5 of AP-088: Evaluation of Mining Scenorios*. Carlsbad, NM: Sandia National Laboratories. ERMS 531138.

Lowry, T.L., 2003b. *Analysis Report, Tasks 2 & 3 of AP-100: Grid Size Conversion ond Generation of SECOTP2D Input*. Carlsbad, NM: Sandia National Laboratories. ERMS 531137.

Lowry, T.S., 2004. *Analysis Report for Inclusion of Omitted Areas in Mining Tronsmissivity Calculations in Response to EPA Comment G-11*. Carlsbad, NM: Sandia National Laboratories. ERMS 538218.

Lowry, T.S. and Kanney, J.F., 2005. *Analysis Report for the CRA-2004 PABC Culebra Flow and Transport Calculations*. Carlsbad, NM: Sandia National Laboratories. ERMS 541508.

MacKinnon, R.J. and Freeze, G., 1997a. *Summary of EPA-Mandated Performance Assessment Verification Test (Replicate 1) and Comparison With the Compliance Certification Application Calculations, Revision 1*. Carlsbad, NM: Sandia National Laboratories. ERMS 422595.

MacKinnon, R.J. and Freeze, G., 1997b. *Summary of Uncertainty and Sensitivity Analysis Results for the EPA-Mandated Performance Assessment Verification Test, Rev 1*. Carlsbad, NM: Sandia National Laboratories. ERMS 420669.

MacKinnon, R.J. and Freeze, G., 1997c. *Supplemental Summary of EPA-Mandated Performance Assessment Verification Tests (All Replicates) and Comparison With the Compliance Certification Application Calculations, Revision 1*. Carlsbad, NM: Sandia National Laboratories. ERMS 414880.

Meigs, L.C., Beauheim, R.L. and Jones, T.L., eds., 2000. Interpretation of Tracer Tests Performed in the Culebra Dolomite at the Waste Isolation Pilot Plant Site. Carlsbad, NM: Sandia National Laboratories. SAND97-3109.

Powers, D.W., Lambert, S.J., Shaffer, S.-E., Hill, L.R. and Weart, W.D., eds., 1978. Geological Characterization Report - (WIPP). Carlsbad, NM: Sandia National Laboratories. SAND78-1596.

Ramsey, J.L., 1997. *WIPP PA User's Manual for SECOTP2D, Version 1.41*. Carlsbad, NM: Sandia National Laboratories. ERMS 245734.

Ramsey, J.L. and Wallace, M., 1996. *Analysis Package for the Culebra Flow and Transport Calculations (Task 3) of the Performance Assessment Analyses Supporting the Compliance Certification Application*. Carlsbad, NM: Sandia National Laboratories. ERMS 240516.

Rudeen, D.K., 2003. *User's Manual for DTRKMF Version 1.00*. Carlsbad, NM: Sandia National Laboratories. ERMS 523246.

Salari, K. and Blaine, R., 1996. *WIPP PA User's Manual for SECOTP2D, Version 1.30*. Carlsbad, NM: Sandia National Laboratories. ERMS 236695.

U.S. DOE, 1996. *Title 40 CFR Part 191 Compliance Certification Application for the Waste Isolation Pilot Plant*. Carlsbad, NM: U.S. Department of Energy Waste Isolation Pilot Plant, Carlsbad Area Office. DOE/CAO-1996-2184.

U.S. DOE, 2004. *Title 40 CFR Part 191 Compliance Recertification Application for the Waste Isolation Pilot Plant*. Carlsbad, NM: U.S. Department of Energy Waste Isolation Pilot Plant, Carlsbad Field Office. DOE/WIPP 2004-3231.

U.S. EPA, 1993. *Title 40 CFR Part 191: Environmental Radiation Protection Standards for the Management and Disposal of Spent Nuclear Fuel, High-Level and Transuranic Radioactive Wastes; Final Rule*. Federal Register, Vol 58, 66398-66416.

U.S. EPA, 1996. *Title 40 CFR Part 194: Criteria for the Certification and Recertification of the Waste Isolation Pilot Plant's Compliance with the 40 CFR Part 191 Disposal Regulations; Final Rule*. Federal Register, Vol. 61, 5223-5245.

U.S. EPA, 1998. *Criteria for the Certification and Recertification of the Waste Isolation Pilot Plant's Compliance with the Disposal Regulations: Certification Decision: Final Rule. Federal Register, Vol. 63.* ERMS 251924.

Vine, J.D., 1963. *Surface Geology of the Nash Draw Quadrangle, Eddy County, New Mexico.* U.S. Geological Survey. Bulletin 1141-B.

Appendix 1 Mining Modification Process Narrative

This appendix describes each step of the mining modification process in sufficient detail to allow it to be reproduced. Tables of input and output files are listed in the Culebra flow chapter of the run control document for PABC-2009 (Long, 2010)

The mining modification (i.e., non-VMS) portion of the analysis in this report can be broken down into 9 major steps:

0. Convert mining areas delineated by a binary ESRI shapefile to ASCII MODFLOW grid data;
1. Checkout AP-114 Task 7 results from CVS repository `Tfields` and modify directory structure associated with realization names (remove `Update` & `Update2` from some of the path names);
2. Enlarge mining areas to include both MODFLOW cells directly over mined areas and cells affected by nearby mined areas (i.e., within the 45° angle-of-draw);
3. Modify hydraulic conductivity fields and internal boundary conditions according to mining shape definition (from step 3) and mining factors from LHS on VMS (see Section A2.5);
4. Run MODFLOW and DTRKMF for each of 700 scenarios (600 mined + 100 non-mined) using 100 meter square elements;
5. Post-process DTRKMF output for plotting CDF and particle track figures.
6. Convert MODFLOW input data from 100 m to 50 m elements (4× total number of elements);
7. Run MODFLOW for each of the 600 mined scenarios using 50 m elements; and
8. Convert MODFLOW budget files from binary to ASCII, renaming them for ftp transfer to VMS to be used as input to VTRAN2 (see Appendix 3).

The commercial off-the-shelf software (COTS) used in the mining modification portion of the analysis is summarized in Table A1-1, and software are discussed when used in the rest of this appendix.

Table A1-1. Commercial off-the-shelf software used in mining modification analysis

Program	Version	Platform	Use
Python	2.3.4	Linux	script interpreter
Bash	3.00.15(1)	Linux	script interpreter
MATLAB	7.9.0.529 (R2009b)	Windows XP	script interpreter / plotting
Gnuplot	4.2.3	Windows XP	plotting
MS-Excel	2007-SP1	Windows XP	plotting / regression
Surfer	9.7.543	Windows XP	plotting

A1.1 Step 0 – Shapefile Conversion and Mapping to Grid

The first step is a binary-to-ASCII file conversion step (in Python) followed by a mapping of the results onto the MODFLOW grid (in MATLAB), and is the only portion of the analysis in this appendix not done on the WIPP PA Pentium 4 cluster. Step 0 is run on a Dell Precision 690 workstation (with two Intel Xeon processors) running Windows XP, Service Pack 2. The shapefile and scripts are located in the CVS repository `MiningMod` with the other files used in the Linux portion of this analysis (in the archive

potash_shapefile.zip, located in the package Auxiliary). The conversion portion of this step was done using the Python script convert_shapefile_to_ASCII.py (see §A4.1 for script listing and Table A1-2 for input/output files), which converts the binary ESRI shapefile polyline data that is used to define the extent of the minable potash ore into a series of ASCII text files (the specification for ESRI shapefiles is outlined in an ESRI (1998) white paper). The single shapefile is comprised of all the files with the base name Measured_Minable_Ore_UTMNAD27 (see file listing in Table A1-5), but the single binary file with the extension .shp contains the polyline data defining the extent of the potash. Since the mining definition is specified as a doubly-connected region (i.e., an area with holes cut out of it), care must be taken to handle polylines nested inside one another (see Figure A1-1); it is known *a priori* that none of the individual polylines intersect.

Table A1-2. Input and output files for Python script convert_shapefile_to_ASCII.py

File	Remark
Inputs[1]	
convert_shapefile_to_ASCII.in	Python input listing filenames
Measured_Minable_Ore_UTMNAD27.shp	single file from potash shapefile containing coordinates of polylines defining potash areas
Outputs	
polyline_dump_matlab_part*nnnn*.dat	54 ASCII listings of UTM NAD27 coordinates each containing data for an individual polyline
polyline_dump_for_gnuplot.dat	ASCII listing of all parts, each separated by two blank lines for plotting to check conversion

1. $nnnn \in \{0000,0001,\ldots,0053\}$

The shapefile has two sets of data important to the present use; the main portion is a listing of double-precision NAD27 UTM x, y coordinates (Zone 13) of the vertices in the polyline in meters (192,528 pairs). The second set of data in the shapefile (needed for this analysis) is a listing of the 53 integer line numbers where this single long list of coordinates is broken into 54 parts.

The 54 parts defined in the shapefile used here are each saved into a different text file (to be read back in by the MATLAB script in the next step), and all the data is also saved into a single text file for plotting and checking in Gnuplot and Surfer; the multi-file (lines 172-191 of §A4.1.2) and single-file (lines 144-170) formats have the same information in them (see Table A1-3 for a comparison of the first few points in two corresponding files). The original binary shapefile and the ASCII files were plotted simultaneously in the program Surfer as a check that the data were extracted from the binary file correctly. Surfer has the ability to plot ESRI shapefiles and the text format exported by the scripts described in this section. The original shapefile and the exported text files were found to be the same.

Table A1-3. Listing of the first five data points in the files `polyline_dump_matlab_part0000.dat` and `polyline_dump_for_gnuplot.dat`.

`589072.390 3612760.518`	`# data from Measured_Minable_Ore_UTMNAD27.shp`
`589078.150 3612765.663`	`# part: 0`
`589077.955 3612765.806`	`589072.4 3612760.5`
`589072.857 3612769.527`	`589078.1 3612765.7`
`589067.671 3612773.240`	`589078.0 3612765.8`
	`589072.9 3612769.5`
	`589067.7 3612773.2`

The MATLAB script `import_polyline_determine_mined_areas.m` (§A4.2 and Table A1-4) utilizes the built-in MATLAB function `inpolygon()` to compare coordinates of model-cell centers to the polylines exported to ASCII in the previous step, determining whether each model cell is inside or outside each of the 54 potash polygons. For the mining-area definitions, none of the polygons intersect and the most of the smaller polygons are inside the largest polygon (the polyline corresponding to part 1), and therefore define small cutout areas where no minable potash is found inside a larger potash area. Model cells are checked with respect to each of the 54 parts of the overall shapefile (lines 58-63 of the MATLAB script, §A4.2). The final calculation of whether a cell is minable or not is determined by comparing what types of polygons (e.g., black, red, and green in Figure A1-1) the cell is located within (lines 65-73 in §A4.2). The following cases are exhaustive for the given set of data:

1. cells outside all polygons have no potash (white areas in Figure A1-1);
2. cells inside one polygon have potash (either black or green areas in Figure A1-1); and
3. cells inside more than one polygon have no potash (red areas in Figure A1-1), because there are no triply-nested polylines.

The two output files `mining_areas_matrix.dat` and `mining_areas_xyz.dat` contain the listing of the cells inside (value of 1) and outside (value of 0) in two different formats (saved as a list of x, y coordinates and mining index for plotting in Gnuplot and also saved as a matrix of mining indices, with no coordinates – used later in the analysis).

Table A1-4. Input and output files for MATLAB script `import_polyline_determine_mined_areas.m`

File	Remark
Inputs[1]	
`polyline_dump_matlab_part`*`nnnn`*`.dat`	54 ASCII listings of UTM NAD27 coordinates each containing data for an individual polyline (see outputs in Table A1-2)
Outputs	
`mining_areas_matrix.dat`	ASCII matrix with indices indicating MODFLOW model cells with minable potash
`mining_areas_xyz.dat`	ASCII x,y,z listing of MF2K model cells with minable potash and their UTM NAD27 coordinates

1. $nnnn \in \{0000, 0001, \ldots, 0053\}$

This process of mapping the shapefile provided by BLM onto the model grid was done in one step for PABC-2004 using the COTS Windows software GMS (Lowry, 2003a). This approach was attempted, but problems appeared associated with the way GMS 7.0 maps the current shapefile, resulting in GMS crashing and not performing the mapping. Technical and developer support from the GMS vendor could not resolve the problem, aside from the assurance that this will be fixed in some future release. Due to this limitation, the manipulation and mapping of the shapefiles to the MODFLOW model grid is given explicitly in terms of the Python and MATLAB scripts here listed and described.

Table A1-5. Directory listing of input scripts, input shapefile, intermediate files, and output files for shapefile conversion (step 0). Files are located in a zip archive saved in the CVS repository `MiningMod` in the package `Auxiliary`.

```
C:\shapefile_conversion>dir
 Volume in drive C is DriveC
 Volume Serial Number is 542A-10F7

 Directory of C:\shapefile_conversion

10/07/2009  01:49 PM    <DIR>          .
10/07/2009  01:49 PM    <DIR>          ..
09/30/2009  04:40 PM                93 convert_shapefile_to_ASCII.in
10/07/2009  10:30 AM             9,184 convert_shapefile_to_ASCII.py
09/30/2009  04:59 PM             2,258 import_polyline_determine_mined_areas.m
06/22/2009  05:27 PM               178 Measured_Minable_Ore_UTMNAD27.dbf
06/22/2009  05:27 PM               426 Measured_Minable_Ore_UTMNAD27.prj
06/22/2009  05:27 PM               132 Measured_Minable_Ore_UTMNAD27.sbn
06/22/2009  05:27 PM               116 Measured_Minable_Ore_UTMNAD27.sbx
06/22/2009  05:27 PM         3,080,816 Measured_Minable_Ore_UTMNAD27.shp
06/22/2009  05:27 PM             2,239 Measured_Minable_Ore_UTMNAD27.shp.xml
06/22/2009  05:27 PM               108 Measured_Minable_Ore_UTMNAD27.shx
09/28/2009  11:06 AM         1,395,622 mining_areas_matrix.dat
09/28/2009  11:06 AM         4,359,400 mining_areas_xyz.dat
09/30/2009  04:35 PM         3,851,461 polyline_dump_for_gnuplot.dat
09/30/2009  04:35 PM         3,240,336 polyline_dump_matlab_part0000.dat
09/30/2009  04:35 PM           766,608 polyline_dump_matlab_part0001.dat
09/30/2009  04:35 PM            49,872 polyline_dump_matlab_part0002.dat
09/30/2009  04:35 PM            58,944 polyline_dump_matlab_part0003.dat
09/30/2009  04:35 PM            33,288 polyline_dump_matlab_part0004.dat
09/30/2009  04:35 PM            33,504 polyline_dump_matlab_part0005.dat
09/30/2009  04:35 PM             8,568 polyline_dump_matlab_part0006.dat
09/30/2009  04:35 PM            16,152 polyline_dump_matlab_part0007.dat
09/30/2009  04:35 PM            20,832 polyline_dump_matlab_part0008.dat
09/30/2009  04:35 PM             6,552 polyline_dump_matlab_part0009.dat
09/30/2009  04:35 PM            12,024 polyline_dump_matlab_part0010.dat
09/30/2009  04:35 PM             9,912 polyline_dump_matlab_part0011.dat
09/30/2009  04:35 PM            11,136 polyline_dump_matlab_part0012.dat
09/30/2009  04:35 PM            14,832 polyline_dump_matlab_part0013.dat
09/30/2009  04:35 PM             8,280 polyline_dump_matlab_part0014.dat
09/30/2009  04:35 PM            10,776 polyline_dump_matlab_part0015.dat
09/30/2009  04:35 PM             6,096 polyline_dump_matlab_part0016.dat
09/30/2009  04:35 PM             5,568 polyline_dump_matlab_part0017.dat
09/30/2009  04:35 PM             7,320 polyline_dump_matlab_part0018.dat
09/30/2009  04:35 PM             9,744 polyline_dump_matlab_part0019.dat
09/30/2009  04:35 PM            10,200 polyline_dump_matlab_part0020.dat
09/30/2009  04:35 PM             4,680 polyline_dump_matlab_part0021.dat
09/30/2009  04:35 PM             4,056 polyline_dump_matlab_part0022.dat
09/30/2009  04:35 PM             7,632 polyline_dump_matlab_part0023.dat
09/30/2009  04:35 PM             5,784 polyline_dump_matlab_part0024.dat
09/30/2009  04:35 PM             5,544 polyline_dump_matlab_part0025.dat
09/30/2009  04:35 PM             5,400 polyline_dump_matlab_part0026.dat
09/30/2009  04:35 PM             3,864 polyline_dump_matlab_part0027.dat
09/30/2009  04:35 PM             5,448 polyline_dump_matlab_part0028.dat
09/30/2009  04:35 PM             4,128 polyline_dump_matlab_part0029.dat
09/30/2009  04:35 PM             3,432 polyline_dump_matlab_part0030.dat
09/30/2009  04:35 PM             6,552 polyline_dump_matlab_part0031.dat
09/30/2009  04:35 PM             4,512 polyline_dump_matlab_part0032.dat
09/30/2009  04:35 PM             5,592 polyline_dump_matlab_part0033.dat
09/30/2009  04:35 PM             4,824 polyline_dump_matlab_part0034.dat
09/30/2009  04:35 PM             3,480 polyline_dump_matlab_part0035.dat
09/30/2009  04:35 PM             2,808 polyline_dump_matlab_part0036.dat
09/30/2009  04:35 PM             3,672 polyline_dump_matlab_part0037.dat
09/30/2009  04:35 PM             2,568 polyline_dump_matlab_part0038.dat
09/30/2009  04:35 PM             1,944 polyline_dump_matlab_part0039.dat
09/30/2009  04:35 PM             1,440 polyline_dump_matlab_part0040.dat
09/30/2009  04:35 PM            24,888 polyline_dump_matlab_part0041.dat
09/30/2009  04:35 PM            27,888 polyline_dump_matlab_part0042.dat
09/30/2009  04:35 PM             1,512 polyline_dump_matlab_part0043.dat
09/30/2009  04:35 PM             2,472 polyline_dump_matlab_part0044.dat
09/30/2009  04:35 PM             1,152 polyline_dump_matlab_part0045.dat
09/30/2009  04:35 PM               360 polyline_dump_matlab_part0046.dat
09/30/2009  04:35 PM               264 polyline_dump_matlab_part0047.dat
09/30/2009  04:35 PM            24,072 polyline_dump_matlab_part0048.dat
09/30/2009  04:35 PM            27,000 polyline_dump_matlab_part0049.dat
09/30/2009  04:35 PM            11,544 polyline_dump_matlab_part0050.dat
09/30/2009  04:35 PM            22,032 polyline_dump_matlab_part0051.dat
09/30/2009  04:35 PM             8,664 polyline_dump_matlab_part0052.dat
09/30/2009  04:35 PM            40,920 polyline_dump_matlab_part0053.dat
              67 File(s)     17,322,705 bytes
               2 Dir(s)  149,001,261,056 bytes free
```

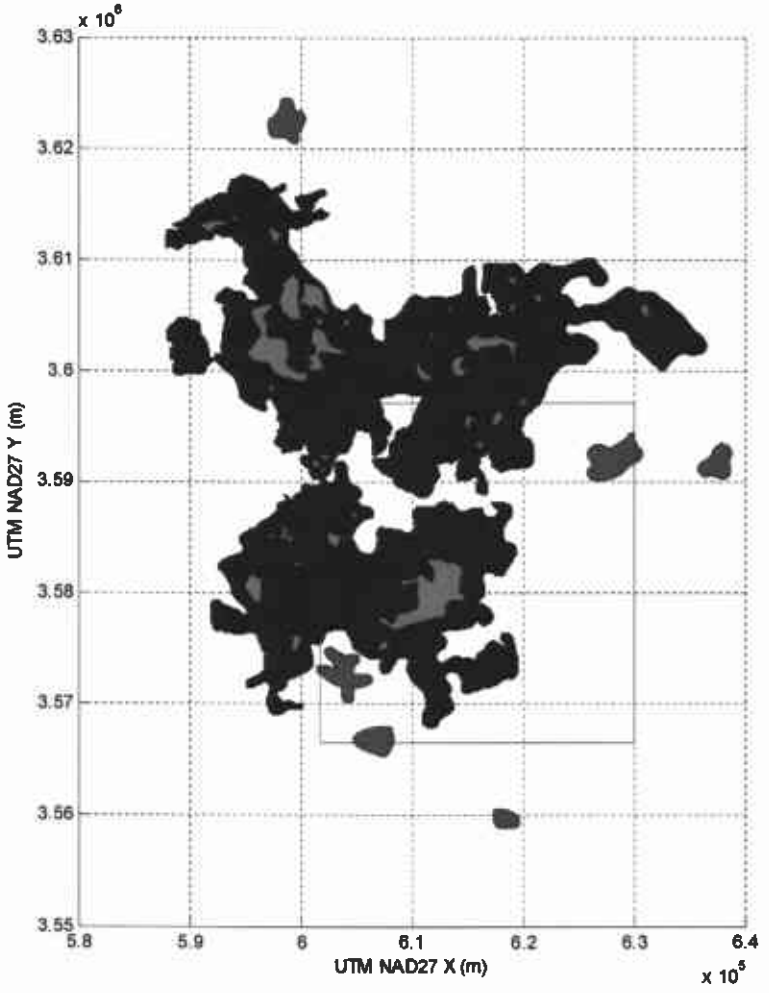

Figure A1-1. 54 polygons defining mining areas, color-coded by their relationship to the large black polygon. Green are outside the large polygon and define mined areas, red are inside the black polygon and define non-mined areas. Blue rectangle indicates PABC-2009 MODFLOW model extents.

The ASCII file `mining_areas_xyz.dat` was uploaded to the Pentium 4 PA cluster and added to the CVS repository `MiningMod` in the package `Inputs`, to be used as input to the Python script that enlarges mining areas to account for the angle-of-draw effect (see next section).

Figure A1-1 illustrates the relationship between the different parts of the polyline and shows the extent of the minable potash beyond the MODFLOW model domain (the area plotted in Figure A1-2). Figure A1-2 indicates the MODFLOW cells (small blue dots) that were determined to be located in mined areas. Both figures were generated by the MATLAB script (§A4.2: Figure A1-1 in lines 28, 35, 37, 41-43 and Figure A1-2 lines 76-77) that computes the mapping of model cells onto the potash mining definitions.

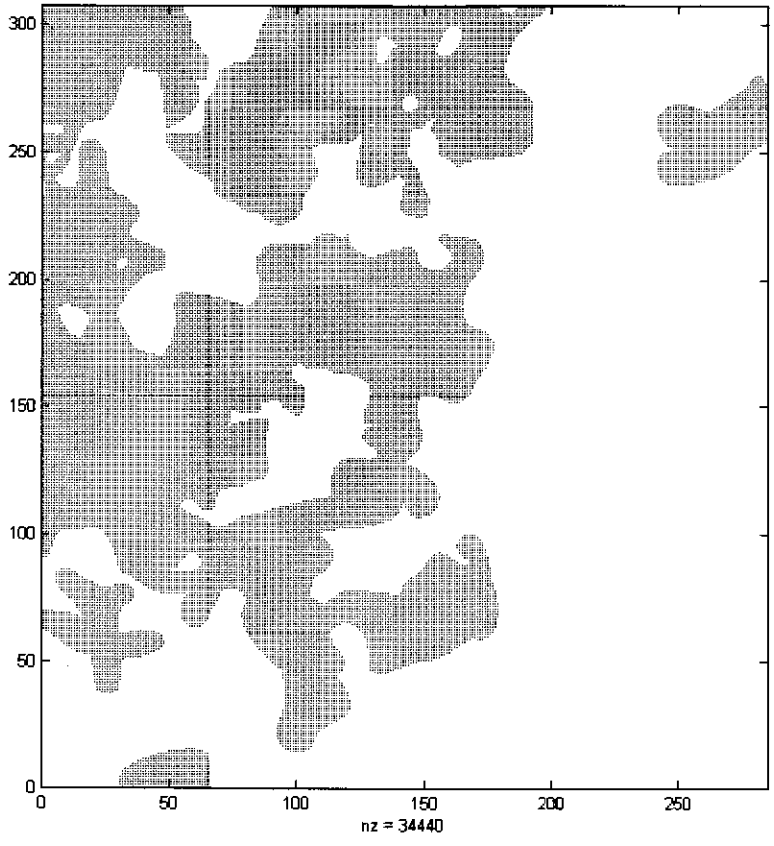

Figure A1-2. MODFLOW model domain with mined model cells marked with a small blue dot. 34,440 of the total 87,188 elements have mining (some cells in the northwest portion of the domain are inactive – see Figure 3-2)

A1.2 Step 1 – MODFLOW File Checkout and Directory Re-structuring

The creation of the directory structure and the process of checking out AP-114 Task 7 MODFLOW files from the CVS repository `Tfield` are handled by the QA-controlled Python program `ReadScript.py`, using the input file `mining_mod.inp` (itself saved in the `RunControl` package of the `MiningMod` CVS repository). See Figure A1-3 for the directory structure in the CVS repository used in this analysis. The Bash shell script `run_mining_mods.sh` (§A4.3) is the main script called by `ReadScript.py` (see last line of input file); this Bash script calls several other scripts and performs minor file manipulations (see Figure A1-4 for the dependency of scripts). The 100 realizations of flow models resulting from AP-114 Task 7 (Hart et al., 2009) are not in a flat directory structure in the CVS repository `Tfields`; most of the 100 final realizations were updated (sometimes twice) as part of the re-calibration effort associated with the freshwater head value at SNL-8 (Hart et al., 2009). The Bash script `run_mining_mods.sh` processes the directory structure and creates the intermediate file `keepers_short` at lines 25-45 (§A4.3).

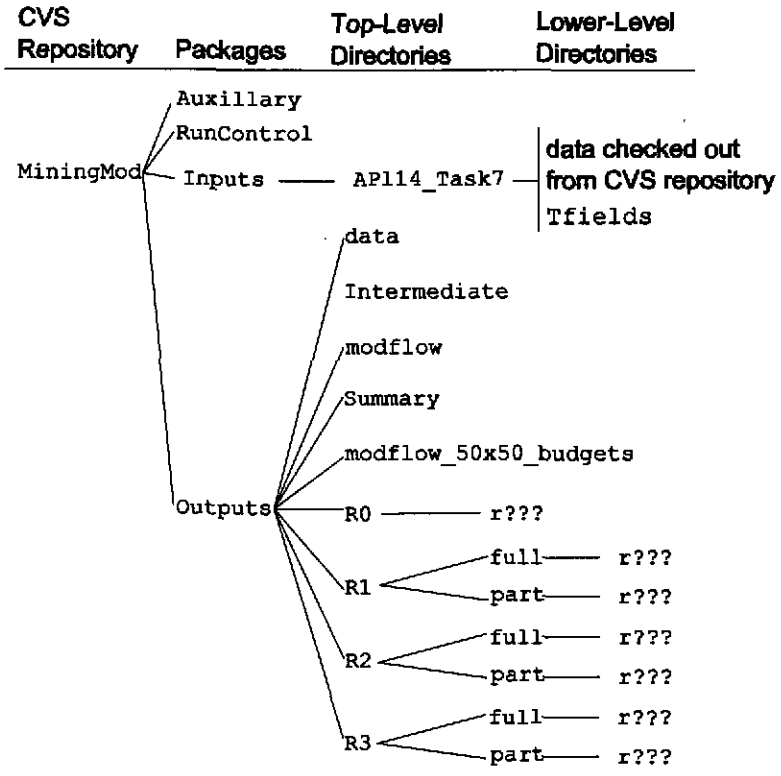

Figure A1-3. Directory structure of `MiningMod` CVS repository; `r???` indicates the 100 realizations (not numbered sequentially) selected in Hart et al., (2009) after simplifying the directory structure (see Table A1-6).

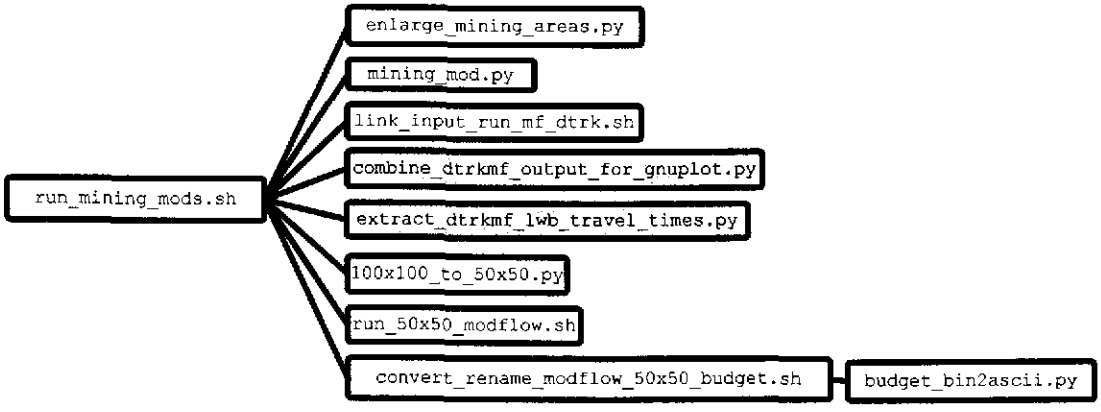

Figure A1-4. Dependency between scripts used in mining modifications on Pentium 4 PA cluster. In the middle column, the execution order is from top to bottom. The two gray boxes indicate scripts only used for post-processing DTRKMF output.

The scripts and input files used in this analysis are in the Inputs package of the CVS repository; the input files used directly from AP-114 Task 7 are exported from that CVS repository (`Tfields`) into the directory `Inputs/AP114_Task7` for use in this analysis, but are not checked back into the `MiningMod` CVS repository. The Outputs package contains files generated as part of this analysis, or

input files modified from their original state in AP-114 Task 7. The two subdirectories `data` and `modflow` in the Outputs package (see Figure A1-3) contain MODFLOW input files that are modified for the 50 m grid from their use in the original 100 m grid. The `Intermediate` top-level subdirectory contains results from intermediate steps in the analysis that are checked back into CVS for completeness. The `Summary` top-level directory contains post-processed DTRKMF results used for plotting figures. The `R0`, `R1`, `R2`, and `R3` top-level directories contain the subdirectories where MODFLOW is executed for each realization; each `r???` leaf in Figure A1-3 represents 100 subdirectories such as `r007`, `r203`, `r861`, etc. (see Table A1-6). The `Auxiliary` package contains a zip archive with the shapefile and scripts associated with step 0 and an MS-Excel spreadsheet associated with the regression analysis shown in Figure 3-21 and Figure 3-22, neither of which are run on the Pentium 4 PA cluster.

Table A1-6. Listing of file `keepers` (original column) with equivalent short name (short column) after modification by `run_mining_mods.sh`

ID	Original	Short	ID	Original	Short	ID	Original	Short	ID	Original	Short
1	Update/r256	r256	26	Update/r060	r060	51	Update/r883	r883	76	Update/r002	r002
2	Update/r902	r902	27	Update/r012	r012	52	Update/r045	r045	77	Update/r053	r053
3	Update/r038	r038	28	r078	r078	53	Update2/r137	r137	78	Update/r861	r861
4	Update/r486	r486	29	r104	r104	54	Update/r279	r279	79	Update2/r465	r465
5	Update/r984	r984	30	Update/r052	r052	55	Update/r694	r694	80	Update/r511	r511
6	r028	r028	31	Update2/r007	r007	56	Update/r361	r361	81	Update/r191	r191
7	Update/r298	r298	32	r102	r102	57	Update/r040	r040	82	Update/r142	r142
8	Update/r791	r791	33	Update/r809	r809	58	Update/r571	r571	83	Update/r061	r061
9	Update/r910	r910	34	r029	r029	59	Update/r440	r440	84	Update/r055	r055
10	Update/r054	r054	35	Update/r921	r921	60	Update/r070	r070	85	Update/r664	r664
11	r098	r098	36	Update/r051	r051	61	Update/r273	r273	86	Update/r515	r515
12	Update2/r327	r327	37	Update/r655	r655	62	Update/r669	r669	87	Update2/r017	r017
13	Update/r657	r657	38	Update/r823	r823	63	r084	r084	88	Update/r001	r001
14	r083	r083	39	Update2/r981	r981	64	Update/r568	r568	89	Update/r203	r203
15	Update/r808	r808	40	r082	r082	65	Update/r037	r037	90	Update2/r940	r940
16	r090	r090	41	Update/r328	r328	66	Update/r276	r276	91	Update/r034	r034
17	Update/r982	r982	42	r027	r027	67	Update/r431	r431	92	Update/r095	r095
18	r076	r076	43	Update/r522	r522	68	Update/r634	r634	93	Update/r041	r041
19	Update/r010	r010	44	Update/r506	r506	69	Update/r652	r652	94	Update/r260	r260
20	Update/r059	r059	45	Update2/r207	r207	70	Update/r752	r752	95	Update2/r013	r013
21	Update/r006	r006	46	r073	r073	71	Update/r064	r064	96	Update/r009	r009
22	Update/r640	r640	47	Update/r707	r707	72	Update/r032	r032	97	Update2/r489	r489
23	r097	r097	48	Update/r814	r814	73	r004	r004	98	Update/r727	r727
24	Update/r922	r922	49	Update/r508	r508	74	Update/r058	r058	99	Update/r806	r806
25	Update/r631	r631	50	Update/r092	r092	75	r074	r074	100	r024	r024

A1.3 Step 2 - Enlarge Mining Areas

The main Bash shell script `run_mining_mods.sh` (line 62 §A4.3) calls the Python script `enlarge_mining_areas.py` (§A4.4 and Table A1-7), which uses the input file `mining_areas_xyz.dat` as the definition of the mined areas (output by `import_polyline_determine_mined_areas.m`, §A4.2), and the UTM NAD27 Zone 13 coordinates of the corners of the WIPP LWB (specified in lines 4 and 5 of the input file `enlarge_mining_areas.in` §A4.4.1). The script writes two arrays as output, indicating where mining effects will be applied in both the full (`New_Full_09.dat`) and partial (`New_Part_09.dat`) mining scenarios.

Table A1-7. Input and output file for Python script `enlarge_mining_areas.py`

File[1]	Remark
Inputs	
`Inputs/mining_areas_xyz.dat`	X,Y coordinates of 100x100-m cells with index indicating presence of minable potash
`Inputs/enlarge_mining_areas.in`	Python script input with filenames, model grid, and WIPP LWB coordinates
Outputs	
`Outputs/mining_factor.dat`	matrix form of input indices for plotting
`Outputs/mining_factor.datx`	x-coordinates for matrix form of plotting
`Outputs/mining_factor.daty`	y-coordinates for matrix form of plotting
`Outputs/New_Full_09.dat`	full mining index as a matrix
`Outputs/New_Part_09.dat`	partial mining index as a matrix

1. CVS repository `MiningMod`

In the Python mining area enlargement script (§A4.4.2), the grid-defined mining areas are read in as (x,y,index) triplets (lines 118-131), converted from the indices 0 (no mining) and 1 (mining) to 0 and 10 (line 127), then the index associated with each model cell center that is located inside the WIPP LWB is increased by 1 (see script lines 135-143 and Table A1-8).

Table A1-8. Mining indices used in `expand_mining_areas.py`

	Mined area	Non-mined area
Inside WIPP LWB	11	1
Outside WIPP LWB	10	0

Mining-related subsidence effects are expanded by cycling through the original array of model cells, and propagating effects from this into a new matrix using the stencil comprised of a 5×5 square of cells centered on the mined cell, with 1 additional affected cell located along the 4 compass directions (see see script lines 168-204 and Figure 3-5).

Inside the WIPP LWB, MODFLOW cells with minable potash are compared to both mining-affected cells and the potash shapefile in Figure 3-12 through Figure 3-14 in Section 3.4.2 of the main text.

Table A1-9. Excerpts from mining_areas_matrix.dat (top), `New_Full_09.dat` (middle), and `New_Part_09.dat` (bottom) for rows 101-129 and columns 71-121 (area including NW corner of WIPP LWB). 0 is not mined or affected, 1 is mined or affected by mining (see Figure A1-5 for location of area).

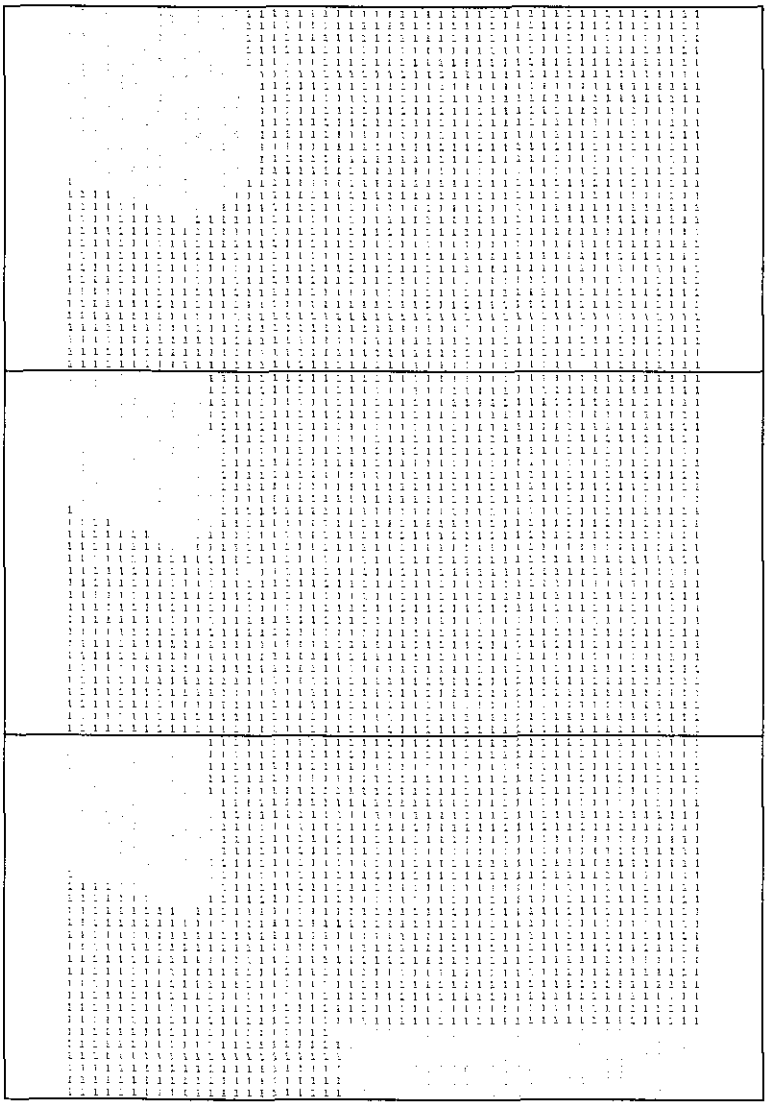

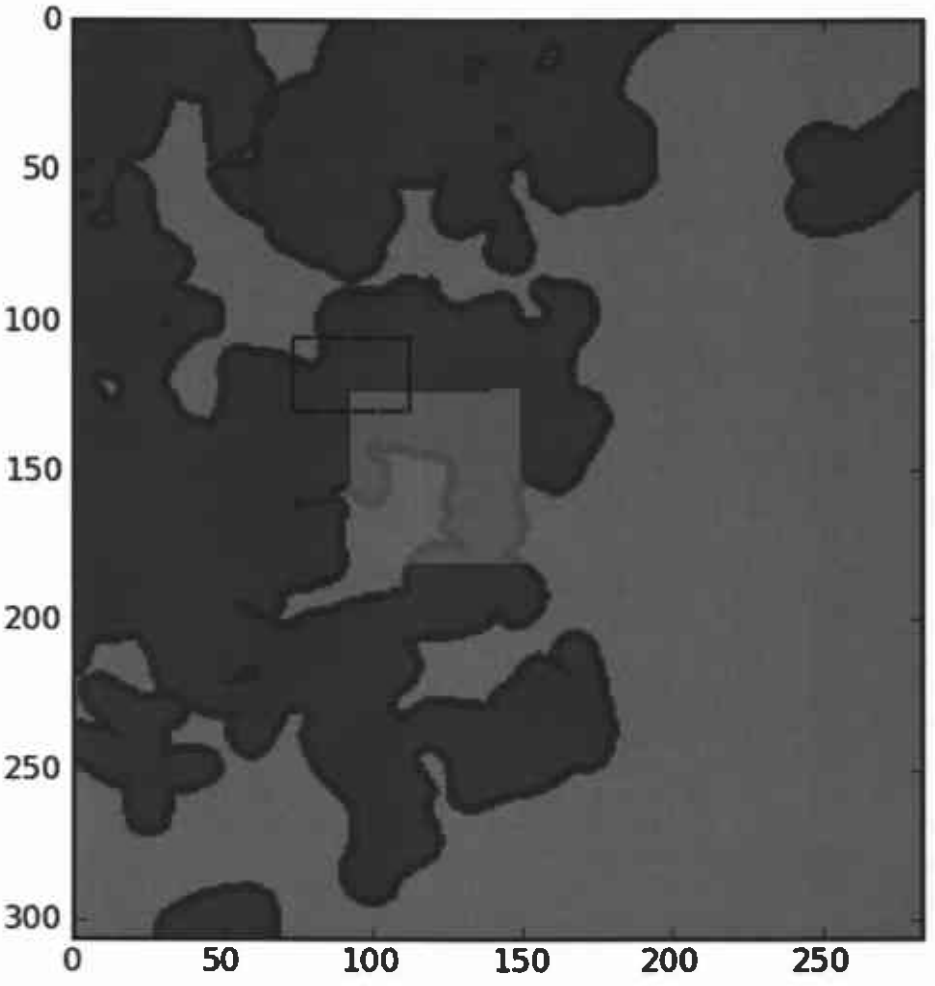

Figure A1-5. Matrices of full, partial, and unexpanded mining factors (region corresponding to Table A1-9 marked with dashed line); maroon cells have minable potash in both mining scenarios, purple indicates the halo of cells affected by mining that are not directly mined, orange cells are only mined in the full-mining scenario (with the corresponding halo of affected full-mining only cells in dark gray), and the background of model cells are unaffected by mining.

A1.4 Step 3 – Perform Mining Modifications

The main Bash shell script `run_mining_mods.sh` (§A4.3) at line 67 calls the Python script `mining_mods.py` (§A4.5.2 and Table A1-10), which uses the definitions of the mining-affected areas from the previous step and the mining factors from VMS (see section A2.5, `sum1_st2d_pabc09_r{1,2,3}.tbl`) to modify the hydraulic conductivity arrays to account for the potential increases in hydraulic conductivity due to mining-related subsidence.

After reading in the input files (lines 113-116 §A4.5.2), the Python script `mining_mods.py` first modifies the boundary conditions in certain mined areas (lines 123-144). Model cells that are specified head and mined (excluding the outermost ring of constant-head cells – handled in lines 146-165) are changed to normal cells, resulting in two new MODFLOW IBOUND arrays, `init_bnds_full.inf` and `init_bnds_part.inf` (lines 167-176).

Lastly, the horizontal hydraulic conductivity is modified by the mining factor (read in lines 186-202), resulting in six new hydraulic conductivity fields for each realization (3 replicates with different mining factors × 2 cases of either partial or full mining, see lines 209-252).

A1.4.1 Modification of Boundary Conditions

The MODFLOW IBOUND array is used to indicate whether cells are active (1), inactive (0), or specified head (negative integers) (Harbaugh et al., 2000). East of the composite M2/H2 + M3/H3 halite margin there exist essentially lithostatic pressure conditions, where pressure is equal to the weight of the overburden. The MODFLOW model developed in AP-114 Tasks 5 and 7 represents this lithostatic area using both very low hydraulic conductivity and specified head set to the land surface elevation (Hart et al., 2008; 2009). Applying the mining factor to these areas without changing the cell from constant head to active would greatly increase the flux flowing into the domain, since the constant-head boundary conditions are a potentially infinite source of water. Since the halite-sandwiched region is not believed to be a large source of water, constant-head cells that are

1. interior to the modeling domain (i.e., not in rows 1 or 307 or in columns 1 or 284),
2. east of the H2/M2 or H3/M3 Rustler halite margins (i.e., in the "halite-sandwiched" region), and
3. affected by mining modifications

are converted to active cells (see individual IBOUND arrays in Figure A1-6 and a composite figure of all three arrays in Figure A1-7).

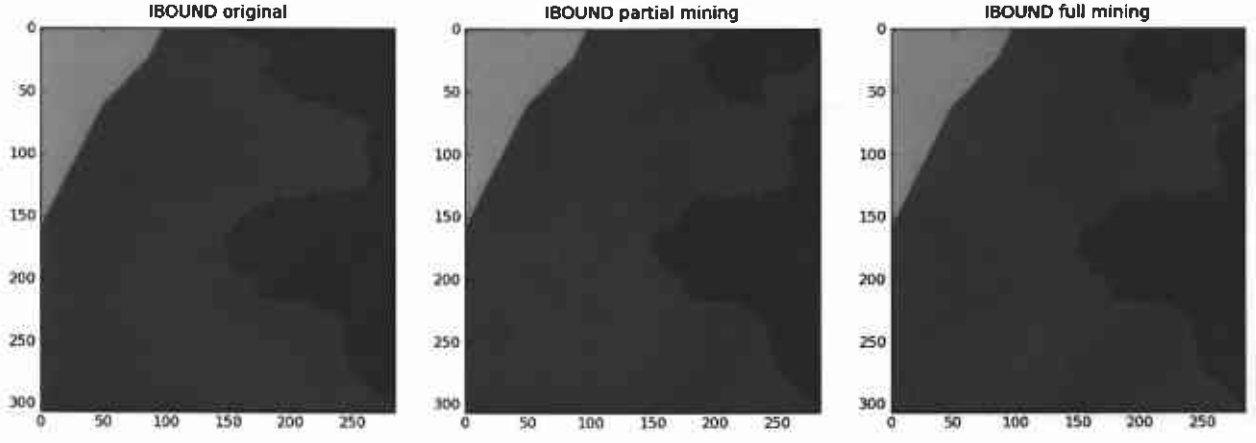

Figure A1-6. MODFLOW IBOUND arrays for original, partial-mining, and full-mining cases. Green is inactive or no-flow (zero), brick red is active (one), blue is specified head (negative integers). The only difference between full- and partial-mining scenarios is near row 175, column 150.

The cells in the outermost row and columns of the domain (aside from those cells in the inactive or no-flow region) are maintained as constant head, even if they correspond to mined regions – only constant-head cells in the interior of the model domain corresponding to the halite-sandwiched region of the Culebra are changed to active cells.

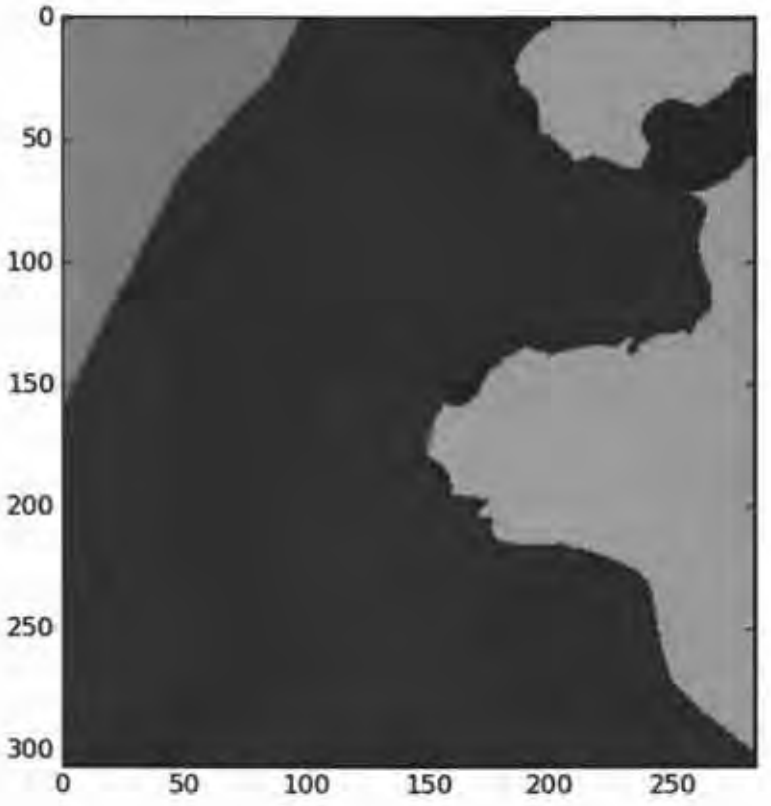

Figure A1-7. Overlay of three original, partial-mining, and full-mining IBOUND arrays given separately in Figure A1-6. The only difference between full and partial mining is a small tan sliver near row 175, column 150.

Table A1-10. Input and output files for Python script `mining_mod.py`

File[1,2]	Remark
Inputs	
`Inputs/keepers_short`	list of 100 realizations with "Update" or "Update2" stripped off (Table A1-6).
`Inputs/mining_mod.in`	Python script input with filenames
`Outputs/New_Full_09.dat`	full mining index (Table A1-7 outputs)
`Outputs/New_Part_09.dat`	partial mining index (Table A1-7 outputs)
`Inputs/AP114_Task7/data/init_bnds.inf`[3]	original MF2K IBOUND array
`Inputs/sum1_st2d_pabc09_r{1,2,3}.tbl`	mining factors from VMS; replicates 1,2,3
`Inputs/AP114_Task7/Outputs/r???/ modeled_K_field.mod`[3]	100 calibrated T-fields from AP-114 Task 7
Outputs	
`Outputs/data/init_bnds_full.inf`	MF2K IBOUND array for full mining
`Outputs/data/init_bnds_part.inf`	MF2K IBOUND array for partial mining
`Outputs/Rn/M/r???/ modeled_mined_K_field.mod`	600 MF2K input mining-modified T-fields

1. CVS repository `MiningMod`
2. $n \in \{1,2,3\}$; $M \in$ {full,part}; $r??? \in \{r256, r902, \textit{etc.}\}$ (see Table A1-6)
3. `Inputs/AP114_Task7/` is the working directory where files checked out from CVS repository `Tfields` are located, see (Long, 2010)

A1.4.2 Modification of Transmissivity Fields

The mining factors are saved in three table files (`sum1_st2d_pabc09_r{1,2,3}.tbl`); the data in these tables, along with the names of the MODFLOW 2000 T-field realizations (MF2K RZN – taken from the file `keepers`) are given in two different ways in Table A1-11 and Table A1-12. Table A1-11 is presented from the viewpoint of the 100 MODFLOW flow-fields and the mining factors that were applied to them for the three replicates. Table A1-12 is presented from the viewpoint of the SECOTP2D vectors, and which MODLFOW flow-field and mining factor was used in each replicate.

Each T-field is modified inside the potash-affected areas uniformly by a mining factor between 1 and 1,000 (MINP_FACT) applied to a selected realization (the integer TRANS_IDX), both variables being sampled by LHS (Kirchner, 2010) for each replicate.

Table A1-11. Mining factors applied to each MODFLOW realization. Keepers id refers to the order the realizations are listed in the keepers file (Table A1-6). First five columns are sorted by MODFLOW realization name, last five columns sorted by order in keepers file.

MF2K rzn	keepers id	R1	R2	R3
r001	88	374.4	487.7	774.5
r002	76	766.0	252.9	72.50
r004	73	356.6	249.1	992.4
r006	21	847.3	756.8	737.6
r007	31	84.52	432.4	592.5
r009	96	384.8	665.2	867.6
r010	19	240.1	979.7	59.88
r012	27	774.2	143.7	875.2
r013	95	783.4	927.2	310.9
r017	87	593.3	614.0	347.2
r024	100	718.3	980.8	377.4
r027	42	579.4	633.7	17.75
r028	6	104.2	228.6	391.3
r029	34	968.6	322.9	707.1
r032	72	637.4	291.5	191.8
r034	91	80.05	62.14	937.3
r037	65	566.1	674.3	416.3
r038	3	149.2	124.6	795.4
r040	57	337.4	996.2	143.2
r041	93	531.6	207.4	813.2
r045	52	732.0	415.2	354.7
r051	36	803.3	451.5	837.5
r052	30	583.5	539.0	153.5
r053	77	721.0	657.3	221.1
r054	10	217.6	402.0	976.7
r055	84	186.2	904.5	28.11
r058	74	956.1	780.6	587.5
r059	20	937.6	831.2	492.3
r060	26	58.89	876.3	383.6
r061	83	298.5	16.25	648.9
r064	71	399.4	103.4	189.2
r070	60	362.8	705.3	562.3
r073	46	983.4	582.3	505.1
r074	75	91.84	936.0	728.1
r076	18	435.1	36.28	851.6
r078	28	920.7	847.9	602.0
r082	40	325.0	827.2	471.1
r083	14	857.1	479.9	716.7
r084	63	320.7	605.5	488.0
r090	16	340.7	425.9	548.9
r092	50	413.8	49.06	689.4

keepers id	MF2K rzn	R1	R2	R3
1	r256	552.2	271.0	829.2
2	r902	444.3	778.6	439.4
3	r038	149.2	124.6	795.4
4	r486	484.9	515.1	38.70
5	r984	947.2	237.0	163.0
6	r028	104.2	228.6	391.3
7	r298	170.5	690.7	802
8	r791	821.7	170.2	208.8
9	r910	124.5	503.6	67.93
10	r054	217.6	402.0	976.7
11	r098	681.8	948.3	112.6
12	r327	39.37	357.3	452.9
13	r657	810.8	86.49	886.4
14	r083	857.1	479.9	716.7
15	r808	796.7	392.2	423.0
16	r090	340.7	425.9	548.9
17	r982	869.8	373.0	530.2
18	r076	435.1	36.28	851.6
19	r010	240.1	979.7	59.88
20	r059	937.6	831.2	492.3
21	r006	847.3	756.8	737.6
22	r640	751.6	599.5	766.5
23	r097	898.1	898.8	126.1
24	r922	289.7	729.1	676.3
25	r631	616.3	713.6	918.5
26	r060	58.89	876.3	383.6
27	r012	774.2	143.7	875.2
28	r078	920.7	847.9	602.0
29	r104	309.0	888.1	842.8
30	r052	583.5	539.0	153.5
31	r007	84.52	432.4	592.5
32	r102	30.83	495.7	274.8
33	r809	13.61	962.8	252.9
34	r029	968.6	322.9	707.1
35	r921	258.5	805.7	107.8
36	r051	803.3	451.5	837.5
37	r655	499.1	118.6	983.0
38	r823	230.7	910.9	281.4
39	r981	111.8	527.7	172.3
40	r082	325.0	827.2	471.1
41	r328	696.7	194.6	757.3

MF2K rzn	keepers id	R1	R2	R3
r095	92	203.6	737.1	326.2
r097	23	898.1	898.8	126.1
r098	11	681.8	948.3	112.6
r102	32	30.83	495.7	274.8
r104	29	309.0	888.1	842.8
r137	53	261.0	442.7	331.8
r142	82	659.5	569.5	558.1
r191	81	744.2	183.5	954.3
r203	89	648.4	91.27	401.7
r207	45	671.8	307.5	298.8
r256	1	552.2	271.0	829.2
r260	94	888.6	958.4	516.5
r273	61	872.8	261.7	364.2
r276	66	137.4	797.5	890.6
r279	54	995.3	620.6	960.4
r298	7	170.5	690.7	802.0
r327	12	39.37	357.3	452.9
r328	41	696.7	194.6	757.3
r361	56	455.0	5.562	946.9
r431	67	912.6	541.0	237.4
r440	59	663.4	77.07	902.6
r465	79	908.9	24.43	615.9
r486	4	484.9	515.1	38.70
r489	97	529.8	136.2	668.9
r506	44	505.9	769.6	460.9
r508	49	478.8	811.7	656.5
r511	80	625.9	851.8	266.1
r515	86	466.9	865.4	302.1
r522	43	404.7	682.8	139.2
r568	64	977.1	344.8	86.60
r571	58	603.1	59.70	444.3
r631	25	616.3	713.6	918.5
r634	68	153.5	469.3	250.2
r640	22	751.6	599.5	766.5
r652	69	179.5	318.3	4.342
r655	37	499.1	118.6	983.0
r657	13	810.8	86.49	886.4
r664	85	544.4	220.1	787.5
r669	62	1.019	572.6	747.9
r694	55	514.0	552.0	574.7
r707	47	67.09	286.8	638.7
r727	98	424.7	648.6	42.97
r752	70	247.5	338.3	214.2
r791	8	821.7	170.2	208.8
r806	99	272.8	179.3	627.4
r808	15	796.7	392.2	423.0
r809	33	13.61	962.8	252.9
r814	48	832.1	383.8	699.4
r823	38	230.7	910.9	281.4
r861	78	44.18	156.2	91.25
r883	51	705.1	748.4	921.9
r902	2	444.3	778.6	439.4
r910	9	124.5	503.6	67.93
r921	35	258.5	805.7	107.8
r922	24	289.7	729.1	676.3
r940	90	196.3	365.2	534.8
r981	39	111.8	527.7	172.3
r982	17	869.8	373.0	530.2
r984	5	947.2	237.0	163.0

keepers id	MF2K rzn	R1	R2	R3
42	r027	579.4	633.7	17.75
43	r522	404.7	682.8	139.2
44	r506	505.9	769.6	460.9
45	r207	671.8	307.5	298.8
46	r073	983.4	582.3	505.1
47	r707	67.09	286.8	638.7
48	r814	832.1	383.8	699.4
49	r508	478.8	811.7	656.5
50	r092	413.8	49.06	689.4
51	r883	705.1	748.4	921.9
52	r045	732.0	415.2	354.7
53	r137	261.0	442.7	331.8
54	r279	995.3	620.6	960.4
55	r694	514.0	552.0	574.7
56	r361	455.0	5.562	946.9
57	r040	337.4	996.2	143.2
58	r571	603.1	59.7	444.3
59	r440	663.4	77.07	902.6
60	r070	362.8	705.3	562.3
61	r273	872.8	261.7	364.2
62	r669	1.019	572.6	747.9
63	r084	320.7	605.5	488.0
64	r568	977.1	344.8	86.60
65	r037	566.1	674.3	416.3
66	r276	137.4	797.5	890.6
67	r431	912.6	541.0	237.4
68	r634	153.5	469.3	250.2
69	r652	179.5	318.3	4.342
70	r752	247.5	338.3	214.2
71	r064	399.4	103.4	189.2
72	r032	637.4	291.5	191.8
73	r004	356.6	249.1	992.4
74	r058	956.1	780.6	587.5
75	r074	91.84	936.0	728.1
76	r002	766.0	252.9	72.50
77	r053	721.0	657.3	221.1
78	r861	44.18	156.2	91.25
79	r465	908.9	24.43	615.9
80	r511	625.9	851.8	266.1
81	r191	744.2	183.5	954.3
82	r142	659.5	569.5	558.1
83	r061	298.5	16.25	648.9
84	r055	186.2	904.5	28.11
85	r664	544.4	220.1	787.5
86	r515	466.9	865.4	302.1
87	r017	593.3	614.0	347.2
88	r001	374.4	487.7	774.5
89	r203	648.4	91.27	401.7
90	r940	196.3	365.2	534.8
91	r034	80.05	62.14	937.3
92	r095	203.6	737.1	326.2
93	r041	531.6	207.4	813.2
94	r260	888.6	958.4	516.5
95	r013	783.4	927.2	310.9
96	r009	384.8	665.2	867.6
97	r489	529.8	136.2	668.9
98	r727	424.7	648.6	42.97
99	r806	272.8	179.3	627.4
100	r024	718.3	980.8	377.4

Table A1-12. Mining factors and MODFLOW flow simulation corresponding to each SECOTP2D vector and replicate

vector	R1			R2			R3		
	TRANS IDX	MF2K RZN	MINP FACT	TRANS IDX	MF2K RZN	MINP FACT	TRANS IDX	MF2K RZN	MINP FACT
1	46	r073	983.4	73	r004	249.1	47	r707	638.7
2	79	r465	908.9	86	r515	865.4	75	r074	728.1
3	93	r041	531.6	91	r034	62.14	70	r752	214.2
4	30	r052	583.5	75	r074	936.0	23	r097	126.1
5	88	r001	374.4	24	r922	729.1	87	r017	347.2
6	36	r051	803.3	41	r328	194.6	51	r883	921.9
7	96	r009	384.8	77	r053	657.3	50	r092	689.4
8	81	r191	744.2	69	r652	318.3	53	r137	331.8
9	95	r013	783.4	36	r051	451.5	94	r260	516.5
10	51	r883	705.1	1	r256	271.0	16	r090	548.9
11	42	r027	579.4	80	r511	851.8	30	r052	153.5
12	85	r664	544.4	70	r752	338.3	78	r861	91.25
13	39	r981	111.8	66	r276	797.5	81	r191	954.3
14	26	r060	58.89	10	r054	402.0	10	r054	976.7
15	94	r260	888.6	55	r694	552.0	49	r508	656.5
16	83	r061	298.5	38	r823	910.9	88	r001	774.5
17	78	r861	44.18	79	r465	24.43	97	r489	668.9
18	19	r010	240.1	100	r024	980.8	96	r009	867.6
19	69	r652	179.5	87	r017	614.0	3	r038	795.4
20	32	r102	30.83	68	r634	469.3	7	r298	802.0
21	62	r669	1.019	71	r064	103.4	33	r809	252.9
22	16	r090	340.7	4	r486	515.1	64	r568	86.60
23	29	r104	309.0	65	r037	674.3	31	r007	592.5
24	77	r053	721.0	2	r902	778.6	76	r002	72.50
25	3	r038	149.2	50	r092	49.06	82	r142	558.1
26	20	r059	937.6	13	r657	86.49	44	r506	460.9
27	68	r634	153.5	57	r040	996.2	1	r256	829.2
28	1	r256	552.2	14	r083	479.9	59	r440	902.6
29	18	r076	435.1	22	r640	599.5	46	r073	505.1
30	27	r012	774.2	93	r041	207.4	20	r059	492.3
31	97	r489	529.8	18	r076	36.28	79	r465	615.9
32	92	r095	203.6	61	r273	261.7	61	r273	364.2
33	76	r002	766.0	56	r361	5.562	83	r061	648.9
34	98	r727	424.7	45	r207	307.5	9	r910	67.93
35	13	r657	810.8	43	r522	682.8	69	r652	4.342
36	70	r752	247.5	96	r009	665.2	42	r027	17.75
37	22	r640	751.6	60	r070	705.3	55	r694	574.7
38	60	r070	362.8	52	r045	415.2	48	r814	699.4
39	7	r298	170.5	20	r059	831.2	34	r029	707.1
40	4	r486	484.9	23	r097	898.8	41	r328	757.3
41	17	r982	869.8	92	r095	737.1	85	r664	787.5
42	58	r571	603.1	59	r440	77.07	74	r058	587.5
43	64	r568	977.1	85	r664	220.1	100	r024	377.4
44	14	r083	857.1	15	r808	392.2	45	r207	298.8
45	15	r808	796.7	76	r002	252.9	80	r511	266.1
46	25	r631	616.3	48	r814	383.8	2	r902	439.4
47	74	r058	956.1	21	r006	756.8	98	r727	42.97
48	99	r806	272.8	51	r883	748.4	72	r032	191.8
49	90	r940	196.3	3	r038	124.6	25	r631	918.5
50	71	r064	399.4	37	r655	118.6	38	r823	281.4
51	35	r921	258.5	7	r298	690.7	58	r571	444.3
52	48	r814	832.1	44	r506	769.6	36	r051	837.5
53	53	r137	261.0	49	r508	811.7	86	r515	302.1
54	75	r074	91.84	19	r010	979.7	73	r004	992.4
55	41	r328	696.7	29	r104	888.1	84	r055	28.11
56	44	r506	505.9	81	r191	183.5	6	r028	391.3
57	10	r054	217.6	28	r078	847.9	39	r981	172.3
58	24	r922	289.7	27	r012	143.7	99	r806	627.4
59	11	r098	681.8	63	r084	605.5	22	r640	766.5
60	56	r361	455.0	42	r027	633.7	28	r078	602.0
61	55	r694	514.0	39	r981	527.7	89	r203	401.7

vector	R1			R2			R3		
	TRANS IDX	MF2K RZN	MINP FACT	TRANS IDX	MF2K RZN	MINP FACT	TRANS IDX	MF2K RZN	MINP FACT
62	63	r084	320.7	12	r327	357.3	40	r082	471.1
63	57	r040	337.4	98	r727	648.6	92	r095	326.2
64	84	r055	186.2	99	r806	179.3	52	r045	354.7
65	86	r515	466.9	25	r631	713.6	57	r040	143.2
66	23	r097	898.1	16	r090	425.9	21	r006	737.6
67	72	r032	637.4	11	r098	948.3	27	r012	875.2
68	5	r984	947.2	30	r052	539.0	37	r655	983.0
69	28	r078	920.7	31	r007	432.4	13	r657	886.4
70	73	r004	356.6	94	r260	958.4	90	r940	534.8
71	33	r809	13.61	17	r982	373.0	91	r034	937.3
72	87	r017	593.3	58	r571	59.70	43	r522	139.2
73	34	r029	968.6	40	r082	827.2	60	r070	562.3
74	40	r082	325.0	8	r791	170.2	8	r791	208.8
75	21	r006	847.3	62	r669	572.6	77	r053	221.1
76	80	r511	625.9	53	r137	442.7	24	r922	676.3
77	49	r508	478.8	74	r058	780.6	17	r982	530.2
78	67	r431	912.6	47	r707	286.8	54	r279	960.4
79	9	r910	124.5	64	r568	344.8	4	r486	38.70
80	91	r034	80.05	9	r910	503.6	95	r013	310.9
81	50	r092	413.8	32	r102	495.7	68	r634	250.2
82	6	r028	104.2	54	r279	620.6	65	r037	416.3
83	59	r440	663.4	82	r142	569.5	14	r083	716.7
84	82	r142	659.5	89	r203	91.27	66	r276	890.6
85	37	r655	499.1	6	r028	228.6	26	r060	383.6
86	61	r273	872.8	35	r921	805.7	12	r327	452.9
87	31	r007	84.52	97	r489	136.2	5	r984	163.0
88	12	r327	39.37	83	r061	16.25	18	r076	851.6
89	65	r037	566.1	67	r431	541.0	71	r064	189.2
90	38	r823	230.7	46	r073	582.3	19	r010	59.88
91	8	r791	821.7	78	r861	156.2	63	r084	488.0
92	89	r203	648.4	84	r055	904.5	15	r808	423.0
93	2	r902	444.3	33	r809	962.8	67	r431	237.4
94	100	r024	718.3	34	r029	322.9	11	r098	112.6
95	54	r279	995.3	95	r013	927.2	32	r102	274.8
96	47	r707	67.09	88	r001	487.7	93	r041	813.2
97	45	r207	671.8	72	r032	291.5	35	r921	107.8
98	52	r045	732.0	5	r984	237.0	56	r361	946.9
99	43	r522	404.7	90	r940	365.2	29	r104	842.8
100	66	r276	137.4	26	r060	876.3	62	r669	747.9

Figure A1-8 and Figure A1-9 show examples of the changes in the T-field due to the mining modifications for a single realization (r440). In Figure A1-8, the color scale is the same between all three plots, and the horizontal black line indicates the location of the longitudinal cross-section (Figure A1-9).

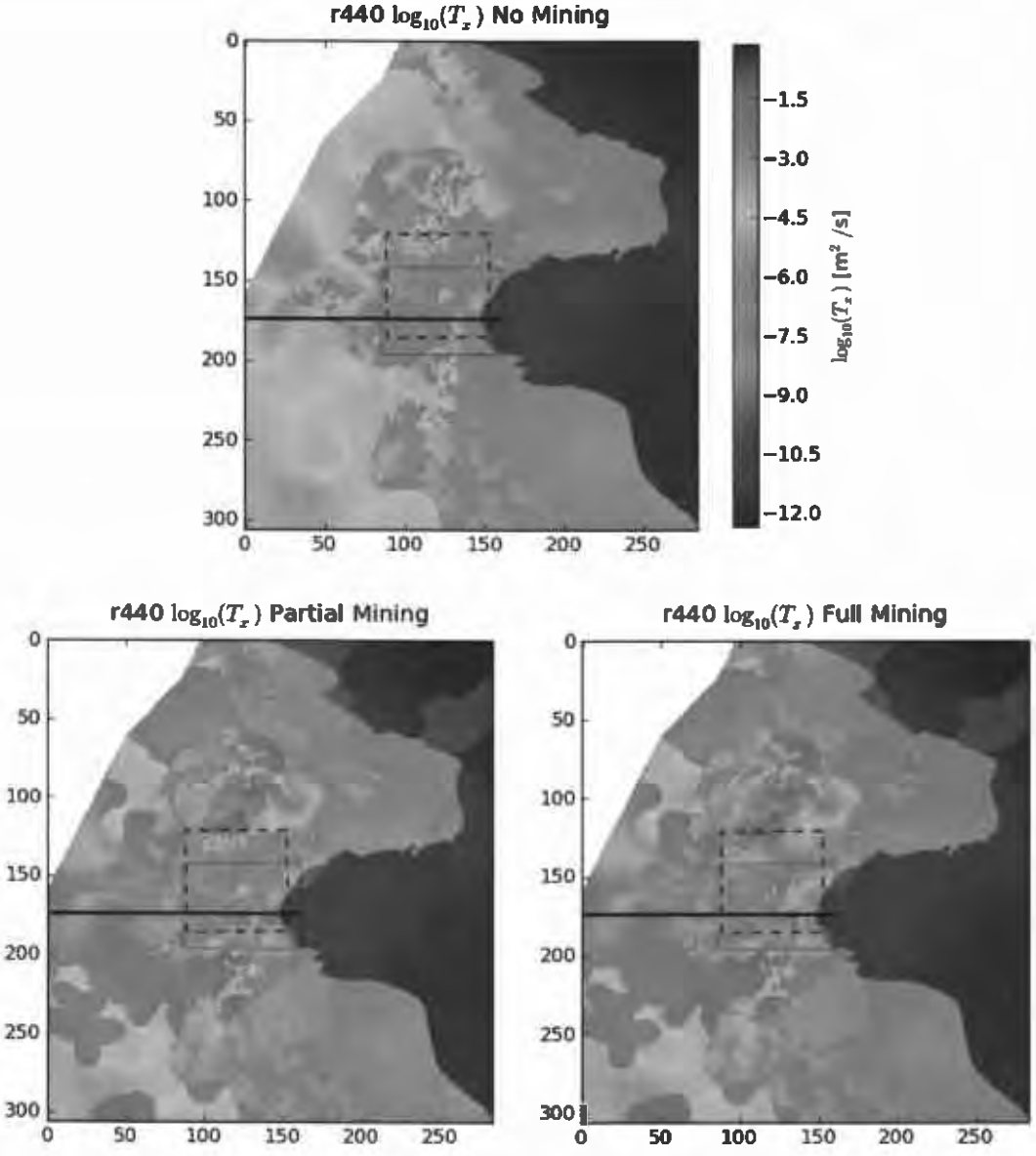

Figure A1-8. Comparison of r440 R2 for non-mined, fully mined, and partially mined scenarios (same color scale in all three plots). Coordinates are cell-based (each cell 100 m on a side); heavy black line indicates location of cross section (Figure A1-9), while LWB (black dashed) and SECOTP2D domain (red) are shown for comparison.

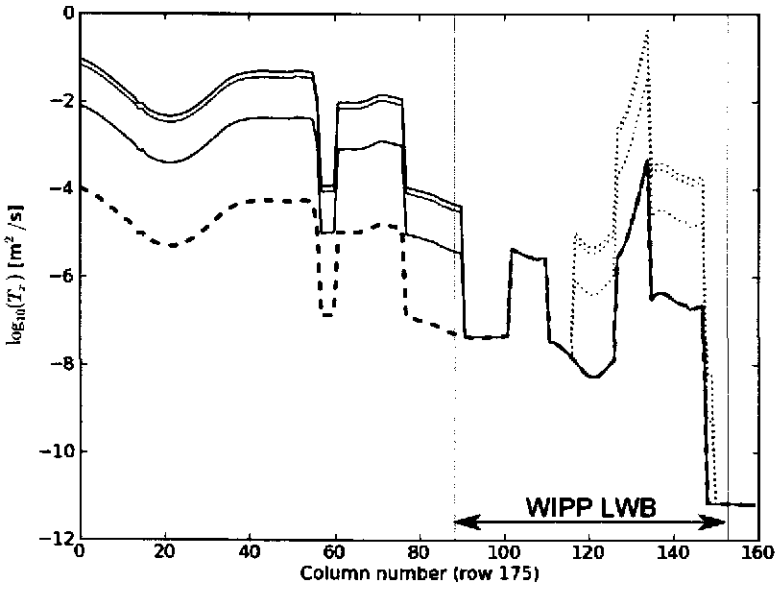

Figure A1-9. Longitudinal cross section through the WIPP LWB (see Figure A1-8 for location) showing all seven T-fields associated with r440. Dashed black line is original non-mined T field, three solid lines are partial-mining scenarios, three dotted lines are full-mining scenarios. Light vertical lines indicate extent of LWB.

A1.5 Step 4 – Run MODFLOW and DTRKMF for Each Realization

Once the mining-modified T-fields and IBOUND arrays are created for the 100 m × 100 m mesh corresponding to each realization and mining scenario, the main Bash shell script `run_mining_mods.sh` (§A4.3) at line 93 calls the Bash shell script `link_input_run_mf_dtrk.sh` (§A4.6), which creates symbolic links to the required MODFLOW (Table A1-13) and DTRKMF (Table A1-14) input files that are the same between all of the 700 scenarios run. Linking is faster and uses less disk space than making hundreds duplicates of common input files. T distribution files (different between each of the 700 realizations) were already put into their corresponding subdirectories by the mining_mods.py script (see Section A1.4.2). The files to be linked are listed in a text input file named `files`, which is read by the Bash shell script. The output from running DTRKMF is used to create CDF plots of the travel time to the WIPP LWB from the C-2737 release point.

Table A1-13. Input and output files for MODFLOW flow calculations (100 m × 100 m grid)

File[1,2]	Remark
Inputs	
Inputs/AP114_Task7/modflow/mf2k_head.ba6[5]	basic package
Inputs/AP114_Task7/modflow/mf2k_head.dis[5]	discretization package
Inputs/AP114_Task7/modflow/mf2k_head.nam[5]	name list
Inputs/AP114_Task7/modflow/mf2k_head.de4.nam[3,5]	name list when DE4 used
Inputs/AP114_Task7/modflow/mf2k_head.oc[5]	output control package
Inputs/AP114_Task7/modflow/mf2k_head.rch[5]	recharge package
Inputs/AP114_Task7/modflow/mf2k_culebra.lmg[5]	LMG solver package
Inputs/AP114_Task7/modflow/mf2k_culebra.lpf[5]	LPF package
Inputs/mf2k_culebra.de4[3]	DE4 solver package
Inputs/AP114_Task7/data/init_bnds.inf[4,5]	non-mined IBOUND array
Inputs/AP114_Task7/data/init_head.mod[5]	initial head array
Inputs/AP114_Task7/data/elev_bot.mod[5]	bottom elevation array
Inputs/AP114_Task7/data/elev_top.mod[5]	top elevation array
Inputs/AP114_Task7/Outputs/*r???*/modeled_A_field.mod[5]	100 A field arrays
Inputs/AP114_Task7/Outputs/*r???*/modeled_R_field.mod[5]	100 R field arrays
Inputs/AP114_Task7/Outputs/*r???*/modeled_S_field.mod[5]	100 S field arrays
Outputs/R*n*/*M*/*r???*/modeled_K_field.mod	600 mined K field arrays
Outputs/R0/*r???*/modeled_K_field.mod	100 non-mined K field arrays
Outputs/data/init_bnds_*M*.inf	2 mined IBOUND arrays
Outputs	
Outputs/R*n*/*M*/*r???*/modeled_head.lst	600 ASCII narrative listings
Outputs/R0/*r???*/modeled_head.lst	100 ASCII narrative listings
Outputs/R*n*/*M*/*r???*/modeled_flow.bud	600 binary flow budgets
Outputs/R0/*r???*/modeled_flow.bud	100 binary flow budgets
Outputs/R*n*/*M*/*r???*/modeled_head.bin	600 binary head files
Outputs/R0/*r???*/modeled_head.bin	100 binary head files
Outputs/R*n*/*M*/*r???*/mf2k_stdout	600 screen outputs
Outputs/R0/*r???*/mf2k_stdout	100 screen outputs
Outputs/R*n*/*M*/*r???*/lmg_err.tmp	error file (not saved)

1. CVS repository MiningMod
2. $n \in \{1,2,3\}$; $M \in$ {full,part}; r??? ∈ {r256, r902, *etc.*} (see Table A1-6)
3. these input files are only used when the LMG solver fails to converge in the allotted time
4. this input file is only used in the 100 non-mined realizations
5. Inputs/AP114_Task7/ is the working directory where files checked out from CVS repository Tfields are located, see (Long, 2010)

The Bash shell script (§A4.6) has two main loops. The first loop (lines 26-70) goes over the 100 original T-fields in their non-mined state (realization R0 in the directory structure — Figure A1-3), setting up input files, running MODFLOW and DTRKMF, for the 100 m grid. The second loop (lines 78-145) does largely the same thing for each of the 600 mining-modified T-fields (100 realizations × 3 replicates R{1,2,3} × 2 mining types {full,part}). Screen output from running MODFLOW and DTRKMF is redirected to text files (mf2k_stdout and dtrkmf_stdout) that are checked into CVS.

Approximately once per every 500 times the algebraic multigrid solver package (LMG) does not converge due to problems associated with large changes in transmissivity as a result of mining (e.g., very high and low transmissivity cells juxtaposed without a smooth transition). To automate the analysis in the case where the model fails to converge, similar to an approach used in AP-114 Task 7 (Hart et al., 2009), a time limit is placed on the execution of MODFLOW when using the LMG solver via the built-in Bash command `ulimit` (see line 8 of the Bash shell script `link_input_run_mf_dtrk.sh`). In each step of the innermost loop, after running MODFLOW, the script checks for the presence of an error file, `lmg_err.tmp` (lines 118-120 in §A4.6), which would be generated if the simulation failed to converge and was terminated by the shell for running longer than the allotted time. When this error file is found, the simulation is restarted using the direct solver package (DE4), which always converges but runs at least 10-20 times slower than the LMG solver. The DE4 solver is part of the standard MODFLOW-2000 executable, but previously was not tested for WIPP use. New tests were added to the test suite to cover the direct solver (Hart, 2010). The time limit defined using `ulimit` is extended to an unlimited amount of time (line 125), and the simulation is re-run with the DE4 solver, concatenating the screen output from this second simulation onto the output from the first simulation (the screen-redirected output file in these restarted cases will include screen output from both simulations).

Table A1-14. Input and output files for DTRKMF particle tracking calculations (100 m × 100 m grid)

File[1,2]	Remark
Inputs	
`Inputs/dtrkmf/wippctrl.inp`	DTRKMF input file
`Inputs/dtrkmf/dtrkmf.in`	DTRKMF screen input
`Outputs/Rn/M/r???/modeled_flow.bud`	600 MF2K mined budgets (see Table A1-13)
`Outputs/R0/r???/modeled_flow.bud`	100 MF2K non-mined budgets
`Inputs/AP114_Task7/data/elev_bot.mod`[3,4]	*Culebra bottom* elevation (`fort.34`)[3]
`Inputs/AP114_Task7/data/elev_top.mod`[3,4]	Culebra top elevation (`fort.33`)[3]
`Inputs/AP114_Task7/modflow/mf2k_head.dis`[4]	MF2K discretization package
Outputs	
`Outputs/Rn/M/r???/dtrk.dbg`	600 ASCII narrative listings
`Outputs/R0/r???/dtrk.dbg`	100 ASCII narrative listings
`Outputs/Rn/M/r???/dtrk.out`	600 ASCII particle tracks
`Outputs/R0/r???/dtrk.out`	100 ASCII particle tracks
`Outputs/Rn/M/r???/dtrkmf_stdout`	600 screen output
`Outputs/R0/r???/dtrkmf_stdout`	100 screen output

1. CVS repository `MiningMod`
2. $n \in \{1,2,3\}$; $M \in$ {full,part}; $r??? \in \{r256, r902, \textit{etc.}\}$ (see Table A1-6)
3. DTRKMF expects these files to be opened on Fortran units 33 and 34, therefore the input files are linked to files named `fort.33` and `fort.34`.
4. `Inputs/AP114_Task7/` is the working directory where files checked out from CVS repository `Tfields` are located, see (Long, 2010)

A1.6 Step 5 – Post-Process DTRKMF Output for Plotting

The main Bash shell script `run_mining_mods.sh` (§A4.3) at lines 104 and 110 calls two Python scripts `combine_dtrkmf_output_for_gnuplot.py` (§A4.7.2) and `extract_dtrkmf_lwb_travel_times.py` (§A4.8.2) to post-process the output from DTRKMF for producing CDF and particle track figures (see Table A1-15). These data are not used further in PA,

but the scripts are included here and the results are checked into CVS for completeness. Each of the 700 realizations produces a DTRKMF output file (`dtrk.out`), where each record or line in the file is a point along the path taken by a particle. The first three columns of output are the time, DTRKMF column, and DTRKMF row indicating the location of each particle. The scripts perform two conversions on this output, printing the results in two different formats.

The row and column output of DTRKMF is converted to UTM NAD27 Zone 13 coordinates (meters), the travel times are adjusted to a 4-m Culebra transport thickness (from the 7.75-m thickness used in the flow calculations), and the results are saved in one of two formats. The Python script `combine_dtrkmf_output_for_gnuplot.py` puts all 100 realizations for each of the seven different mining / replicate combinations into a single file (resulting in seven large text files with two carriage returns between the points associated with particle tracks for each realization); this allows plotting of the "horsetail plots" of particles using Gnuplot (Figure 3-11 through Figure 3-14). The Python script `extract_dtrkmf_lwb_travel_times.py` extracts the last particle location from each file (the last row), saving them to seven different files, each with 100 rows indicating travel time to the WIPP LWB for each of the realizations. These data are then further processed to create an additional seven files with the particles sorted by travel time and a cumulative probability column (going from 0.01 to 1.0 in steps of 0.01), for creation of a CDF plot (Figure 3-9).

Table A1-15. Input and output files for DTRKMF post-processing Python scripts

File[1,2]	Remark
Inputs	
`Inputs/combine_dtrkmf_output_for_gnuplot.in`	Python inputs with filenames and coordinates
`Inputs/extract_dtrkmf_lwb_travel_times.in`	Python inputs with filenames and coordinates
`Outputs/R0/r???/dtrk.out`	100 DTRKMF ASCII particle tracks
`Outputs/Rn/M/r???/dtrk.out`	600 DTRKMF ASCII particle tracks
Outputs	
`Outputs/Summary/dtrk_all_realizations_Rn_M.dat`	6 summaries of 100 full particle traces
`Outputs/Summary/dtrk_nomining_all_realizations.dat`	summary of 100 non-mined particle traces
`Outputs/Summary/wipplwb_results_Rn_M.out`	6 summaries of time and location each realization's particle exits the LWB
`Outputs/Summary/wipplwb_results_Rn_M.sort`	6 summaries of sorted time and cumulative probability for particles exiting the LWB
`Outputs/Summary/wipplwb_results_nomining.out`	summaries of time and location each non-mined realization's particle exits the LWB
`Outputs/Summary/wipplwb_results_nomining.sort`	summary of sorted time and cumulative probability for non-mined realization's particles exiting the LWB

1. CVS repository $CVSLIB/MiningMod
2. $n \in \{1,2,3\}$; $M \in$ {full,part}; r??? $\in \{r256, r902,\ etc.\}$ (see Table A1-6)

A1.7 Step 6 – Convert MODFLOW Input Data to Transport Mesh

The SECOTP2D transport mesh is comprised of 50 m square elements, while the MODFLOW mesh used for calibration is made up of 100 m square elements. Each square 100 m MODFLOW element is sub-divided into four equal-sized square elements, with the properties of the larger cells copied directly into the smaller cells without averaging or smoothing. The boundary head is the only property that is smoothed in the transition from the coarser to the finer mesh. The main Bash shell script `run_mining_mods.sh` (§A4.3) at line 121 calls the Python script `100x100_to_50x50.py` (§A4.9.2 and Table A1-16), which reads in the two MODFLOW IBOUND arrays (full and partial mining), the top and bottom elevation arrays, the starting head array and the four different parameter fields for each realization: 300 non-mined parameter fields (anisotropy, recharge, and storage) + 100 realizations × 3 replicates × 2 mining types for hydraulic conductivity = 900 total expanded parameter fields. The corresponding quadrupled input files are saved to re-run MODFLOW for creating the inputs to SECOTP2D (the original 100 unmodified T-fields are not re-run, since they were only needed for comparison in the particle track and CDF results and figures).

Table A1-16. Input and output files for Python script `100x100_to_50x50.py`

File[1,2,3]	Remark
Inputs	
`Inputs/100x100_to_50x50.in`	Python input file with filenames
`Outputs/data/init_bnds_full.inf`	full-mining IBOUND (see Table A1-7 outputs)
`Outputs/data/init_bnds_part.inf`	partial-mining IBOUND (see Table A1-7 outputs)
`Inputs/AP114_Task7/data/elev_top.mod`[4]	Culebra top elevation field
`Inputs/AP114_Task7/data/elev_bot.mod`[4]	Culebra bottom elevation field
`Inputs/AP114_Task7/data/init_head.mod`[4]	Initial and specified head field
`Inputs/AP114_Task7/Outputs/`*r???*`/modeled_`*W*`_field.mod`[4]	300 calibrated non-mined property fields
`Outputs/R`*n*`/`*r???*`/modeled_K_field.mod`	600 mined T-fields
Outputs	
`Outputs/data/init_bnds_full.inf.50`	full-mining IBOUND for 50 m grid
`Outputs/data/init_bnds_part.inf.50`	partial-mining IBOUND for 50 m grid
`Outputs/data/elev_top.mod.50`	Culebra top elevation for 50 m grid
`Outputs/data/elev_bot.mod.50`	Culebra bottom elevation for 50 m grid
`Outputs/data/init_head.mod.50`	Initial and specified head for 50 m grid
`Outputs/R0/`*r???*`/modeled_`*W*`_field.mod.50`	300 non-mined properties for 50 m grid
`Outputs/R`*n*`/`*r???*`/modeled_K_field.mod.50`	600 mined T-fields for 50 m grid

1. CVS repository `MiningMod`
2. $n \in \{1,2,3\}$; $M \in$ {full,part}; r??? $\in \{r256, r902, \textit{etc.}\}$ (see Table A1-6)
3. $W \in \{A, R, S\}$
4. `Inputs/AP114_Task7/` is the working directory where files checked out from CVS repository `Tfields` are located, see (Long, 2010)

At lines 148-159 of the `100x100_to_50x50.py` Python script, the top and bottom elevations are converted to the finer mesh; Table A1-17 illustrates a small subsection of the two matrices. Since no manipulation besides expanding the grid was necessary, the values were treated as strings (no conversion to floating point) to increase the execution speed of the script and prevent changes to the input data due to conversion. The bottom elevation array was treated similarly; the value in each cell is exactly 7.75 m lower than the top elevation, in both the coarse and finer mesh grids.

Table A1-17. Northwest corner of Culebra top elevation field; top half is original field (4×4), bottom half is expanded field corresponding to same area (8×8). Four and 16 cells are colored-coded to illustrate correspondence.

911.91	911.99	912.08	912.18				
911.89	911.98	912.09	912.21				
911.86	911.96	912.08	912.21				
911.79	911.90	912.03	912.18				
911.91	911.91	911.99	911.99	912.08	912.08	912.18	912.18
911.91	911.91	911.99	911.99	912.08	912.08	912.18	912.18
911.89	911.89	911.98	911.98	912.09	912.09	912.21	912.21
911.89	911.89	911.98	911.98	912.09	912.09	912.21	912.21
911.86	911.86	911.96	911.96	912.08	912.08	912.21	912.21
911.86	911.86	911.96	911.96	912.08	912.08	912.21	912.21
911.79	911.79	911.90	911.90	912.03	912.03	912.18	912.18
911.79	911.79	911.90	911.90	912.03	912.03	912.18	912.18

The initial head array was smoothed (see lines 162-219) along the exterior two rows or columns of the domain and therefore the input file was converted to floating point (unlike the top elevation array). The smoothing was accomplished by first copying the data into the finer mesh without averaging (line 171), then applying a smoothing stencil to the head data (see script lines 180-216 and examples in Table A1-18 and Figure A1-10).

Table A1-18. Initial head along north edge of model domain (row 1) in original (top) and expanded (bottom) starting head.

942.800	942.834	942.867	942.899	942.931

942.780	942.808	942.825	942.842	942.858	942.875	942.891	942.907	942.923	942.939

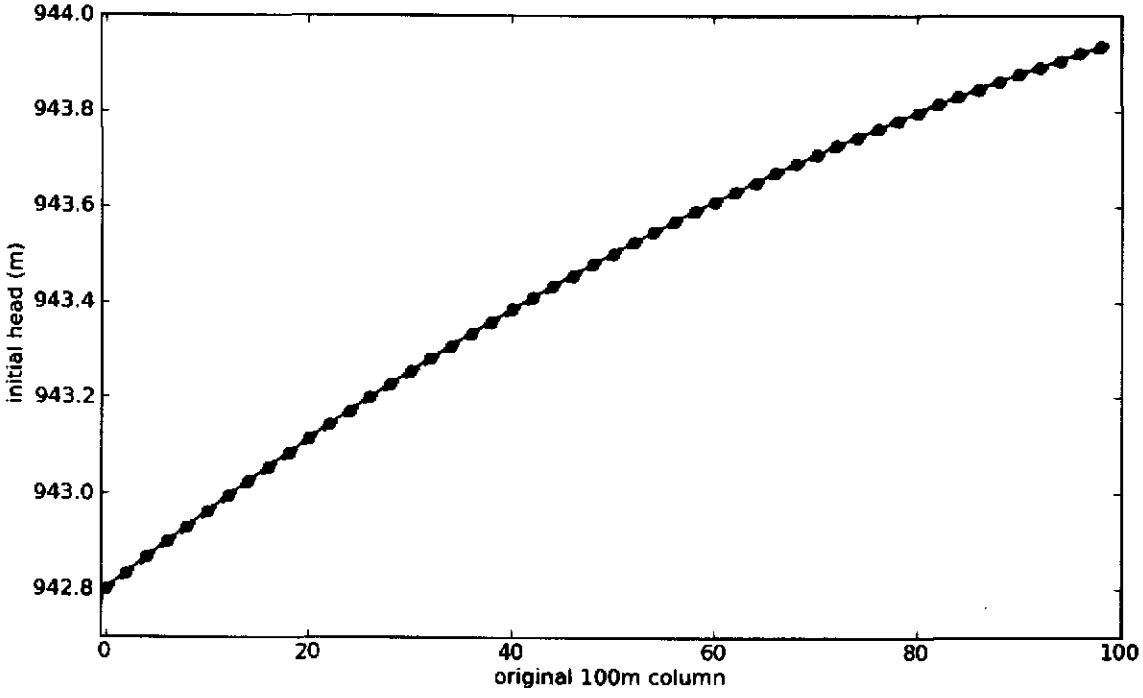

Figure A1-10. Comparison of initial head arrays for original and expanded grids. First 100 columns of first row (north boundary) in the original (red circles) and first two rows of the expanded (blue dots) model

The MODFLOW IBOUND arrays (one for full and another for partial mining) are expanded and copied into the quadrupled grid in the same manner as the top and bottom elevation arrays (see lines 222-240 of script and Table A1-19). The anisotropy (A), recharge (R), and storativity (S) arrays are expanded to the finer grid for each of the 100 realizations – 300 fields total – in lines 243-260 of the Python script. Like the IBOUND arrays, the top & bottom elevation arrays, and the T-fields, these A-, R-, and S-fields are read in and written as strings, avoiding the string-to-float conversion overhead and potential rounding errors.

Table A1-19. Section of IBOUND arrays at southeast corner of domain for 100 m grid (top) and 50 m grid (bottom). -1 (in red) indicates specified head; 1 indicates an active cell.

```
  1   1   1   1  -1  -1  -1  -1  -1  -1
  1   1   1   1   1  -1  -1  -1  -1  -1
  1   1   1   1   1   1  -1  -1  -1  -1
  1   1   1   1   1   1   1  -1  -1  -1
  1   1   1   1   1   1   1   1  -1  -1
  1   1   1   1   1   1   1   1   1  -1
  1   1   1   1   1   1   1   1   1  -1
  1   1   1   1   1   1   1   1   1  -1
  1   1   1   1   1   1   1   1   1  -1
 -1  -1  -1  -1  -1  -1  -1  -1  -1  -1
```

```
  1   1   1   1   1   1   1   1  -1  -1  -1  -1  -1  -1  -1  -1  -1  -1  -1
  1   1   1   1   1   1   1   1  -1  -1  -1  -1  -1  -1  -1  -1  -1  -1  -1
  1   1   1   1   1   1   1   1   1   1  -1  -1  -1  -1  -1  -1  -1  -1  -1
  1   1   1   1   1   1   1   1   1   1  -1  -1  -1  -1  -1  -1  -1  -1  -1
  1   1   1   1   1   1   1   1   1   1   1  -1  -1  -1  -1  -1  -1  -1  -1
  1   1   1   1   1   1   1   1   1   1   1   1  -1  -1  -1  -1  -1  -1  -1
  1   1   1   1   1   1   1   1   1   1   1   1   1  -1  -1  -1  -1  -1  -1
  1   1   1   1   1   1   1   1   1   1   1   1   1   1  -1  -1  -1  -1  -1
  1   1   1   1   1   1   1   1   1   1   1   1   1   1   1  -1  -1  -1  -1
  1   1   1   1   1   1   1   1   1   1   1   1   1   1   1   1  -1  -1  -1
  1   1   1   1   1   1   1   1   1   1   1   1   1   1   1   1   1  -1  -1
  1   1   1   1   1   1   1   1   1   1   1   1   1   1   1   1   1  -1  -1
  1   1   1   1   1   1   1   1   1   1   1   1   1   1   1   1   1  -1  -1
  1   1   1   1   1   1   1   1   1   1   1   1   1   1   1   1   1  -1  -1
  1   1   1   1   1   1   1   1   1   1   1   1   1   1   1   1   1  -1  -1
  1   1   1   1   1   1   1   1   1   1   1   1   1   1   1   1   1  -1  -1
  1   1   1   1   1   1   1   1   1   1   1   1   1   1   1   1   1  -1  -1
 -1  -1  -1  -1  -1  -1  -1  -1  -1  -1  -1  -1  -1  -1  -1  -1  -1  -1  -1
 -1  -1  -1  -1  -1  -1  -1  -1  -1  -1  -1  -1  -1  -1  -1  -1  -1  -1  -1
```

Table A1-20. Filenames of corresponding MODFLOW input files for 100 m and 50 m grid problems

Type	Original 100 m grid input filename	Quadrupled 50 m grid input filename
Culebra elevations	`elev_{top,bot}.mod`	`elev_{top,bot}.mod.50`
Initial heads	`init_head.mod`	`init_head.mod.50`
IBOUND array	`init_bnds_{part,full}.inf`	`init_bnds_{part,full}.inf.50`
T,A,R and S arrays	`modeled_{T,A,R,S}_field.mod`	`modeled_{T,A,R,S}_field.mod.50`
Name list	`mf2k_head.nam`	`mf2k_head_50.nam`
Discretization package	`mf2k_head.dis`	`mf2k_head_50.dis`

Aside from the data arrays, there are a few MODFLOW input files that reference the number of rows and columns in the domain, and therefore must also be modified (see Table A1-20). These input files are modified from the original versions checked out from AP-114 Task 7 in the Bash shell script `run_mining_mods.sh` (§A4.3 lines 130-152) using `sed` substitute `"s/original/replace/"` commands.

A1.8 Step 7 – Run MODFLOW Using the Finer Transport Mesh

Very similar to the Bash shell script `link_input_run_mf_dtrkmf.sh` (§A4.6) discussed in Section A1.5, the main Bash shell script `run_mining_mods.sh` (§A4.3) at line 162 calls the Bash shell script `run_50x50_modflow.sh` (§A4.10), which prepares the required input files and executes MODFLOW for each of the 600 cases (100 realizations × 2 mining types (full or partial) × 3 replicates (R1,R2,R3) =

600), but unlike the script that executes the 100 m MODFLOW model, the script that drives the 50 m MODFLOW model does not additionally run DTRKMF after each flow simulation. The 2-minute time limit is enforced to handle cases where the LMG solver does not converge (see previous discussion for details); the fraction of runs that do not converge for the quadrupled grid is a larger proportion than for the original coarser mesh, approximately 1 in 100. When the LMG solver converges, it does so in less than 10 seconds; the direct solver always works, but has a run time of several minutes.

The only result used from running MODFLOW with the finer mesh is the cell-by-cell flow budget, which is used as an input (after some pre-processing) for SECOTP2D.

A1.9 Step 8 – Convert Binary MODFLOW Budget Files to ASCII for VTRAN2

The main Bash shell script `run_mining_mods.sh` (§A4.3) at line 173 calls the Bash shell script `convert_rename_modflow_50x50_budget.sh` (§A4.11), which loops over the 600 MODFLOW simulations using the finer transport mesh, calling the Python script `budget_bin2ascii.py` (§A4.12) in each directory, renaming and moving the resulting ASCII output to a common directory.

A1.9.1 Binary to ASCII Budget File Conversion

The Python script `budget_bin2ascii.py` (§A4.12.2) reads the MODFLOW binary cell-by-cell budget file, and writes an ASCII file that is comprised of two matrices, separated by a blank line. The binary budget files for the Culebra MODFLOW model have the structure outlined in Table A1-21 (two header records and some data). The first header record is formatted in little-endian format with the following data: two integers (`kstp` and `kper`), a 16-character string (`text`), and three integers (`ncol`, `nrow`, and `nlays` – see line 130 of §A4.12.2). Based on the value in the text field in the first header; the value is either read in as qx (`FLOW RIGHT FACE`), qy (`FLOW FRONT FACE`), or it is skipped (lines 150, 154, and 158). The second header is not used.

Table A1-21. General structure of a data block in a MODFLOW budget files

Header1: (`kstp,kper,text,ncol,nrow,nlay`)
Header2: (discarded)
data

The ASCII budget is saved as two large matrices in scientific notation (specified in line two of the input file) in the natural, unwrapped format. Each matrix for the PABC-2009 MODFLOW model is 307 rows by 284 columns, with a blank line between the matrices.

A single realization (r440) is plotted for each of the two mining scenarios and three replicates in Figure A1-11, to illustrate the effect mining type and mining multiplier have on the resulting transport flow-field, here only showing the portion of the flowfield used for transport analysis in SECOTP2D. The WIPP LWB, WIPP panels, and release point are indicated in the six plots.

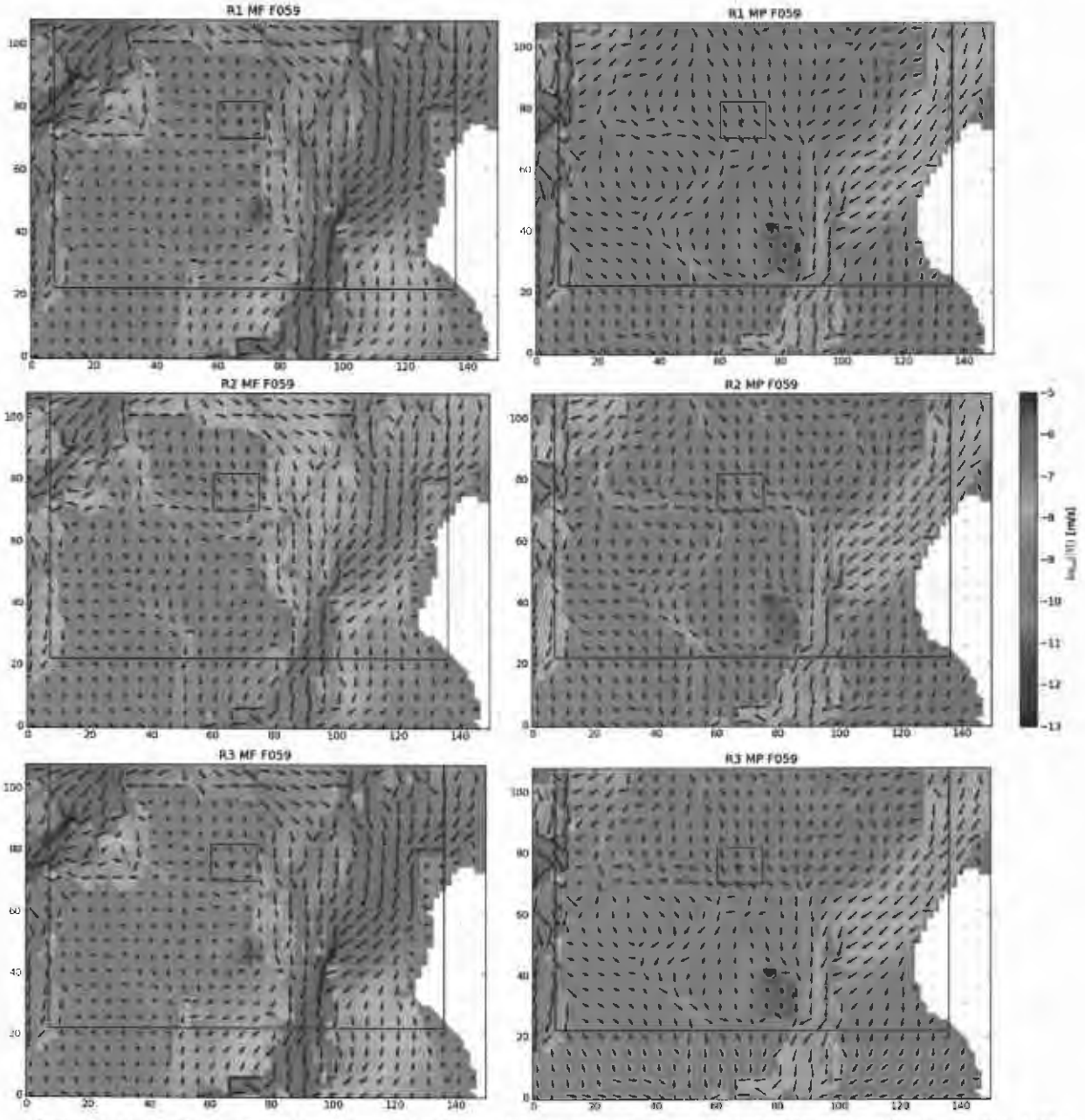

Figure A1-11. VTRAN2 output ($\log_{10}$ Darcy velocity in m/s) corresponding to a single MODFLOW realization (r440). Left column is full mining, right column is partial mining; mining factors: R1=663.4, R2=77.07, R3=902.6. Color scale is the same between all figures, relative vector length scaling is not.

Appendix 2 SECOTP2D Transport Process Narrative

This appendix describes the methods used to organize and implement the SECOTP2D Culebra radionuclide transport calculations.

The SECOTP2D solute transport code is used in conjunction with a preprocessor (PRESECOTP2D) and a postprocessor (POSTSECOTP2D). In addition, several utility codes are used to sample from the probability distributions for subjectively uncertain parameters, define the mesh, set material properties and set model parameters. These codes and their use are described in the following sections. All of these codes are located in the WIPP Software Configuration Management System (SCMS) (Long, 2010) and are run on the WIPP PA Alpha Cluster. All codes used in the analysis, with the exception of the VTRAN2 utility code, are qualified per Nuclear Waste Management Procedure NP 19-1: Software Requirements (Chavez, 2006). The VTRAN2 utility is qualified for use in this analysis per Nuclear Waste Management Procedure NP 9-1: Analyses (Chavez, 2008). VTRAN2 code validation testing is presented in Appendix 3.

The computations are divided into several steps according to the number of times a particular code is run, for efficiency, and to allow for inspection of intermediate results. Digital Command Language (DCL) run control scripts have been written to orchestrate the calculations in each step. Using these scripts, the calculations were performed under formal run control procedures by the WIPP PA Run Control Coordinator. See the PABC-2009 Run Control Report (Long, 2010) for detailed information on the WIPP PA Run Control System.

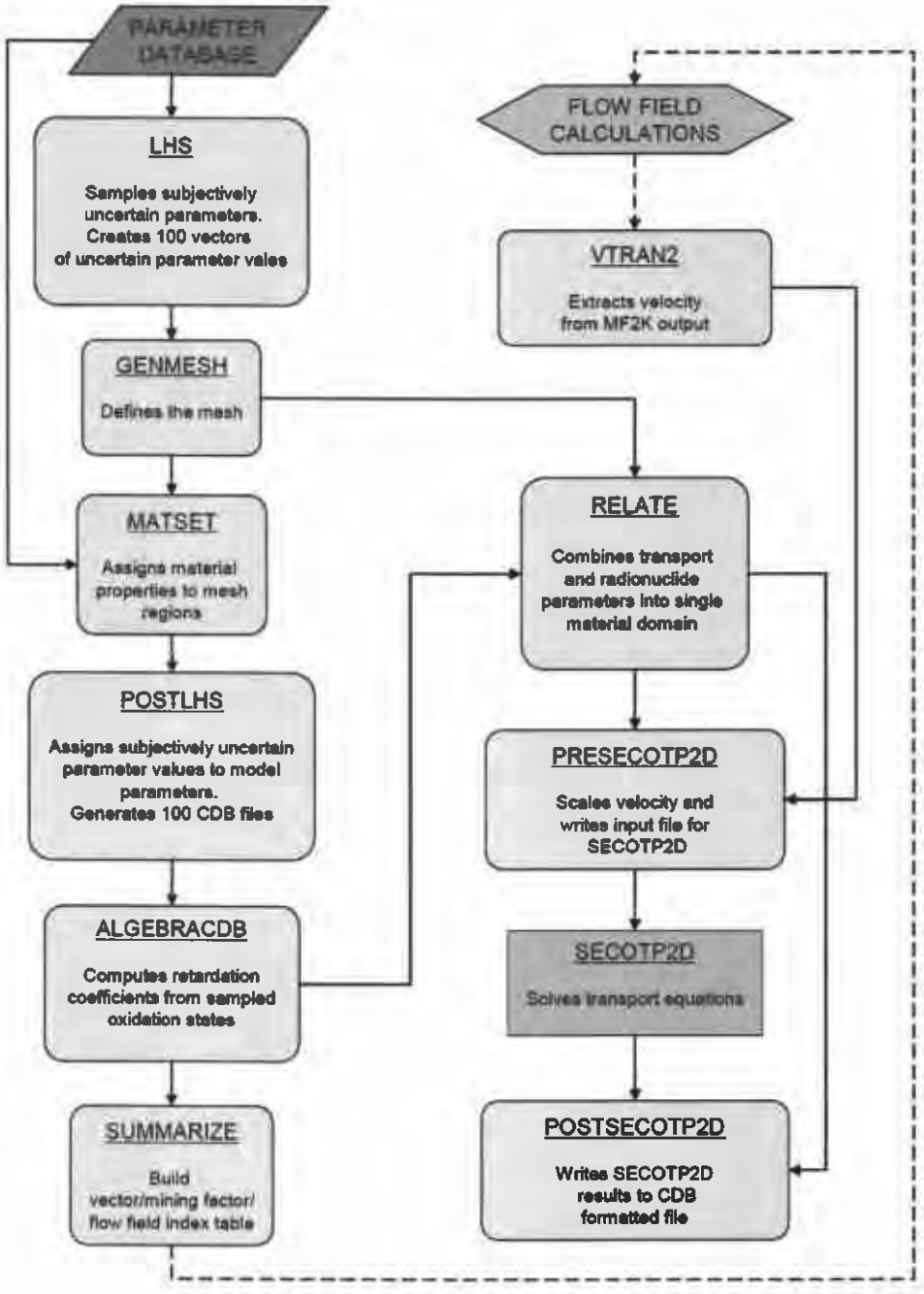

Figure A2-1. Culebra transport calculation flowchart

A2.1 Step 0 – Sampling of Subjectively Uncertain Parameters

The subjectively uncertain Culebra transport parameters were not sampled in isolation. Instead, all subjectively uncertain parameters used in the PABC-2009 were sampled at once at the beginning of the PA calculations in order to impose the appropriate correlations. The Latin hypercube sampling code LHS was used for this purpose. The LHS sampling is reported in (Kirchner, 2010).

A2.2 Step 1 – Mesh Generation and Material Property Assignment

Step 1 is run once. The Step 1 script uses GENMESH version 6.08 to generate the computational grid and MATSET version 9.10 to assign material properties to element blocks. The Step 1 script, GENMESH and MATSET executables, script input and log files, as well as the input and output files for GENMESH and MATSET are listed in Table A2-1.

The GENMESH input file specifies a uniform computational mesh consisting of 50 m square cells, with 151 cells in the x-direction, and 109 cells in the y-direction. All cells are 4 m thick.

The MATSET input file specifies 13 element blocks. Block 1 is for Culebra physical transport properties. Block 2 is for global properties. Block 3 is for reference constants. Blocks 4 through 7 are for the atomic weights and half-lives of radionuclide species ^{241}Am, ^{239}Pu, ^{230}Th, and ^{234}U, respectively. Blocks 8 through 13 are for the distribution coefficients and molecular diffusion coefficients for the species/oxidation state combinations Am(III), Pu(III), Pu(IV), Th(IV), U(IV), and U(VI), respectively.

MATSET assigns the values of deterministic model parameters to the appropriate element blocks. For uncertain model parameters, the median value is assigned to the appropriate element blocks.

Table A2-1. Step 1 input and output files

	File Names	CMS Library	CMS Class
SCRIPT	EVAL_GENERIC_STEP1.COM	LIBPABC09_EVAL	GENERIC_STEP1_V1.4
Input	EVAL_ST2D_PABC09_STEP1.INP	LIBPABC09_EVAL	PABC09-0
Log	EVAL_ST2D_PABC09_STEP1.LOG	LIBPABC09_ST2D	PABC09-0
GENMESH	GM_PA96.EXE	LIBGM	PA96
Input	GM_ST2D_PABC09.INP	LIBPABC09_ST2D	PABC09-0
Output	GM_ST2D_PABC09.CDB	LIBPABC09_ST2D	PABC09-0
Output	GM_ST2D_PABC09.DBG	Not kept	Not kept
MATSET	MATSET_QA0910.EXE	LIBMS	QA0910
Input	MS_ST2D_PABC09.INP	LIBPABC09_ST2D	PABC09-0
Input	GM_ST2D_PABC09.CDB	LIBPABC09_ST2D	PABC09-0
Output	MS_ST2D_PABC09.CDB	LIBPABC09_ST2D	PABC09-0
Output	MS_ST2D_PABC09.DBG	Not kept	Not kept

A2.3 Step 2 – Uncertain Parameter Assignments

Step 2 is run once per replicate. The Step 2 script uses POSTLHS version 4.07A to assign the sampled parameter values to the appropriate element block properties. The Step 2 script, POSTLHS executable, script input and log files, as well as the input and output files for POSTLHS are shown in Table A2-2.

POSTLHS loops over all 100 vectors in the replicate. The result is 100 CAMDAT database (CDB) files per replicate, with each CDB file containing the sampled parameter values for that replicate/vector combination. Sampled values for physical parameters for replicates R1, R2, and R3 are shown in Table A2-3.

Table A2-2. Step 2 input and output files

	File names[1,2]	CMS Library	CMS Class
SCRIPT	EVAL_GENERIC_STEP2.COM	LIBPABC09_EVAL	GENERIC_STEP2_V1.2
Input	EVAL_ST2D_PABC09_STEP2_R*r*.INP	LIBPABC09_EVAL	PABC09-0
Log	EVAL_ST2D_PABC09_STEP2_R*r*.LOG	LIBPABC09_ST2D	PABC09-0
POSTLHS	POSTLHS_QA0407A.EXE	LIBLHS	QA0407A
Input	LHS3_DUMMY.INP	LIBPABC09_LHS	PABC09-0
Input	LHS2_PABC09_R*r*.TRN	LIBPABC09_LHS	PABC09-0
Input	MS_ST2D_PABC09.CDB	LIBPABC09_ST2D	PABC09-0
Output	LHS3_ST2D_PABC09_R*r*_V*vvv*.CDB	LIBPABC09_ST2D	PABC09-0
Output	LHS3_ST2D_PABC09_R*r*.DBG	LIBPABC09_ST2D	PABC09-0

1. $r \in \{1,2,3\}$
2. $vvv \in \{001,002,\ldots,100\}$ for each r

Table A2-3. Sampled values of uncertain SECOTP2D physical parameters for all three replicates

	R1				R2				R3			
vector	APOROS	DPOROS	HMBLKLT	CLIMTIDX	APOROS	DPOROS	HMBLKLT	CLIMTIDX	APOROS	DPOROS	HMBLKLT	CLIMTIDX
1	3.47E-4	1.44E-1	2.73E-1	1.09E+0	4.47E-4	1.81E-1	2.37E-1	1.01E+0	4.72E-4	1.57E-1	4.45E-1	1.11E+0
2	1.17E-4	2.20E-1	1.73E-1	1.17E+0	3.59E-3	1.99E-1	7.37E-2	1.05E+0	2.01E-3	1.81E-1	2.93E-1	1.69E+0
3	3.08E-4	1.33E-1	4.27E-1	1.20E+0	6.14E-3	1.09E-1	3.13E-1	1.90E+0	1.35E-4	1.89E-1	3.62E-1	1.23E+0
4	2.76E-3	1.74E-1	2.10E-1	1.01E+0	2.71E-4	1.19E-1	2.70E-1	1.06E+0	5.82E-3	1.53E-1	1.98E-1	1.20E+0
5	7.70E-3	1.97E-1	4.37E-1	1.04E+0	7.17E-3	1.32E-1	1.14E-1	2.14E+0	8.13E-3	1.76E-1	1.23E-1	1.17E+0
6	1.51E-3	1.07E-1	2.50E-1	1.59E+0	2.40E-4	1.84E-1	4.91E-1	1.23E+0	7.47E-3	1.48E-1	2.92E-1	1.65E+0
7	2.13E-3	1.93E-1	3.47E-1	1.19E+0	1.91E-4	1.84E-1	1.64E-1	1.07E+0	1.99E-3	1.75E-1	3.33E-1	1.01E+0
8	9.46E-4	1.49E-1	3.67E-1	1.12E+0	2.85E-3	1.13E-1	4.82E-1	2.00E+0	3.08E-4	1.73E-1	3.05E-1	1.01E+0
9	8.13E-4	2.09E-1	5.26E-2	1.17E+0	7.52E-4	1.00E-1	2.31E-1	1.14E+0	7.68E-4	1.18E-1	1.27E-1	1.08E+0
10	4.18E-3	1.77E-1	3.98E-1	1.13E+0	2.47E-4	1.15E-1	1.70E-1	1.11E+0	1.39E-3	2.22E-1	1.83E-1	1.16E+0
11	5.22E-4	1.72E-1	2.34E-1	1.15E+0	9.99E-4	1.77E-1	4.40E-1	1.25E+0	1.40E-4	1.68E-1	1.72E-1	1.66E+0
12	2.58E-4	1.89E-1	3.38E-1	1.24E+0	9.51E-3	2.04E-1	2.82E-1	1.08E+0	5.56E-3	1.78E-1	3.79E-1	2.17E+0
13	1.65E-4	1.75E-1	2.99E-1	1.07E+0	9.58E-3	1.06E-1	4.96E-1	1.04E+0	1.50E-4	1.74E-1	8.53E-2	1.12E+0
14	8.58E-3	1.62E-1	4.21E-1	1.24E+0	1.09E-4	1.17E-1	1.84E-1	1.23E+0	3.06E-3	1.30E-1	2.41E-1	1.75E+0
15	1.82E-4	1.36E-1	1.07E-1	1.21E+0	3.59E-4	1.75E-1	3.86E-1	1.21E+0	1.60E-3	1.88E-1	1.42E-1	1.11E+0
16	4.95E-4	1.85E-1	4.66E-1	1.03E+0	1.58E-3	1.22E-1	1.52E-1	1.18E+0	2.02E-4	2.14E-1	1.11E-1	1.19E+0
17	1.46E-4	1.03E-1	1.97E-1	1.16E+0	8.29E-3	1.87E-1	3.35E-1	1.13E+0	4.65E-3	1.20E-1	1.67E-1	1.62E+0
18	4.46E-4	1.90E-1	4.64E-1	1.75E+0	4.98E-4	1.38E-1	8.94E-2	1.14E+0	9.39E-3	2.04E-1	4.09E-1	1.20E+0
19	7.08E-4	1.84E-1	4.99E-1	1.16E+0	3.35E-3	2.27E-1	3.05E-1	1.12E+0	1.62E-4	1.81E-1	4.49E-1	1.10E+0
20	6.27E-4	1.57E-1	3.63E-1	1.62E+0	4.69E-3	1.11E-1	3.69E-1	1.58E+0	2.76E-4	1.02E-1	9.53E-2	1.17E+0
21	1.66E-3	1.63E-1	3.20E-1	1.07E+0	7.10E-4	2.24E-1	3.25E-1	1.20E+0	1.88E-4	1.71E-1	3.86E-1	1.86E+0
22	2.26E-3	1.15E-1	2.86E-1	1.01E+0	1.26E-4	1.64E-1	3.92E-1	1.21E+0	4.35E-3	1.00E-1	1.76E-1	1.20E+0
23	1.20E-4	1.79E-1	4.16E-1	1.14E+0	1.32E-3	1.64E-1	9.21E-2	1.17E+0	9.87E-4	2.28E-1	3.95E-1	2.20E+0
24	1.61E-3	1.02E-1	4.90E-1	1.71E+0	5.63E-3	1.16E-1	2.59E-1	2.08E+0	5.02E-3	1.82E-1	2.45E-1	1.19E+0
25	8.64E-4	1.61E-1	4.08E-1	1.24E+0	1.89E-4	1.53E-1	5.39E-2	1.85E+0	1.75E-3	1.28E-1	4.96E-1	2.15E+0
26	5.27E-3	1.76E-1	2.65E-1	1.13E+0	2.12E-3	2.42E-1	2.73E-1	1.08E+0	6.54E-3	1.51E-1	4.74E-1	1.12E+0
27	1.26E-3	1.04E-1	3.73E-1	1.18E+0	5.26E-3	1.72E-1	1.32E-1	1.93E+0	3.86E-3	1.91E-1	4.39E-1	1.11E+0
28	6.98E-3	1.58E-1	4.86E-1	2.07E+0	8.89E-4	1.29E-1	2.02E-1	1.03E+0	1.56E-4	1.24E-1	1.38E-1	1.87E+0
29	9.67E-4	1.70E-1	2.93E-1	1.13E+0	5.07E-3	1.33E-1	6.58E-2	1.20E+0	1.34E-3	1.83E-1	1.19E-1	2.01E+0
30	1.13E-4	1.81E-1	1.52E-1	1.88E+0	2.05E-3	1.62E-1	2.05E-1	1.10E+0	2.75E-4	1.31E-1	2.77E-1	1.82E+0
31	2.10E-4	1.67E-1	2.40E-1	1.11E+0	2.46E-3	1.86E-1	4.02E-1	1.15E+0	6.68E-4	1.07E-1	2.48E-1	1.13E+0
32	1.09E-3	1.13E-1	8.01E-2	1.17E+0	7.63E-3	1.02E-1	1.74E-1	1.05E+0	9.37E-4	1.17E-1	6.79E-2	1.16E+0
33	1.83E-4	1.24E-1	3.21E-1	1.24E+0	6.20E-4	1.26E-1	1.88E-1	1.06E+0	4.98E-4	1.85E-1	4.67E-1	1.07E+0
34	5.73E-4	1.15E-1	3.03E-1	1.10E+0	1.80E-4	1.74E-1	4.11E-1	1.15E+0	5.54E-4	1.12E-1	3.74E-1	1.22E+0
35	2.30E-4	1.52E-1	2.16E-1	1.19E+0	2.25E-4	1.20E-1	1.24E-1	1.19E+0	5.03E-4	1.66E-1	1.57E-1	1.12E+0
36	4.80E-3	1.21E-1	1.14E-1	1.54E+0	1.80E-3	1.76E-1	4.82E-1	1.08E+0	3.53E-4	1.35E-1	3.17E-1	1.05E+0
37	2.84E-4	1.17E-1	4.05E-1	1.10E+0	1.73E-3	1.12E-1	4.60E-1	1.20E+0	5.43E-4	2.00E-1	7.08E-2	1.19E+0
38	2.65E-4	1.19E-1	2.05E-1	2.15E+0	1.48E-4	1.17E-1	4.16E-1	1.74E+0	3.18E-3	1.77E-1	2.72E-1	1.04E+0
39	5.27E-4	1.76E-1	6.35E-2	1.22E+0	9.44E-4	1.09E-1	4.58E-1	1.09E+0	1.49E-3	1.02E-1	2.01E-1	1.25E+0
40	1.28E-4	1.73E-1	2.47E-1	1.03E+0	3.40E-4	1.03E-1	4.06E-1	1.18E+0	4.18E-4	1.23E-1	4.94E-1	1.15E+0
41	2.28E-4	1.48E-1	4.44E-1	1.03E+0	3.27E-4	1.68E-1	1.93E-1	1.12E+0	2.68E-3	1.15E-1	4.69E-1	1.22E+0
42	8.95E-4	1.66E-1	3.82E-1	1.16E+0	6.40E-3	1.19E-1	1.76E-1	2.05E+0	6.08E-3	1.16E-1	4.89E-1	1.21E+0
43	4.14E-3	1.68E-1	3.56E-1	1.05E+0	2.76E-4	1.24E-1	3.76E-1	1.15E+0	8.48E-3	1.79E-1	4.22E-1	1.02E+0
44	4.67E-3	1.09E-1	1.02E-1	1.04E+0	1.65E-3	1.88E-1	4.31E-1	2.02E+0	4.14E-4	1.71E-1	1.85E-1	1.55E+0
45	5.92E-4	1.20E-1	2.60E-1	1.02E+0	1.10E-4	1.71E-1	3.17E-1	1.67E+0	2.17E-3	1.09E-1	4.80E-1	1.19E+0
46	1.01E-3	2.28E-1	2.56E-1	1.05E+0	1.40E-4	1.80E-1	1.31E-1	1.00E+0	2.62E-4	1.33E-1	4.54E-1	1.14E+0
47	7.56E-4	1.46E-1	1.13E-1	1.15E+0	3.87E-3	1.79E-1	8.44E-2	1.12E+0	3.94E-4	1.62E-1	5.84E-2	1.95E+0
48	5.64E-3	1.39E-1	3.09E-1	1.08E+0	8.81E-3	1.75E-1	2.88E-1	1.20E+0	1.80E-4	1.03E-1	3.29E-1	1.14E+0
49	3.64E-3	1.65E-1	2.83E-1	1.06E+0	2.36E-3	1.65E-1	1.55E-1	1.53E+0	7.01E-4	1.82E-1	3.47E-1	1.24E+0
50	3.49E-3	1.69E-1	1.42E-1	1.06E+0	2.01E-4	1.04E-1	4.36E-1	1.61E+0	1.06E-3	1.72E-1	2.07E-1	1.07E+0
51	3.35E-4	1.82E-1	3.12E-1	1.11E+0	8.22E-4	1.44E-1	1.40E-1	1.16E+0	6.24E-4	1.58E-1	1.16E-1	1.15E+0
52	9.82E-3	1.84E-1	3.84E-1	1.21E+0	4.34E-4	2.11E-1	1.21E-1	1.97E+0	5.97E-4	1.11E-1	4.02E-1	1.57E+0
53	2.04E-3	1.53E-1	2.30E-1	1.02E+0	5.63E-4	1.56E-1	3.97E-1	1.10E+0	1.22E-4	1.54E-1	2.09E-1	1.18E+0
54	1.44E-3	1.30E-1	2.37E-1	1.05E+0	1.11E-3	1.85E-1	1.39E-1	1.22E+0	1.13E-4	1.60E-1	4.19E-1	1.23E+0
55	7.61E-4	1.10E-1	2.78E-1	1.09E+0	4.22E-3	1.82E-1	2.09E-1	1.02E+0	8.35E-4	2.13E-1	4.35E-1	1.18E+0
56	4.39E-3	1.06E-1	2.68E-1	1.00E+0	5.10E-4	1.51E-1	1.48E-1	1.16E+0	2.41E-3	1.19E-1	2.17E-1	1.09E+0
57	2.90E-3	1.10E-1	3.77E-1	1.94E+0	5.35E-4	1.73E-1	4.25E-1	1.81E+0	2.13E-4	1.49E-1	2.71E-1	2.10E+0
58	3.28E-4	1.12E-1	1.35E-1	1.23E+0	2.21E-3	1.69E-1	5.97E-2	1.25E+0	1.56E-3	1.20E-1	2.59E-1	1.21E+0
59	1.24E-3	1.86E-1	4.48E-1	1.19E+0	4.14E-3	1.01E-1	9.79E-2	1.24E+0	6.91E-3	1.13E-1	1.34E-1	1.09E+0
60	6.83E-4	1.73E-1	8.39E-2	1.11E+0	3.63E-4	1.79E-1	2.79E-1	1.09E+0	7.59E-3	1.64E-1	2.87E-1	1.22E+0

	R1				R2				R3			
vector	APOROS	DPOROS	HMBLKLT	CLIMTIDX	APOROS	DPOROS	HMBLKLT	CLIMTIDX	APOROS	DPOROS	HMBLKLT	CLIMTIDX
61	1.91E-3	1.68E-1	3.31E-1	1.23E+0	4.50E-3	1.14E-1	3.51E-1	1.16E+0	2.52E-3	1.05E-1	4.29E-1	2.10E+0
62	1.01E-4	1.28E-1	4.38E-1	1.00E+0	4.01E-4	1.20E-1	3.42E-1	1.64E+0	9.02E-4	1.86E-1	2.81E-1	1.01E+0
63	8.75E-3	1.41E-1	1.57E-1	1.22E+0	1.39E-3	1.67E-1	2.97E-1	1.22E+0	2.39E-4	1.09E-1	2.98E-1	1.06E+0
64	9.38E-3	2.38E-1	1.78E-1	1.81E+0	5.82E-4	1.18E-1	4.71E-1	1.02E+0	2.96E-3	1.30E-1	3.11E-1	1.07E+0
65	2.37E-3	2.03E-1	3.93E-1	1.07E+0	1.70E-4	1.91E-1	4.74E-1	1.01E+0	1.93E-4	1.65E-1	8.08E-2	2.05E+0
66	5.85E-3	1.86E-1	3.28E-1	1.04E+0	2.59E-4	1.89E-1	2.64E-1	1.14E+0	7.25E-4	1.08E-1	4.25E-1	1.04E+0
67	5.22E-3	1.45E-1	1.28E-1	1.25E+0	1.83E-3	1.15E-1	4.22E-1	1.02E+0	3.20E-4	1.70E-1	4.61E-1	1.05E+0
68	2.64E-3	1.03E-1	4.56E-1	2.01E+0	8.61E-3	1.88E-1	2.53E-1	1.17E+0	8.25E-4	1.37E-1	3.36E-1	1.98E+0
69	2.56E-3	1.54E-1	1.46E-1	1.21E+0	1.16E-3	1.31E-1	3.56E-1	1.09E+0	7.07E-3	1.17E-1	5.41E-2	1.08E+0
70	1.10E-3	1.11E-1	4.72E-1	1.57E+0	6.89E-3	1.45E-1	4.49E-1	1.19E+0	1.73E-4	1.77E-1	3.13E-1	1.03E+0
71	4.26E-4	1.28E-1	2.19E-1	1.98E+0	1.93E-3	2.19E-1	3.58E-1	1.05E+0	3.67E-4	2.36E-1	3.38E-1	1.21E+0
72	1.98E-4	1.78E-1	4.74E-1	2.02E+0	3.03E-4	1.06E-1	1.03E-1	1.01E+0	1.27E-4	1.61E-1	1.50E-1	1.05E+0
73	1.07E-4	1.80E-1	7.48E-2	1.66E+0	1.48E-3	1.49E-1	2.43E-1	1.79E+0	2.28E-3	1.43E-1	2.56E-1	1.17E+0
74	4.01E-4	2.46E-1	4.91E-1	2.18E+0	7.55E-3	1.46E-1	3.31E-1	1.19E+0	6.32E-4	1.58E-1	3.53E-1	2.24E+0
75	3.68E-4	1.88E-1	8.65E-2	2.08E+0	3.16E-3	2.48E-1	6.96E-2	1.74E+0	1.28E-3	1.39E-1	7.34E-2	1.79E+0
76	1.34E-3	1.64E-1	4.82E-1	1.15E+0	1.10E-3	1.61E-1	2.28E-1	1.11E+0	9.70E-3	1.64E-1	9.49E-2	1.08E+0
77	8.20E-3	1.87E-1	1.62E-1	1.22E+0	1.05E-3	1.06E-1	1.07E-1	1.70E+0	5.36E-3	1.14E-1	3.72E-1	1.02E+0
78	6.13E-3	1.61E-1	1.26E-1	1.07E+0	1.27E-3	1.11E-1	1.96E-1	1.10E+0	1.01E-4	1.69E-1	2.13E-1	1.24E+0
79	3.81E-3	1.42E-1	3.57E-1	1.02E+0	4.77E-4	1.86E-1	4.52E-1	2.19E+0	1.01E-3	1.83E-1	8.82E-2	1.07E+0
80	1.77E-3	1.25E-1	5.64E-2	1.50E+0	7.69E-4	1.12E-1	2.18E-1	1.03E+0	4.97E-3	1.14E-1	4.12E-1	1.13E+0
81	3.04E-3	1.19E-1	1.65E-1	1.18E+0	1.20E-3	1.40E-1	1.61E-1	1.11E+0	1.06E-4	1.25E-1	4.84E-1	1.01E+0
82	2.00E-4	2.33E-1	1.72E-1	1.04E+0	1.65E-4	1.82E-1	2.45E-1	1.24E+0	3.69E-3	1.19E-1	3.60E-1	1.53E+0
83	3.19E-3	1.79E-1	2.89E-1	1.91E+0	2.57E-3	1.28E-1	3.07E-1	1.13E+0	4.08E-3	1.62E-1	3.90E-1	1.93E+0
84	2.50E-4	1.63E-1	4.11E-1	2.11E+0	2.93E-4	1.48E-1	5.86E-2	1.07E+0	2.23E-4	1.45E-1	1.64E-1	1.04E+0
85	1.37E-4	2.22E-1	9.59E-2	1.12E+0	6.72E-4	1.60E-1	3.01E-1	1.15E+0	2.83E-3	1.10E-1	1.62E-1	1.71E+0
86	4.68E-4	1.88E-1	1.84E-1	1.10E+0	1.24E-4	1.83E-1	4.87E-1	2.12E+0	2.93E-4	1.86E-1	3.23E-1	1.18E+0
87	1.44E-4	1.17E-1	4.54E-1	1.08E+0	1.19E-4	1.68E-1	3.20E-1	1.07E+0	4.41E-3	1.41E-1	2.36E-1	1.16E+0
88	1.53E-3	1.34E-1	7.10E-2	1.08E+0	3.29E-3	1.36E-1	2.51E-1	2.19E+0	1.15E-3	1.87E-1	1.05E-1	1.91E+0
89	2.45E-3	1.23E-1	1.93E-1	1.84E+0	4.94E-3	1.78E-1	3.70E-1	1.22E+0	1.17E-4	1.12E-1	2.26E-1	1.10E+0
90	3.39E-3	1.83E-1	6.59E-2	1.12E+0	2.94E-3	1.62E-1	2.23E-1	1.18E+0	8.97E-3	1.89E-1	3.69E-1	1.11E+0
91	1.18E-3	1.12E-1	1.85E-1	2.20E+0	3.76E-3	1.66E-1	3.45E-1	1.55E+0	2.31E-3	1.80E-1	2.64E-1	1.00E+0
92	3.93E-4	1.14E-1	9.39E-2	1.23E+0	1.02E-4	1.58E-1	8.14E-2	1.12E+0	3.41E-4	1.06E-1	2.32E-1	1.03E+0
93	6.39E-3	1.38E-1	1.21E-1	1.19E+0	6.35E-4	1.90E-1	3.63E-1	1.05E+0	1.10E-3	1.42E-1	1.90E-1	1.23E+0
94	1.84E-3	1.17E-1	3.36E-1	1.14E+0	8.34E-4	1.55E-1	3.96E-1	1.02E+0	3.53E-3	2.49E-1	4.55E-1	1.14E+0
95	7.32E-3	1.08E-1	3.47E-1	1.10E+0	1.32E-4	1.35E-1	2.14E-1	2.25E+0	1.73E-3	1.84E-1	2.23E-1	1.06E+0
96	6.64E-3	1.82E-1	1.38E-1	2.24E+0	2.16E-4	1.63E-1	1.11E-1	1.23E+0	1.89E-3	2.44E-1	1.45E-1	1.13E+0
97	6.56E-4	1.71E-1	4.31E-1	1.78E+0	5.80E-3	1.71E-1	3.80E-1	1.03E+0	2.50E-4	1.90E-1	3.97E-1	1.25E+0
98	1.56E-4	1.59E-1	3.88E-1	1.70E+0	3.89E-4	2.34E-1	2.89E-1	1.86E+0	3.34E-3	1.46E-1	5.92E-2	1.09E+0
99	2.98E-4	1.00E-1	2.23E-1	1.17E+0	1.54E-4	1.41E-1	4.43E-1	1.24E+0	1.26E-3	1.68E-1	9.97E-2	1.06E+0
100	1.72E-4	1.16E-1	2.03E-1	1.20E+0	2.70E-3	1.70E-1	4.68E-1	1.04E+0	4.42E-4	1.66E-1	3.44E-1	1.02E+0

A2.4 Step 3 – Evaluation of Oxidation-State-Dependent Parameters

Step 3 is run once per replicate. The Step 3 script loops over all 100 vectors in the replicate, invoking ALGEBRACDB version 2.35 and RELATE version 1.43 for each vector. The Step 3 script, ALGEBRACDB and RELATE executables, script input and log files, as well as the input and output files for ALGEBRACDB and RELATE are shown in Table A2-5

The ALGEBRACDB code selects the sampled distribution coefficient and molecular diffusion coefficient based upon the value of the sampled oxidation state. The distribution coefficient is then used to calculate the retardation factor. The RELATE code is used to remove all element blocks except for CULEBRA (all required non-CULEBRA block properties are transferred to the CULEBRA block). Sampled values for chemical parameters are shown in Table A2-4.

Table A2-4. Sampled values of uncertain K_d parameter; OXSTAT indicates whether the U and Pu species are in their high or low oxidation states for each vector and replicate

	R1					R2					R3				
vector	OXSTAT	MKD_AM	MKD_PU	MKD_TH	MKD_U	OXSTAT	MKD_AM	MKD_PU	MKD_TH	MKD_U	OXSTAT	MKD_AM	MKD_PU	MKD_TH	MKD_U
1	H	9.72E-2	7.50E-3	5.64E+0	3.33E-3	H	1.48E-2	2.81E+0	2.00E-3	6.33E-5	H	1.93E-2	2.69E+0	1.82E-3	7.67E-4
2	L	4.37E-2	1.59E-1	3.10E-3	2.39E-1	H	6.49E-3	1.20E-3	1.47E-1	9.95E-3	L	7.98E-3	1.88E-2	8.79E-4	1.96E+0
3	L	3.69E-2	6.52E-2	1.16E-3	6.87E-3	H	9.00E-2	2.34E-1	4.44E-3	1.60E-4	L	2.49E-1	1.26E-1	4.72E-2	7.22E-2
4	L	1.42E-1	4.79E-2	1.86E-2	7.19E-1	H	2.11E-1	5.68E-2	1.09E-1	4.05E-5	H	1.01E-1	5.38E-4	3.26E-3	5.22E-5
5	H	1.08E-2	2.89E-3	1.44E-3	3.69E-3	L	1.59E-2	1.26E-2	7.98E-2	3.75E+0	L	6.67E-3	2.45E-1	1.05E+0	2.71E+0
6	H	1.59E-2	2.79E-1	2.10E-2	6.62E-5	H	4.13E-2	3.23E+0	3.64E-3	7.24E-3	H	1.16E-1	5.02E-2	1.26E-1	9.94E-3
7	L	7.19E-2	9.35E-3	3.90E-3	6.44E-4	L	6.20E-2	7.90E-2	2.58E-2	2.90E-3	H	1.18E-2	3.04E+0	6.74E-1	7.37E-5
8	H	1.72E-1	5.51E-1	8.03E+0	1.52E-3	L	9.30E-3	3.38E-1	9.35E-1	6.07E-4	L	1.23E-2	2.91E-2	8.85E-2	4.91E-2
9	H	3.14E-2	2.22E-1	1.25E-2	1.31E-4	L	1.29E-2	2.24E-2	9.49E-2	1.12E+0	L	3.25E-1	2.39E-2	1.06E-3	2.07E+0
10	L	7.90E-3	2.66E-1	3.29E-2	3.47E+0	H	2.24E-1	1.37E-3	9.89E-3	1.80E-3	L	1.32E-1	2.10E-1	2.95E+0	8.87E-2
11	L	2.30E-1	1.51E-1	4.30E-2	3.07E-3	H	4.57E-2	1.68E-2	7.25E-2	1.82E-4	H	5.01E-2	3.28E+0	3.95E-2	3.29E-4
12	H	2.02E-2	3.50E-1	1.18E+0	2.98E-3	H	6.40E-2	1.51E+0	6.45E-4	3.51E-4	H	1.93E-1	7.72E+0	2.43E-1	8.22E-3
13	H	1.04E-2	4.18E+0	6.29E+0	4.95E-3	H	1.39E-1	3.28E-3	7.38E-1	2.57E-3	L	5.21E-3	1.46E-1	7.64E-4	1.24E-3
14	H	1.41E-2	1.96E-1	2.01E+0	4.43E-4	L	2.02E-2	9.20E-2	2.63E-1	1.88E-1	L	3.16E-1	9.72E-2	1.81E-1	3.42E+0
15	L	6.89E-2	1.72E-1	2.66E-1	3.95E+0	L	1.11E-2	1.83E-2	8.75E-4	5.91E-3	L	4.44E-2	9.35E-3	2.07E-1	1.01E+0
16	L	3.00E-2	1.10E-1	5.44E-1	7.64E-4	H	2.15E-2	1.22E-2	2.83E-2	6.79E-3	H	1.04E-1	2.11E-3	5.79E-3	1.12E-3
17	L	5.91E-3	1.57E-2	1.80E+0	3.53E-2	H	1.82E-2	6.45E-3	4.36E-1	2.62E-4	L	2.20E-1	4.00E-1	4.99E-2	1.45E-3
18	L	6.21E-3	7.70E-3	4.58E-3	1.14E-2	H	1.74E-1	6.89E+0	6.43E+0	2.54E-4	H	1.61E-2	8.72E-2	1.38E-3	3.16E-3
19	L	8.78E-3	5.57E-2	1.84E-3	1.49E-2	L	2.93E-1	5.59E-2	1.12E-2	1.63E+0	H	1.59E-1	8.01E-3	2.34E-3	2.97E-4
20	L	7.65E-2	1.03E-2	6.66E-2	1.32E-3	L	2.36E-1	1.69E-2	6.49E-1	2.26E-3	L	8.56E-2	1.79E-2	3.26E-2	1.27E-2
21	L	9.23E-2	2.50E-2	1.80E-3	6.74E+0	L	1.15E-2	5.24E-2	1.19E+0	6.70E-2	L	5.69E-2	3.33E-2	7.43E-1	5.57E-4
22	L	8.04E-2	9.42E-2	1.50E-1	3.49E-3	L	2.76E-2	1.18E-1	6.86E-4	3.98E-1	H	3.45E-1	8.09E-2	6.83E-3	5.72E-4
23	H	7.70E-3	5.78E-1	1.10E-3	4.10E-5	L	5.73E-2	2.01E-1	1.64E-1	3.14E-2	H	1.75E-1	1.36E+0	2.77E-1	6.29E-4
24	H	3.58E-1	3.02E+0	4.24E-1	1.28E-3	H	2.62E-1	7.93E-1	2.18E+0	1.32E-2	L	2.74E-1	9.08E-3	1.70E-2	7.66E-4
25	L	2.82E-1	1.07E-2	1.34E-1	1.43E-3	H	2.99E-2	8.83E-2	1.69E-2	1.33E-3	H	4.03E-2	1.41E-2	7.34E-2	7.00E-3
26	H	1.50E-2	6.72E-2	8.25E-2	1.05E-4	H	2.45E-1	7.76E-4	8.35E+0	1.17E-3	L	2.06E-2	8.08E-3	1.08E-1	7.64E-1
27	H	2.13E-2	1.71E-1	1.01E+0	1.61E-4	H	7.06E-2	1.94E-2	1.67E-3	2.26E-4	H	1.30E-2	1.96E-2	7.36E-3	7.13E-4
28	L	2.61E-1	5.79E-3	9.06E-2	2.20E-1	H	6.17E-3	7.50E-2	1.08E-3	7.87E-4	L	5.73E-3	3.64E-2	3.52E+0	2.22E-1
29	L	1.98E-1	2.06E-1	1.56E+0	2.05E-3	H	3.61E-1	1.21E+0	2.39E+0	1.75E-2	L	8.25E-3	3.91E-2	4.13E+0	1.10E-1
30	H	1.33E-2	1.13E-3	6.24E-4	1.69E-2	L	2.84E-2	5.78E-3	3.57E+0	1.30E-1	L	7.09E-2	2.02E-1	5.69E-4	9.66E-3
31	L	1.63E-1	3.96E-2	1.11E-2	1.10E+0	L	5.17E-3	2.80E-2	1.00E-3	6.94E+0	L	2.90E-2	1.93E-1	3.61E-2	6.42E-3
32	L	2.67E-2	1.64E-1	1.03E-1	4.84E-3	H	5.16E-2	6.11E-2	3.88E-2	6.58E-5	H	2.31E-1	4.30E-3	1.57E-3	6.51E-3
33	L	1.44E-2	1.04E-1	2.67E+0	8.06E-3	H	1.55E-1	2.36E-2	5.27E-3	5.60E-5	H	9.69E-3	1.55E-1	1.52E-2	5.74E-3
34	L	1.13E-1	2.00E-2	5.03E-1	4.21E-1	L	1.12E-1	7.72E-3	5.05E+0	1.48E+0	H	2.70E-2	2.75E-2	2.25E+0	9.60E-4
35	L	3.51E-2	3.04E-2	3.45E-1	9.31E-1	L	4.73E-2	1.07E-1	4.68E-1	1.96E-3	L	6.94E-3	1.73E-2	7.04E+0	1.83E+0
36	H	3.25E-2	1.51E+0	8.98E-4	3.77E-3	H	1.24E-1	8.21E-4	1.92E-3	1.51E-2	H	1.11E-1	5.87E-3	5.36E-2	6.48E-5
37	L	6.25E-3	2.29E-1	7.44E-3	2.19E-2	L	3.21E-2	4.49E-2	5.28E-2	8.98E-3	H	1.51E-1	4.57E-1	2.48E-3	4.77E-4
38	L	1.14E-2	1.87E-1	1.99E-1	1.52E-3	H	7.35E-3	1.13E-2	4.05E+0	1.86E-2	L	1.76E-2	5.02E-2	9.72E-3	8.23E-2
39	L	1.28E-2	1.25E-2	1.42E+0	4.79E-1	H	2.04E-2	2.05E-1	7.47E-4	3.78E-4	H	7.59E-2	3.85E-1	3.49E-1	3.72E-5
40	H	6.56E-2	2.15E+0	2.18E-1	7.35E-3	L	3.65E-2	3.95E-1	3.53E-2	4.74E-2	H	9.19E-3	8.32E-4	1.48E-1	1.81E-2
41	L	6.09E-2	1.84E-2	9.16E-3	2.70E-2	L	3.43E-2	1.01E-2	1.28E-2	4.96E-3	L	2.11E-1	1.35E-1	9.75E+0	2.83E-3
42	L	5.51E-3	6.36E-3	2.24E+0	4.24E-3	L	4.42E-2	1.10E-1	1.27E-1	4.33E-1	H	4.14E-2	3.14E-1	2.10E-2	1.16E-4
43	L	2.08E-1	1.22E-1	9.67E-4	1.79E-3	L	9.96E-2	1.21E-2	5.80E+0	3.54E-3	L	3.88E-2	1.31E-2	3.40E-1	1.74E-3
44	H	9.35E-3	2.11E-3	4.36E+0	8.66E-4	L	5.46E-2	1.73E-1	5.84E-2	6.24E+0	H	2.99E-1	3.51E-1	6.18E+0	1.30E-2
45	H	1.28E-1	6.20E-4	7.58E-2	9.95E-4	H	1.40E-1	1.48E-2	1.20E-3	4.22E-3	H	7.50E-2	6.55E+0	1.62E+0	1.46E-4
46	H	2.26E-2	2.06E-2	1.07E+0	3.20E-5	L	3.89E-1	1.86E-1	3.20E-1	8.30E-3	H	1.23E-1	1.93E-2	1.57E-1	2.04E-4
47	L	7.37E-2	1.34E-2	2.73E-3	6.59E-2	H	5.00E-2	6.38E-1	5.22E-2	1.11E-3	H	1.70E-2	1.27E-3	3.91E-3	2.29E-4
48	H	1.22E-2	3.11E-3	8.46E-3	5.19E-4	H	1.06E-1	4.01E-3	8.22E-3	3.34E-5	L	9.40E-2	2.75E-1	8.70E-1	3.88E+0
49	L	1.76E-1	1.18E-2	2.21E-3	3.43E-1	H	1.24E-2	1.17E-1	1.44E+0	1.38E-4	H	1.85E-1	1.48E+0	8.31E-3	3.66E-4
50	L	4.48E-2	8.85E-2	1.67E-2	2.85E-3	H	7.30E-2	1.02E-3	1.06E+0	4.78E-4	H	5.44E-3	1.01E+0	1.16E-2	1.39E-3
51	H	1.29E-1	3.27E-1	3.04E+0	1.86E-2	L	6.90E-2	2.24E-1	5.85E-4	3.05E-3	H	1.61E-1	3.77E-2	8.03E+0	6.78E-5
52	H	2.07E-2	1.19E+0	1.38E+0	7.82E-3	L	9.72E-3	1.10E-2	8.15E+0	1.62E-1	H	7.11E-3	6.34E-3	1.14E-3	3.47E-5
53	H	3.32E-2	4.77E-2	5.58E-2	5.79E-3	H	5.85E-3	1.66E+0	8.98E-1	5.05E-4	L	1.21E-1	6.55E-2	1.39E+0	2.50E-3
54	H	1.66E-2	1.24E-2	3.27E-1	1.85E-3	L	8.44E-2	1.52E-1	1.45E-2	1.63E-2	L	1.56E-2	6.95E-3	5.86E-2	3.50E-2
55	L	5.02E-3	6.82E-3	4.63E+0	1.54E+0	L	3.50E-2	2.41E-2	2.99E+0	3.74E-1	H	2.02E-2	1.68E-1	7.97E-1	1.27E-3
56	H	2.40E-2	1.12E+0	1.37E-2	4.28E-3	H	3.70E-1	1.83E-3	1.51E-3	2.08E-4	L	2.34E-2	6.34E-3	6.65E-4	2.66E-1
57	H	8.94E-3	3.91E-1	7.37E-4	2.84E-4	H	2.79E-1	5.04E-2	2.52E+0	3.76E-5	L	2.49E-2	1.60E-2	1.41E-2	1.95E-1
58	L	7.27E-3	3.96E-1	5.04E-2	9.42E+0	H	1.20E-1	1.15E-1	1.76E-1	1.12E-2	H	1.46E-2	9.64E+0	9.54E-1	2.86E-4
59	L	1.79E-2	4.30E-2	2.54E-1	3.83E-1	L	9.81E-2	3.70E-2	2.94E-2	6.22E-1	H	2.37E-1	2.48E-3	6.83E-2	5.22E-4

	R1					R2					R3				
vector	OXSTAT	MKD_AM	MKD_PU	MKD_TH	MKD_U	OXSTAT	MKD_AM	MKD_PU	MKD_TH	MKD_U	OXSTAT	MKD_AM	MKD_PU	MKD_TH	MKD_U
60	H	5.40E-2	5.17E-3	6.63E-3	1.55E-2	H	1.87E-2	2.23E-3	4.04E-3	5.88E-5	L	5.47E-2	1.28E-2	2.37E-2	5.33E-1
61	L	4.16E-2	8.40E-2	4.07E-3	1.27E+0	L	2.95E-1	1.45E-2	3.02E-3	4.75E-3	L	8.95E-2	8.35E-2	4.93E-3	9.88E-3
62	L	1.04E-1	1.75E-2	8.67E-1	4.61E+0	L	7.51E-3	3.15E-1	2.06E-1	7.12E-1	L	6.36E-2	5.74E-3	4.14E-1	5.94E-2
63	L	1.78E-2	6.87E-2	2.47E-2	9.16E-1	H	3.47E-1	5.16E-1	6.44E-3	1.41E-3	H	2.14E-2	5.83E-2	1.23E-3	1.27E-4
64	L	4.75E-2	2.33E-2	8.33E+0	5.43E-3	H	4.01E-2	1.52E-3	1.34E-2	6.19E-3	L	3.53E-2	5.04E-3	2.61E-2	1.09E+0
65	H	2.45E-2	1.62E-3	7.02E+0	1.03E-2	H	1.29E-1	1.13E+0	9.76E+0	8.39E-5	H	6.32E-3	8.21E-1	1.24E-2	4.40E-3
66	H	2.78E-2	7.53E-1	2.36E-3	1.29E-2	H	9.34E-2	8.91E+0	7.52E-3	1.99E-3	L	1.11E-2	4.48E-2	2.94E-1	3.06E-1
67	H	1.51E-1	7.05E-3	3.07E-2	1.34E-4	H	8.07E-3	6.39E+0	2.15E-2	4.60E-3	L	1.38E-1	1.44E-2	5.13E+0	1.39E-1
68	H	1.01E-1	2.87E-2	5.30E-3	1.19E-4	L	1.76E-2	7.19E-3	4.00E-2	7.67E-4	H	6.93E-2	2.27E+0	8.56E+0	8.29E-5
69	L	1.59E-1	5.13E-2	2.94E-1	1.77E+0	L	5.91E-2	5.58E-3	4.75E-2	1.26E+0	H	1.85E-2	3.67E+0	1.03E-1	2.65E-4
70	H	3.97E-1	4.54E-2	9.69E+0	1.50E-4	L	2.47E-2	1.54E-1	9.00E-3	3.44E+0	L	1.42E-1	2.96E-1	5.92E-1	5.01E+0
71	H	5.91E-2	1.40E-3	1.18E-1	4.00E-4	L	1.80E-1	1.81E-1	2.32E-2	4.79E-1	L	2.59E-1	4.87E-2	4.72E-3	2.29E+0
72	L	8.40E-3	1.28E-2	3.68E-2	3.19E+0	H	2.40E-2	3.64E+0	5.51E-1	2.79E-4	L	1.09E-2	2.60E-1	1.32E-1	1.28E-1
73	H	2.07E-1	6.84E-1	5.60E-3	1.16E-3	H	8.12E-2	1.29E-1	2.01E+0	1.22E-2	H	1.99E-1	4.53E+0	5.24E-4	3.78E-3
74	H	8.45E-2	2.58E-3	1.11E-1	9.83E-5	H	1.08E-2	1.65E-3	4.81E+0	4.62E-5	L	5.97E-2	4.13E-2	4.09E-3	1.67E-2
75	H	1.88E-2	5.14E+0	2.32E+0	3.41E-4	L	5.59E-3	8.68E-2	3.73E-1	1.14E+0	L	1.38E-2	1.72E-1	1.29E+0	9.05E-1
76	H	2.19E-1	4.77E+0	9.97E-3	1.21E-2	H	6.96E-3	7.12E-4	1.76E+0	1.40E-2	L	1.03E-2	3.43E-1	3.62E-3	4.47E-3
77	H	6.92E-3	1.71E-2	3.38E+0	4.51E-5	L	3.19E-1	3.17E-2	9.98E-2	8.18E-1	L	6.26E-2	1.67E-2	2.71E-2	1.38E+0
78	L	5.06E-2	2.56E-2	1.28E-3	1.17E+0	L	2.25E-2	7.15E-2	3.91E-1	5.80E-2	L	3.41E-2	4.39E-2	4.71E+0	3.15E-2
79	L	1.22E-1	2.98E-1	5.20E-4	7.64E-2	L	2.48E-1	6.16E-3	5.25E-4	1.26E-2	L	4.79E-2	3.34E-1	2.99E-2	7.30E-4
80	L	3.34E-1	1.94E-1	5.71E-1	5.74E-4	L	1.05E-2	3.35E-2	2.53E-1	1.78E+0	L	8.06E-2	1.08E-1	2.84E-3	6.05E-1
81	L	6.74E-3	1.88E-2	1.49E-2	1.86E-2	H	3.09E-2	3.35E-2	1.58E+0	1.99E-2	L	5.17E-2	1.87E-1	6.43E-3	1.90E-2
82	L	1.35E-1	8.01E-2	4.57E-2	2.48E-2	L	8.15E-3	2.65E-1	3.00E-1	2.72E-1	L	7.63E-3	1.15E-1	5.62E-1	2.76E+0
83	H	8.89E-2	6.17E+0	7.21E-1	6.19E-4	L	1.62E-1	1.01E-1	6.05E-1	2.03E-3	H	5.49E-3	6.43E-2	4.35E-1	6.65E-4
84	H	5.27E-2	5.72E-3	1.68E-1	1.11E-2	L	1.65E-2	2.82E-1	1.30E-3	2.69E-2	H	2.86E-1	5.12E+0	2.06E-3	1.36E-4
85	L	2.38E-1	3.48E-2	6.60E-1	6.16E-2	L	2.07E-1	1.64E-1	2.82E-3	9.85E-4	H	3.63E-2	1.50E-2	2.21E-1	2.75E-3
86	H	5.64E-2	5.00E-1	2.28E-2	9.18E-3	L	1.83E-1	1.12E-2	1.30E+0	2.65E+0	L	4.48E-2	3.15E-1	8.30E-2	1.61E-3
87	H	2.82E-1	1.60E+0	4.02E+0	7.12E-5	L	1.17E-1	2.64E-2	6.58E-2	5.50E-1	L	9.24E-3	2.03E-2	4.94E-1	1.43E-1
88	H	4.06E-2	4.20E-2	1.57E-3	1.44E-3	H	3.83E-2	4.84E-3	2.46E-3	1.23E-4	H	9.57E-2	1.57E+0	1.91E+0	4.53E-5
89	L	5.39E-3	8.55E-3	5.43E+0	1.65E-1	L	1.51E-2	2.65E-2	1.43E-3	2.97E-1	H	3.93E-1	3.06E-1	1.82E-2	4.81E-3
90	H	1.86E-1	5.90E-4	3.89E-1	7.65E-5	H	2.54E-2	5.89E+0	8.04E-1	3.09E-4	L	3.81E-1	1.31E-1	1.82E+0	7.09E-1
91	L	2.95E-1	1.34E-1	7.83E-1	1.95E-1	L	6.62E-3	9.52E-2	3.15E+0	9.47E-2	H	3.23E-2	5.72E+0	2.37E+0	3.54E-3
92	H	1.17E-2	3.22E-2	6.10E-2	6.62E-3	L	1.34E-2	3.53E-2	5.89E-3	3.16E+0	H	3.06E-2	1.87E-3	9.53E-4	7.49E-3
93	H	3.08E-1	2.24E-3	3.27E+0	1.62E-3	H	1.91E-1	2.04E-3	6.78E-3	1.56E-2	L	6.07E-3	2.84E-1	1.15E+0	4.43E+0
94	H	3.73E-1	1.89E-1	2.76E-2	3.66E-5	L	7.73E-2	3.84E-2	1.84E-2	7.10E-4	H	2.61E-2	2.23E-2	1.68E-3	2.41E-4
95	L	3.92E-2	3.59E-1	3.39E-3	1.46E-1	H	9.15E-3	2.51E-2	1.31E-1	5.97E-4	H	8.81E-3	4.06E-2	6.02E+0	1.75E-2
96	H	2.50E-1	2.67E+0	5.82E-4	5.41E-3	H	8.71E-3	4.13E+0	3.45E-3	7.62E-3	H	1.73E-1	3.70E-3	1.05E-2	3.07E-5
97	L	1.12E-1	2.55E-1	1.78E-1	3.51E-1	L	1.47E-1	4.15E-2	4.28E+0	4.33E-3	H	2.80E-2	1.33E-1	7.40E-4	2.15E-3
98	H	9.65E-3	1.79E-3	7.46E-4	4.29E-5	L	3.31E-1	2.48E-2	2.25E-1	1.20E-1	H	2.23E-2	1.70E-3	3.19E+0	1.21E-3
99	H	2.58E-2	9.64E-2	6.43E-3	1.79E-3	H	1.40E-2	1.80E-1	7.39E+0	1.50E-4	L	3.57E-1	2.54E-1	2.75E+0	5.72E+0
100	H	3.41E-1	7.64E-4	2.65E-3	4.13E-3	H	5.39E-3	5.10E-3	2.26E-3	1.16E-4	H	1.33E-2	5.89E-4	3.80E+0	9.68E-3

Table A2-5. Step 3 script, executables, input, and output files

	File names[1,2]	CMS Library	CMS Class
SCRIPT	EVAL_ST2D_STEP3.COM	LIBPABC09_EVAL	ST2D_STEP3_V1.0
Input	EVAL_ST2D_PABC09_STEP3_Rr.INP	LIBPABC09_EVAL	PABC09-0
Log	EVAL_ST2D_PABC09_STEP3_Rr.LOG	LIBPABC09_ST2D	PABC09-0
ALGEBRACDB	ALGEBRACDB_PA96.EXE	LIBALG	PA96
Input	ALG_ST2D_PABC09.INP	LIBPABC09_ST2D	PABC09-0
Input	LHS3_ST2D_PABC09_Rr_Vvvv.CDB	LIBPABC09_ST2D	PABC09-0
Output	ALG_ST2D_PABC09_Rr_Vvvv.CDB	LIBPABC09_ST2D	PABC09-0
Output	ALG_ST2D_PABC09_Rr_Vvvv.DBG	Not kept	Not kept
RELATE	RELATE_PA96.EXE	LIBREL	
Input	REL_ST2D_PABC09.INP	LIBPABC09_ST2D	PABC09-0
Input	GM_ST2D_PABC09.CDB	LIBPABC09_ST2D	PABC09-0
Input	ALG_ST2D_PABC09_Rr_Vvvv.CDB	LIBPABC09_ST2D	PABC09-0
Output	REL_ST2D_PABC09_Rr_Vvvv.CDB	LIBPABC09_ST2D	PABC09-0
Output	REL_ST2D_PABC09_Rr_Vvvv.DBG	Not kept	Not kept

1. $r \in \{1,2,3\}$
2. $vvv \in \{001,002,\ldots,100\}$ for each r

A2.5 Step 4 – Tabulation of Mining Factors and Flow-Field Indices

Step 4 is run once per replicate. The Step 4 script fetches all 100 ALGEBRACDB output files produced in Step 3, then runs SUMMARIZE version 2.20 on them. The Step 4 script, SUMMARIZE executable, script input and log files as well as the input and output files for SUMMARIZE are shown in Table A2-6.

The SUMMARIZE code is used to construct tables of the uncertain mining factor parameter CULEBRA:MINP_FAC and the flow-field index parameter CULEBRA:TRANSIDX (flow-field index = INT[CULEBRA:TRANSIDX]. These tables are transferred to the WIPP PA Pentium Cluster for use in the Culebra flow calculations (see Section A1.4). Each table contains four columns: the vector number, time (not used), MINP_FAC, and TRANSIDX.

Table A2-6. Step 4 script, executables, input and output files

	File names[1,2]	CMS Library	CMS Class
SCRIPT	EVAL_ST2D_STEP4.COM	LIBPABC09_EVAL	GENERIC_STEP4_V1.0
Input	EVAL_ST2D_PABC09_STEP4_Rr.INP	LIBPABC09_EVAL	PABC09-0
Output	SUM1_ST2D_PABC09_Rr.INP	LIBPABC09_ST2D	PABC09-0
Log	EVAL_ST2D_PABC09_STEP4_Rr.LOG	LIBPABC09_ST2D	PABC09-0
SUMMARIZE	SUMMARIZE_QA_0220.EXE	LIBSUM	QA0220
Input	SUM1_ST2D_PABC09_Rr.INP	LIBPABC09_ST2D	PABC09-0
Input	ALG_ST2D_PABC09_Rr_Vvvv.CDB	LIBPABC09_ST2D	PABC09-0
Output	SUM1_ST2D_PABC09_Rr.TBL	LIBPABC09_ST2D	PABC09-0
Output	SUM1_ST2D_PABC09_Rr.LOG	Not kept	Not kept
Output	SUM1_ST2D_PABC09_Rr_ERROR.LOG	Not kept	Not kept

1. $r \in \{1,2,3\}$
2. $vvv \in \{001,002,\ldots,100\}$ for each r

A2.6 Step 5 – Flow-Field Extraction

The rules for converting the MODFLOW output data (volumetric flux) to SECOTP2D input data (Darcy velocity) described in Section 4.1.2 were implemented in the Fortran code VTRAN2. VTRAN2 neither models physical phenomena nor solves differential equations that model physical phenomena. Rather, it is a utility code that processes the output data produced by a modeling code and formats that data for use in another modeling code. VTRAN2 has been qualified for this analysis per Nuclear Waste Management Procedure NP 9-1: Analysis (Chavez, 2008). The source code listing, build information, and verification testing for VTRAN2 are provided in Appendix 3.

The VTRAN2 code takes five command line arguments, four required and one optional. All arguments are the names of input or output files, descriptions of which follow:

1. ***cmd_file*** is an input ASCII format command file. The command file describes the MODFLOW mesh, the SECOTP2D mesh, the x- and y-direction offsets between the two meshes and the format that was used to write the MODFLOW velocities into the ASCII budget file (see below).
2. ***bud_file*** is an input ASCII format MODFLOW budget file containing the volumetric flux values for each cell in the groundwater flow modeling mesh.
3. ***trn_file*** is a binary format output file containing the groundwater flow velocities for the transport domain (including the ghost cells) in the format required by the SECOTP2D transport code.
4. ***dbg_file*** is an output ASCII format diagnostic/debug file containing information about the VTRAN2 run.
5. ***txt_file*** is an optional output ASCII format file containing the same data as the `trn_file`.

A sample command line that executes VTRAN2 is shown below:

```
$ VTRAN2 TEST.CMD TEST.BUD TEST.TRN TEST.DBG TEST.TXT
```

The flow-fields obtained from the Culebra flow calculations introduce the concept of mining scenarios into the transport calculations. The Step 5 script is run once per replicate/mining scenario combination. The script loops over all 100 flow-field indices in the replicate/scenario combination, using the VTRAN2 utility code to extract the mining-modified Culebra flow-fields (corresponding to the sub-domain used in the Culebra transport calculations) from the MODFLOW output files. The script, executable, script input and log files, along with the input and output files for the VTRAN2 utility are shown in Table A2-7.

Table A2-7. Step 5 script, executable, input and output files

	File Names[1,2,3]	CMS Library	CMS Class
SCRIPT	EVAL_ST2D_STEP5.COM	LIBPABC09_EVAL	ST2D_STEP5_V1.0
Script Input	EVAL_ST2D_PABC09_STEP5_R*r*_M*m*.INP	LIBPABC09_EVAL	PABC09-0
Log	EVAL_ST2D_PABC09_STEP5_R*r*_M*m*.LOG	LIBPABC09_MF2K	PABC09-0
VTRAN2	VTRAN2.EXE	LIBPABC09_MF2K	VTRAN2_V1.1
Input	VTRAN2_PABC09.INP	LIBPABC09_MF2K	PABC09-0
Input	MF2K_PABC09_R*r*_M*m*_F*fff*.OUT	LIBPABC09_MF2K	PABC09-0
Output	MF2K_PABC09_R*r*_M*m*_F*fff*.TRN	LIBPABC09_MF2K	PABC09-0
Output	VTRAN2_ST2D_PABC09_R*r*_M*m*_F*fff*.DBG	Not kept	Not kept

1. $r \in \{1,2,3\}$
2. $m \in \{F, P\}$
3. $fff \in \{001,002,\ldots,100\}$ for each r and each m

A2.7 Step 6 – Transport Calculations

The Step 6 script runs the SECOTP2D suite of codes (PRESECOTP2D version 1.22, SECOTP2D version 1.41A, and POSTSECOTP2D version 1.04) to calculate radionuclide transport through the Culebra. Two DCL run control scripts are used in Step 6. The master script is invoked once for each replicate/scenario combination. The master script loops over all 100 vectors for each replicate/scenario combination. For each vector, the master script performs the following steps:

- Use GROPECDB version 2.12 to extract the value of the CULEBRA:TRANSIDX parameter from the ALGEBRACDB output file generated in Step 3. The value of this parameter indicates the flow-field index to use with the vector.
- Write input file for slave script
- Run the slave script

The slave script then runs PRESECOTP2D, SECOTP2D, and POSTSECOTP2D for that vector. Both the master and the slave scripts produce log files to record their actions. In the paragraphs that follow, the input and output files for the generic case are described, then the procedure followed to re-run certain replicate/scenario/vector combinations with a modified PRESECOTP2D input file to overcome numerical stability problems is described.

Table A2-8. Step 6 script, executables, input and output files (general case)

	File Names[1,2,3,4,5]	CMS Library	CMS Class
MASTER SCRIPT	EVAL_ST2D_STEP6_MASTER.COM	LIBPABC09_EVAL	ST2D_STEP6_V1.0
Input	EVAL_ST2D_PABC09_STEP6_R*r*_M*m*.INP	LIBPABC09_EVAL	PABC09-0
Log	EVAL_ST2D_PABC09_STEP6_R*r*_M*m*.LOG	LIBPABC09_ST2D	PABC09-0
SLAVE SCRIPT	EVAL_ST2D_STEP6_MASTER.COM	LIBPABC09_EVAL	ST2D_STEP6_V1.0
Log	EVAL_ST2D_PABC09_STEP6_R*r*_M*m*_V*vvv*.LOG	LIBPABC09_ST2D	PABC09-0
GROPECDB	GROPECDB_PA96.EXE	LIBGR	PA96
Input	GROPE_ST2D_PABC09.INP	LIBPABC09_ST2D	PABC09-0
Input	ALG_ST2D_PABC09_R*r*_V*vvv*.CDB	LIBPABC09_ST2D	PABC09-0
Output	GROPE_ST2D_PABC09_R*r*_M*m*_V*vvv*.TXT	Not kept	Not kept
PRESECOTP2D	PRESECOTP2D_QA0122.EXE	LIBST2D	QA0122
Input	ST2D1_PABC09.INP	LIBPABC09_ST2D	PABC09-0
Input	REL_ST2D_PABC09_R*r*_V*vvv*.CDB	LIBPABC09_ST2D	PABC09-0
Input	MF2K_PABC09_R*r*_M*m*_F*fff*.TRN	LIBPABC09_MF2K	PABC09-0
Output	ST2D2_PABC09_R*r*_M*m*_V*vvv*.INP	Not kept	Not kept
Output	ST2D1_PABC09_R*r*_M*m*_V*vvv*.PRP	Not kept	Not kept
Output	ST2D1_PABC09_R*r*_M*m*_V*vvv*.VEL	Not kept	Not kept
Output	ST2D1_PABC09_R*r*_M*m*_V*vvv*.DBG	Not kept	Not kept
SECOTP2D	SECOTP2D_QA0141A.EXE	LIBST2D	QA0141A
Input	ST2D2_PABC09_R*r*_M*m*_V*vvv*.INP	Not kept	Not kept
Input	ST2D1_PABC09_R*r*_M*m*_V*vvv*.PRP	Not kept	Not kept
Input	ST2D1_PABC09_R*r*_M*m*_V*vvv*.VEL	Not kept	Not kept
Output	ST2D2_PABC09_R*r*_M*m*_V*vvv*.BIN	Not kept	Not kept
Output	ST2D2_PABC09_R*r*_M*m*_V*vvv*.DBG	Not kept	Not kept
POSTSECOTP2D	POSTSECOTP2D_QA0104.EXE	LIBST2D	QA0104
Input	ST2D2_PABC09_R*r*_M*m*_V*vvv*.BIN	Not kept	Not kept
Input	REL_ST2D_PABC09_R*r*_V*vvv*.CDB	LIBPABC09_ST2D	PABC09-0
Output	ST2D3_PABC09_R*r*_M*m*_V*vvv*.CDB	LIBPABC09_ST2D	PABC09-0
Output	ST2D3_PABC09_R*r*_M*m*_V*vvv*.DBG	LIBPABC09_ST2D	PABC09-0

1. $r \in \{1,2,3\}$
2. $m \in \{F, P\}$
3. $fff \in \{001,002,\ldots,100\}$ for each m
4. $vvv \in \{001,002,\ldots,100\}$ for each m
5. flow-field index matched with number through the TRANSIDX parameter for each vector

In the few instances where SECOTP2D failed due to numerical instability using the generic numerical control parameters, a new PRESECOTP2D input file was submitted by the analyst and the case was re-run in a manner similar to that described above. In order to track these cases, a special tag ("MOD") was inserted into the PRESECOTP2D input file name, as well as the master script input file and log file names. The vectors for each combination of replicate and mining scenario that required modified PRESECOTP2D input files are shown in Table A2-9. The modified file names for each vector are shown in

Table A2-10. Other files have the same names as for the generic case. Files in the libraries from the previous runs were replaced with files from the re-run.

Table A2-9. Step 6 modified input runs

	Full Mining (MF)	Partial Mining (MP)
R1	6, 35, 63, 65, 88, 95	46, 88
R2	-	2, 9, 26, 27, 40, 99
R3	49	32, 52, 53, 69

Table A2-10. Step 6 modified input run file names

	File Names[1,2,3]	CMS Library	CMS Class
MASTER SCRIPT			
Input	EVAL_ST2D_PABC09_STEP6_Rr_Mm_Vvvv_MOD.INP	LIBPABC09_EVAL	PABC09-0
Log	EVAL_ST2D_PABC09_STEP6_Rr_Mm_Vvvv_MOD.LOG	LIBPABC09_ST2D	PABC09-0
PRESECOTP2D			
Input	ST2D1_PABC09_Rr_Vvvv.INP	LIBPABC09_ST2D	PABC09-0

1. $r \in \{1,2,3\}$
2. $m \in \{F, P\}$
3. $vvv \in \{001,002, \ldots ,100\}$ for each m

Appendix 3 VTRAN2 Utility

This appendix provides the source listing, build information, and a summary of testing for the Fortran utility code VTRAN2. VTRAN2 was originally written for PABC-2004 (Lowry and Kanney, 2005) and was used to extract the groundwater flow velocity data from ASCII versions of the MODFLOW cell-by-cell flow budget files (see Sections 4.1.1 and A2.6). The VTRAN source code and input files were trivially changed from PABC-2004 to accommodate a MODFLOW grid 568 elements wide (previously 448 elements).

A3.1 VTRAN2 Build Info

The Fortran source code file for the VTRAN2 utility (`VTRAN2.F`) is shown in Table A3-1. This file is archived in CMS library `LIBPABC09_MF2K`, class `VTRAN2_V1.1` on the WIPP PA Alpha Cluster.

Table A3-1. `VTRAN2.F` source listing

```
      PROGRAM VTRAN

C
C
C     nrowmf - number of rows cells in the mf2k grid
C     ncolmf - number of columns in the mf2k grid
C
C     ncx - number of cells in x-direction in the st2d grid
C     ncy - number of cells in y-direction in the st2d grid
C
C     jshftx - x offset of transport domain (# of cells in col direction)
C     ishfty - y offset of transport domain (# of cells in row direction)
C
C
      PARAMETER (nfmat = 2, mxfile=5)

      CHARACTER*80 author, date, title
      CHARACTER*80 filenm(mxfile)
      CHARACTER*80 fmat(nfmat),rdfmat
      CHARACTER*80 fnmcmd, fnmbud, fnmtrn, fnmdbg, fnmvel

      INTEGER ierr
      INTEGER iunscr, iuncmd, iunbud, iuntrn, iundbg, iunvel
      INTEGER nfiles, nfiler
      INTEGER nrowmf, ncolmf, ncx, ncy
      INTEGER istart, ishift, jstart, jshift
      INTEGER match, irdfmt
      DOUBLE PRECISION time
      DOUBLE PRECISION ayz_inv, axz_inv, dx, dy, dz
      DOUBLE PRECISION, ALLOCATABLE :: qxin(:,:), qyin(:,:)
      DOUBLE PRECISION, ALLOCATABLE :: qxout(:,:), qyout(:,:)

      LOGICAL wrtvel

C----------------------
C.....Setup
C----------------------

C.....Assign file unit numbers

      nfiles = 5

      iunscr = 6
      iuncmd = 11
      iunbud = 12
      iuntrn = 13
      iundbg = 14
      iunvel = 15

C.....Valid budget file input formats
C     modified these format statements to accommidate the 2009PABC
C     MODFLOW model which was bigger than the previous 448 width

      fmat(1) = '(568e16.8)'
      fmat(2) = '(568e24.16)'
```

```
C-----------------------------------------
C.....Process command line (get file names)
C-----------------------------------------

C      WRITE(iunscr,*) 'VTRAN >> Processing command line'

C.....Required args  (1-4) are fnmcmd, fnmbud, fnmtrn, fnmdbg
C.....Optional arg (5) is fnmvel

      CALL filcmdlin( nfiles, nfiler, filenm )

C      write(iunscr,*) 'nfiler = ', nfiler

      IF ( nfiler .GT. nfiles ) THEN
         CALL QAABORT( 'VTRAN>> Too many command line arguments')
      ELSE
         IF ( nfiler .LT. nfiles-1 ) THEN
            CALL QAABORT( 'VTRAN>> Too few command line arguments')
         ENDIF
      ENDIF

      fnmcmd = filenm(1)
      fnmbud = filenm(2)
      fnmtrn = filenm(3)
      fnmdbg = filenm(4)

      IF (nfiler .eq. nfiles ) THEN
         wrtvel = .true.
         fnmvel = filenm(5)
      ELSE
         wrtvel = .false.
         fnmvel = 'None'
      ENDIF

C          write(iunscr,*) 'fnmcmd is ', fnmcmd
C          write(iunscr,*) 'fnmbud is ', fnmbud
C          write(iunscr,*) 'fnmtrn is ', fnmtrn
C          write(iunscr,*) 'fnmdbg is ', fnmdbg
C          write(iunscr,*) 'fnmvel is ', fnmvel

C.....Open Diagnostics/Debug file

      OPEN (UNIT=iundbg, FILE=fnmdbg, STATUS='UNKNOWN',IOSTAT=ierr)
      IF ( ierr .NE. 0 ) THEN
         CALL QAABORT ('Error opening command file')
      ENDIF

C-------------------------
C.....Process command file
C-------------------------

C      WRITE(iunscr,*) 'VTRAN >> Processing command file'

C.....Open command file

      OPEN (UNIT=iuncmd, FILE=fnmcmd, STATUS='OLD',
     +      READONLY, IOSTAT=ierr)
      IF ( ierr .NE. 0 ) THEN
         WRITE(iundbg,*) 'Error opening command file'
         CALL QAABORT ('Error opening command file')
      ENDIF

C.....Read from command file

      READ (iuncmd,*)
      READ (iuncmd,10) author
      READ (iuncmd,*)
      READ (iuncmd,10) date
      READ (iuncmd,*)
      READ (iuncmd,10) title
      READ (iuncmd,*)
      READ (iuncmd,10) rdfmat
      READ (iuncmd,*)
      READ (iuncmd,*) iscrn
      READ (iuncmd,*)
      READ (iuncmd,*) ncolmf, nrowmf
      READ (iuncmd,*)
      READ (iuncmd,*) jshftx, ishfty, ncx, ncy
      READ (iuncmd,*)
      READ (iuncmd,*) dx, dy, dz
```

```
 10   FORMAT(A80)
 11   FORMAT(3e01.3)
C.....Close command file

      CLOSE (UNIT=iuncmd,STATUS='KEEP')

C.....Send diagnostic ouput to screen or to debug file

      IF (iscrn .EQ. 0 ) THEN
        iunscr = iundbg
      ENDIF

C.....Echo input

      WRITE(iunscr,20) fnmcmd, fnmbud, fnmtrn, fnmdbg, fnmvel

 20   FORMAT (1X, 'command file                    = ',A80/
     +        1X, 'budget file                     = ',A80/
     +        1X, '(binary) velocity transfer file = ',A80/
     +        1X, 'diagnostic/debug file           = ',A80/
     +        1X, '(ascii) velocity output file    = ',A80
     +       )


      WRITE(iunscr,50) author, date, title, rdfmat
      WRITE(iunscr,100) iscrn, ncolmf, nrowmf,
     +                  jshftx, ishfty, ncx, ncy,
     +                  dx, dy, dz

 50   FORMAT(1X,' author   = ' A80/
     +       1X,' date     = ',A80/
     +       1X,' title    = ',A80/
     +       1X,' format   = ',A80
     +       )
 100  FORMAT(1X,' iscrn    = ',i5 /
     +       1X,' ncolmf   = ',i5 /
     +       1X,' nrowmf   = ',i5 /
     +       1X,' jshftx   = ',i5 /
     +       1X,' ishfty   = ',i5 /
     +       1X,' ncx      = ',i5 /
     +       1X,' ncy      = ',i5 /
     +       1X,' dx       = ',e10.4 /
     +       1X,' dy       = ',e10.4 /
     +       1X,' dz       = ',e10.4
     +      )

C.....Assign correct format number

      irdfmt = 0
      match  = 0
      DO i=1,nfmat
         IF( LLE(rdfmat,fmat(i)) .AND. LLE(fmat(i),rdfmat)) THEN
         irdfmt = i
         match = 1
         ENDIF
      ENDDO

      IF ( match .ne.1 ) THEN
         WRITE(iunscr,*) 'Invalid input format'
         CALL QAABORT ('Invalid input format')
      ENDIF

      WRITE(iunscr,150) irdfmt, rdfmat
 150  FORMAT(1X,'Using input format (',i2, ') = ',A80)

C.....Sanity check. Since ghost cells are added, we must have:
C.....jshftx >= 1 and ishifty >= ncy+1

      IF ( jshftx .LT. 1 ) THEN
         WRITE(iunscr,*) 'Invalid jshftx value'
         CALL QAABORT ('Invalid jshftx value')
      ENDIF

      IF ( ishfty .LT. (ncy+1) ) THEN
         WRITE(iunscr,*) 'Invalid ishfty value'
         CALL QAABORT ('Invalid ishfty value')
      ENDIF

C---------------------
C.....Allocate memory
C---------------------
```

```
C.....Mf2k grid is (1:ncolmf,1:nrowmf).
C.....Ghost cells placed around transport domain, so ST2D grid is
C.....(0:ncx,0:ncy). Thus qxout and qyout are padded to account for
C.....required ghost cells

      ALLOCATE( qxin(1:ncolmf,1:nrowmf),
     +          qyin(1:ncolmf,1:nrowmf),
     +          qxout(0:ncx+1,0:ncy+1),
     +          qyout(0:ncx+1,0:ncy+1),
     +          STAT=ierr )

      IF ( ierr .NE. 0 ) THEN
         WRITE(iunscr,*) 'Error allocating memory'
         CALL QAABORT ('Error allocating memory')
      ENDIF

C----------------------
C.....Read budget file
C----------------------

      WRITE(iunscr,*) 'VTRAN >> Reading budget file'

      OPEN (UNIT=iunbud, FILE=fnmbud, FORM='FORMATTED',
     +                   STATUS='OLD', IOSTAT=ierr)
      IF ( ierr .NE. 0 ) THEN
         WRITE(iunscr,*) 'Error opening budget file'
         CALL QAABORT ('Error opening budget file')
      ENDIF

      DO i=1,nrowmf
         READ(iunbud,rdfmat) (qxin(j,i),j=1,ncolmf)
      END DO
      READ(iunbud,*)
      DO i=1,nrowmf
         READ(iunbud,rdfmat) (qyin(j,i),j=1,ncolmf)
      END DO

C.....Close budget file

      CLOSE (UNIT=iunbud,STATUS='KEEP')

C.....Budget file contains volume fluxes, so must divide
C.....by area of cell face perpendicular to flow direction
C.....to get specific discharge (darcy velocity)

C.....X direction

      ayz_inv = 1.d0/(dy*dz)
      DO i=1,nrowmf
         DO j=1,ncolmf
           qxin(j,i) = qxin(j,i) * ayz_inv
         END DO
      END DO

C.....Y direction

      axz_inv = 1.d0/(dx*dz)
      DO i=1,nrowmf
         DO j=1,ncolmf
           qyin(j,i) = qyin(j,i) * axz_inv
         END DO
       END DO

C-----------------------
C.....Process velocities
C-----------------------

      WRITE(iunscr,*) 'VTRAN >> Processing velocities'

C.....Now grab velocities for internal cells and ghost cells.
C.....Let (l,m) be indices of the ST2D grid cells, ranging from 0:ncx+1
C.....and 0:ncy+1, repsectively. We must compute the corresponding
C.....MF2K indices. The computed mf2k indices must account for:
C.....  1) The offset of the ST2D grid origin
C.....  2) The opposite sense of the y-coord in the two meshes
C.....  3) ST2D face-centered velocities of a given cell are defined
C.....     at the trailing edges of cells (defined according to sense of
C.....     the ST2D axes) while the MF2K face-centered velocities are
C.....     defined at the "right" and "front"  faces of the cell.
```

```
      DO m=0,ncy+1
         DO l=0,ncx+1
            j = jshftx + l
            i = ishfty + 1 - m
            qxout(l,m) = qxin(j-1,i)
            qyout(l,m) = qyin(j,i)
         END DO
      END DO

C.... For ST2D, face centered velocities defined at trailing edges
C     of cells. Ghost cells are placed around the computational domain,
C     but cells on left and bottom do not have defined velocities associated
C     with them. Consider the x-dimension with limits [0,x1], with ncx
C     regular cells and a ghost cell on each side of the domain. Then
C       u(0,m) is not defined,
C       u(1,m) = u at x=0, and
C       u(ncx+1,m) = u at x1
C     Similarly, Consider the y-dimension with limits [0,y1], with ncx
C     regular cells and a ghost cell on each side of the domain. Then
C       v(l,0) is not defined,
C       v(l,1) = v at y=0, and
C       v(l,ncy+1) = v at y1

C.....Zero out the undefined components

      DO m=0,ncy+1
         qxout(0,m) = 0.D0
      END DO

      DO l=0,ncx+1
         qyout(l,0) = 0.D0
      END DO

C.....Change sign of y-velocities. Modflow convention is that
C.....flow is positive in direction of increasing row numbers.
C.....But row numbers increase in negative y-direction.

      DO m=0,ncy+1
         DO l=0,ncx+1
            qyout(l,m) = -qyout(l,m)
         END DO
      END DO

C-------------------------------
C.....Write velocity transfer file
C-------------------------------

      WRITE(iunscr,*) 'VTRAN >> Writing velocity transfer file'

C.....Open the file

      OPEN (UNIT=iuntrn, FILE=fnmtrn, FORM='UNFORMATTED',
     -      STATUS='UNKNOWN',IOSTAT=ierr)
      IF ( ierr .NE. 0 ) THEN
         WRITE(iunscr,*) 'Error opening velocity transfer file'
         CALL QAABORT ('Error opening velocity transfer file')
      ENDIF

C.....Write the following line because sf2d wrote it and
C.....st2d1 expects it (but does not use them)

      time = 0.d0
      WRITE(iuntrn) ncx, ncy, time

C.....Write velocities to output file. Include the undefined
C.....components, since ST2D1 expects them. (ST2D1 reads
C.....them in, but does not write them to the velocity file
C.....it passes to ST2D2)

      WRITE(iuntrn) ( ( qxout(l,m), l=0,ncx+1),m=0,ncy+1 )
      WRITE(iuntrn) ( ( qyout(l,m), l=0,ncx+1),m=0,ncy+1 )

C.....Close output file

      CLOSE (UNIT=iuntrn,STATUS='KEEP')

C-----------------------------------
C.....Write ascii velocity output file
C-----------------------------------

      IF ( wrtvel ) THEN
```

```
      WRITE(iunscr,*) 'VTRAN >> Writing ascii velocity output file'

C.....Open the file

C      OPEN (UNIT=iunvel, FILE=fnmvel, FORM='FORMATTED',
C     +      STATUS='UNKNOWN',IOSTAT=ierr)

      irecl = 568*(23+1)
      OPEN (UNIT=iunvel, FILE=fnmvel, FORM='FORMATTED',
     +      STATUS='UNKNOWN',RECL=irecl,IOSTAT=ierr)

      IF ( ierr .NE. 0 ) THEN
         WRITE(iunscr,*) 'Error opening ascii velocity output file'
         CALL QAABORT ('Error opening ascii velocity outpuit file')
      ENDIF

C.....Write the following line because sf2d wrote it and
C.....st2d1 expects it (but does not use them)

      time = 0.d0
      WRITE(iunvel,200) ncx, ncy, time
 200  FORMAT(1x,2(i5,2x),e16.8)

C.....Write velocities to output file

C     changed implied do-loops to one explicit, one implied
C     and added a blank line between the arrays for easier reading
C
      DO m=0,ncy+1
          WRITE(iunvel,rdfmat) ( qxout(l,m), l=0,ncx+1)
      enddo
      write(iunvel,*) '    '
      do m=0,ncy+1
          WRITE(iunvel,rdfmat) ( qyout(l,m), l=0,ncx+1)
      enddo

C.....Close output file

      CLOSE (UNIT=iunvel,STATUS='KEEP')

      ENDIF

C-------------
C.....Clean up
C-------------

      WRITE(iunscr,*) 'VTRAN >> Cleaning up'

      DEALLOCATE(qxin,qxout,qyin,qyout)

      WRITE(iunscr,*) 'VTRAN >> Normal Completion'
      CLOSE (UNIT=iundbg,STATUS='KEEP')

C     Signal normal completion

      STOP 'VTRAN >> Normal Completion'
      END
```

The VTRAN2 utility was compiled using the compile and link commands listed in Table A 3-2. The files and storage locations associated with building the VTRAN2 utility are given in Table A3-3.

Table A 3-2. VTRAN2 VMS build and link commands

```
$ F90 /DEBUG/NOOPTIMIZE VTRAN2.F
$ LINK /EXEC=VTRAN2.EXE VTRAN2.OBJ, CAMCON_LIB/LIB, CAMSUPES_LIB/LIB
```

Table A3-3. VTRAN2 build info

Description	File	CMS Library	CMS Class

Source code	VTRAN2.F	LIBPABC09_MF2K	VTRAN2_V1.1
VTRAN2 executable	VTRAN2.EXE	LIBPABC09_MF2K	VTRAN2_V1.1

A3.2 VTRAN2 Verification

Test cases for the VTRAN2 utility were slightly modified from those developed for Lowry and Kanney (2005) and executed by the Run Control Coordinator. The executable and input/output files used for the test are shown in Table A3-4.

Table A3-4. VTRAN2 test files

Description	File	CMS Library	CMS Class
VTRAN2 executable	VTRAN2.EXE	LIBPABC09_MF2K	VTRAN2_V1.1
Test 1			
Input command file	VTRAN_TEST_1.CMD	LIBPABC09_MF2K	VTRAN2_V1.1
Input budget file	VTRAN_TEST_1.BUD	LIBPABC09_MF2K	VTRAN2_V1.1
Output binary velocity file	VTRAN_TEST_1.TRN	LIBPABC09_MF2K	VTRAN2_V1.1
Output ASCII velocity file	VTRAN_TEST_1.VEL	LIBPABC09_MF2K	VTRAN2_V1.1
Output debug file	VTRAN_TEST_1.DBG	LIBPABC09_MF2K	VTRAN2_V1.1
Test 2			
Input command file	VTRAN_TEST_2.CMD	LIBPABC09_MF2K	VTRAN2_V1.1
Input budget file	VTRAN_TEST_2.BUD	LIBPABC09_MF2K	VTRAN2_V1.1
Output binary velocity file	VTRAN_TEST_2.TRN	LIBPABC09_MF2K	VTRAN2_V1.1
Output ASCII velocity file	VTRAN_TEST_2.VEL	LIBPABC09_MF2K	VTRAN2_V1.1
Output debug file	VTRAN_TEST_2.DBG	LIBPABC09_MF2K	VTRAN2_V1.1

The VTRAN2 utility code was verified using two test cases. Case 1 demonstrates the conversion of volumetric flux to Darcy velocities, the sign change of the y-direction velocities, and the inclusion of ghost nodes. Case 2 demonstrates that the indexing selects the correct subregion.

Both test cases use the mesh layout shown in Figure A3-1. The volume fluxes are specified on the 10×15 cell mesh. The 4×3 cell sub-region outlined in red represents the transport domain. The dashed lines indicate the ghost nodes. We run VTRAN2 such that it writes the output in both ASCII and binary format, so we can visually inspect the ASCII file to verify the results.

A3.2.1 VTRAN2 Verification Test Case 1

In this test we use a uniform volume flux ($Q_x = Q_y = 1$), and choose $dx = 1$, and $dy = dz = 2$ in the VTRAN2 command file such that $A_x = 4$ and $A_y = 2$. Thus, for the transport mesh, we will have $u = 0.25$ and $v = 0.5$ for all cell faces except for the left and bottom boundaries. $u = 0$ at the left boundary and $v = 0$ at the bottom because the respective velocity at these faces is undefined in the SECOTP2D convention.

The command file (VTRAN2_TEST_1.CMD), and the budget file (VTRAN2_TEST_1.BUD) are shown in Table A3-5 and Table A3-6, respectively. Running VTRAN2 with these input files produces the ASCII velocity file (VTRAN2_TEST_1.VEL) and the diagnostic file (VTRAN2_TEST_1.DBG) shown in Table

A3-7 and Table A3-8, respectively. We note that u and v are 0.25 and -0.5, as expected. We also note that the 4×3 cell transport domain has been appropriately padded with ghost cells to make a 6×5 array for each velocity component.

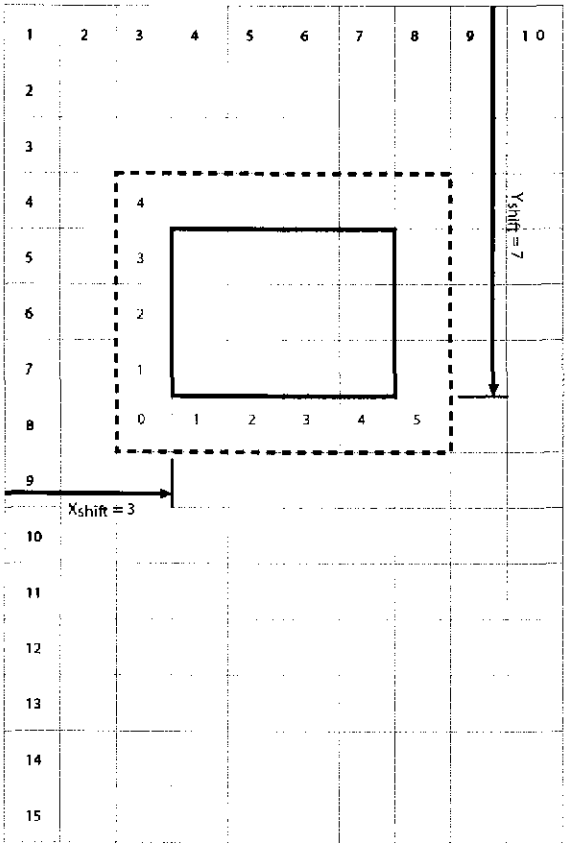

Figure A3-1. Mesh for VTRAN2 verification

Table A3-5. VTRAN2_TEST_1.CMD

```
* author
Joseph F. Kanney
* date
2003.09.24
* title
vtran2 test 1
* input format type
(568e16.8)
* iscrn > 0 will print to screen, otherwise to dbg file
0
* ncol nrow
10 15
* jshftx ishfty ncx ncy
3 7 4 3
* dx dy dz (3e10.3)
1.000E+00 2.000E+00 2.000E+00
```

Table A3-6. VTRAN2_TEST_1.BUD

```
0.10000000E+01 0.10000000E+01 0.10000000E+01 0.10000000E+01 0.10000000E+01 0.10000000E+01 0.10000000E+01 0.10000000E+01 0.10000000E+01 0.10000000E+01
0.10000000E+01 0.10000000E+01 0.10000000E+01 0.10000000E+01 0.10000000E+01 0.10000000E+01 0.10000000E+01 0.10000000E+01 0.10000000E+01 0.10000000E+01
0.10000000E+01 0.10000000E+01 0.10000000E+01 0.10000000E+01 0.10000000E+01 0.10000000E+01 0.10000000E+01 0.10000000E+01 0.10000000E+01 0.10000000E+01
0.10000000E+01 0.10000000E+01 0.10000000E+01 0.10000000E+01 0.10000000E+01 0.10000000E+01 0.10000000E+01 0.10000000E+01 0.10000000E+01 0.10000000E+01
0.10000000E+01 0.10000000E+01 0.10000000E+01 0.10000000E+01 0.10000000E+01 0.10000000E+01 0.10000000E+01 0.10000000E+01 0.10000000E+01 0.10000000E+01
0.10000000E+01 0.10000000E+01 0.10000000E+01 0.10000000E+01 0.10000000E+01 0.10000000E+01 0.10000000E+01 0.10000000E+01 0.10000000E+01 0.10000000E+01
0.10000000E+01 0.10000000E+01 0.10000000E+01 0.10000000E+01 0.10000000E+01 0.10000000E+01 0.10000000E+01 0.10000000E+01 0.10000000E+01 0.10000000E+01
0.10000000E+01 0.10000000E+01 0.10000000E+01 0.10000000E+01 0.10000000E+01 0.10000000E+01 0.10000000E+01 0.10000000E+01 0.10000000E+01 0.10000000E+01
0.10000000E+01 0.10000000E+01 0.10000000E+01 0.10000000E+01 0.10000000E+01 0.10000000E+01 0.10000000E+01 0.10000000E+01 0.10000000E+01 0.10000000E+01
0.10000000E+01 0.10000000E+01 0.10000000E+01 0.10000000E+01 0.10000000E+01 0.10000000E+01 0.10000000E+01 0.10000000E+01 0.10000000E+01 0.10000000E+01
0.10000000E+01 0.10000000E+01 0.10000000E+01 0.10000000E+01 0.10000000E+01 0.10000000E+01 0.10000000E+01 0.10000000E+01 0.10000000E+01 0.10000000E+01
0.10000000E+01 0.10000000E+01 0.10000000E+01 0.10000000E+01 0.10000000E+01 0.10000000E+01 0.10000000E+01 0.10000000E+01 0.10000000E+01 0.10000000E+01
0.10000000E+01 0.10000000E+01 0.10000000E+01 0.10000000E+01 0.10000000E+01 0.10000000E+01 0.10000000E+01 0.10000000E+01 0.10000000E+01 0.10000000E+01
0.10000000E+01 0.10000000E+01 0.10000000E+01 0.10000000E+01 0.10000000E+01 0.10000000E+01 0.10000000E+01 0.10000000E+01 0.10000000E+01 0.10000000E+01
0.10000000E+01 0.10000000E+01 0.10000000E+01 0.10000000E+01 0.10000000E+01 0.10000000E+01 0.10000000E+01 0.10000000E+01 0.10000000E+01 0.10000000E+01

0.10000000E+01 0.10000000E+01 0.10000000E+01 0.10000000E+01 0.10000000E+01 0.10000000E+01 0.10000000E+01 0.10000000E+01 0.10000000E+01 0.10000000E+01
0.10000000E+01 0.10000000E+01 0.10000000E+01 0.10000000E+01 0.10000000E+01 0.10000000E+01 0.10000000E+01 0.10000000E+01 0.10000000E+01 0.10000000E+01
0.10000000E+01 0.10000000E+01 0.10000000E+01 0.10000000E+01 0.10000000E+01 0.10000000E+01 0.10000000E+01 0.10000000E+01 0.10000000E+01 0.10000000E+01
0.10000000E+01 0.10000000E+01 0.10000000E+01 0.10000000E+01 0.10000000E+01 0.10000000E+01 0.10000000E+01 0.10000000E+01 0.10000000E+01 0.10000000E+01
0.10000000E+01 0.10000000E+01 0.10000000E+01 0.10000000E+01 0.10000000E+01 0.10000000E+01 0.10000000E+01 0.10000000E+01 0.10000000E+01 0.10000000E+01
0.10000000E+01 0.10000000E+01 0.10000000E+01 0.10000000E+01 0.10000000E+01 0.10000000E+01 0.10000000E+01 0.10000000E+01 0.10000000E+01 0.10000000E+01
0.10000000E+01 0.10000000E+01 0.10000000E+01 0.10000000E+01 0.10000000E+01 0.10000000E+01 0.10000000E+01 0.10000000E+01 0.10000000E+01 0.10000000E+01
0.10000000E+01 0.10000000E+01 0.10000000E+01 0.10000000E+01 0.10000000E+01 0.10000000E+01 0.10000000E+01 0.10000000E+01 0.10000000E+01 0.10000000E+01
0.10000000E+01 0.10000000E+01 0.10000000E+01 0.10000000E+01 0.10000000E+01 0.10000000E+01 0.10000000E+01 0.10000000E+01 0.10000000E+01 0.10000000E+01
0.10000000E+01 0.10000000E+01 0.10000000E+01 0.10000000E+01 0.10000000E+01 0.10000000E+01 0.10000000E+01 0.10000000E+01 0.10000000E+01 0.10000000E+01
0.10000000E+01 0.10000000E+01 0.10000000E+01 0.10000000E+01 0.10000000E+01 0.10000000E+01 0.10000000E+01 0.10000000E+01 0.10000000E+01 0.10000000E+01
0.10000000E+01 0.10000000E+01 0.10000000E+01 0.10000000E+01 0.10000000E+01 0.10000000E+01 0.10000000E+01 0.10000000E+01 0.10000000E+01 0.10000000E+01
0.10000000E+01 0.10000000E+01 0.10000000E+01 0.10000000E+01 0.10000000E+01 0.10000000E+01 0.10000000E+01 0.10000000E+01 0.10000000E+01 0.10000000E+01
0.10000000E+01 0.10000000E+01 0.10000000E+01 0.10000000E+01 0.10000000E+01 0.10000000E+01 0.10000000E+01 0.10000000E+01 0.10000000E+01 0.10000000E+01
0.10000000E+01 0.10000000E+01 0.10000000E+01 0.10000000E+01 0.10000000E+01 0.10000000E+01 0.10000000E+01 0.10000000E+01 0.10000000E+01 0.10000000E+01
```

Table A3-7. VTRAN2_TEST_1.VEL

```
     4       3    0.00000000E+00
  0.00000000E+00  0.25000000E+00  0.25000000E+00  0.25000000E+00  0.25000000E+00  0.25000000E+00
  0.00000000E+00  0.25000000E+00  0.25000000E+00  0.25000000E+00  0.25000000E+00  0.25000000E+00
  0.00000000E+00  0.25000000E+00  0.25000000E+00  0.25000000E+00  0.25000000E+00  0.25000000E+00
  0.00000000E+00  0.25000000E+00  0.25000000E+00  0.25000000E+00  0.25000000E+00  0.25000000E+00
  0.00000000E+00  0.25000000E+00  0.25000000E+00  0.25000000E+00  0.25000000E+00  0.25000000E+00

  0.00000000E+00  0.00000000E+00  0.00000000E+00  0.00000000E+00  0.00000000E+00  0.00000000E+00
 -0.50000000E+00 -0.50000000E+00 -0.50000000E+00 -0.50000000E+00 -0.50000000E+00 -0.50000000E+00
 -0.50000000E+00 -0.50000000E+00 -0.50000000E+00 -0.50000000E+00 -0.50000000E+00 -0.50000000E+00
 -0.50000000E+00 -0.50000000E+00 -0.50000000E+00 -0.50000000E+00 -0.50000000E+00 -0.50000000E+00
 -0.50000000E+00 -0.50000000E+00 -0.50000000E+00 -0.50000000E+00 -0.50000000E+00 -0.50000000E+00
```

Table A3-8. VTRAN3_TEST_1.DBG

```
command file                   = VTRAN2_TEST_1.CMD
budget file                    = VTRAN2_TEST_1.BUD
(binary) velocity transfer file = VTRAN2_TEST_1.TRN
diagnostic/debug file          = VTRAN2_TEST_1.DBG
(ascii) velocity output file   = VTRAN2_TEST_1.VEL
 author   = Joseph F. Kanney
 date     = 2003.09.24
 title    = vtran2 test 1
 format   = (568e16.8)
 iscrn    =      0
 ncolmf   =     10
 nrowmf   =     15
 jshftx   =      3
 ishfty   =      7
 ncx      =      4
 ncy      =      3
 dx       = 0.1000E+01
 dy       = 0.2000E+01
 dz       = 0.2000E+01
Using input format ( 1) = (568e16.8)
VTRAN >> Reading budget file
VTRAN >> Processing velocities
VTRAN >> Writing velocity transfer file
VTRAN >> Writing ascii velocity output file
VTRAN >> Cleaning up
VTRAN >> Normal Completion
```

A3.2.2 VTRAN2 Verification Test Case 2

In this test, we specify a synthetic volume flux field on the 10×15 mesh such that the modulus of the velocity component equals the row number and the fractional part equals the column number. Thus the cell number is embedded in the value of the flux component. We then specify $dx = dy = dz = 1$ in the

VTRAN2 command file. In this way, we can visually inspect the velocity file to verify that the correct row and column indices are extracted.

The command file (VTRAN2_TEST_2.CMD), and the budget file (VTRAN2_TEST_2.BUD) are shown in Table A3-9 and Table A3-10, respectively. Running VTRAN2 with these input files produces the ASCII velocity file (VTRAN2_TEST_2.VEL) and the diagnostic file (VTRAN2_TEST_2.DBG) shown in Table A3-11 and Table A3-12, respectively. We note from the velocity component values that the correct translation of indices between the two meshes has been effected.

Table A3-9. VTRAN2_TEST_2.CMD

```
* author
Joseph F. Kanney
* date
2003.09.24
* title
vtran2 test 2
* input format type
(568e16.8)
* iscrn > 0 will print to screen, otherwise to dbg file
0
* ncol nrow
10 15
* jshftx ishfty ncx ncy
3 7 4 3
* dx dy dz (3e10.3)
1.000E+00 1.000E+00 1.000E+00
```

Table A3-10. VTRAN2_TEST_2.BUD

```
0.10100000E+01 0.10200000E+01 0.10300000E+01 0.10400000E+01 0.10500000E+01 0.10599999E+01 0.10700001E+01 0.10800000E+01 0.10900000E+01 0.11000000E+01
0.20100000E+01 0.20200000E+01 0.20300000E+01 0.20400000E+01 0.20500000E+01 0.20599999E+01 0.20699999E+01 0.20799999E+01 0.20899999E+01 0.20999999E+01
0.30100000E+01 0.30200000E+01 0.30300000E+01 0.30400000E+01 0.30500000E+01 0.30599999E+01 0.30699999E+01 0.30799999E+01 0.30899999E+01 0.30999999E+01
0.40100002E+01 0.40200000E+01 0.40300002E+01 0.40400000E+01 0.40500002E+01 0.40599999E+01 0.40700002E+01 0.40799999E+01 0.40900002E+01 0.40999999E+01
0.50100002E+01 0.50200000E+01 0.50300002E+01 0.50400000E+01 0.50500002E+01 0.50599999E+01 0.50700002E+01 0.50799999E+01 0.50900002E+01 0.50999999E+01
0.60100002E+01 0.60200000E+01 0.60300002E+01 0.60400000E+01 0.60500002E+01 0.60599999E+01 0.60700002E+01 0.60799999E+01 0.60900002E+01 0.60999999E+01
0.70100002E+01 0.70200000E+01 0.70300002E+01 0.70400000E+01 0.70500002E+01 0.70599999E+01 0.70700002E+01 0.70799999E+01 0.70900002E+01 0.70999999E+01
0.80100002E+01 0.80200005E+01 0.80299997E+01 0.80400000E+01 0.80500002E+01 0.80600004E+01 0.80699997E+01 0.80799999E+01 0.80900002E+01 0.81000004E+01
0.90100002E+01 0.90200005E+01 0.90299997E+01 0.90400000E+01 0.90500002E+01 0.90600004E+01 0.90699997E+01 0.90799999E+01 0.90900002E+01 0.91000004E+01
0.10010000E+02 0.10020000E+02 0.10030000E+02 0.10040000E+02 0.10050000E+02 0.10060000E+02 0.10070000E+02 0.10080000E+02 0.10090000E+02 0.10100000E+02
0.11010000E+02 0.11020000E+02 0.11030000E+02 0.11040000E+02 0.11050000E+02 0.11060000E+02 0.11070000E+02 0.11080000E+02 0.11090000E+02 0.11100000E+02
0.12010000E+02 0.12020000E+02 0.12030000E+02 0.12040000E+02 0.12050000E+02 0.12060000E+02 0.12070000E+02 0.12080000E+02 0.12090000E+02 0.12100000E+02
0.13010000E+02 0.13020000E+02 0.13030000E+02 0.13040000E+02 0.13050000E+02 0.13060000E+02 0.13070000E+02 0.13080000E+02 0.13090000E+02 0.13100000E+02
0.14010000E+02 0.14020000E+02 0.14030000E+02 0.14040000E+02 0.14050000E+02 0.14060000E+02 0.14070000E+02 0.14080000E+02 0.14090000E+02 0.14100000E+02
0.15010000E+02 0.15020000E+02 0.15030000E+02 0.15040000E+02 0.15050000E+02 0.15060000E+02 0.15070000E+02 0.15080000E+02 0.15090000E+02 0.15100000E+02

0.10100000E+01 0.10200000E+01 0.10300000E+01 0.10400000E+01 0.10500000E+01 0.10599999E+01 0.10700001E+01 0.10800000E+01 0.10900000E+01 0.11000000E+01
0.20100000E+01 0.20200000E+01 0.20300000E+01 0.20400000E+01 0.20500000E+01 0.20599999E+01 0.20699999E+01 0.20799999E+01 0.20899999E+01 0.20999999E+01
0.30100000E+01 0.30200000E+01 0.30300000E+01 0.30400000E+01 0.30500000E+01 0.30599999E+01 0.30699999E+01 0.30799999E+01 0.30899999E+01 0.30999999E+01
0.40100002E+01 0.40200000E+01 0.40300002E+01 0.40400000E+01 0.40500002E+01 0.40599999E+01 0.40700002E+01 0.40799999E+01 0.40900002E+01 0.40999999E+01
0.50100002E+01 0.50200000E+01 0.50300002E+01 0.50400000E+01 0.50500002E+01 0.50599999E+01 0.50700002E+01 0.50799999E+01 0.50900002E+01 0.50999999E+01
0.60100002E+01 0.60200000E+01 0.60300002E+01 0.60400000E+01 0.60500002E+01 0.60599999E+01 0.60700002E+01 0.60799999E+01 0.60900002E+01 0.60999999E+01
0.70100002E+01 0.70200000E+01 0.70300002E+01 0.70400000E+01 0.70500002E+01 0.70599999E+01 0.70700002E+01 0.70799999E+01 0.70900002E+01 0.70999999E+01
0.80100002E+01 0.80200005E+01 0.80299997E+01 0.80400000E+01 0.80500002E+01 0.80600004E+01 0.80699997E+01 0.80799999E+01 0.80900002E+01 0.81000004E+01
0.90100002E+01 0.90200005E+01 0.90299997E+01 0.90400000E+01 0.90500002E+01 0.90600004E+01 0.90699997E+01 0.90799999E+01 0.90900002E+01 0.91000004E+01
0.10010000E+02 0.10020000E+02 0.10030000E+02 0.10040000E+02 0.10050000E+02 0.10060000E+02 0.10070000E+02 0.10080000E+02 0.10090000E+02 0.10100000E+02
0.11010000E+02 0.11020000E+02 0.11030000E+02 0.11040000E+02 0.11050000E+02 0.11060000E+02 0.11070000E+02 0.11080000E+02 0.11090000E+02 0.11100000E+02
0.12010000E+02 0.12020000E+02 0.12030000E+02 0.12040000E+02 0.12050000E+02 0.12060000E+02 0.12070000E+02 0.12080000E+02 0.12090000E+02 0.12100000E+02
0.13010000E+02 0.13020000E+02 0.13030000E+02 0.13040000E+02 0.13050000E+02 0.13060000E+02 0.13070000E+02 0.13080000E+02 0.13090000E+02 0.13100000E+02
0.14010000E+02 0.14020000E+02 0.14030000E+02 0.14040000E+02 0.14050000E+02 0.14060000E+02 0.14070000E+02 0.14080000E+02 0.14090000E+02 0.14100000E+02
0.15010000E+02 0.15020000E+02 0.15030000E+02 0.15040000E+02 0.15050000E+02 0.15060000E+02 0.15070000E+02 0.15080000E+02 0.15090000E+02 0.15100000E+02
```

Table A3-11. VTRAN2_TEST_2.VEL

```
   4      3    0.00000000E+00
 0.00000000E+00  0.80299997E+01  0.80400000E+01  0.80500002E+01  0.80600004E+01  0.80699997E+01
 0.00000000E+00  0.70300002E+01  0.70400000E+01  0.70500002E+01  0.70599999E+01  0.70700002E+01
 0.00000000E+00  0.60300002E+01  0.60400000E+01  0.60500002E+01  0.60599999E+01  0.60700002E+01
 0.00000000E+00  0.50300002E+01  0.50400000E+01  0.50500002E+01  0.50599999E+01  0.50700002E+01
 0.00000000E+00  0.40300002E+01  0.40400000E+01  0.40500002E+01  0.40599999E+01  0.40700002E+01

 0.00000000E+00  0.00000000E+00  0.00000000E+00  0.00000000E+00  0.00000000E+00  0.00000000E+00
-0.70300002E+01 -0.70400000E+01 -0.70500002E+01 -0.70599999E+01 -0.70700002E+01 -0.70799999E+01
-0.60300002E+01 -0.60400000E+01 -0.60500002E+01 -0.60599999E+01 -0.60700002E+01 -0.60799999E+01
-0.50300002E+01 -0.50400000E+01 -0.50500002E+01 -0.50599999E+01 -0.50700002E+01 -0.50799999E+01
-0.40300002E+01 -0.40400000E+01 -0.40500002E+01 -0.40599999E+01 -0.40700002E+01 -0.40799999E+01
```

Table A3-12. VTRAN2_TEST_2.DBG

```
command file                     = VTRAN2_TEST_2.CMD
budget file                      = VTRAN2_TEST_2.BUD
(binary) velocity transfer file = VTRAN2_TEST_2.TRN
diagnostic/debug file            = VTRAN2_TEST_2.DBG
(ascii) velocity output file     = VTRAN2_TEST_2.VEL
 author    = Joseph F. Kanney
 date      = 2003.09.24
 title     = vtran2 test 2
 format    = (568e16.8)
 iscrn     =      0
 ncolmf    =     10
 nrowmf    =     15
 jshftx    =      3
 ishfty    =      7
 ncx       =      4
 ncy       =      3
 dx        = 0.1000E+01
 dy        = 0.1000E+01
 dz        = 0.1000E+01
Using input format ( 1) = (568e16.8)
VTRAN >> Reading budget file
VTRAN >> Processing velocities
VTRAN >> Writing velocity transfer file
VTRAN >> Writing ascii velocity output file
VTRAN >> Cleaning up
VTRAN >> Normal Completion
```

A4 Script Source Listing

The scripts listed in this appendix neither model physical phenomena nor solve differential equations that model physical phenomena. Rather they are utility codes that process inputs and outputs for other modeling codes (i.e., MODFLOW, DTRKMF, and SECOTP2D).

A4.1 Python script convert_shapefile_to_ASCII.py

A4.1.1 Input File

```
Measured_Minable_Ore_UTMNAD27
polyline_dump_matlab_part    .dat
polyline_dump_for_gnuplot.dat
```

A4.1.2 Script

```
# Copyright (c) 2008
#   Zach Steindler (steiza@gmail.com, http://code.google.com/p/pyshapefile/)
#
# All rights reserved.
#
# Redistribution and use in source and binary forms, with or without modification,
# are permitted provided that the following conditions are met:
#
# Redistributions of source code must retain the above copyright notice,
# this list of conditions and the following disclaimer.
#
# Redistributions in binary form must reproduce the above copyright notice,
# this list of conditions and the following disclaimer in the documentation
# and/or other materials provided with the distribution.
#
# Neither the name of the original author nor the names of contributors
# may be used to endorse or promote products derived from this software
# without specific prior written permission.
#
# THIS SOFTWARE IS PROVIDED BY THE COPYRIGHT HOLDERS AND CONTRIBUTORS "AS IS"
# AND ANY EXPRESS OR IMPLIED WARRANTIES, INCLUDING, BUT NOT LIMITED TO, THE
# IMPLIED WARRANTIES OF MERCHANTABILITY AND FITNESS FOR A PARTICULAR PURPOSE
# ARE DISCLAIMED. IN NO EVENT SHALL THE COPYRIGHT OWNER OR CONTRIBUTORS BE
# LIABLE FOR ANY DIRECT, INDIRECT, INCIDENTAL, SPECIAL, EXEMPLARY, OR CONSEQUENTIAL
# DAMAGES (INCLUDING, BUT NOT LIMITED TO, PROCUREMENT OF SUBSTITUTE GOODS OR
# SERVICES; LOSS OF USE, DATA, OR PROFITS; OR BUSINESS INTERRUPTION) HOWEVER
# CAUSED AND ON ANY THEORY OF LIABILITY, WHETHER IN CONTRACT, STRICT LIABILITY,
# OR TORT (INCLUDING NEGLIGENCE OR OTHERWISE) ARISING IN ANY WAY OUT OF THE USE
# OF THIS SOFTWARE, EVEN IF ADVISED OF THE POSSIBILITY OF SUCH DAMAGE.

import struct
_POINT_PAIR_SIZE = 16

class ShapefileData(object):
    """A python class for loading shapefiles."""

    def __init__(self, base_filename):
        """Initializes ShapefileData with path to shapefile data.

        Args:
            base_filename: Base path to shapefile data. base_filename + '.shp'
              and base_filename + '.dbf' should exist.
        """
        self.base_filename = base_filename

    def load_bounding_box(self):
        """Loads boundry information from .shp file"""
        shp_fd = open('%s.shp' % self.base_filename, 'rb')
        shp_fd.seek(36)

        self.file_xmin, self.file_ymin, self.file_xmax, self.file_ymax = \
                struct.unpack('dddd', shp_fd.read(32))

        shp_fd.close()

    def load_objects(self, x = 0, y = 0, radius = 0):
        """Loads information from .shp file; only loads information within
           bounds if specified.

           Args:
             x: x coordinate at center of bounding box
             y: y coordinate at center of bounding box
             radius: size of bounding box
        """
        self.load_bounding_box()
        self.items = {}

        if x == 0 or y == 0 or radius == 0:
            self.data_xmin = self.file_xmin
            self.data_xmax = self.file_xmax
            self.data_ymin = self.file_ymin
            self.data_ymax = self.file_ymax
        else:
            self.data_xmin = x - radius
            self.data_xmax = x + radius
```

```
            self.data_ymin = y - radius
            self.data_ymax = y + radius

        shp_fd = open('%s.shp' % self.base_filename, 'rb')
        shp_fd.seek(100)

        while True:
            # Process record header
            record_header = shp_fd.read(12)
            if record_header == '':
                break

            record_number, record_length = struct.unpack('>LL',
                    record_header[:8])

            record_shape = struct.unpack('<L', record_header[8:])[0]

            # Process record body
            if record_shape == 0:
                # Record is null
                pass

            elif record_shape == 1:
                # Record is a point
                object_point = shp_fd.read(_POINT_PAIR_SIZE)
                x, y = struct.unpack('dd', object_point)

                if self.data_xmin > x or self.data_xmax < x:
                    continue
                if self.data_ymin > y or self.data_ymax < y:
                    continue

                self.items[record_number] = {'type': 'point',
                        'point': {'x': x, 'y': y}}

            elif record_shape == 3 or record_shape == 5:
                # Record is a polyline
                object_header = shp_fd.read(40)
                object_xmin, object_ymin, object_xmax, object_ymax, \
                        nparts, points = struct.unpack('ddddii', object_header)

                if object_xmax < self.data_xmin or \
                        object_xmin > self.data_xmax or \
                        object_ymax < self.data_ymin or \
                        object_ymin > self.data_ymax:

                    # added partial handling of parts  (KK 09/09)
                    part_list = shp_fd.read((4 * nparts) +
                        (_POINT_PAIR_SIZE * points))
                    print 'TODO: learn to handle this case?! (not needed for WIPP data)'

                    continue

                # read in list of indicies to first point in each part (KK 09/09)
                part_list = shp_fd.read((4 * nparts))
                self.parts = list(struct.unpack('i'*nparts, part_list))

                self.items[record_number] = {'type': 'polyline', 'points': []}

                object_points = shp_fd.read(_POINT_PAIR_SIZE * points)
                for i in xrange(0, len(object_points), _POINT_PAIR_SIZE):
                    x, y = struct.unpack('dd', object_points[i:i+_POINT_PAIR_SIZE])
                    self.items[record_number]['points'].append({'x': x, 'y':y})

            else:
                raise UnknownShape
        shp_fd.close()

    def dump_polyline_to_file(self,rec_num=1,fn='polyline_dump_for_gnuplot.dat'):
        """save each part of the polyline as a group, separated
        by two blank lines.  Intended for plotting in Gnuplot.
        Added by Kris Kuhlman, Sept 2009"""

        fh = open(fn,'w')
        # save filename in a comment at top of file
        fh.write('# data from %s.shp\n'%self.base_filename)

        # number of parts
        npar = len(self.parts)

        # number of points (end of last part)
        npts = len(self.items[rec_num]['points'])

        self.parts.append(npts)

        for i in xrange(npar):
            fh.write('# part: %i\n'%i)
            p = self.items[rec_num]['points'][self.parts[i]:self.parts[i+1]]
            for pt in p:
                # save data with 10cm precision (good enough for plotting)
```

```
                # make file a bit smaller and quicker to parse by GnuPlot
                fh.write('%.1f %.1f\n'%(pt['x'],pt['y']))
            fh.write('\n\n')

        fh.close()

    def dump_polyline_to_files(self,rec_num=1,fn=['polyline_dump_matlab_part','.dat']):
        """save each part of the polyline as a file, Intended for
        importing into Matlab. Added by Kris Kuhlman, Sept 2009"""

        # number of parts
        npar = len(self.parts)

        # number of points (end of last part)
        npts = len(self.items[rec_num]['points'])

        self.parts.append(npts)

        for i in xrange(npar):
            # save file with index between prefix and suffix given as arguments
            fh = open('%s%4.4i%s'%(fn[0],i,fn[1]),'w')
            p = self.items[rec_num]['points'][self.parts[i]:self.parts[i+1]]
            for pt in p:
                # write points with 0.1cm precision (UTM is in meters)
                fh.write('%.3f %.3f\n'%(pt['x'],pt['y']))
            fh.close()

# following added by KK 09/09
if __name__ == '__main__':

    from sys import argv

    # this script just drives the pyshapefile Python library
    # to open (then dump to ASCII) the potash mining definitions shapefile
    # read an input file with same basename but '.in' instead of '.py'

    fin = open(argv[0].replace('.py','.in'),'r')
    shpfn = fin.readline().strip()
    matfn = fin.readline().strip().split()
    gnufn = fin.readline().strip()
    fin.close()

    print '####################'
    print 'shpfn:',shpfn
    print 'matfn:',matfn
    print 'gnufn:',gnufn
    print '####################'

    shp = ShapefileData(shpfn)

    # read in shapefile polyline data
    shp.load_objects()

    # dump polylines to a single text file for plotting in GnuPlot
    shp.dump_polyline_to_file(fn=gnufn)

    # dump each part of polyline to a single file
    # for reading / processing in Matlab

    shp.dump_polyline_to_files(fn=matfn)
```

A4.2 MATLAB script `import_polyline_determine_mined_areas.m`

```
% this MATLAB script reads in the ASCII parts of the polyline defined
% in the BLM mining areas shapefile, determining whether each
% cell in the model domain is inside the mining region  an
% integer matrix indicating whether the cell is mined is the result.

% NB: this script takes about 2 hours to run on my desktop

prefix = 'polyline_dump_matlab_part';
suffix = '.dat';
numpart = 54;

% use cells (rather than more common arrays) to allow variable-length parts
p = cell(numpart,2);

for i=1:numpart
    p{i,1} = {load([prefix,sprintf('%4.4i',i-1),suffix])};
end

% first cell is the main polygon; all other cells will be checked with
% reference to that one.  0=outside, 1=inside

% since no polylines intersect, just check to see if the first point of a
% given polyline is inside or outside the big polyline.

p{1,2} = {-1};

% plot individual parts of polyline as areas (patches) for checking
patch(p{1,1}(:,1),p{1,1}(:,2),'k')
hold on;

for i=2:numpart
    p{i,2} = {inpolygon(p{i,1}(1,1),p{i,1}(1,2), ...
        p{1,1}(:,1),p{1,1}(:,2))};
    if p{i,2} == 1
        patch(p{i,1}(:,1),p{i,1}(:,2),'r')
    else
        patch(p{i,1}(:,1),p{i,1}(:,2),'g')
    end
end

daspect([1,1,1])
xlabel('UTM NAD27 X (m)')
ylabel('UTM NAD27 Y (m)')

% model grid
nrow = 307;
ncol = 284;
x0 = 601700.0;
x1 = 630000.0;
dx = 100.0;
y0 = 3566500.0;
y1 = 3597100.0;
dy = 100.0;

[X,Y] = meshgrid(x0:dx:x1,y0:dy:y1);
result = zeros(nrow,ncol,numpart);

for i=numpart:-1:1
    display(i);
    tic
    result(:,:,i) = inpolygon(X,Y,p{i,1}(:,1),p{i,1}(:,2));
    toc
end

% this assumes that the only polygon that surrounds any other polygons
% is the "big" one that is the first entry.  None of the other polygons
% intersect or surround one another.

%  black            red                 green
% big_polygon - nested_polygons + external_polygons

final = result(:,:,1) - sum(result(:,:,[p{:,2}]==1),3) + ...
    sum(result(:,:,[p{:,2}]==0),3);

% plot for checking
figure()
spy(final)

save('mining_areas_matrix.dat','-ascii','final')
out = [reshape(X,nrow*ncol,1),reshape(Y,nrow*ncol,1), ...
       reshape(final,nrow*ncol,1)];

save('mining_areas_xyz.dat','-ascii','out')
```

A4.3 Bash shell script run_mining_mods.sh

```
#!/bin/bash

# this script assumes the following directory substructure
# created in ReadScript.py, where CWP='cwd'
#
#  CWP/Inputs
#  CWP/Inputs/bin                       (MF2K & DTRKMF binaries)
#  CWP/Inputs/AP114_Task7
#  CWP/Inputs/AP114_Task7/data          (MF2K data files)
#  CWP/Inputs/AP114_Task7/modflow       (MF2K package files)
#  CWP/Inputs/AP114_Task7/Outputs       (modeled_{K,A,R,S}_field.mod)
#  CWP/Outputs/                         (results of this analysis)
#  CWP/RunControl
#

verbose=True

# the script is started from the "CWP" directory

echo '## run_mining_mods.sh starting directory: ' 'pwd' '##'

# modify the path of "updated" T-fields, so they are all at the
# same level in the directory structure (simplifying scripts elsewhere)

if [ ${verbose} == True ]; then
    echo "## create a list of realizations without Update{,2} directory components ##"
fi

if [ -a ./Inputs/keepers_short ]; then
    # delete any pre-existing files here,
    # since file is concatenated to in next loop
    rm ./Inputs/keepers_short
fi

for d in 'cat ./Inputs/keepers'; do
  bn='basename ${d}'
  # test whether it is a compound path
  # if compound, move up a directory
  if [ ${d} != ${bn} ]; then
      mv ./Inputs/AP114_Task7/Outputs/${d}/ ./Inputs/AP114_Task7/Outputs/
  fi

  # create a new 'keepers' list without Update or Update2 directories
  echo ${bn} >> ./Inputs/keepers_short
done

if [ ${verbose} == True ]; then
    echo "## run mining modifications ##"
fi

cd Outputs

# make links of mining mod input files and scripts into
# the current Outputs working directory
for f in 'cat ../Inputs/files_minmod'; do
  ln -s ../Inputs/${f} ./${f}
done

# python script creates partial/full mining factor
# arrays from GIS definition of mining areas
# extending area to account for 45-degree angle of repose
python enlarge_mining_areas.py

# python script creates 600 mining-modified T fields
# and 2 mining-modified MODFLOW IBOUND arrays
# this script creates directory hierarchy in Outputs/
python mining_mod.py

# ------------------------------------------------------
# run 100x100 m grid MODFLOW2K and DTRKMF

if [ ${verbose} == True ]; then
    echo "## run MODFLOW2K and DTRKMF ##"
fi

# MODFLOW name file using direct solver (use when LMG solver fails)
sed -e "s/LMG           8 mf2k_culebra\.lmg/DE4           8 mf2k_culebra.de4/" \
    <../Inputs/AP114_Task7/modflow/mf2k_head.nam \
    >../Outputs/modflow/mf2k_head.de4.nam

# adjust MODFLOW LMG solver tolerance and turn on PCG pre-conditioner
sed -e "s/3\.0 2\.2 5\.4 0/3.0 2.2 5.4 1/" \
    -e "s/2 50 1\.0E-08 1.0 1/2 50 1.0E-10 1.0 1/" \
    <../Inputs/AP114_Task7/modflow/mf2k_culebra.lmg \
    >../Outputs/modflow/mf2k_culebra.lmg

# sed doesn't modify files in-place
mv ../Outputs/modflow/mf2k_culebra.lmg \
```

```
    ../Inputs/AP114_Task7/modflow/mf2k_culebra.lmg

# creates links for common files into each of 600 mining-modified
# T fields and runs MODFLOW and DTRKMF (this is 100x100 m grid)
./link_input_run_mf_dtrk.sh

# ------------------------------------------------------
if [ ${verbose} == True ]; then
    echo "## extract DTRKMF output ##"
fi

# combine all 100 realizations of results for each
# mining scenario into a single file for easier plotting
# travel times are converted to 4m thickness

python combine_dtrkmf_output_for_gnuplot.py

# extract time required to exit LWB from dtrkmf results
# also sort results for plotting of travel-time CDFs
# travel times here are converted to 4m thickness

python extract_dtrkmf_lwb_travel_times.py

# ------------------------------------------------------
# convert 100x100 m grid to 50x50 m grid

if [ ${verbose} == True ]; then
    echo "## convert MODFLOW2K inputs to 50x50m grid ##"
fi

# create spatially-variable model property files
# for 50x50m grid from 100x100m grid
python 100x100_to_50x50.py

# create other 50x50 MODFLOW input files from 100x100 files
# using find/replace in sed

if [ ${verbose} == True ]; then
    echo "## create MF2K inputs for 50x50m grid ##"
fi

# change MODFLOW name file to point to expanded input files
# s/find/replace/ is a sed regexp, '.' in the left hand side
# must be escaped with a backslash, or it means "any character"
# a trailing "g" means apply globally (otherwise finds one occurrence)
sed -e "s/modeled_head\.lst/modeled_head_50.lst/" \
    -e "s/modeled_head\.bin/modeled_head_50.bin/" \
    -e "s/modeled_flow\.bud/modeled_flow_50.bud/" \
    -e "s/\.mod/.mod.50/g" \
    -e "s/\.inf/.inf.50/" \
    -e "s/mf2k_head\.dis/mf2k_head_50.dis/" \
     <../Inputs/AP114_Task7/modflow/mf2k_head.nam \
     >../Outputs/modflow/mf2k_head_50.nam

# input file for direct solver
# this is used when LMG doesn't work, which is ~1% of the time
sed -e "s/LMG           8 mf2k_culebra\.lmg/DE4           8 mf2k_culebra.de4/" \
     <../Outputs/modflow/mf2k_head_50.nam \
     >../Outputs/modflow/mf2k_head_50.de4.nam

# change MODFLOW discretization file to new # rows & cols
sed -e "s/307 284/614 568/" \
     <../Inputs/AP114_Task7/modflow/mf2k_head.dis \
     >../Outputs/modflow/mf2k_head_50.dis

# ------------------------------------------------------
# run MODFLOW on refined grid to create budget files
# for SECOTP2D, located inside each subdirectory

if [ ${verbose} == True ]; then
    echo "## run MODFLOW2K on 50x50 m grid ##"
fi

./run_50x50_modflow.sh

# ------------------------------------------------------
# convert budget files to ASCII and copy resulting ASCII files
# (all with same name, but in different directories) into a
# single directory, renaming files appropriately

if [ ${verbose} == True ]; then
    echo "## convert binary budgets to ASCII and move VTRAN2 input files to single location ##"
fi

./convert_rename_modflow_50x50_budget.sh

# the files saved into this directory are inputs to VTRAN2,
# which prepares these files for use by SECOTP2D

if [ ${verbose} == True ]; then
    echo "## end of 'run_mining_mods.sh' Bash shell script ##"
fi
```

A4.4 Python script enlarge_mining_areas.py

A4.4.1 Input File

```
601700.0 3566500.0
284 307
100.0 100.0
616941.0 610495.0 610567.0 617015.0 616941.0
3585109.0 3585068.0 3578623.0 3578681.0 3585109.0
mining_areas_xyz.dat
mining_factor.dat
New_Full_09.dat
New_Part_09.dat
True
```

A4.4.2 Script

```
# this script takes the output of ArcGIS and creates the full and partial mining
# factor files that are used in the mining modification calculation.

from math import floor
from itertools import izip
from sys import exit,argv

##########################################
# read in input data
try:
    # input name has same name as script ending with ".in", instead of ".py"
    scrfname = argv[0]
    inpfname = scrfname.replace('.py','.in')
    fin = open(inpfname,'r')
except IOError:
    print 'ERROR: %s input file "%s" not found.' %(scrfname,inpfname)
    exit(1)

x0,y0 = [float(x) for x in fin.readline().strip().split()]  # UTM NAD27 (m) modflow grid origin
nx,ny = [int(x)   for x in fin.readline().strip().split()]  # number of cells
dx,dy = [float(x) for x in fin.readline().strip().split()]  # cell size (meters)

wipp = []
wipp.append([float(x) for x in fin.readline().rstrip().split()]) # x-coordinate (closed CCW loop)
wipp.append([float(x) for x in fin.readline().rstrip().split()]) # y
wipp = zip(*wipp)

# file with GIS mining data
fnminingin = fin.readline().strip()
# file for saving mining factor into matrix form for debugging
fnminfactout = fin.readline().strip()
# files for full and partial mining indices (output for other scripts)
fnfullminout = fin.readline().strip()
fnpartminout = fin.readline().strip()

# print status/debugging to screen?
verbose = fin.readline().strip()
fin.close()

verbose = verbose[0] == 'T' or verbose[0] == 't'

if verbose:
    print 'echo input'
    print '=============================='
    print "x0,y0",x0,y0
    print "nx,ny",nx,ny
    print "dx,dy",dx,dy
    print "wipp",wipp
    print "fnminingin",fnminingin
    print "fnminfactout",fnminfactout
    print "fnfullminout",fnfullminout
    print "fnpartminout",fnpartminout
    print '=============================='

##################################################

nel = ny*nx

##################################################
# define functions

def wipp_inside(x,y):
    """ given a line segment between points P0=(x0,y0) and P1=(x1,y1)
    a third point P=(x,y) has the following relationship to the line segment.
    f = (y-y0)(x1-x0) - (x-x0)(y1-y0)
    if f<0 then P is to the right of the line,
    if f>0 it is on the left (=0 is on the line)
    if a point is on the left of all CCW line segments defining
    a convex polygon (such as the wipp boundary), then it is inside the polygon
    http://ozviz.wasp.uwa.edu.au/~pbourke/geometry/insidepoly/"""

    f = True
```

```
        for (p0,p1) in zip(wipp[0:-1],wipp[1:]):
            # to be inside the following must be > 0 for all 4 sides
            if (y-p0[1])*(p1[0]-p0[0])-(x-p0[0])*(p1[1]-p0[1]) <= 0.0:
                f = False
                break
        return f

def matsave(filename,m):
    """Writes file as a list of lists as a 2D array (passed in as integers)
    Outer list is rows, inner lists are columns (C-major order)."""
    f = open(filename,'w')
    for row in m:
        f.write(' '.join(['%2i'%val for val in row]) +'\n')
    f.close()

def minsave(filename,m):
    """Save mining matrices, taking the 3 cells of padding into account"""
    f = open(filename,'w')
    for row in m[3:-3]: # leave off first and last 3 rows
        # leave off first and last 3 columns of each row
        f.write(' '.join(['%2i'%val for val in row[3:-3]]) +'\n')
    f.close()

def reshapecv2m(v,order='C'):
    """Reshape a vector that was previously reshaped in C-style order from a matrix,
    back into a matrix (here a list of lists)."""
    if order=='C':
        # row-major order (MODFLOW, C, Python/numpy)
        m = [None]*ny
        for i,(lo,hi) in enumerate(izip(xrange(0, nel-nx+1, nx), xrange(nx, nel+1, nx))):
            m[i] = v[lo:hi]
        return m
    elif order=='F':
        # column-major order (Fortran, Matlab)
        m = [None]*nx
        for i,(lo,hi) in enumerate(izip(xrange(0, nel-ny+1, ny), xrange(ny, nel+1, ny))):
            m[i] = v[lo:hi]
        # transpose rows/columns and flip in y-direction
        return zip(*m)[::-1]


################################################

# read in definition of mining on 100x100 grid
if verbose:
    print 'reading GIS data:',fnminingin

fin = open(fnminingin,'r')
m = []
for line in fin:
    # data are "X Y index" (index=1.0 for potash mining, index=0.0 for outside potash)
    m.append([float(x) for x in line.strip().split()])
    m[-1][2] = 10*int(m[-1][2]) # convert to integer and make index (0,10)

if verbose:
    print len(m),'lines of data read;',len(m[0]),'columns'
    # save coordinates of points inside LWB for checking algorithm

count = 0

# check if inside LWB
for pt in m:
    if wipp_inside(pt[0],pt[1]):
        # add one
        pt[2] += 1
        count += 1

if verbose:
    print count,'cells inside LWB, out of',len(m)

minl = reshapecv2m(zip(*m)[2],order='F')

# save un-expanded mining areas in matrix format for comparison
if verbose:
    print 'saving matrix indicating areas with ore to',fnminfactout
    matsave(fnminfactout,minl)
    matsave(fnminfactout+'x',reshapecv2m(zip(*m)[0],order='F'))
    matsave(fnminfactout+'y',reshapecv2m(zip(*m)[1],order='F'))

# 0  = not mined, outside LWB
# 1  = not mined, inside LWB
# 10 = mined,     outside LWB
# 11 = mined,     inside LWB

# pad the target array (list of lists) to allow easier indexing at boundaries
minp = [None]*(ny+6)
minf = [None]*(ny+6)
for i in xrange(len(minp)):
    minp[i] = [0]*(nx+6)
    minf[i] = [0]*(nx+6)
```

```
166 v5 = [1,1,1,1,1]

168 if verbose:
        print 'expand mining'
170 for i in xrange(ny):
        i2 = i+3
172     for j in xrange(nx):
            j2 = j+3
174         # is there mining in this cell?
            # either inside or outside LWB (full mining case)
176         if minl[i][j] > 9:
                # expand the mining using a 5x5 square, centered on this cell
178             minf[i2-2][j2-2:j2+3] = v5
                minf[i2-1][j2-2:j2+3] = v5
180             minf[i2  ][j2-2:j2+3] = v5
                minf[i2+1][j2-2:j2+3] = v5
182             minf[i2+2][j2-2:j2+3] = v5

184             # expand mining an additional cell in compass directions
                minf[i2+3][j2] = 1
186             minf[i2-3][j2] = 1
                minf[i2][j2-3] = 1
188             minf[i2][j2+3] = 1

190         # is there mining in this cell AND is it outside the LWB?
            # (partial mining case)
192         if minl[i][j] == 10:
                # expand the mining using a 5x5 square
194             minp[i2-2][j2-2:j2+3] = v5
                minp[i2-1][j2-2:j2+3] = v5
196             minp[i2  ][j2-2:j2+3] = v5
                minp[i2+1][j2-2:j2+3] = v5
198             minp[i2+2][j2-2:j2+3] = v5

200             # expand mining an additional cell in compass directions
                minp[i2+3][j2] = 1
202             minp[i2-3][j2] = 1
                minp[i2][j2-3] = 1
204             minp[i2][j2+3] = 1

206 if verbose:
        print 'saving full mining factor array:',fnfullminout
208 minsave(fnfullminout,minf)

210 if verbose:
        print 'saving partial mining factor array:',fnpartminout
212 minsave(fnpartminout,minp)
```

A4.5 Python script mining_mod.py

A4.5.1 Input File

```
284 307
%.11e
../Inputs/keepers_short
New_Full_09.dat
New_Part_09.dat
../Inputs/AP114_Task7/data/init_bnds.inf
init_bnds_full.inf
init_bnds_part.inf
sum1_st2d_pabc09_r1.tbl  sum1_st2d_pabc09_r2.tbl  sum1_st2d_pabc09_r3.tbl
../Inputs/AP114_Task7/Outputs
modeled_K_field.mod
modeled_mined_K_field.mod
True
```

A4.5.2 Script

```
# This script does the actual mining modifications to the T fields and
# MODFLOW boundary conditions.
#
#  INPUTS:  2 integer arrays indicating where full/partial mining occurs
#           100 MODFLOW T fields from calibration
#           1 MODFLOW IBOUND array (specification of active/BC/inactive status)
#           3 mining factor lists (100 numbers 1<=x<=1000)
#
#  OUTPUTS: 600 mining-modified T fields (100 realizations, 2 mining types, 3 replicates)
#           2 mining-modified MODFLOW ibound arrays
#
# this script should be run from the ./Outputs directory

from glob import  glob
from os import makedirs,remove
from os.path import split,exists
from itertools import chain
from sys import exit,argv

########################################
# read in input data
try:
    # input name has same name as script ending with ".in", instead of ".py"
    scrfname = argv[0]
    inpfname = scrfname.replace('.py','.in')
    fin = open(inpfname,'r')
except IOError:
    print 'ERROR: %s input file "%s" not found.' %(scrfname,inpfname)
    exit(1)

# number of columns, rows in model grid
nx,ny = [int(x) for x in fin.readline().rstrip().split()]
outfmt = fin.readline().strip()  # python format for K fields
fnrznlist = fin.readline().strip()  # filname of shortened realization list (keepers_short)
fnfullminin = fin.readline().strip()  # full mining indicator field (input)
fnpartminin = fin.readline().strip()  # partial mining "" "" (input)
fnIBOUNDin = fin.readline().strip()  # path to MF2K IBOUND array file (input)
fnIBOUNDfout = fin.readline().strip() # path to full-mining-modified IBOUND (out)
fnIBOUNDpout = fin.readline().strip() # "" partial "" ""
fnminfact = fin.readline().strip().split()  # list of 3 filenames for mining factors from VMS
pathrzn = fin.readline().strip()       # base path to all 100 AP114_Task 7 realizations
fnKfieldin = fin.readline().strip()  # filename of K (aka T) field (in)
fnKfieldout = fin.readline().strip()  # filename for mining-modified K field (out)
verbose = fin.readline().strip()       # True to print status output (False = no)
fin.close()

verbose = verbose[0] == 'T' or verbose[0] == 't'

if verbose:
    print 'echo input'
    print '=================='
    print 'nx,ny',nx,ny
    print 'outfmt',outfmt
    print 'fnrznlist',fnrznlist
    print 'fnfullminin',fnfullminin
    print 'fnpartminin',fnpartminin
    print 'fnIBOUNDin',fnIBOUNDin
    print 'fnIBOUNDfout',fnIBOUNDfout
    print 'fnIBOUNDpout',fnIBOUNDpout
    print 'fnminfact',fnminfact
    print 'pathrzn',pathrzn
    print 'fnKfieldin',fnKfieldin
    print 'fnKfieldout',fnKfieldout
    print '=================='

ncl = nx*ny

########################################
# define functions
def intload(filename):
```

```
    """Reads file (a 2D integer array) as a list of lists.
    Outer list is rows, inner lists are columns."""
    f = open(filename,'r')
    m = [[int(v) for v in line.rstrip().split()] for line in f]
    f.close()
    return m

def intsave(filename,m):
    """Writes file as a list of lists as a 2D integer array, space-separated format '%2i'.
    Outer list is rows, inner lists are columns."""
    f = open(filename,'w')
    for row in m:
        f.write(' '.join(['%2i' % col for col in row]) + '\n')
    f.close()

def floatload(filename):
    """Reads file (a list of real numbers, one number each row) into a list of floats."""
    f = open(filename,'r')
    m = [float(line.rstrip()) for line in f]
    f.close()
    return m

def floatsave(filename,m):
    """Writes file as a list floats, one value per row, format '%.11e'."""
    f = open(filename,'w')
    f.write('\n'.join([outfmt%num for num in m]) +'\n')
    f.close()

def debugsave(filename,m,n):
    f = open(filename,'w')
    for val,flag in zip(m,n):
        f.write(outfmt%val + ' %5i'%flag  +'\n')
    f.close()

def reshapem2v(m):
    """Reshapes a rectangular matrix into a vector in same fashion as numpy.reshape(),
    which is C-major order"""
    return list(chain(*m))

########################################
if verbose:
    print 'read files'
# read in mining definitions and modflow ibound array (all 2D integer matrices)
full = intload(fnfullminin)
part = intload(fnpartminin)
ibound = intload(fnIBOUNDin)

iboundf = []
iboundp = []

if verbose:
    print 'adjust BC'
# turn off constant head nodes where mining modification happens
for j in xrange(ny):
    rowf = []
    rowp = []
    for i in xrange(nx):

        #  1 in mining file indicates mining
        # -1 in ibound array indicates constant head
        # new ibound array for full mining
        if full[j][i] == 1 and ibound[j][i] == -1:
            rowf.append(1)
        else:
            rowf.append(ibound[j][i])

        # new ibound array for partial mining
        if part[j][i] == 1 and ibound[j][i] == -1:
            rowp.append(1)
        else:
            rowp.append(ibound[j][i])

    iboundf.append(rowf)
    iboundp.append(rowp)

# make the northeast far row/column is still specified head at the outermost row/col
# these are columns 99:284 in row 1 and all rows in rightmost column for
# CRA 2009 PABC MODFLOW model
for i in xrange(98,nx):
    iboundf[0][i] = -1
    iboundp[0][i] = -1

for j in xrange(ny):
    iboundf[j][-1] = -1
    iboundp[j][-1] = -1

# make sure south row is all constant head
for j in xrange(nx):
```

```
159         iboundf[-1][j] = -1
            iboundp[-1][j] = -1
161
    # make sure south part of western boundary (row 159:307) is all constant head
163 for j in xrange(159,ny):
            iboundf[j][0] = -1
165         iboundp[j][0] = -1

167 # create similar subdirectories in the Outputs subdir for modified input
    # files, rather than just putting them back in the Inputs directory
169 # with the unmodified files checked out of CVS
    for dir in ['../Outputs/data','../Outputs/modflow']:
171         if not exists(dir):
                makedirs(dir)
173
    # save two mining-modified MODFLOW IBOUND arrays to disk
175 intsave('../Outputs/data/'+fnIBOUNDfout,iboundf)
    intsave('../Outputs/data/'+fnIBOUNDpout,iboundp)
177
    if verbose:
179         print 'reshape mining'
    # reshape 2D matrix of integer mining indicators to
181 # vector same shape as T fields
    full = reshapem2v(full)
183 part = reshapem2v(part)
    min = [full,part]
185
    if verbose:
187         print 'read mining factors'
    # read in 3 lists of random mining factors
189 # skip first 3 rows (header), mining factor is third column
    minp_fact = [None]*3
191 transidx = [None]*3

193 for i,infn in enumerate(fnminfact):
            fh = open(infn,'r')
195         data = fh.read().strip()
            fh.close()
197
            # read in list of mining factors (floating point 1.0 to 1000.0)
199         minp_fact[i] = [float(line.split()[2]) for line in data.splitlines()[3:]]

201         # read in mapping from order in "keepers" -> SECOTP vector order (integer index 1:100)
            transidx[i] =  [int(float(line.strip().split()[3])) for line in data.splitlines()[3:]]
203
    # loop over all 100 realizations ()
205 fin = open(funtlist,'r')
    rzns = [x.strip() for x in fin.readlines()]  # list of 100 MODFLOW realizations in proper order
207 fin.close()

209 for i,rzn in enumerate(rzns):
            if verbose:
211             print i,rzn # print status to screen

213         # path into realization directory
            d = pathrzn + '/' + rzn
215
            # get the original T fields from the calibration results (1D double-precision vector)
217         K = floatload(d +'/'+ fnKfieldin)

219         # write unmodififed T field to R0 directory
            # create rzn subdirectories
221         path = './R0/' + rzn
            if not exists(path):
223             makedirs(path)
            Kfn = path + '/'+ fnKfieldin
225         if exists(Kfn):
                remove(Kfn)
227         floatsave(Kfn+'.bak',K)  # to copmare with the linked version

229         # perform mining modifications and copy results to directory
            # creating directory structure for 3 replicates and full/partial mining
231         for j,r in enumerate(['R1','R2','R3']):
                for m,t in enumerate(['full','part']):
233                 Kmin = [None]*nel
                    for n,val in enumerate(K):
235                     if min[m][n] == 1:
                            # apply mining factor, lookup the current flow realization (0-based)
237                         # in the transidx list (1-based) and take that mining factor
                            Kmin[n] = val*minp_fact[j][transidx[j].index(i+1)]
239                     else:
                            Kmin[n] = val
241
                    # save mining modified K into directory tree
243                 # create realization directory if it doesn't exist yet
                    mfn = '/'.join([r,t,rzn])
245                 if not exists(mfn):
                        makedirs(mfn)
```

```
247         floatsave(mfn +'/'+ fnKfieldout,Kmin)

249         # debugging version has both K values and mining factors
            # (for comparison with original K field)
251         if verbose:
                debugsave(mfn +'/'+ fnKfieldout+'.dbg',Kmin,min[m])
```

A4.6 Bash shell script `link_input_run_mf_dtrk.sh`

```
#!/bin/bash

verbose=True

crfile=lmg_err.tmp

# set a 1 minute timeout for LMG solver (usually runs in ~2 seconds)
ulimit -S -t 60

# use absolute paths with ln -s
path='pwd'

# this should point to the working directory where ReadScript.py was run
# which the parent directory of the current Output directory
# where this script was started
based='dirname ${path}'

if [ ${verbose} == True ]; then
    echo "current dir:" ${path}
    echo "base dir:" ${based}
fi

########################################
# re-run no-mining scenario in the "R0" directory
r=0
for d in 'cat ${based}/Inputs/keepers_short'; do
  cd R0/${d}

  echo "current directory:" 'pwd'

  # input files that are the same for every realization
  for f in 'cat ${based}/Inputs/files'; do
    # the "files" list includes directories in the names too
    ln -sf ${based}/${f} .
  done

  # handle ibound array separately (here use AP114 Task7 version)
  ln -sf ${based}/Inputs/AP114_Task7/data/init_bnds.inf .

  # realization-specific files
  for x in {R,A,S,K}; do
    ln -sf ${based}/Inputs/AP114_Task7/Outputs/${d}/modeled_${x}_field.mod .
  done

  # delete any old budget file, so dtrkmf throws
  # an error if modflow doesn't run
  if [ -a modeled_flow.bud ]; then
      rm modeled_flow.bud
  fi

  # run MF2K
  if [ ${verbose} == True ]; then
      ${based}/Inputs/bin/mf2k_1.6.release  mf2k_head.nam | tee mf2k_stdout
  else
      ${based}/Inputs/bin/mf2k_1.6.release  mf2k_head.nam >mf2k_stdout
  fi

  # dtrkmf reads .dis file, but not .nam file (why?)
  ln -sf ./elev_bot.mod ./fort.34
  ln -sf ./elev_top.mod ./fort.33

  # run DTRKMF
  if [ ${verbose} == True ]; then
      ${based}/Inputs/bin/dtrkmf_v0100 <dtrkmf.in | tee dtrkmf_stdout
  else
      ${based}/Inputs/bin/dtrkmf_v0100 <dtrkmf.in >dtrkmf_stdout
  fi

  cd ../..
done

if [ ${verbose} == True ]; then
    echo " running mining-modified MODFLOW realizations"
fi

########################################
# run mining modified cases in directories R1,R2 and R3
for r in {1,2,3}; do
  for t in {"full","part"}; do
    for d in 'cat ${based}/Inputs/keepers_short'; do
      cd R${r}/${t}/${d}

      if [ ${verbose} == True ]; then
          echo "current directory:" 'pwd'
      fi

      # input files that are the same for every realization
      for f in 'cat ${based}/Inputs/files'; do
        ln -sf ${based}/${f} .
```

```
90          done
92          # handle ibound array separately (here use mining-modified one)
            ln -sf ${based}/Outputs/data/init_bnds_${t}.inf ./init_bnds.inf
94
            # realization-specific files (not including K, use mining-modified one)
96          for x in {R,A,S}; do
              ln -sf ${based}/Inputs/AP114_Task7/Outputs/${d}/modeled_${x}_field.mod .
98          done
100         ln -sf modeled_mined_K_field.mod modeled_K_field.mod
102         if [ -a modeled_flow.bud ]; then
                rm modeled_flow.bud
104         fi
106         # make sure there are no error files laying around
            if [ -s ${erfile} ]; then
108             rm -f ${erfile}
            fi
110
            # run MF2K with LMG solver
112         if [ ${verbose} == True ]; then
                ${based}/Inputs/bin/mf2k_1.6.release mf2k_head.nam | tee mf2k_stdout
114         else
                ${based}/Inputs/bin/mf2k_1.6.release mf2k_head.nam >mf2k_stdout
116         fi
118         # check for presence of non-zero sized error file.
            # Re-run with direct solver, which is very slow but always works
120         if [ -s ${erfile} ]; then
122             ln -sf ${based}/Outputs/modflow/mf2k_head.de4.nam .
                ln -sf ${based}/Inputs/mf2k_culebra.de4 .
124
                ulimit -S -t unlimited
126             # concatenate log file to the end of other file
                ${based}/Inputs/bin/mf2k_1.6.release mf2k_head.de4.nam \
128                 >>mf2k_stdout
                ulimit -S -t 60
130         fi
132         ln -sf ./elev_bot.mod ./fort.34
            ln -sf ./elev_top.mod ./fort.33
134
            # DTRKMF
136         if [ ${verbose} == True ]; then
                ${based}/Inputs/bin/dtrkmf_v0100 <dtrkmf.in | tee dtrkmf_stdout
138         else
                ${based}/Inputs/bin/dtrkmf_v0100 <dtrkmf.in >dtrkmf_stdout
140         fi
142         cd ../../..
          done
144     done
    done
146
    ulimit -S -t unlimited
```

A4.7 Python script combine_dtrkmf_output_for_gnuplot.py

A4.7.1 Input File

```
601700.0  3597100.0
100.0  100.0
dtrk.out
dtrk_nomining_all_realizations.dat
dtrk_all_realizations  .dat
True
```

A4.7.2 Script

```
# put all the particle tracks together into one file for simpler
# plotting of the "cloud" of particles using gnuplot
#
# INPUT:  700 dtrkmf output files
# OUTPUT: 7 merged files with all particle tracks together
#           each realization separated by two blank lines
#

from glob import glob
from sys import exit,argv

##################################################
# read input data
try:
    # input name has same name as script ending with ".in", instead of ".py"
    scrfname = argv[0]
    inpfname = scrfname.replace('.py','.in')
    fin = open(inpfname,'r')
except IOError:
    print 'ERROR: %s input file "%s" not found.' %(scrfname,inpfname)
    exit(1)

# grid origin for dtrkmf I,J -> UTM NAD27 x,y conversion
x0,y0 = [float(x) for x in fin.readline().rstrip().split()]
dx,dy = [float(x) for x in fin.readline().rstrip().split()]
fndtrkout =      fin.readline().strip()  # dtrkmf output filename
fnnominingout = fin.readline().strip()   # output filename
fnminingout =   fin.readline().strip().split()  # prefix & suffix of output file
verbose =       fin.readline().strip()

verbose = verbose[0] == 'T' or verbose[0] == 't'

if verbose:
    print 'echo input'
    print '=================='
    print 'x0,y0',x0,y0
    print 'dx,dy',dx,dy
    print 'fndtrkout',fndtrkout
    print 'fnnominingout',fnnominingout
    print 'fnminingout',fnminingout
    print '=================='

########################################

rep=['R1','R2','R3']
min=['full','part']
for r in rep:
    for m in min:
        ofn = fnminingout[0]+'_'+r+'_'+m+fnminingout[1]
        if verbose:
            print 'output:',ofn
        fout = open(ofn,'w')
        for f in glob('/'.join([r,m,'r???',fndtrkout])):
            if verbose:
                print 'input:',f
            # read in all results (except first header line)
            fh = open(f,'r')
            results = [l.split() for l in fh.readlines()[1:]]
            fh.close()
            # write a gnuplot-friendly header for each realization
            fout.write('# %s \n' % f)
            # write x,y location and time
            for pt in results:
                # convert from I,J to x,y
                x = float(pt[1])*dx + x0
                y = y0 - float(pt[2])*dy
                # convert from 7.75-m to 4-m Culebra
                t = float(pt[0])/7.75*4.0
                fout.write('%.1f,%.1f,%.8e\n' % (x,y,t))

            # 2 blank lines between each realization
            fout.write('\n\n')
        fout.close()

# nomining case
r='R0'
```

```
78  if verbose:
        print 'output:',fnnominingout
80  fout = open(fnnominingout,'w')
    for f in glob('/'.join([r,'r???',fndtrkout])):
82      if verbose:
            print 'input:',f
84      fh = open(f,'r')
        results = [l.split() for l in fh.readlines()[1:]]
86      fh.close()
        fout.write('# %s \n' % f)
88      for pt in results:
            x = float(pt[1])*dx + x0
90          y = y0 - float(pt[2])*dy
            t = float(pt[0])/7.75*4.0
92          fout.write('%.1f,%.1f,%.8e\n' % (x,y,t))

94      fout.write('\n\n')
    fout.close()
```

A4.8 Python script extract_dtrkmf_lwb_travel_times.py

A4.8.1 Input File

```
601700.0  3597100.0
100.0  100.0
dtrk.out
wipplwb_results_nomining.out
wipplwb_results  .out  .sort
True
```

A4.8.2 Script

```
# extract the final time from each DTRKMF output file.  This corresponds
# to the travel time from the release point at the center of the
# waste panels (C-2737) to the WIPP LWB.
#
# INPUTS:  700 DTRKMF output files (600 mining + 100 no-mining)
# OUTPUTS: 7 summary files with travel time to cross WIPP LWB
#             and x,y location of crossing point.
#          7 summary files with cumulative probability, travel
#             time to the WIPP LWB, files sorted by travel time.

from glob import glob
from sys import exit,argv

#####################################################
# read input data
try:
    # input name has same name as script ending with ".in", instead of ".py"
    scrfname = argv[0]
    inpfname = scrfname.replace('.py','.in')
    fin = open(inpfname,'r')
except IOError:
    print 'ERROR: %s input file "%s" not found.' %(scrfname,inpfname)
    exit(1)

# grid origin for dtrkmf I,J -> UTM NAD27 x,y conversion
x0,y0 = [float(x) for x in fin.readline().rstrip().split()]
dx,dy = [float(x) for x in fin.readline().rstrip().split()]
fndtrkout = fin.readline().strip()  # dtrkmf output filename
fnnominingout = fin.readline().strip()   # output filename
fnminingout = fin.readline().strip().split()  # prefix & suffix of output file
verbose = fin.readline().strip()

verbose = verbose[0] == 'T' or verbose[0] == 't'

if verbose:
    print 'echo input'
    print '=================='
    print 'x0,y0',x0,y0
    print 'dx,dy',dx,dy
    print 'fndtrkout',fndtrkout
    print 'fnnominingout',fnnominingout
    print 'fnminingout',fnminingout
    print '=================='

########################################

# loop over all the mining scenarios
for r in ['R1','R2','R3']:
    for scen in ['full','part']:
        ofn = fnminingout[0]+'_'+r+'_'+scen+fnminingout[1]
        if verbose:
            print 'output:',ofn
        fout = open(ofn,'w')
        for d in glob('/'.join([r,scen,'r???'])):

            # open file, get last row (t,col,row,...)
            ifn = d +'/'+ fndtrkout
            if verbose:
                print 'input:',ifn
            fin = open(ifn,'r')
            pt = fin.readlines()[-1].split()
            fin.close()

            # save coordinates of exit point
            x = float(pt[1])*dx + x0
            y = y0 - float(pt[2])*dy

            # save travel time (coverting to 4m thick Culebra
            # from 7.75m MODFLOW results)
            t = float(pt[0])/7.75*4.0

            fout.write('%.8e,%.1f,%.1f,%s\n' % (t,x,y,d[-4:]))

        # write each 100 realizations to different file
        fout.close()

# the non-mining scenario
```

```
r='R0'
if verbose:
    print 'output:',fnnominingout
fout = open(fnnominingout,'w')
for d in glob(r+'/r???'):

    ifn = d +'/'+ fndtrkout
    if verbose:
        print 'input:',ifn
    fin = open(ifn,'r')
    pt = fin.readlines()[-1].split()
    fin.close()

    x = float(pt[1])*dx + x0
    y = y0 - float(pt[2])*dy
    t = float(pt[0])/7.75*4.0
    fout.write('%.8e,%.1f,%.1f,%s\n' % (t,x,y,d[-4:]))

fout.close()

########################################
# read data back in and pre-process for making CDF figures

nr = 100 # number of realizations

# cumulative probability vector
p = [float(j+1)/float(nr) for j in range(nr)]

# ####################################
# add first column with cumulative p values
# and sort each column from shortest to largest travel time
for ifn in glob(fnminingout[0]+'*'+fnminingout[1]):
    fin = open(ifn,'r')
    t = [(float(line.split(',')[0]),line.rstrip().split(',')[-1]) for line in fin]
    fin.close()

    # this sorting approach taken from Python Library reference
    tmplist = [(x[0],x) for x in t]
    tmplist.sort()
    t = [x for (key,x) in tmplist]

    ofn = ifn.replace(fnminingout[1],fnminingout[2])

    if verbose:
        print ifn,'->',ofn

    # give sorted files a different exentsion
    fout = open(ofn,'w')
    for prob,(time,name) in zip(p,t):
        fout.write('%.2f,%.8e,%s\n' % (prob,time,name))
    fout.close()
```

A4.9 Python script 100x100_to_50x50.py

A4.9.1 Input File

```
284  307  100
../Inputs/AP114_Task7/data/
elev_top.mod  elev_bot.mod
elev_top.mod.50  elev_bot.mod.50
init_head.mod
init_head.mod.50
./data/
init_bnds.inf  init_bnds_part.inf  init_bnds_full.inf
init_bnds.inf.50  init_bnds_part.inf.50  init_bnds_full.inf.50
../Inputs/AP114_Task7/Outputs/
modeled_A_field.mod  modeled_R_field.mod  modeled_S_field.mod  modeled_K_field.mod
modeled_A_field.mod.50  modeled_R_field.mod.50  modeled_S_field.mod.50  modeled_K_field.mod.50
%.11e
True
```

A4.9.2 Script

```
# this script expands the MODFLOW input files from the 100x100m grid
# used in AP-144 to the 50x50m grid used by SECOTP2D (AP-145)
#
# INPUTS:  2 integer IBOUND arrays
#          2 real top/bottom elevation arrays
#          1 real starting head array
#          2400 real parameter fields (4 params x 100 realizations x 3 replicates x 2 mining types)
#
# OUTPUTS: 2 integer expanded (50x50m) IBOUND arrays
#          2 expanded real top/bottom elevation arrays
#          1 expanded real starting head array
#          2400 expanded real parameter fields and associated directory structure:

from glob import glob
from itertools import chain,izip
from sys import exit,argv

################################################
# read input data
try:
    # input name has same name as script ending with ".in", instead of ".py"
    scrfname = argv[0]
    inpfname = scrfname.replace('.py','.in')
    fin = open(inpfname,'r')
except IOError:
    print 'ERROR: %s input file "%s" not found.' %(scrfname,inpfname)
    exit(1)

# columns, rows, and realizations in 100x100m MODFLOW model
nx,ny,nf = [int(x) for x in fin.readline().rstrip().split()]
pathMF2Kdata =     fin.readline().strip()      # relative paths to AP114 Task7 files
fnelevin =         fin.readline().strip().split() # elevation files (input)
fnelevout =        fin.readline().strip().split() # " " (output)
fninitheadin =     fin.readline().strip()         # starting head file (input)
fninitheadout =    fin.readline().strip()         # " " (output)
pathMF2Kdataout =  fin.readline().strip()      # path to resulting modified arrays
fnIBOUNDin =       fin.readline().strip().split() # IBOUND arrays (input)
fnIBOUNDout =      fin.readline().strip().split() # " " " (outputs)
pathMF2KOutputs =  fin.readline().strip()         # path to AP114 Task 7 Outputs
fnfieldsin =       fin.readline().strip().split() # {A,R,S,K} fiels (input)
fnfieldsout =      fin.readline().strip().split() # " " " (output)
outfmt =           fin.readline().strip()  # valid Python format for MF2K output
verbose =          fin.readline().strip()
fin.close()

verbose = (verbose[0] == 'T' or verbose[0] == 't')

if verbose:
    print 'echo input'
    print '=================='
    print 'nx,ny,nf',nx,ny,nf
    print 'pathMF2Kdata',pathMF2Kdata
    print 'fnelevin',fnelevin
    print 'fnelevout',fnelevout
    print 'fninitheadin',fninitheadin
    print 'fninitheadout',fninitheadout
    print 'pathMF2Kdataout',pathMF2Kdataout
    print 'fnIBOUNDin',fnIBOUNDin
    print 'fnIBOUNDout',fnIBOUNDout
    print 'pathMF2KOutputs',pathMF2KOutputs
    print 'fnfieldsin',fnfieldsin
    print 'fnfieldsout',fnfieldsout
    print 'outfmt',outfmt
    print '=================='

nel = nx*ny

################################################
# define functions
```

```
70
    # only float{load,save} below convert from string to numeric values
72  # other functions only work with strings for increased speed and to
    # eliminate possible changes in trailing significant figures from conversions
74  def matload(filename):
        """Reads file (a 2D array) as a list of lists of strings.
76      Outer list is rows, inner lists are columns."""
        f = open(filename,'r')
78      m = [line.rstrip().split() for line in f]
        f.close()
80      return m

82  def matsave(filename,m):
        """Writes file as a list of lists as a 2D array (passed in as strings)
84      Outer list is rows, inner lists are columns
        (column-major or C-style order)."""
86      f = open(filename,'w')
        for row in m:
88          f.write(' '.join(row) + '\n')
        f.close()
90
    def floatload(filename):
92      """Reads file (a list of strings, one per row) into a list of floats."""
        f = open(filename,'r')
94      m = [float(line.rstrip()) for line in f]
        f.close()
96      return m

98  def floatsave(filename,m):
        """Writes file as a list floats, one value per row."""
100     f = open(filename,'w')
        f.write('\n'.join([outfmt % num for num in m]) + '\n')
102     f.close()

104 def vecload(filename):
        """Reads file (a list of real numbers, one number each row)
106     into a list (no conversion)."""
        f = open(filename,'r')
108     m = [line.rstrip() for line in f]
        f.close()
110     return m

112 def vecsave(filename,m):
        """Writes file as a list floats, one value per row."""
114     f = open(filename,'w')
        f.write('\n'.join(m) + '\n')
116     f.close()

118 # these 3 reshaping routines are generic
    # they work on either strings, floats, or integers
120 def reshapem2v(m):
        """Reshapes a rectangular matrix into a vector in
122     row-major (C-style) order"""
        return list(chain(*m))
124
    def reshapev2m(v):
126     """Reshape a vector that was previously reshaped in row-major
        order from a matrix, back into a matrix (here a list of lists)."""
128     m = [None]*ny
        for i,(lo,hi) in enumerate(izip(xrange(0, ncl-nx+1, nx),
130                                     xrange(nx, ncl+1, nx))):
            m[i] = v[lo:hi]
132     return m

134 def doublem(m):
        """create a matrix that is doubled in both rows and cols, with
136     entries copied from each larger cell into the 4 smaller cells
        associated with it."""
138     md = [None]*(2*ny)
        for i,row in enumerate(m):
140         drow = list(chain(*[(x,x) for x in row]))
            md[2*i] =   drow
142         md[2*i+1] = drow
        return md
144

146 ################################################
    # top and bottom elevations (double-precision vectors)
148 if verbose:
        print 'top/bot elevations'
150
    inbased  = pathMF2Kdata
152 outbased = pathMF2Kdataout

154 for fin,fout in zip(fnelevin,fnelevout):
        ifn = inbased + fin
156     ofn = outbased + fout
        if verbose:
158         print ifn,'->',ofn
        vecsave(ofn,reshapem2v(doublem(reshapev2m(vecload(ifn)))))
```

```
160
    #@@@@@@@@@@@@@@@@@@@@@@
162 # initial / boundary head (double-precision vectors)
    if verbose:
164     print 'initial head'

166 infname = inbased + fninitheadin
    outfname = outbased + fninitheadout
168 if verbose:
        print infname,'->',outfname
170
    mout = doublem(reshapev2m(floatload(infname)))
172
    # build up empty "matrices"
174 fact = []
    res = []
176 for j in range(2*ny):
        fact.append([0.0 for x in range(2*nx)])
178     res.append([0.0 for x in range(2*nx)])

180 # need to smooth and average heads along exterior boundaries,
    # need to do conversion to floats (avoided elsewhere)
182
    # first & last two rows (each boundary cell converted to 2 cells)
184 for row in [0,1,-2,-1]:
        deltah = []
186     # compute smoothing factor
        for p,v,n in zip(mout[row][0:-2], mout[row][1:-1], mout[row][2:]):
188         # one of these two terms =0, because neighboring values are copies
            deltah.append(v-p + v-n)
190
        # apply smoothing factor
192     for i in xrange(1,len(mout[row])-1):
            # factor 1/4 is distance between centers of smaller cells
194         # relative to distance between centers of larger cells
            fact[row][i] = - 0.25*deltah[i-1]
196
    mtout = zip(*mout)
198
    # first & last two columns :: zip(*"list of lists") essentially a transpose
200 for col in [0,1,-2,-1]:
        deltah = []
202     for p,v,n in zip(mtout[col][0:-2], mtout[col][1:-1], mtout[col][2:]):
            deltah.append(v-p + v-n)
204
        for i in xrange(1,len(mtout[col])-1):
206         fact[i][col] = - 0.25*deltah[i-1]

208 # apply factors
    for i,row in enumerate(fact):
210     for j,val in enumerate(row):
            # don't smooth transition between Land surface constant head and
212         # that specified by the parametric surface
            if abs(fact[i][j]) < 20.0:
214             res[i][j] = fact[i][j] + mout[i][j]
            else:
216             res[i][j] = mout[i][j]

218 # save results
    floatsave(outfname,reshapem2v(res))
220
    #@@@@@@@@@@@@@@@@@@@@@@
222 # ibound arrays (integer matrices)
    if verbose:
224     print 'ibound'

226 for fin,fout in zip(fnIBOUNDin[0:1],fnIBOUNDout[0:1]):
        ifn = inbased + fin
228     ofn = outbased + fout
        if verbose:
230         print ifn,'->',ofn
        matsave(ofn,doublem(matload(ifn)))
232
    for fin,fout in zip(fnIBOUNDin[1:],fnIBOUNDout[1:]):
234     # these files were mining modified and are
        # already in the "output" directory
236     ifn = outbased + fin
        ofn = outbased + fout
238     if verbose:
            print ifn,'->',ofn
240     matsave(ofn,doublem(matload(ifn)))

242 #@@@@@@@@@@@@@@@@@@@@@@
    # A,R and S fields (DP vectors, same for all 3 mining scenarios)
244 if verbose:
        print 'anisotropy, recharge, and storativity'
246
    inbased = pathMF2KOutputs
248 # save mining-agnostic files in the R0/r??? set of sub-directories
    outbased = './R0/'
```

```
250
    realizations = glob(inbased+'r???')
252
    for r in realizations:
254     rzn = r.split('/')[-1] # get just the 'r???' part
        for fin,fout in zip(fnfieldsin[0:3],fnfieldsout[0:3]):
256         ifn = r +'/'+ fin
            ofn = outbased + rzn +'/'+ fout
258         if verbose:
                print ifn,'->',ofn
260         vecsave(ofn,reshapem2v(doublem(reshapev2m(vecload(ifn)))))

262
    #@@@@@@@@@@@@@@@@@@@@
264 # K fields (different for each realization and mining scenario)
    if verbose:
266     print 'hydraulic conductivity'

268 # R[1-3] are replicates (not including non-mining case R0)
    # * is {full,part} mining
270 # r??? is T-field realization
    realizations = glob('R[1-3]/*/r???/')
272
    for r in realizations:
274     # these files are already in ./Outputs, since they are modified
        ifn = r + fnfieldsin[3]
276     ofn = r + fnfieldsout[3]
        if verbose:
278         print ifn,'->',ofn
        vecsave(ofn,reshapem2v(doublem(reshapev2m(vecload(ifn)))))
```

A4.10 Bash shell script run_50x50_modflow.sh

```
#!/bin/bash

verbose=True

# use absolute paths with ln
path='pwd'
based='dirname ${path}'

erfile=lmg_err.tmp

#set -o xtrace

mfexe=mf2k_1.6.release
#mfexe=mf2k_dp_1.6.release

# set a 2 minute timeout for LMG solver (usually runs in ~4 seconds)
ulimit -S -t 120

if [ ${verbose} == True ]; then
    echo "current dir:" ${path}
    echo "base dir:" ${based}
fi

########################################
# run mining modified cases in directories R1,R2 and R3
for r in {1,2,3}; do
  for t in {"full","part"}; do
    for d in 'cat ${based}/Inputs/keepers_short'; do
      cd R${r}/${t}/${d}

      if [ ${verbose} == True ]; then
          echo 'current dir:' R${r} ${t} ${d}
      fi

      # input files that are the same for every realization
      for f in 'cat ${based}/Inputs/files.50'; do
        ln -sf ${based}/${f} .
      done

      # handle ibound array separately
      ln -sf ${based}/Outputs/data/init_bnds_${t}.inf.50 ./init_bnds.inf.50

      # realization-specific files (not including K - use modified one)
      # were saved into the R0/r??? subdirectory structure
      for x in {R,A,S}; do
        ln -sf ${based}/Outputs/R0/${d}/modeled_${x}_field.mod.50 .
      done

      # make sure there are no error files laying around
      if [ -s ${erfile} ]; then
          rm -f ${erfile}
      fi

      # run MF2K with LMG solver (fast, works 99% of the time)
      if [ ${verbose} == True ]; then
          ${based}/Inputs/bin/${mfexe}  mf2k_head_50.nam \
              | tee mf2k_stdout.50
      else
          ${based}/Inputs/bin/${mfexe}  mf2k_head_50.nam \
              >mf2k_stdout.50
      fi

      # there are two potential reasons that MF2K may need to be re-run with de4
      # ------------------------------------------------------------------------
      # 1) MF2K runs to completion, but the solver does not converge
      #    grep has to be used to check for this statement in the listing file
      # 2) MF2K never finishes, therefore the timelimit must be
      #    used to kill MF2K, producing an error file.

      # If either condition is met re-run with direct solver,
      # which is very slow but always works

      # check for and write out the type of failure
      fail=0
      if grep 'FAILED TO CONVERGE IN TIME STEP   1 OF STRESS PERIOD   1' modeled_head_50.lst; then
          fail=1
          messg=non-converged
      elif [ -s ${erfile} ]; then
          fail=2
          messg=timed-out
      fi

      if [[ ${fail} > 0 ]]; then
          if [ ${verbose} == True ]; then
              echo 'Convergence problem' ${messg} 'in:' R${r} ${t} ${d} 'use DE4 solver'
          fi

          ln -sf ${based}/Outputs/modflow/mf2k_head_50.de4.nam .
```

```
            ln -sf ${based}/Inputs/mf2k_culebra.dc4 .

            ulimit -S -t unlimited
            # concatenate log file to the end of other file
            ${based}/Inputs/bin/${mfexe} mf2k_head_50.de4.nam \
                >>mf2k_stdout.50
            ulimit -S -t 120
        fi

        cd ../../..
      done
    done
done

# unset limit set at top of script
ulimit -S -t unlimited
```

A4.11 Bash shell script `convert_rename_modflow_50x50_budget.sh`

```
#!/bin/bash

# this script traverses the directory structure, converting
# the 50x50m MF2K budget files to ASCII format, and
# copies them to a common directory (renaming them uniquely),
# then zips up the budget files for ftp transfer to VMS

verbose=True
buddir=modflow_50x50_budgets

if [ -d ${buddir} ]; then
    echo "budget destination directory exists"
else
    mkdir ${buddir}
fi

# copy output from each of 600 directories to common directory
# renaming files using directory structure
for r in {1,2,3}; do
  for t in {'full','part'}; do
    index=0
    for d in `cat ../Inputs/keepers_short`; do

      # increment counter
      let index++

      # save a zero-padded integer as a string for writing as filename
      fff=`printf "%03d" ${index}`

      cd R${r}/${t}/${d}

      # link local versions of python script and its input file
      ln -sf ../../../../Inputs/budget_bin2ascii.{py,in} .

      # run binary -> ascii Python converter script
      python budget_bin2ascii.py

      # use F and P like VMS is expecting
      if [ ${t} == full ]; then
          typ=F
      else
          typ=P
      fi

      if [ ${verbose} == True ]; then
          echo "current dir:" `pwd` "-> MF2K_PABC09_R${r}_M${typ}_F${fff}.OUT"
      fi

      # move ascii file to common directory while modifying file name
      # to conform to what VMS expects
      mv modeled_flow_50.asciibud \
          ../../../${buddir}/MF2K_PABC09_R${r}_M${typ}_F${fff}.OUT

      cd ../../..
    done
  done
done

# zip up files by replicate, for easier transfer to VMS.
# The files are >2GB all zipped up, so it has to be
# broken into three files to stay below that 32-bit file-size limit

##cd ${buddir}
##for rep in {R1,R2,R3}; do
##  # fastest compression is good enough, therfore use -1
##  # -T tests the archive after creating it
##   zip -T1 modflow_budgets_${rep} MF2K_PABC09_${rep}_*.OUT
##done
##cd ..
```

A4.12 Python script budget_bin2ascii.py

A4.12.1 Input File

```
modeled_flow.bud
%24.16e
modeled_flow.asciibud
True
```

A4.12.2 Script

```
# this script reads in the binary MODFLOW budget files, saved in
# the compact format.  ASCII arrays (with one blank line between them)
# for "FLOW RIGHT FACE" and "FLOW FRONT FACE" (qx and qy) are saved to file
#
# INPUT:  MODFLOW binary budget file
# OUTPUT: ASCII file with qx and qy matricies
#
# NB: this script assumes one layer in binary file, if there is more than one
# the last layer present will overwrite the previous layers in the ASCII file

import struct
from itertools import izip
from sys import exit,argv

if __name__ == "__main__":
    ###################################################
    # read input data
    try:
        # input name has same name as script ending with ".in", instead of ".py"
        scrfname = argv[0]
        inpfname = scrfname.replace('.py','.in')
        fin = open(inpfname,'r')
    except IOError:
        print 'ERROR: %s input file "%s" not found.' %(scrfname,inpfname)
        exit(1)

    fnbinaryin = fin.readline().strip()  # MODFLOW binary budget file
    outfmt = fin.readline().strip()      # desired ASCII format (valid Python format)
    fnasciiout = fin.readline().strip()  # ASCII output file
    verbose = fin.readline().strip()
    fin.close()

    verbose = verbose[0] == 'T' or verbose[0] == 't'

    if verbose:
        print 'echo input'
        print '=================='
        print 'fnbinaryin',fnbinaryin
        print 'outfmt',outfmt
        print 'fnasciiout',fnasciiout
        print '=================='

###################################################
# define class and functions needed below

class FortranFile(file):
    """ modified from May 2007 Enthought-dev mailing list post by Neil Martinsen-Burrell"""

    def __init__(self,fname, mode='r', buf=0):
        file.__init__(self, fname, mode, buf)
        self.ENDIAN = '<'  # little endian
        self.di = 4  # default integer, usually 4 bytes, might be 8 on 64-bit platform
        self.dr = 4  # default real, double-precision is 8 bytes, single is 4

    def readReals(self):
        """Read in an array of reals (default precision) with error checking
        prec=d is 'double precision' or 64-bit reals, while prec=f is 'single-
        precision' with 32-bit reals."""
        if self.dr == 8:
            prec='d'  # double
        elif self.dr == 4:
            prec='f'  # float
        else:
            print 'incorrectly specified defanlt real'
            exit(1)

        h = struct.unpack(self.ENDIAN+'i',self.read(self.di))[0] # read header
        data_str = self.read(h)
        if h % self.dr != 0:
            raise IOError('Error reading array of reals from data file')
        num = h/self.dr
        reals = struct.unpack(self.ENDIAN+str(num)+prec,data_str)
        if struct.unpack(self.ENDIAN+'i',self.read(self.di))[0] != h:  # check against footer
            raise IOError('Error reading array of reals from data file')
        return list(reals)

    def readInts(self):
        """Read in an array of integers with error checking"""
        h = struct.unpack('i',self.read(self.di))[0] # read header
```

```
        data_str = self.read(h)
        len_int = struct.calcsize('i')
        if h % len_int != 0:
            raise IOError('Error reading array of integers from data file')
        num = h/len_int
        ints = struct.unpack(str(num)+'i',data_str)
        if struct.unpack(self.ENDIAN+'i',self.read(self.di))[0] != h: # check against footer
            raise IOError('Error reading array of integers from data file')
        return list(ints)

    def readRecord(self):
        """Read a single fortran record (potentially mixed reals, ints, and characters)"""
        dat = self.read(self.di) # read header
        if len(dat) == 0:
            raise IOError('Empy record header')
        h = struct.unpack(self.ENDIAN+'i',dat)[0]
        data_str = self.read(h)
        if len(data_str) != h:
            raise IOError('Didn''t read enough data')
        check = self.read(self.di)
        if len(check) != self.di:
            raise IOError('Didn''t read enough data')
        if struct.unpack(self.ENDIAN+'i',check)[0] != h: # check against footer
            raise IOError('Error reading record from data file')
        return data_str

def reshapev2m(v,nx,ny):
    """Reshape a vector that was previously reshaped in C-major order from a matrix,
    back into a C-major order matrix (here a list of lists)."""
    m = [None]*ny
    n = nx*ny
    for i,(lo,hi) in enumerate(izip(xrange(0, n-nx+1, nx), xrange(nx, n+1, nx))):
        m[i] = v[lo:hi]
    return m

def floatmatsave(filehandle,m):
    """Writes array to open filehandle.
    Outer list is rows, inner lists are columns."""

    for row in m:
        f.write(''.join([outfmt % col for col in row]) + '\n')

################################################

if __name__ == "__main__":

    # open binary file
    ff = FortranFile(fnbinaryin)

    # format of MODFLOW header in binary budget file
    fmt = '<2i16s3i'  # little endian, 2 integers, 16-character string, 3 integers

    while True:
        try:
            # read in header
            h = ff.readRecord()

        except IOError:
            # exit while loop
            break

        else:
            # unpack header
            kstp,kper,text,ncol,nrow,nlay = struct.unpack(fmt,h)
            if verbose:
                print kstp,kper,text,ncol,nrow,nlay

            # second header read but not needed
            throw_away = ff.readRecord()

            if text.strip() == 'FLOW RIGHT FACE':
                qx = ff.readReals()
                assert len(qx) == nrow*ncol, 'qx array is not expected size; check binary format'

            elif text.strip() == 'FLOW FRONT FACE':
                qy = ff.readReals()
                assert len(qy) == nrow*ncol, 'qy array is not expected size; check binary format'

            else: # text.strip() == 'CONSTANT HEAD' (and potentially other cases)
                num = ff.readInts()[0]

                # there are "num" Constant head records consisting of default integers
                # and reals (4 or 8 bytes each),
                # padded fore and aft by default inteters (4 bytes each on 32-bit)
                # second argument to seek (1) incates a seek relative to current position

                jump = num*(3*ff.di + ff.dr)
                if verbose:
                    print 'num:',num,'jump:',jump
```

```
                ff.seek(jump,1)
170
        ff.close()
173
        # save ASCII file
174     f = open(fnasciiout,'w')
        floatmatsave(f,reshapev2m(qx,ncol,nrow))
176     f.write('\n')
        floatmatsave(f,reshapev2m(qy,ncol,nrow))
178     f.close()
```